UNIVERSITE D'ABOMEY - CALAVI (UAC)

INSTITUT NATIONAL DE L'EAU

Registered under N°: 397

A DISSERTATION

Submitted

In partial fulfillment of the requirements for the degree of

DOCTOR of Philosophy (PhD) of the University of Abomey-Calavi (Benin Republic)

In the framework of the

Graduate Research Program on Climate Change and Water Resources (GRP-CCWR)

By

Gnibga Issoufou Yangouliba

Public defense on: 07/28/2023

======

IMPACTS OF CLIMATE, LAND USE, AND WATER MANAGEMENT CHANGES ON THE HYDROPOWER POTENTIALS OF THE BAGRE DAM, BURKINA FASO

======

Supervisors:

SINTONDJI Luc Ollivier, Full Professor, Université d'Abomey-Calavi, Benin
DIPAMA Jean-Marie, Full Professor, Université Joseph Ki-Zerbo, Burkina Faso
KOCH Hagen, Associate Researcher, Potsdam Institute for Climate Impact Research (PIK), Germany

======

Reviewers:

SOGBEDJI Mianikpo Jean, Full Professor, Université de Lomé, Togo
NGOUNOU NGATCHA Benjamin**,** Full Professor, Université de Ngaoundéré, Cameroun
AKPONIKPE I. Pierre, Full Professor, Université d'Abomey-Calavi, Benin

======

JURY

KOUNOUHEWA Basile	Full Professor, Université d'Abomey-Calavi, Benin	President
SOGBEDJI Mianikpo Jean	Full Professor, Université d'Abomey-Calavi, Benin	Reviewer
NGOUNOU NGATCHA Benjamin	Full Professor, Université de Ngaoundéré, Cameroun	Reviewer
AKPONIKPE I. Pierre	Full Professor, Université de Parakou, Benin	Reviewer
GUEDJE Kossi François	Associate Professor, Université d'Abomey-Calavi, Benin	Examiner
SINTONDJI Luc Ollivier	Full Professor, Université d'Abomey-Calavi, Benin	Supervisor
DIPAMA Jean-Marie	Full Professor, Université Joseph Ki-Zerbo, Burkina Faso	Co-Supervisor
KOCH Hagen	Associate Researcher, PIK, Germany	Co-Supervisor

DEDICACE

To my mother, Safoura Kanguélégué.

ACKNOWLEDGMENT

This PhD work is realized in the framework of the West African Science Service Center on Climate Change and Adapted Land use (WASCAL) and funded by the **German Ministry of Education and Research (BMBF) in collaboration with the Benin Ministry of Higher Education and Scientific Research** (MESRS). I am also grateful to the Society of Wetland Scientists (SWS) for its grant support.

I am grateful to my supervisors, Prof. Luc Ollivier Sintondji, Prof. Jean-Marie Dipama, and Dr. Hagen Koch, for their support and assistance during this exciting journey.

A special thanks to my adviser Dr. Stefan Liercsh and my co-supervisor Dr. Hagen Koch, for their availability, their patience, and the fruitful collaboration during my scientific stay at Postdam Institute for Climate Impact Reasearch (PIK) in Germany.

I would like to thank also Dr. Yacouba Yira (CNRST, Burkina Faso), Dr. Moussa Sidibe (World Bank), Dr. Isaac Larbi (University of Environment and Sustainable Development, Ghana), Dr. Andrew Manoba Limantol (University of Environment and Sustainable Development, Ghana), Dr. Benewindé Jean-Bosco Zoungrana (University Joseph Ki-Zerbo, Burkina Faso), Dr. Patricia Ouedraogo (University of Fada N'Gourma, Burkina Faso) Dr. Kwame Oppong Hackman (WASCAL Competence Center, Burkina Faso), Dr. Oble Neya, and Benjamin Bonkoungou for their advices and scientific collaborations.

I am grateful to the WASCAL Benin staff for bearing with the students thoughout the three years. Thanks for the management, the efforts, and the encouragements.

My gratitude goes also to my colleagues of the WASCAL fourth batch, especially those from the GRP-CCWR.

My last gratitude, but not the least, goes to my family and friends. Thanks a lot for your blessings, encouragements, supports, and prayers. This work is yours.

ABSTRACT

This study focused on the impacts of climate, land use, and water management changes on the hydropower potentials of the Bagré dam in Burkina Faso. The specific objectives are (i) the analysis of hydro-climatic variability and upstream reservoir management impact on the hydropower generation at the Bagré dam, (ii) the determination of the past and future land use/land cover (LULC) dynamics in the Nakambé River Basin (NRB), (iii) the assessment of climate and LULC changes impacts on the hydropower potentials at the Bagré dam, and (iv) the assessment of impacts of changed water management on the hydropower potentials at the Bagré dam. Datasets used were comprised of historically observed and reanalysis climate (W5E5), and hydrological time series for break years detection, trend analysis, and correlation investigation. In addition, Landsat images (1990, 2005, 2020) and ground truth data were used for LULC mapping and projection. Downscaled and Bias corrected data from the Inter-Sectoral Impact Model Intercomparison Project (ISIMIP3b) Global Climate Models, water management, and reservoirs parameters data were integrated into the Soil and Water Integrated Management (SWIM) model to assess changes in hydropower generation for the mid (2035-2065) and far (2065-2095) future due to climate, land use, and water management changes. The results showed an annual positive trend in hydropower generation and inflow due to the construction of the Ziga dam in 2000 and its management change in 2005, respectively. In terms of LULC dynamics, from 1990 to 2020, woodland and shrubland decrease to the benefit of cropland, bare land/built-up, and water bodies. By 2050, woodland and shrubland may continue to decrease under the Business-as-usual (BAU) scenario. However, under an afforestation scenario, woodland and shrubland would slightly increase even though cropland will be the dominated land use of the basin. The results also showed that hydropower generation would increase in the mid (15-24%) and far (1.7-35%) future under climate change scenarios, relative to the baseline period (1984-2014). Furthermore, the future LULC change could increase the hydropower potential. Yet, the increment would be less under an afforestation scenario compared to a BAU LULC. For the hydropower generation change, climate change is responsible for 60-98% while LULC change is responsible for 2-40%. The future water allocation from Ziga reservoir would reduce the inflow by -2 m^3/s in the future. This inflow decrease, in addition to the increasing water withdrawals for irrigation supply at the Bagré dam would cause a strong decrease in hydropower generation, which could be more pronounced under SSP126 and BAU LULC, compared to SSP370 and afforestation scenarios. This work pointed out the challenges for the Bagré dam operation to supply

electricity in the future and can be used as a guideline for policy makers to address the future impacts of climate, land use, and water management changes on water resources in the NRB.

Key words: ISIMIP3b, Land Use and Land Cover Change, SWIM Model, Water Management, Hydropower Generation, Nakambé River Basin.

SYNTHÈSE DE LA THÈSE

Résumé

Cette étude est axée sur les impacts du changement climatique, de l'utilisation des terres et de la gestion de l'eau sur le potentiel hydroélectrique du barrage de Bagré au Burkina Faso. Les objectifs spécifiques sont (i) l'analyse de la variabilité hydro-climatique et de l'impact de la gestion des réservoirs en amont sur la production d'énergie hydroélectrique du barrage de Bagré, (ii) la détermination de la dynamique actuelle et future de l'utilisation des terres et du couvert végétal (LULC) dans le bassin versant du Nakambé (NRB), (iii) l'évaluation des impacts du changement climatique et de LULC sur le potentiel hydroélectrique du barrage de Bagré, et (iv) l'évaluation des impacts des changements dans la gestion de l'eau sur le potentiel hydroélectrique du barrage de Bagré. Les données utilisées se composent des séries chronologiques historiques de données hydrologiques et climatiques observées et des données de réanalyse (W5E5) pour la détection des années de rupture, l'analyse des tendances et l'investigation des corrélations. De plus, des images Landsat (1990, 2005, 2020) et des données de terrain ont été utilisées pour la cartographie et la projection de LULC. Des données de modèles climatiques globaux ayant subies la descente d'échelle et corrigées de biais (ISIMIP3b), la gestion de l'eau et les paramètres des réservoirs ont été utilisées. Ces dernières ont été intégrées au modèle de gestion intégrée des sols et de l'eau (SWIM) pour évaluer les changements dans la production d'hydroélectricité à moyen (2035-2065) et long termes (2065-2095) dus aux changements du climat, de LULC et de la gestion de l'eau. Les résultats montrent une tendance positive annuelle de la production hydroélectrique et du débit entrant à Bagré du fait respectivement de la construction en amont du barrage de Ziga en 2000 et de son changement de gestion en 2005. En termes de la dynamique de LULC, de 1990 à 2020, les zones boisées et la végétation arbustive ont diminué au profit des champs, des sols nus/bâtis et des plans d'eau. D'ici à 2050, les zones boisées et la végétation arbustive pourraient continuer à diminuer dans le cadre du scénario du statu quo. Toutefois, dans le cadre d'un scénario de reboisement, les zones boisées et la végétation arbustive augmenteraient légèrement, même si les champs restent la principale utilisation des terres dans le bassin. Les résultats ont également montré que, par rapport à la période de référence (1984-2014), la production hydroélectrique augmenterait à moyen (15 - 24 %) et à long terme (1,7 - 35 %) selon les scénarii de changement climatique. En outre, le futur changement de LULC pourrait augmenter le potentiel

hydroélectrique du barrage de Bagré. Cependant, l'augmentation serait moindre dans le cadre d'un scénario de reboisement que celui d'un statu quo. Les changements futurs de la production hydroelectrique seraient la consequence du changement climatique (60 - 98%) que celui du changement de LULC (2 - 40%). Enfin, la distribution future de l'eau à partir du réservoir de Ziga va réduire le débit à Bagré de 2 m^3/s. Cette diminution du débit, en plus de l'augmentation des prélèvements d'eau pour l'irrigation dans le barrage de Bagré, pourraient entraîner une forte diminution de la production hydroélectrique, plus prononcée dans les scénarii optimiste et du statu quo, comparativement aux scenarii pessimiste et de reboisement. Les resultats de cette étude mettent en évidence les défis de l'exploitation du barrage de Bagré pour fournir de l'électricité dans les années à venir. Ce travail peut être utilisé comme un outil d'aide à la décision par les décideurs politiques et gestionnaires pour s'adapter aux impacts futurs du climat, de l'utilisation des terres et des changements de gestion de l'eau dans le bassin.

Mots-clés: ISIMIP3b, Utilisation des terrres, Modèle SWIM, Gestion de l'eau, Production hydroélectrique, Bassin versant du Nakambé.

Introduction

L'électricité est essentielle au développement de la société. Elle est utilisée dans de nombreuses activités telles que l'agriculture, l'industrie, l'élevage, l'éducation, etc. Cependant, la volonté de garantir la durabilité de l'utilisation des ressources naturelles et de contribuer à la réduction des émissions de gaz à effet de serre (GES) a conduit à la promotion des énergies renouvelables. En effet, l'hydroélectricité est l'une des plus importantes sources d'energie renouvelable au monde et joue un rôle essentiel dans la réduction des émissions des GES. Au Burkina Faso, la production d'électricité repose principalement sur des centrales thermiques (206 MW). La capacité de production de ses cinq barrages hydroélectriques est de 36 MW: Bagré (16 MW), Kompienga (15,4 MW), Niofila (1,8 MW) Tourni (0,6 MW) et Samendeni (2 MW). La capacité de production nationale est inférieure à la demande, entraînant des importations d'électricité de Côte d'Ivoire, du Ghana et du Togo. Cette situation de dependance entraine de multiples delestages et un coût élevé de l'électricité (96 à 165 francs CFA le KWh). En 2011, sur 1025 GWh/a d'électricité fournie, près de 50% ont été importés. La quantité produite par la Société

Nationale Burkinebè d'Electricité (SONABEL) était de 530 GWh/a (448 GWh/a provenant de centrales thermiques et 82 GWh/a de centrales hydroélectriques). Selon une étude realisée dans le cadre du projet « SE4ALL » en 2016, la production hydroélectrique nationale a baissé de 30% entre 2008 et 2011 en raison de la baisse du niveau d'eau dans les barrages hydroélectriques, qui eux mêmes dépendent des écoulements et des précipitations annuelles. Pourtant, l'utilisation des terres et la gestion de l'eau ont un grand impact sur les écoulements, ce qui pourrait également impacter le niveau d'eau des barrages et la production d'hydroélectricité. Cette étude se fixe pour objectif d'évaluer les impacts des changements climatique, d'utilisation des terres et de la gestion de l'eau sur le potentiel hydroélectrique du barrage de Bagré. De facon spécifique, il s'agit de : (i) analyser la variabilité hydro-climatique et l'impact de la gestion des réservoirs en amont sur la production d'énergie hydroélectrique du barrage de Bagré, (ii) déterminer la dynamique passée et future de LULC dans le bassin versant du Nakambé, (iii) évaluer les impacts du changement climatique et de LULC sur le potentiel hydroélectrique du barrage de Bagré, et (iv) évaluer les impacts des changements de gestion de l'eau sur le potentiel hydroélectrique du barrage de Bagré.

Zone d'étude

Le bassin versant du Nakambé est situé dans le haut-bassin de la Volta Blanche au Burkina Faso. Sa superficie est d'environ 32 623 km^2. Le barrage de Bagré a été construit en 1992 dans la vallée du bassin. Il a une capacité de stockage d'eau de 1,7 milliard de m^3. C'est un barrage à usages multiples dont l'objectif principal est de couvrir 20% des besoins nationaux en électricité. La centrale hydroélectrique installée a une capacité de 16 MW. Le barrage est également utilisé pour la pêche et l'irrigation de plus de 6 000 ha de terres amenagées.

Données, matériels et méthodes

Données

Quatre types de données ont été utilisés dans le cadre de la presente étude. Le premier type est composé de données climatiques à pas de temps journalier. Ces données proviennent des observations et des

réanalyses (W5E5) et comprennent les precipitations, la temperature minimale, maximale et moyenne, l'humidité relative et la radiation solaire de 1985 à 2015. En plus de ces données historiques, des données climatiques (1979-2100) de dix modèles globaux (ISIMIP3b) reduite d'echelle et corrigés de biais ont été utilisées. Le deuxième groupe de données concerne des images Landsat de 1990, 2005 et 2020 qui ont servi à la caractérisation de la dynamique de l'utilisation des terres dans le bassin versant. Le troisième type se compose de données hydrométriques et hydrologiques journalières notamment les débits du fleuve Nakambé à Niaogho (1964-1997), les volumes et les prélèvements d'eau de neuf réservoirs (1993-2018). Le dernier type de données sont d'ordre environemental et se compose de cartes de sols, d'utilisation des terres et des pentes.

Materiels et Méthodes

Les données climatiques d'observation ont servi à la validation des données de W5E5. Les tendances d'évolution de ces séries chronologiques historiques de données climatiques réanalysées (W5E5), et hydrologiques ont été analysées à travers le test de Mann-Kendall modifié. Ensuite, l'utilisation du test de Pettitt et du test d'homogénéité normale standard ont permis de détecter les années de ruptures dans ces séries. Par ailleurs, le test de corrélation de Spearman a été utilisé pour analyser l'influence des variables hydro-climatiques sur la production hydroélectrique du barrage de Bagré.

Quant à la dynamique de l'utilisation des terres dans le bassin, c'est la plateforme Google Earth Engine qui a servi pour la classification des images à l'aide de la méthode du « Random Forest ». La qualité de la classification a été évaluée à travers le coefficient de Kappa. Après avoir validé la projection de la carte de LULC en 2020, les cartes de LULC en 2050 (selon le scenario du statu quo ou de reboisement) ont été generées en utilisant la méthode du « Markov Chain Multi Layer Perceptron Neural Network » du Land Change Modeler.

Le modèle SWIM a servi à l'evaluation de l'impact des changements climatique, de l'utilisation des terres et de la gestion de l'eau sur le potentiel de production hydroélectrique du barrage de Bagré. La méthodologie adoptée a consisté à caler (1980-1984) et valider (1987-1991) le modèle à pas de temps mensuel à la station de Niaogho. La performance du modèle a été évaluée à travers les coefficients de détermination (R^2) et de Nash-Sutcliffe (NSE), et le pourcentage de biais (PBias). Trois scénarios ont

servi pour évaluer les impacts possibles des changements climatiques et d'utilisation des terres sur les débits et la production hydroélectrique:

(i) évaluation de l'impact du changement climatique (SSP126 et SSP370) sur la production hydroélectrique en faisant tourner le modèle SWIM avec la carte d'utilisation des terres de 2005 et ISIMIP3b pour le moyen (2035-2065) et long terme (2065-2095) ;

(ii) évaluation de l'impact des changements d'utilisation des terres sur la production hydroélectrique en faisant tourner le modèle SWIM calibré avec W5E5 (1979-2019) et les cartes d'utilisation des terres de 2050 ;

(iii) évaluation de l'impact des changements combinés du climat et de l'utilisation des terres en faisant tourner le modèle SWIM avec les modèles ISIMIP3b et les deux scénarios de changement d'utilisation des terres de 2050.

Les changements de débit entrant et de production hydroélectrique ont été évalués en estimant les changements relatifs et absolus des médians du débit entrant et de production hydroélectrique au cours de la période 2035-2065 et 2065-2095, par rapport à la période 1984-2014.

Enfin, le changement de gestion de l'eau a consisté à augmenter les prélèvements d'eau à Ziga et Bagré afin d'évaluer leurs impacts sur le débit et la production hydroélectrique.

Résultats et discussion

Variabilité hydro-climatique et impact de la gestion des réservoirs en amont sur la production d'énergie hydroélectrique du barrage de Bagré

Les résultats montrent une tendance annuelle positive significative pour les précipitations, le débit et la production hydroélectrique. L'augmentation du niveau d'eau n'est pas significative en raison du mode de gestion des barrages. Les années de rupture observées dans la production hydroélectrique (2002) et le débit (2006) sont principalement dues respectivement à la construction du barrage de Ziga en 2000 et à son changement de gestion en 2005. Cela est confirmé par le test de corrélation de Spearman qui montre une corrélation modérée entre le barrage de Ziga et la production hydroélectrique à Bagré. À l'échelle mensuelle,

la production hydroélectrique diminue de 30,36 MWh et 16,82 MWh respectivement en mai et juin à cause de l'augmentation significative des prélèvements pour l'irrigation (1,94 hm^3 en mai et 0,67 hm^3 en juin).

Dynamique actuelle et future de l'utilisation des terres et du couvert végétal (LULC) dans le bassin versant du Nakambé (NRB)

En ce qui concerne la dynamique de LULC, les résultats ont montré des changements significatifs au niveau des unités de LULC. De 1990 à 2020, les zones boisées et la végétation arbustive ont diminué respectivement de 45 % et 68 %, tandis que les champs et les sols nus/bâtis ont augmenté respectivement de 51 % et 75 %. De 2020 à 2050, les résultats montrent que, dans le cadre du scénario du statu quo, les sols nus/bâtis et les plans d'eau pourraient continuer à augmenter respectivement de 99 % et de 1 %. En revanche, les champs, la végétation arbustive et les zones boisées pourraient diminuer respectivement de 33 %, 34 % et 47 %. Dans le scénario de reboisement, le contraire du statu quo pourrait se manifester. Alors que les zones boisées, la végétation arbustive et les champs augmenteraient respectivement de 22 %, 52 % et 18 %, entre 2020 et 2050, la zone couverte par les plans d'eau et les sols nus/bâtis diminuerait respectivement de 6,2 % et 39 %.

Impacts du changement climatique et de LULC sur le potentiel hydroélectrique du barrage de Bagré

Le futur climat dans la NRB serait plus humide par rapport à la période de référence (1984-2014). Selon le scenario optimiste, la période 2035-2065 serait humide dans la NRB, avec une augmentation des précipitations annuelles de 10,7 %. Cette augmentation pourrait favoriser une augmentation du débit entrant du barrage et de la production hydroélectrique de 21,1% et 15,6%, respectivement. Cependant, l'augmentation des précipitations de 8% au cours de la période 2065-2095 entraînerait une diminution du débit de 8%, mais une augmentation de la production hydroélectrique de 1,7%. En raison des températures élevées et de la forte évapotranspiration, une augmentation des précipitations sur le bassin n'implique pas nécessairement une augmentation de débit et de la production hydroélectrique. Certains mois pourraient connaitre une diminution du débit et de la production hydroélectrique. Par exemple, le débit diminue en juillet, tandis que la production hydroélectrique diminue en juillet et en août. Ces diminutions pourraient être la conséquence de la baisse des précipitations mensuelles en avril et mai dans un avenir lointain. Globalement, le débit et la production hydroélectrique pourraient augmenter au cours de la période 2035-2065, tandis que la période 2065-2095 connaîtrait un retour à la production hydroélectrique de la période de référence.

Dans le cadre du scenario pessimiste, les conditions climatiques sont beaucoup plus humides que celui du scenario optimiste. En effet, l'augmentation des précipitations annuelles de 21% et 24%, respectivement au cours des périodes 2035-2065 et 2065-2095, induit des augmentations de débit respectives de 54,5% et 75,1% par rapport à la période de référence. Par conséquent, la production hydroélectrique devrait augmenter de 24,4 % et de 35,8 % respectivement pendant les périodes 2035-2065 et 2065-2095 par rapport à la période 1984-2014. Cependant, cette augmentation de la production hydroélectrique cache des disparités de diminution à l'échelle mensuelle, particulièrement durant les mois de juin à août dans le cadre du scenario optimiste. En outre, le futur changement de LULC pourrait augmenter le potentiel de production hydroélectrique. Toutefois, l'augmentation serait moindre dans le cadre d'un scénario de reboisement que dans celui d'un scenario du statu quo. En effet, dans le cadre d'un scénario de reboisement, les résultats des effets combinés des changements climatique et d'utilisation des terres sont semblables à ceux des seuls impacts du changement climatique. Les débits et la production hydroélectrique évoluent de manière similaire entre 2035-2065 et 2065-2095. Dans le cadre du scenario optimiste, le débit au barrage de Bagré augmente de 20,9% au cours de la période 2035-2095 et diminue de 7,8% pour la période 2065-2095 par rapport au scénario de référence. Néanmoins, la production hydroélectrique pourrait augmenter dans le futur même si le taux d'augmentation pendant la période 2035-2065 (14,9%) est plus élevé que celle de la période 2065-2095 (1,9%). Dans le cadre du scenario pessimiste, une augmentation du débit de 53,8 % et 74 % est prévue respectivement pour les périodes 2035-2065 et 2065-2095. Par conséquent, la production hydroélectrique pourrait augmenter de 23,2 % et 34,4 % respectivement pendant les périodes 2035-2065 et 2065-2095. Dans le cadre d'un scénario de statu quo, une augmentation du débit et de la production hydroélectrique respective de 16,9 % et 5,9 % est attendue dans le cadre d'un scenario optimiste pendant la période 2035-2065. Cependant, de 2065 à 2095, une diminution de 3,1 % du débit est attendue, tandis qu'une augmentation de 3,8 % de la production hydroélectrique est prévue. Dans le cadre du scenario pessimiste, les conditions plus humides pourraient entrainer une augmentation du débit de 40,6 % et de 58,1 % respectivement à moyen et à long terme. Par conséquent, la production hydroélectrique augmenterait également de 8,1 % et 12,4 % respectivement pendant les périodes 2035-2065 et 2065-2095 par rapport à la période de référence. En termes de contribution au changement de la production hydroélectrique, le changement climatique est

responsable de 60 à 98 %, tandis que le changement de LULC est responsable de 2 à 40 % selon les scenarii.

Impacts des changements dans la gestion de l'eau sur le potentiel hydroélectrique du barrage de Bagré

Le changement de gestion de l'eau du barrage de Ziga pour fournir de l'eau potable à la ville de Ouagadougou entraînerait une diminution du débit au niveau du barrage de Bagré. Cependant, comparée aux impacts du changement climatique et/ou d'utilisation des terres, cette baisse serait moins sévère et se situe entre 1,4 et 2 m^3/s. Par conséquent, le débit mensuel pourrait être légèrement impacté. Cela signifie que l'augmentation des prélèvements de 0,196 m^3/s à 2,3 m^3/s au barrage de Ziga n'affecterait pas significativement le débit au barrage de Bagré dans le futur. Au contraire, la production d'énergie hydroélectrique au barrage de Bagré diminuerait ou augmenterait selon les scénarii climatique, d'utilisation des terres et la période considérée. Quel que soit la période considérée, l'augmentation des prélèvements d'eau à Bagré pour l'irrigation conduirait à une diminution de la production hydroélectrique dans le cadre des scenarii optimiste et d'utilisation des terres. Cependant, le taux de réduction dans un futur lointain serait plus élevé que celle d'un futur moyen. Cela pourrait s'expliquer par les taux de changement que subira la pluviométrie durant ces deux périodes. En effet, la période 2035-2065 devrait être beaucoup plus humide que celle de 2065-2095. Cependant, dans le cadre d'un scenario pessimiste, une augmentation de la production hydroélectrique est attendue, sauf dans le cadre du statu quo. A l'échelle mensuelle, les futurs prélèvements d'eau pour l'irrigation affecteront fortement la production hydroélectrique et certains mois pourraient connaitre des baisses de près de 4 MW par rapport à la période de référence.

Conclusion

En conclusion, l'étude a montré qu'à l'échelle annuelle, l'augmentation significative de la pluviométrie combinée à la gestion du barrage de Ziga a eu un impact positif sur le débit entrant et la production hydroélectrique du barrage de Bagré. Cependant, cette augmentation annuelle cache des disparités car la production d'hydroélectricité diminue en mai et juin en raison de l'augmentation significative des prélèvements d'eau pour l'irrigation. La dynamique de l'occupation des terres de 1990 à 2020 a montré

une diminution continue de la végétation naturelle, une augmentation continue des champs, des sols nus/bâtis et des plans d'eau. La tendance des unités d'occupation des terres a montré de très importants effets des activités humaines sur le changement de l'état de surface du bassin. D'une part, la future carte de LULC en 2050, basée sur le scénario du statu quo, a montré que la pression humaine exacerberait davantage la végétation naturelle, avec une diminution probable des terres cultivées. D'autre part, dans le cadre du scénario de boisement, la végétation naturelle pourrait augmenter tandis que les sols nus/bâtis pourraient diminuer. Ces différents changements de climat et de l'occupation des terres pourraient entrainer une augmentation du potentiel hydroélectrique du barrage de Bagré. Cette augmentation serait plus accrue selon le scenario climatique pessimiste que celui optimiste. Cependant, les changements de gestion de l'eau pourraient réduire la capacité de production hydroélectrique du barrage de Bagré.

TABLE OF CONTENTS

DEDICACE ..... **ii**

ACKNOWLEDGMENT ..... **iii**

ABSTRACT ..... **iv**

SYNTHÈSE DE LA THÈSE ..... **vi**

TABLE OF CONTENTS ..... **xv**

CHAPTER 1: GENERAL INTRODUCTION **1**

1.1. Context and problem statement 1

1.1.1. Context of the study 1
1.1.2. Problem statement 3

1.2. Literature review 5

1.2.1. Hydropower dams 5
1.2.2. Climate change and climate models 6
1.2.3. Land use and land cover changes 8
1.2.4. Water resources management 10
1.2.5. Hydrological modelling 11
1.2.6. Impacts of climate, land use and water management changes on hydropower generation 13

1.3. Research questions 18

1.4. Thesis objectives 18

1.5. Hypothesis 18

1.6. Novelty 19

1.7. Scope of the thesis 19

1.8. Expected results and benefits 19

1.9. Outline of the thesis 20

CHAPTER 2: STUDY AREA **21**

2.1. Localization 21

2.2. Relief 22

2.3. Vegetation 23

2.4. Climate 23
2.5. Hydrography 24
2.6. Soil and land use 24
2.6.1. Soils 24
2.6.2. Land use 26
2.7. Demography, environmental, social and economic activities 27
2.8. Partial Conclusion 27

CHAPTER 3: DATA, MATERIALS AND METHODS 29
3.1. Data 29
3.1.1. Station and Gridded Climate Data 29
3.1.2. Hydrological data 30
3.1.3. Landsat images and reference data 30
3.1.4. Global Climate Models 31
3.1.5. SWIM model inputs data 32
3.2. Methods 35
3.2.1. Hydro-climatic trend and upstream dam management impact on hydropower generation 35
3.2.2. Land use land cover classification and future land use prediction 40
3.2.3. Assessment of impact of climate and LULC changes on hydropower generation at the Bagré dam 44
3.2.4. Assessment of impact of water management changes on hydropower generation at the Bagré dam 54
3.3. Partial Conclusion 55

CHAPTER 4: HYDRO-CLIMATIC VARIABILITY AND UPSTREAM WATER MANAGEMENT IMPACTS ON HYDROPOWER GENERATION AT THE BAGRÉ DAM 56
4.1. W5E5 datasets performance 56
4.2. Homogeneity and trend analysis of annual hydro-climatic variables and hydropower generation 58
4.3. Trend analysis of monthly hydro-climatic variables and hydropower generation 61
4.4. Relationship between hydro-climatic variables, ENSO and hydropower generation 64
4.5. Discussion 65
4.6. Partial conclusion 68

CHAPTER 5: PAST AND FUTURE LAND USE LAND COVER DYNAMICS IN THE NAKAMBÉ RIVER BASIN 69
5.1. Accuracy of Land Use and Land Cover Classification 69
5.2. Land Use and Land Cover maps in 1990, 2005, and 2020 70

5.3. Changes in Land Use and Land Cover between 1990-2005, 2005-2020, and 1990-2020 72
5.4. Contributors to cropland and bare land/built-up increase 72
5.5. Spatial trend of anthropogenic land uses 73
5.6. Land use change driver variables and potential transition mapping 74
5.7. LULC model validation 75
5.8. Future LULC dynamics 78
5.9. Discussion 80
5.10. Partial conclusion 82

CHAPTER 6: IMPACTS OF CLIMATE AND LAND USE CHANGES ON HYDROPOWER GENERATION 84

6.1. Global climate models projections and hydrological modelling parameterization 84
6.1.1. Performance of ISIMIP3b 84
6.1.2. Climate projections in the NRB 86
6.1.3. Parameters' sensitivity, calibration and validation of SWIM 91
6.2. Impacts of climate change on inflow and hydropower generation 93
6.2.1. Changes in inflow and hydropower generation under climate change impact 93
6.2.2. Changes in seasonal inflow and hydropower generation under climate change impact 94
6.3. Impact of land use change on inflow and hydropower generation 98
6.4. Impact of combined climate and land use changes on inflow and hydropower generation 99
6.4.1. Changes in inflow and hydropower generation under combined impact of climate and land use changes 99
6.4.2. Changes in seasonal inflow and hydropower generation under combined effects of climate and land use changes 101
6.5. Discussion 108
6.6. Partial conclusion 110

CHAPTER 7: IMPACT OF FUTURE WATER ALLOCATION ON HYDROPOWER GENERATION 111

7.1. Impact of future water management on inflow and hydropower generation in the context of climate change 111
7.1.1. Changes in inflow and hydropower generation under future water management and climate change .. 111
7.1.2. Changes in seasonal inflow and hydropower generation under water management and climate changes 112
7.2. Changes in inflow and hydropower generation under water management and LULC changes 116
7.3. Changes in inflow and hydropower generation under the combined impacts of future water management, LULC and climate changes 117
7.3.1. Changes in inflow and hydropower generation under the combined impacts of future water management, climate and land use changes 117

7.3.2. Changes in seasonal inflow and hydropower generation due to future water management under combined effects of climate and land use changes 118
7.4. Discussion 125
7.5. Partial conclusion 126

CHAPTER 8: GENERAL CONCLUSION AND PERSPECTIVES 127
8.1. Conclusions 127
8.2. Recommendations 129
8.3. Perspectives 130

REFERENCES xxiv

ANNEX lvi

List of Acronyms

AEN	:	Agence de l'Eau du Nakambé
ANAM	:	National Meteorological Agency
BAU	:	Business-As-Usual
BUNASOLS	:	Bureau National des Sols
CA-MC	:	Cellular Automata-Markov Chain
CART	:	Classification and Regression Trees
CILSS	:	Comité permanent Inter-Etats de Lutte contre la Sécheresse dans le Sahel
CIREG	:	Climate information for Integrated Renewable Electricity Generation
CORDEX	:	Coordinated Regional Climate Downscaling Experiment
DEM	:	Digital Elevation Model
DGRE	:	Direction Générale des Ressources en Eaux
ENSO	:	El Niño – Southern Oscillation
FAO	:	Food and Agriculture Organization of the United Nations
GCMs	:	Global Climate Models
GEE	:	Google Earth Engine
GFDRR	:	Global Facility for Disaster Reduction and Recovery
GHG	:	Greenhouse Gas
HBV	:	Hydrologiska Byrans Vattenbalansavdelning
HWSD	:	Harmonized World Soils Database
IFC	:	International Finance Coorporation
IHA	:	International Hydropower Association
INSD	:	Institut National de la Statistique et du Développement
IPCC	:	Intergovernmental Panel on Climate Change
ISIMIP	:	Inter-Sectoral Impact Model Intercomparison Project
KNN	:	K-Nearest Neighbour
LCM	:	Land Change Modeler
LVQ	:	Learning Vector Quantization
LULC	:	Land Use/Land Cover
LULCC	:	Land Use/Land Cover Changes
MCM	:	Markov Chain Model
MLP	:	Multi-Layer Perceptron
NRB	:	Nakambé River Basin
NRMSE	:	Normalized Root Mean Square Error
NSE	:	Nash-Sutcliffe Efficiency
PBias	:	Percentage of Bias
RCMs	:	Regional Climate Models
RCP	:	Representative Concentration Pathway
RF	:	Random Forest
SCS	:	Soil Conservation Service
SDG	:	Sustainable Development Goals
SE4ALL	:	Sustainable Energy for All

SGB	:	Stochastic Gradient Boosting
SNHT	:	Standard Normal Homogeneity Test
SONABEL	:	Société Nationale Burkinabè d'Electricité
SSP	:	Shared Socioeconomic Pathways
STMC	:	Stochastic Markov Chain
SVM	:	Support Vector Machines
SWAT	:	Soil and Water Assessment Tool
SWIM	:	Soil and Water Integrated Management
UNEP	:	United Nations Environmental Program
UNEP-GEF	:	United Nations Environment Program - Global Environment Facility
UPDEA	:	Union des Producteurs,Transporteurs et Distributeurs d'Énergie électrique d'Afrique
WASCAL	:	West African Science Service Center on Climate Change and Adapted Land use
WEAP	:	Water Evaluation and Planning System

List of figures

Figure 1. Location of the NRB, Bagré dam, climate and hydrological stations 22
Figure 2. Land use land cover of 2020 (A) and spatial distribution of reservoirs (B) in the NRB.....26
Figure 3. Spatial distribution of soil layers (HWSD) in the NRB 34
Figure 4. LULC mapping and modelling Flowchart.....43
Figure 5. SWIM model structure (Krysanova et al., 2022).....45
Figure 6. Flowchart of SWIM model set up, calibration, and validation for the NRB.....50
Figure 7. Mean monthly observed and W5E5 of rainfall, min and max temperature, relative humidity, and solar radiation at Ouagadougou (A) and Ouahigouya (B) from 1985-2015. 57
Figure 8. Annual trend of climatic variables.....59
Figure 9. Annual trend of hydrological variables. 60
Figure 10. Correlation coefficients between the hydro-climatic variables, ENSO and hydropower generation anomalies.....64
Figure 11. Comparison of ENSO index and hydropower generation anomaly. 65
Figure 12. LULC maps of 1990, 2005, and 2020 71
Figure 13. Percent of changes of LULC units between 1990-2005, 2005-2020, and 1990-2020 72
Figure 14. Contribution to net changes in cropland and bare land/built-up (in km^2) for 1990-2005, 2005-2020 and 1990-2020.....73
Figure 15. Spatial trend of conversion from all LULC classes to cropland (a) and bare land-built-up (b) during the period 1990-2005......74
Figure 16. Spatial trend of conversion from all LULC classes to cropland (a) and bare land-built-up (b) during the period 2005-2020......74
Figure 17. Explanatory variables used for the transition potential mapping. 75
Figure 18. Actual classified and simulated LULC for 2020 77
Figure 19. Projected future LULC maps for 2050 under the BAU and Afforestation scenarios.....79
Figure 20. Changes in average annual rainfall and mean temperature from 2035-2065 (A) and 2065-2095 (B), compared to 1984-2014. 87

Figure 21. Monthly absolute changes in rainfall and mean temperature during the periods 2035-2065 (A, B) and 2065-2095 (C, D) relative to 1984-2014 under SSP126. 89
Figure 22. Monthly absolute changes in rainfall and mean temperature during the periods 2035-2065 (A, B) and 2065-2095 (C, D) relative to 1984-2014 under SSP370 90
Figure 23. Calibration and validation of discharge at Wayen station 92
Figure 24. Calibration and validation of discharge at Niaogho station 93
Figure 25. Monthly absolute changes in inflow and hydropower generation during the periods 2035-2065 (A, B) and 2065-2095 (C, D) relative to 1984-2014 under SSP126 96
Figure 26. Monthly absolute changes in inflow and hydropower generation during the periods 2035-2065 (A, B) and 2065-2095 (C, D) relative to 1984-2014 under SSP370 97
Figure 27. Monthly inflow (A) and hydropower generation (B) under different land use land cover scenarios 98
Figure 28. Monthly absolute changes in inflow and hydropower generation during the periods 2035-2065 (A, B) and 2065-2095 (C, D) relative to 1984-2014 under SSP126 and LULC 2050 AFF 103
Figure 29. Monthly absolute changes in inflow and hydropower generation during the periods 2035-2065 (A, B) and 2065-2095 (C, D) relative to 1984-2014 under SSP370 and LULC 2050 AFF 104
Figure 30. Monthly absolute changes in inflow and hydropower generation during the periods 2035-2065 (A, B) and 2065-2095 (C, D) relative to 1984-2014 under SSP126 and LULC 2050 BAU 106
Figure 31. Monthly absolute changes in inflow and hydropower generation during the periods 2035-2065 (A, B) and 2065-2095 (C, D) relative to 1984-2014 under SSP370 and LULC 2050 BAU 107
Figure 32. Monthly absolute changes in inflow and hydropower generation due to water management and climate changes (SSP126) during the periods 2035-2065 (A, B) and 2065-2095 (C, D) relative to 1984-2014 114
Figure 33. Monthly absolute changes in inflow and hydropower generation due to water management and climate changes (SSP370) during the periods 2035-2065 (A, B) and 2065-2095 (C, D) relative to 1984-2014 115
Figure 34. Monthly inflow (A) and hydropower generation (B) due to water management change under various LULC 117

Figure 35. Monthly absolute changes in inflow and hydropower generation due to water management under climate (SSP126) and afforestation land use changes during the periods 2035-2065 (A, B) and 2065-2095 (C, D) relative to 1984-2014.....120
Figure 36. Monthly absolute changes in inflow and hydropower generation due to water management under climate (SSP370) and afforestation land use changes during the periods 2035-2065 (A, B) and 2065-2095 (C, D) relative to 1984-2014.....121
Figure 37. Monthly absolute changes in inflow and hydropower generation due to water management under climate (SSP126) and BAU land use changes during the periods 2035-2065 (A, B) and 2065-2095 (C, D) relative to 1984-2014.....123
Figure 38. Monthly absolute changes in inflow and hydropower generation due to water management under climate (SSP370) and BAU land use changes during the periods 2035-2065 (A, B) and 2065-2095 (C, D) relative to 1984-2014.....124

List of tables

Table 1. Summary of the literature review on climate change, LULC, and water management changes on discharge and hydropower in West Africa....16
Table 2. Protected areas within the NRB....27
Table 3. Observed and Reanalysis climate data used in the study....30
Table 4. Characteristics of Landsat satellite images used....31
Table 5. Sample sizes of LULC units for 1990, 2005, and 2020....31
Table 6. Global climate models and their spatial resolution before and after downscaling....32
Table 7. HWSD in the NRB....33
Table 8. Equivalence of LULC units with SWIM land use....34
Table 9. Reservoirs and their capacity storage used in SWIM....35
Table 10. Probability of changes used for BAU and afforestation scenarios....44
Table 11. Period of calibration and validation of discharge and reservoir volumes....52
Table 12. Mean withdrawals from Bagré and Ziga under baseline and future water management....54
Table 13. Comparison statistics of monthly observed climate variables and monthly W5E5 products at Ouagadougou (south of the basin) and Ouahigouya (north of the basin) stations....56
Table 14. Modified Mann Kendall, Pettitt's test and SNHT statistics of annual hydro-climatic variables and hydropower in the NRB....58
Table 15. Modified Mann Kendall statistics of monthly climatic variables in the NRB....62
Table 16. Modified Mann Kendall statistics of monthly hydrological variables in the NRB....63
Table 17. Spearman correlation coefficient between annual hydropower generation and hydro-climatic variables....64
Table 18. Confusion matrix of the LULC classification in 1990....69
Table 19. Confusion matrix of the LULC classification in 2005....69
Table 20. Confusion matrix of the LULC classification in 2020....69
Table 21. Proportion of LULC units in 1990, 2005 and 2020....70
Table 22. Proportion of classified and simulated LULC units in 2020 and their associated errors....76

Table 23. Proportion of LULC units in 2050 under the BAU and afforestation scenarios and their percentage of changes 79
Table 24. Comparison statistics of monthly ISIMIP3b rainfall and mean temperature and monthly observations and W5E5 products at Ouagadougou and Ouahigouya stations.....85
Table 25. Median and mean annual rainfall and temperature and percentage of changes over 1984-2014, 2035-2065, and 2065-2095 86
Table 26. Performance of the calibration and validation of daily (Wayen) and monthly (Niaogho) discharges, and daily reservoir volumes 92
Table 27. Multi-models hydro-climatic median changes during 1984-2014, 2035-2065, and 2065-2095 under SSP126 and SSP370 94
Table 28. Changes in median inflow and hydropower generation for different land use land cover scenarios.....98
Table 29. Multi-models median hydro-climatic variables changes during 1984-2014, 2035-2065, and 2065-2095 under SSP126 and SSP370, and afforestation LULC 2050.....99
Table 30. Contribution of climate and afforestation LULCC to inflow and hydropower changes 100
Table 31. Multi-models hydro-climatic median changes during 1984-2014, 2035-2065, and 2065-2095 under SSP126 and SSP370, and Business as usual LULC 2050 100
Table 32. Contribution of climate and BAU LULCC to inflow and hydropower changes 101
Table 33. Multi-models hydro-climatic median changes during 1984-2014, 2035-2065, and 2065-2095 under future water management and climate changes 111
Table 34. Changes in median inflow and hydropower generation for different land use land cover and water management scenarios 116
Table 35. Multi-models hydro-climatic median changes during 1984-2014, 2035-2065, and 2065-2095 under future water management, climate and afforestation land use changes.....118
Table 36. Multi-models hydro-climatic median changes during 1984-2014, 2035-2065, and 2065-2095 under future water management, climate and BAU land use changes.....118

CHAPTER 1: GENERAL INTRODUCTION

This chapter presents a general overview of the study. It presents the background and states the problem of the study. The different objectives and hypothesis are also defined. Lastly, the chapter reviews the previous studies related to hydropower dams, water management, climate change and climate models, land use and land cover changes, and impacts of climate, land use, and water management changes on hydropower dams at global and local scale.

1.1. Context and problem statement

This section addresses the context and highlights the problem statement of the study.

1.1.1. Context of the study

Electricity is essential for societal development. It is used for many activities such as agriculture, industry, livestock, education, etc. For long time, many countries have developed using energy from fuel combustion. However, the need to reach sustainability in natural resources use and to reduce greenhouse gas (GHG) emissions led to the promotion of renewable energy. Indeed, hydropower generation is one of the largest renewable electricity generation sources in the world (Shrestha et al., 2020) and plays an essential role in the reduction of GHG emissions (Berga, 2016). At global scale, hydropower generation accounts for 16% of the total electricity generated in the world (IHA, 2018). China is the largest producer of hydropower in the world with an installed hydropower capacity of about 390 GW in 2020, representing 18% of the nation's electricity generation capacity (Liu et al., 2020).

In Africa, hydropower remains one of the main renewable resources with over 37 GW of installed capacity and accounts for 15% of its total electricity production, which is predicted to reach 23% in 2040 (IHA, 2020). Even though representing 17% of the world's population, almost half of Africans do not have access to electricity. Many African countries such as Ethiopia, South Africa, Angola, Egypt, the Democratic Republic of Congo, Zambia, Mozambique, Nigeria Ghana and Burkina Faso rely on hydropower dams to supply electricity to their population. However, due to the population growth, electricity demand in Africa is expected to triple by 2040 (IHA, 2020). In West Africa for instance, the population is expected to reach 1 billion inhabitants in 2050 (United Nations, 2011). To cope with that, over 50 hydropower projects are currently under construction, with more than 15 GW of installed generation capacity expected to be commissioned by 2025

(IHA, 2020). Nevertheless, some of dam projects do not take into account the impact that climate and land use/land cover (LULC) changes (LULCC) can have on the hydropower generation (Obahoundje and Diedhiou, 2022).

Climate change has a major impact on hydropower generation (Boadi and Owusu, 2017; de Souza Dias et al., 2018; Liu et al., 2020; Mousavi et al., 2018; Sridharan et al., 2019). According to Beilfuss (2012), African countries have not been able to meet their development targets due to climate variability and change impacts on hydropower generation. The reliance on climate sensitive sectors such as hydropower has become a challenge to sustainable development as a result of climate variability and change impacts on power generation (Okudzeto et al., 2014). A study conducted by Owusu et al. (2008) showed that the declining total rainfall in the Volta Basin since the early 1970s had a serious negative impact on hydropower generation at the Akosombo Hydropower Dam. According to Obahoundje et al. (2018), the operation of some hydropower dams in West Africa rely strongly on the hydro-climatic condition of the sub-regions. Hydro-climatic parameters have been varying in West Africa these last decades. Over the whole region, the increase of temperature varied from 0.2 to 0.8 °C since the end of 1970s, and maxima temperatures have increased about 1.5 °C from 1960 to 2010 (Ringard et al., 2014). In parallel, West Africa countries have experienced chronic below average annual rainfall since the 1970s, although a return to wetter conditions has been observed in the 1990s and 2000s (Lebel and Ali, 2009). Rainfall has decreased in some regions, while it increased in others (Ringard et al., 2014). These variations have an impact on river discharges and water levels of reservoirs. For instance, a variation of -2 to 5% in the annual rainfall leads to a change of -20 to 10% in river discharge in the Niger River basin (Stanzel et al. 2018). The decrease in rivers discharge had led to decreasing water levels in several reservoirs. West Africa reservoirs have been impacted by climate variability especially the 1970s and 1980s drought, and the situation is worsening with a rapid population growth and poor land management (Adeyeri, 2019). Lake Tchad for instance experienced a significant decrease in lake water area (6,000 km^2 in 1972, and 1,700 km^2 in 2001) (Vissin, 2007). In fact, the amount of power generated at a hydropower station is dependent on the inflow rate, the hydraulic head (related to water level), and the overall energy conversion efficiency of the generating plant (Kaunda et al., 2012).

In addition to climate, hydropower generation can be impacted by changes in land surfaces conditions (Obahoundje et al., 2018). Akpoti et al. (2016) stated that land cover practice in the

Volta River Basin could be favourable to the Bui dam hydropower generation. Land use practices as the construction of large dams could have an influence on surrounding climate and can lead to microclimatic changes (Obahoundje et al., 2018). Many studies showed that LULCC have a strong effect on potential evapotranspiration (Obahoundje et al., 2017), water holding capacity (Gil Mahe et al., 2005), and the catchment runoff generation (Amoussou et al., 2012; Faye et al., 2015; Lin et al., 2015). Any change in runoff generation affects the hydrodynamics of the river and consequently hydropower generation (Obahoundje et al., 2018).

1.1.2. Problem statement

Burkina Faso is a Sahelian country that faces a big challenge of electricity supply. Indeed, less than 14% of the population had access to electricity in 2010 (INSD, 2020). In 2011, the country had an installed electricity generating capacity of 311 MW. The electricity production is mainly based on thermic power plants (206 MW). Installed hydropower generation capacity is less than 36 MW (SE4ALL, 2016), including five hydropower dams: Bagré (18 MW), Kompienga (15.4 MW), Niofila (1.8 MW) Tourni (0.6 MW) and Samendeni (2 MW). The installed generation capacity is far less than the demand, leading to high of electricity imports from Cote d'Ivoire, Ghana and Togo. Besides, power shortages are estimated to occur 11 times per month (IFC, 2010)and the electricity price (96 to 165 CFA Franc per KWh) is among the highest in Africa (UPDEA, 2009). In 2011, of 1025 GWh/a supplied electricity, almost 50% was imported. The quantity produced by the National Electricity Company (SONABEL) was 530 GWh/a (448 GWh/a from thermic power plants and 82 GWh/a from hydropower plants). According to SE4ALL (2016), the national hydropower production decreased by 30% between 2008 and 2011 because of the decrease of water level in the hydropower dams, which depends on the annual rainfall (Kanazue et al., 2004).

Burkina Faso is characterised by high spatiotemporal rainfall variability, leading to a strong fluctuation of discharges, which has negative impacts on water resources availability (Karambiri, 2017). Ibrahim et al. (2014) analysed its rainy season characteristics (1961-2009) and noticed an increase of high frequency of low rainfall (between 0.1 mm/day and 5 mm/day) and some heavy maximum daily rainfall. They also projected an increase of length of the mean dry spell as well as a late cessation of the rainy season by 2050. (Thiombiano, 2011) analysed the climate variability on water resources in the Nakambé River Basin (NRB) between 1940 and 2008, and found that

rainfall decreased while temperature increased. These changes led to an increase of evaporation rate and a decrease of infiltration, runoff (Ibrahim, 2012) and dam's water levels.

In addition, the NRB has been experiencing accelerated degradation of its environment since the 1970s (Thiombiano, 2011). For instance, more than 400 reservoirs were built in the upstream basin. Most of these reservoirs are small in terms of storage capacity. However, considering the impact of the cascade reservoir schemes and their management, they can have a strong impact on river discharge. As climate change is reported to induce a reduction in crop yield by 24% in the country by 2080 (Cline, 2008), it could lead to more deforestation and migration of people towards wetter lands (around rivers and dams). These land use changes might have an impact on the operation of the Bagré dam, also affecting the operation of the Akossombo dam (Boadi and Owusu, 2017).

The Bagré dam, located in the NRB, is the largest and built as second hydropower dam of the country in 1992. Initially, the dam was expected to store water in order to firstly generate hydropower for the country, as well as to support irrigation, fishing, livestock, and tourism (Bidon, 1995; Zoungrana, 2007). However, it was noticed in 2013 that the Bagré dam faced a very strong decrease in its volume. The reservoir was filled to only 26% of its normal capacity[1]. This was the worst situation that dam has ever faced since its operation started. The decrease in volume in 2013 led to a temporary stop of operation of the Bagré dam by SONABEL. The power shortages experienced by Ouagadougou (Burkina Faso's capital) over the past decade are partly explained by the recorded low water levels in this reservoir, which should provide 20% of Ouagadougou's electricity supply (Bidon, 1995). Moreover, Yanogo (2012) identified irrigation water demand as an important cause of the annual decline in the Bagré's reservoir water level as the amount of water used for irrigation has increased from 2.15 hm^3 in 1997 to 142.4 hm^3 in 2008. This points to the importance of water management in the NRB. One of the strategies planned in the country to supply the electricity demand and future needs as well as reducing GHG emissions is based on building of new hydropower dams. The key question that arises from all these ascertainments is: what is the impact of climate, land use and water management changes on the hydropower generation of the Bagré dam?

[1] Agence Ecofin of 26th June 2013, https://www.agenceecofin.com/electricite/2606-11972-burkina-faso-les-barrages-de-bagre-et-de-kompienga-sont-en-berne

1.2. Literature review

1.2.1. Hydropower dams

Hydropower is a renewable energy source based on water flow and its drop from higher to lower levels that constitutes the energy potential (Thapar, 2008). Since the late 19th century, hydropower has developed as a clean, safe, and reliable source of power and energy service (Corà et al., 2020). In addition, it requires low maintenance and operating cost and the dams built are capable to provide hydroelectricity for a long period of time (Sawsan et al., 2019). Considering their purpose, hydropower dams can be classified into single purpose and multipurpose. The first aims to produce only electricity while the second is used to produce electricity, irrigation, domestic, and industrial water supply, fishery, flood control, etc. Regarding their generating capacity, hydropower plants are classified as (Sawsan et al., 2019):

(i) large >100 MW;
(ii) medium: 25 and 100 MW;
(iii) small: 1-25 MW;
(iv) mini: 100 KW-1 MW;
(v) micro: 5-100 KW and
(vi) pico <5 KW.

A study by the International Hydropower Association (IHA) shows that the world installed hydropower capacity was 1,360 Gigawatts (GW) in 2021, and the region of East Asia and Pacific remains the leader of hydropower production. China alone has a hydropower installed capacity of 390 GW. It is followed by Brazil (109 GW), the USA (102 GW), Canada (82 GW), Russia (55.7 GW), India (51.4 GW), Japan (49.6 GW), Norway (33.4 GW) and Turkey (31.5 GW) (IHA, 2021). In Africa, the installed hydropower capacity was 38 GW in 2021 (IHA, 2021). Eastern and Southern Africa are the leaders in hydropower generation in the continent as Ethiopia, Angola and South Africa are the top three with more than 3 GW of installed hydropower capacity for each country (IHA, 2021). In West Africa, Nigeria and Ghana are the top hydropower producers with an installed capacity of 2.1 and 1.6 GW, respectively. In Burkina Faso, the installed hydropower capacity is 34 MW (IHA, 2021).

The first hydropower dam of Burkina Faso was built in 1988 in Kompienga. Thereafter, many other hydropower schemes have been developed (Bagré, Niofila, Tourni, Samandeni) in the country. These hydropower dams have multipurpose functions and contribute to improve live conditions by providing electricity and water for irrigation to achieve food sufficiency, the first objective of the Ministry of agriculture. The main objective of the Bagré dam is to supply electricity to Ouagadougou. In addition, water is taken directly from the reservoir to supply irrigation water needs. Due to the competition between water use for hydropower and irrigation during the dry season, a priority is set to stop hydropower generation of the dam when the reservoir water level is at 226.7 m asl. In this situation, water withdrawals for irrigation are still permitted. Thus, considering the management implemented, the first objective of the dam is to produce more hydropower during the rainy season, when it is at maximum water level almost every year, while during the dry season, the priority is put on the irrigation. The "Bagré Pôle" is in charge of land development and irrigation aspects whereas the SONABEL is in charge of the hydropower generation.

Most of hydropower dams in Burkina Faso were built at the expense of natural vegetation, cropland and displacement of villages. Collier (2004) reported that hydropower dams have many advantages by providing clean and low-cost electricity, but large hydropower projects are reported to negatively impact the downstream environment. Therefore, the World Commission of Dams calls to build and operate hydropower schemes by considering climate change, environmental, and social factors.

1.2.2. Climate change and climate models

The United Nations defines climate change as a long-term shift in weather patterns. It is considered as one of the major threats faced by many regions across the world (Khalid et al., 2017). The Sixth Assessment Report of the Intergovernmental Panel on Climate Change (IPCC) published in 2021 highlighted an increase in global temperature of about +1.2 °C in 2020 compared to the period of 1850–1900, and temperature is expected to increase by 1.4–4.4 °C until 2100 under the lowest and highest Greenhouse Gases emissions scenarios (SSP1-1.9 and SSP5-8.5), respectively (IPCC, 2021). The rate of the increase depends on the location. In the Eastern Himalayas, for instance, the mean temperature increased by 0.02 °C per year while in Nepal the rate of increase was 0.04 °C per year from 1977 to 2000 (Khalid et al., 2017). The monsoon rainfall also experienced a decrease

from the 1950s to the 1980s but more extreme events since the 1950s (DSB, 2011; IPCC, 2021). For instance, some droughts in East and West Africa are attributed to the increase of sea surface temperatures (SSTs) in the Indian and the Atlantic Oceans (DSB, 2011). Whereas, Western Europe experienced in 2021 a huge flooding causing 179 deaths in Germany and 36 in Belgium (WMO, 2021). Many studies also project a severe decrease of future rainfall in West Africa (Karambiri et al., 2011; Kwawuvi et al., 2022). To assess the impact of climate change, climate models' outputs are required.

Climate models have been demonstrated to reproduce observed features of recent climate and past climate changes (Randall et al., 2007). This reproducing climate variables is more confident for temperature than rainfall, and at large and continental scales. However, many improvements have been made in climate models since the first Coupled Model Intercomparison Project (CMIP) in 1995. In fact, many studies reported that Global Climate Models (GCMs) outputs are not well adapted for climate impacts studies in West Africa because of the coarse resolution, the biases they contain, and the lack of data in the region (Karambiri et al., 2011; Sylla et al., 2013). Therefore, the use of Regional Climate Models (RCMs) outputs is suggested as they have a higher spatial resolution (Awotwi et al., 2015). Many studies used Coordinated Regional Climate Downscaling Experiment (CORDEX-Africa) RCMs to assess the impacts of climate change in the region (Diasso and Abiodun, 2017; Kwawuvi et al., 2022; Rummukainen, 2010; Sarr et al., 2015). CORDEX has a resolution of 0.44°x0.44°. However, the performance of GCMs and RCMs in representing observed climate and trends differs from one model to another (Knutti et al., 2013). The CIMP6 provides a prospect for more precise climate assessments (Ogega et al., 2021). The capability of CIMP6 GCMs to reproduce West African climate has been established, even though biases still exist when it comes to extreme events (Ajibola et al., 2020). GCMs and RCMs outputs are reported to contain biases that must be corrected before their use (Teutschbein and Seibert, 2012). Because the projection from one single model is not reliable, Sylla et al. (2015) recommend the use of multi models when studying climate change impacts in West Africa. The third phase of Inter-Sectoral Impact Model Intercomparison Project (ISIMIP) uses GCMs outputs from the CMIP6. ISIMIP3b delivers data of 10 bias corrected and statistical downscaling models developed by Lange (2019). Thanks to the downscaling method that is stochastic and the better adjusting spatial variability, ISIMIP3b is reliable in preserving trends. In other words, a bias adjustment method is applied at

the spatial resolution of the climate simulation data and a statistical downscaling method is applied to the bias adjusted climate simulation data for the purpose of increasing its spatial resolution to that of the climate observation data, W5E5 (Stefan Lange, 2019). The bias adjustment is based on a parametric quantile mapping, a robust method to adjust biases in all percentiles of a distribution and to preserve trends in these percentiles (Lange, 2019). More details on ISIMIP3b can be found in Lange (2019, 2021).

1.2.3. Land use and land cover changes

The dynamics of LULC are described as a process of change of the Earth's land cover at temporal and spatial scales (Hassen et al., 2021). This change is increasingly becoming a global concern because of its impacts on terrestrial and aquatic ecosystems (Sibanda and Ahmed, 2021). More than 75% of the Earth's land surface is already degraded and this share could reach 90% by 2050 (Cherlet et al. 2018). Between 1960 and 2019, almost one-third of the Earth's land surface has been changed (Winkler et al., 2021). These authors further emphasized a global net loss of forest area of 0.8 million km² but an expansion in global agriculture of 1.0 million km². However, these trends vary from one region to another. In Africa for instance, the natural vegetation of most places has been transformed to anthropogenic land uses (Barnieh et al., 2020; Bullock et al., 2021; Findell et al., 2017). Between 2012 and 2017, the continent's natural vegetation areas decreased significantly in favour of impervious areas (Nowak and Greenfield, 2020). This is due to population growth and the gradual drying up of soils due to climate change (UNEP, 2004). In West Africa, between 1975 and 2013, large areas of savannah, open forest and woodland were converted to cropland and urban areas (Barnieh et al., 2020; CILSS, 2016). Statistically, one third of the forest cover disappeared, while bare land areas increased by 47% over a period of 40 years (CILSS, 2016).

From 1975 to 2013, the Mono River Basin for instance, saw an increase of 350% in farmland and decreases of -46% and -33% in woodland and shrubland, respectively (Koubodana et al., 2019). Additionally, these authors projected that between 2013 and 2027, agricultural area could rise by 28% while woodland and shrubland areas could decrease by -10% and -21%, respectively. Many studies in the Volta Basin have also shown a change from natural vegetation to cropland and built-up areas. For example, Braimoh and Vlek (2004) estimated 5% as the annual rate of natural vegetation conversion to cropland from 1984 to 1999 on an area of 5,400 km^2 located between the White Volta and Oti River Basins. Within the White Volta Basin, built-up areas increased by 46%,

cropland increased by 49%, whereas forest and woodland decreased between 1990 and 2015 in the Nawuni sub-basin (Baatuuwie, 2015). In the Bankandi-Loffing sub-basin, a part of the Black Volta Basin in Burkina Faso, an annual conversion of 3.3% of savanna to cropland and settlement was observed between 2007 and 2013 (Idrissou et al., 2022; Yira et al., 2016). This rapid LULCC is a major setback to sustainable development (Akinyemi, 2021; Akpoti et al., 2016; Bessah et al., 2020; Dimobe et al., 2017; Nut et al., 2021). Thereafter, an assessment of LULCC could provide a better understanding of the interactions between natural vegetation and anthropogenic activities (Floreano and de Moraes, 2021; Gupta and Sharma, 2020).

Several studies in the Upper NRB have found an increase of bare land and cropland areas over the last decades (Karambiri et al., 2011; Mahe et al., 2005; R. Yonaba et al., 2021). However, only a few studies have attempted to assess the dynamics of past and future LULC over the entire basin, affecting the hydrological processes upstream of the largest reservoir, the Bagré dam, in Burkina Faso, with particular emphasis on its annual water storage. Moreover, most of these studies used the maximum likelihood classification method for LULC mapping. This method is based on the resemblance of neighbouring pixels. Despite its capability to provide acceptable results, the maximum likelihood classification method is parametric and assumes normal distribution of data (Shetty, 2019). Nevertheless, several non-parametric machine learning algorithms not relying on normal distribution of the sample data have been developed and are used in LULC assessment. These comprise mainly Random Forest (RF), Support Vector Machines (SVM), Classification and Regression Trees (CART), K-Nearest Neighbour (KNN), Learning Vector Quantization (LVQ), and Stochastic Gradient Boosting (SGB) (Dimobe et al., 2017; Forkuor et al., 2017; Gislason et al., 2006; Hackman et al., 2017; Nery et al., 2016; Shetty, 2019; Zoungrana et al., 2015). Among these non-parametric classifiers, a consensus seems to have been reached on the effectiveness of RF. s

Moreover, although various methods, such as the Cellular Automata-Markov Chain (CA-MC), Markov Chain Model (MCM), Stochastic Markov Chain (STMC), Multi-Layer Perceptron (MLP) Neural Network and Markov Chain Model, and Combined Markov-FLUS Model (Bozkaya et al., 2015; Dey et al., 2021; Girma et al., 2022; Sinha et al., 2020; Yang et al., 2022) have been developed to project future LULC, the most reliable technique is using the Multi-Layer Perceptron Neural Network and Markov Chain Model, which is a robust machine learning algorithm for these projections (Eastman et al., 2020; Hussien et al., 2022).

1.2.4. Water resources management

The concept of water resources management includes many activities related to water. Thus, Savenije and Hoekstra (2002) stated that these activities are basically: monitoring, modelling, exploration, assessment, design of measures and strategies, implementation of policy, operation and maintenance, and evaluation of water resources. They further emphasized that water resources management also covers institutional reform at local, national, and international scale for a period of time. Water resources are managed for water supply (industry, domestic, hydropower, irrigation), protection against floods and other objectives. To do so, dams are often built on the rivers to store water for agricultural and domestic supply or downstream flood alleviation. For example, on the Euphrates and Tigris Rivers in Turkey, 22 dams were built and 19 hydropower plants were installed to increase the domestic electricity production and develop a vast irrigation scheme for agriculture (Berkun, 2010). In China, the rapid hydropower development on the Mekong River led to changes in the flow's patterns (Piman et al., 2016). Yet, many dams are planned to be built upstream of the same river and could jeopardize the downstream flow regimes and the hydropower generation (Piman et al., 2016). For Koch et al. (2013), the reservoir operation or management option is very important because it plays a key role depending on the purpose of the dam.

In West Africa, several dams were built in order to better manage water at basin or transboundary basin level. The two biggest are the Akosombo Dam in Ghana, and the Kainji Dam in Nigeria. The Akosombo was built in 1965 on the Volta River. In the upstream basin, in Burkina Faso, more than 400 small reservoirs including the Bagré dam, a multipurpose dam, were built. The objective of these reservoirs is to supply water for hydropower, irrigation, industrial and drinking purpose. However, as these cascade reservoirs are constructed on the same river Nakambé, the management of one has an impact on the others. The population in the region is expected to increase in the future. This will lead to higher water demands from various users. One of the strategies to cope with these future needs is to build more reservoirs. The Nakambé Water Agency in charge of the water management in the basin could face to many problems if a reasonable scheme and water management plan is not considered. As stated by Loucks and Eelco (2016), a good water resources management plan is very important to sustain this resource for future generations, especially in the

Sahel region where water is very scarce. To support better management of water resources, hydrological models are set up and used in various regions.

1.2.5. Hydrological modelling

To assess the impact of climate, land use and water management changes on hydropower generation, it is necessary to assess first the impacts of these changes on dam inflow. To do so, there is a necessity to use a hydrological model. Hydrological models are tools that are used to estimate hydrological components of the water cycle (Dutta and Sarma, 2021). In West Africa, many authors have used several models for hydrological studies.

The first group has used lumped rainfall-runoff models or simple water balance methods. Lumped models are based on empirical methods by the use of mathematical equations and are exactly associated to the physical processes of the basin (Darbandsari and Coulibaly, 2020). A water balance model was used by Stanzel et al. (2018) to investigate the impacts of climate change on all West African river's basins. The Water Evaluation and Planning System (WEAP) model was used in the Volta River Basin to assess the performance of existing and planned irrigation and hydropower schemes under climate change scenario (McCartney et al., 2012). Kwakye and Bárdossy (2020) assessed the performance of the Hydrologiska Byrans Vattenbalansavdelning (HBV) model for hydrological modelling in the Black Volta Basin, and found that the model is suitable for supporting management of the water resources and hydropower generation in the basin. Afterwards, Yira et al. (2021) also assessed the impact of climate change on discharge and hydropower in the Bamboi catchment, part of the Black Volta Basin, using the HBV light model. The model was able to simulate discharge in the basin with a Nash-Sutcliffe Efficiency (NSE) varying from 0.59 to 0.66. Using the GR2M model, Karambiri et al. (2011) were able to evaluate the impacts of climate change on runoff in the NRB. The GR2M calibration and validation showed good performance of NSE (> 0.7). Furthermore, Gbohoui et al. (2021) used the Budyko type models, based on the water balance, to quantify the contributions of climate and environment to historical change of runoff in the NRB.

The second group of authors used distributed models. These models are not widely used in the region because they require a lot of fine scale data that are often not available in Africa. Nevertheless, authors such as Dembélé et al. (2022) used the fully distributed mesoscale

Hydrologic Model (mHM), capable to simulate dominant hydrological processes with seamless spatiotemporal patterns in the modelling domain (Kumar et al., 2013), in the Volta River Basin. Using satellite products as climate inputs, the model showed its ability and reliability in reproducing the spatiotemporal patterns of the basin hydrological processes. Moreover, Andersen et al. (2001) successfully validated the distributed MIKE SHE model in the Senegal River Basin. Furthermore, a study by Komi et al. (2017) used LISFLOOD model in the Oti River basin, part of the Volta River Basin, for flood hazard modelling processes. The performance of the model was very good with NSE > 0.87.

The third group of authors used semi-distributed models. Semi-distributed models are conceptual models that consider land sue and soil as model inputs. Yira et al. (2017) and Hounkpè et al. (2019) successfully used the Water flow and balance Simulation Model (WaSiM) to simulate water balance components and flood characteristics in the Dano and Zou catchments, respectively. The Variable Infiltration Capacity (VIC) model, a semi-distributed model that solves the energy and water balances at the grid-scale (Liang et al., 1994), was used in the Volta basin to investigate the impact of climate variability on hydrological droughts (Gebrechorkos et al., 2022). In Burkina Faso and Cote d'Ivoire, the CEQUEAU model was used to assess the hydrological behavior of the Nakambé, Agneby, and Boubo River basins (Desconnets et al., 1998; Goula et al., 2009; Kouadio et al., 2015). Giertz et al. (2006) used the semi-distributed model UHP-HRU to assess soil water availability and consumption in the Oueme River basin within Benin. The widely used Soil and Water Assessment Tool (SWAT) was effectively used by Larbi (2019), Hounkpè et al. (2019), Okafor (2019) and Yonaba et al. (2021) to assess the impacts of climate and LULC change on water resources in Ghana, Benin and Burkina Faso, respectively. These studies showed the ability of SWAT to simulate the observed runoff with satisfactory NSE and KGE coefficients according to Moriasi et al. (2007). The Soil and Water Integrated Management (SWIM) model, derived from SWAT and MATSALU (a model developed in Estonia for the agricultural basin of the Matsalu Bay to evaluate several management scenarios for eutrophication control), was also used in the region (Krysanova et al., 2015).

SWIM is a spatially semi-distributed model, integrating hydrology, vegetation, erosion, and nutrient dynamics at the river basin scale (Krysanova et al., 2000; Krysanova et al., 2015). The model has been already applied in Germany, Brazil, China, and Africa (Obangui, Niger and Volta

River basins) (Aich et al., 2014; Krysanova et al., 2015; Liersch et al., 2023). It was used in the Elbe River basin to find strategies to reduce nutrient concentrations and improve the environmental status (Krysanova et al., 2015). In the Niger River basin, the model was successfully used to assess the impact of climate change and water management including the water allocation and inundation (Liersch et al., 2012) and the reservoir (Koch et al., 2013) modules. Furthermore, Liersch et al. (2023) successfully used the SWIM model in the Volta River basin, where the Nakambé River basin is located. Overall, more than 67% of the studies that applied the SWIM model in hydrology obtained a satisfactory of NSE > 0.7 for both calibration and validation periods (Krysanova et al., 2015). However, it was also reported that SWIM performs lowly when anthropogenic water management in watersheds are not supported by data (Krysanova et al., 2015). In the NRB, where more than 400 small dams were built upstream of the Bagré dam, data on water management for the 9 biggest dams were available to be used in the SWIM model.

1.2.6. Impacts of climate, land use and water management changes on hydropower generation

Climate change is affecting water resources, resulting in changing frequencies and intensities of droughts and floods. In both cases, it can affect the economy and human lives. This situation jeopardizes the efforts of countries in the achievement of the Sustainable Development Goals (SDG) 6 and 7 on ensuring "availability and sustainable management of water and sanitation" and "access to affordable, reliable, sustainable and modern energy" for all. In terms of sustainable and affordable energy, hydropower generation is among the recommended solutions. However, many studies showed that climate change will affect the performance of hydropower dams. In China for instance, the national hydropower generation may at first decrease in the 2030s and then may increase in the 2070s due to climate change (Sun et al., 2022). A study by Tamm et al. (2016) showed an overall increase of hydropower generation is expected in far future in Estonia. They further argue that the increasing rate depends mainly on the climate models used. In Iran, a decrease in rainfall by 2070 will reduce the Seimareh's hydropower plant performance with dam inflows and electricity production declining by 5.2 to 13.4% and 8.4 to 16.3%, respectively (Goodarzi et al., 2020). Seven hydropower dams' vulnerability to climate change were investigated in India by Ali et al. (2018). The authors found that the projected increase of rainfall by 18 ± 14.6% under Representative Concentration Pathway (RCP) 8.5 will lead to an increase of mean annual inflow

and hydropower generation by 45% and 25%, correspondingly. However, it was reported that the monthly hydropower generation will decline from May to June for the snow-dominated Nathpa Jhakri and Bhakra Nangal hydropower projects.

In Africa, several studies attempted to assess the impact of climate change on the existing hydropower dams (Liersch et al., 2017; Nonki et al., 2021; Obahoundje et al., 2017, 2021b, 2022; Oyerinde et al., 2016). Nonki et al. (2021), using the HBV-light model, found that hydropower generation could decline at the Lagdo dam in Cameroon by 2095. A study conducted by Liersch et al. (2017) on the on building Grand Ethiopian Renaissance Dam showed that the baseline hydropower generation of 13 TWh/a could slightly increase in the future due to climate change. In West Africa, climate change is reported to negatively affect the hydropower potential of the Nangbeto dam in the Mono River Basin (Obahoundje et al., 2021a; 2021b). In the Volta River Basin, climate change could reduce the average annual hydropower generation by about 30% in the far future (McCartney et al., 2012). In the Black Volta, part of the Volta, the hydropower generation of the Bui dam may decline in 2040 under climate change scenario (Obahoundje et al., 2017). Apart from climate change, LULCC and water abstraction will also affect hydropower generation (Obahoundje and Diedhiou, 2022).

According to Wei et al. (2013) and Descroix et al. (2018), LULCC has a significant impact on runoff. Its impacts on hydropower generation have been reported by several studies (Kouame et al., 2019; Leta et al., 2022). Bahati et al. (2021) assessed the impacts of climate change and LULCC on the Muzizi hydropower potential in Uganda. Using REMO and RCA4 climate models, they found that hydropower will increase by 124% and 76% under both RCPs 4.5 and 8.5, respectively in the 2050s. In West Africa, many studies assessed the effects of LULCC on runoff (Hounkpe et al., 2019; Larbi, 2019; Obahoundje and Diedhiou, 2022), but few attempted to relate it to hydropower generation. In the Black Volta, a study by Obahoundje et al. (2017) showed that the combined effects of climate and LULCC will affect the future generation at the hydropower plant of the Bui dam. The authors found that an increase in cropland area would lead to increasing runoff and hydropower generation. When reviewing the existing studies of climate and land use changes impacts in West Africa, Obahoundje and Diedhiou (2022) concluded that land-use changes on hydropower generation have received little attention from policy makers and dam managers in West Africa. Therefore, it is crucial to include LULCC impacts in hydropower generation

assessment, as it helps to draw accurate planning and adaptation strategies for sustainable development (Lienou, 2013).

On the other hand, water management is affecting discharge and hydropower potentials (Annys et al., 2020; Koch et al., 2020; Liersch et al., 2013; Lobanova et al., 2016; McCartney et al., 2012; Meema et al., 2021). In Ethiopia, the management of the Tekeze hydropower dam led to a decline in high flows and increase in low flows downstream (Annys et al., 2020). McCartney et al. (2012) showed that the reduction in technical performance of reservoirs will be greater under climate and water abstraction changes scenario in the Volta basin. Liersch et al. (2013), investigating the impact of water management and climate change in the Inner Niger Delta, found that climate change and upstream reservoir management could substantially decrease peak discharges during the rainy season. Another study of Amisigo et al. (2014) estimated the mean annual hydropower coverage between 75% and 95% (depending on the management scenario) for the Bagré dam by 2050. In the NRB, Desconnets et al. (1998) attempted to demonstrate the impact of 15 upstream reservoirs on runoff at Wayen station, using the CEQUEAU-ONU model. They found that reservoirs' management reduced the discharge, where the effects of reservoirs is particularly significant for the first months of the rainy season (June and July). Many other dams were constructed in the 2000s in the NRB with large capacity storages (example of 200 Mm^3 for Ziga) to supply irrigation demand and domestic water supply. However, in the context of climate change and population growth, there is a need to investigate how current and future withdrawals from upstream reservoirs will affect Bagré dam inflow. In addition, the Bagré reservoir is also used to supply irrigation. Less than half of the potential agricultural area of 30,000 hectares has been developed for irrigation (Zoungrana, 2007). The development of the remaining area would also impact the hydropower generation by the Bagré reservoir.

Table **1** provides a summary of all the papers used in the literature review, according to the type of research carried out in West Africa.

Table 1. Summary of the literature review on climate change, LULC, and water management changes on discharge and hydropower in West Africa

Basin / Catchment /	Period of study	Hydrological Model used	CC - LULC - Water Management impacts / model ability	Discharge / Hydropower	Authors
Niger River	1970 - 2001		Water management	Discharge & Hydropower	Koch et al. (2013)
Niger River	1960 - 2100	SWIM	LULC & CC	Discharge	Aich et al. (2014)
Volta River	1960-2100		CC & Water management	Discharge & Hydropower	Liersch et al. (2023)
West Africa River	2026 - 2065	Water Balance Model	CC	Discharge	Stanzel et al. (2018)
Volta River	2021 - 2100	SWAT & WEAP	CC & Water Management		McCartney et al. (2012)
Mono	1970 - 2090	WEAP	CC & LULC	Discharge & Hydropower	Obahoundje et al. (2021b)
Black Volta	2000 - 2040	WEAP	CC & LULC		Obahoundje et al. (2017)
Black Volta	1961 – 2005	HBV	Model ability	Discharge	Kwakye and Bárdossy (2020)
Bamboi	1983 - 2099	HBV light	CC	Discharge & Hydropower	Yira et al. (2021)
Nakambe & Senegal River	1970 - 2050	GR2M	CC	Discharge	Karambiri et al. (2011)

Nakambe River at Wayen	1965-1994	Budyko model	CC & Environment	Discharge	Gbohoui et al. (2021)
Volta River	1991 - 2100	Hydrologic Model (mHM)	CC	Discharge	Dembélé et al. (2022)
Senegal River	1986 - 1996	MIKE SHE	Model ability	Discharge	Andersen et al. (2001)
Oti River	2001-2007	LISFLOOD	Model ability	Discharge	Komi et al. (2017)
Dano	1971 - 2050	WaSiM	CC	Discharge	Yira et al. (2017);
Zou	1991 - 2010	SWAT & WaSiM	LULC	Discharge	Hounkpè et al. (2019)
Niger River	1961-2100	IHACRES	CC	Discharge & Hydropower	Oyerinde et al. (2016)
Nakambé	1985 – 1996		Water management		Desconnets et al. (1998)
Agneby	1983 - 2001	CEQUEAU	LULC	Discharge	Goula et al. (2009)
Boubo	1983 - 2001		LULC		Kouadio et al. (2015)
Vea					Larbi (2019)
Dano	1971 - 2050	SWAT	CC & LULC	Discharge	Okafor (2019)
Nakambé					Yonaba et al. (2021)

1.3. Research questions

The main research questions of this study are listed below.

- How did past hydro-climatic variability and upstream water management impact hydropower generation at the Bagré dam?
- What are the dynamics of past and future land use/land cover change in the NRB?
- How will future climate and land use changes impact the hydropower generation at the Bagré dam?
- What is the impact of future water management on hydropower generation at the Bagré dam?

1.4. Thesis objectives

The main objective of this study is to evaluate the potential of hydropower generation at the Bagré dam in the context of climate, land use, and water management changes. The specific objectives are:

- to analyse the impacts of hydro-climatic variability and upstream water management on the hydropower generation at the Bagré dam;
- to determine the dynamics of past and future land use/land cover in the NRB;
- to assess the impacts of climate and land use/land cover changes on the hydropower potential at the Bagré dam;
- to assess the impact of water management changes on the hydropower potential at the Bagré dam.

1.5. Hypothesis

Following these research questions, four assumptions were formulated:

- hydropower generation at the Bagré dam is in positive correlation with the trend of rainfall, inflow, water level, and upstream water management;
- the dynamics of LULC in the NRB are marked by the expansion of anthropogenic land use;
- future climate and LULC changes will increase the hydropower generation at the Bagré dam;

- water management changes will negatively impact the seasonal hydropower generation at the Bagré dam.

1.6. Novelty

The impacts of climate and land use changes on hydropower generation were analysed in several studies at global scale. While most of these studies used CORDEX RCMs, this study used GCMs from ISIMIP3b to assess the impact of climate change on hydropower under the new updated Representative Concentration Pathway called Shared Socioeconomic Pathways (SSP). In addition, this study considered the impact of water management changes on hydropower generation. The impacts are assessed in two ways. First the upstream water management effects on the Bagré's inflow are examined, second the change of Bagré dam operation on its hydropower generation is analysed. All this was done using two scenarios (afforestation and Business as Usual - BAU) of LULC, that can support policy making for better management of water resources in the basin. The results of this study were also used for further investigations in the CIREG (Climate information for Integrated Renewable Electricity Generation; https://cireg.pik-potsdam.de/homepage-en/) project by providing insight of LULCC on the hydropower potential of the Bagré dam.

1.7. Scope of the thesis

The impacts of climate, land use, and water management changes on hydropower generation is the main focus of this study. Future climate projections impact on hydropower generation were assessed using individual climate models and the ensemble median. The study also takes into account the contribution of each factor (climate, land use and water management impact) in the changes in inflow and hydropower generation at the Bagré dam. However, return flows from water withdrawals for irrigation are not taken into account in the model.

1.8. Expected results and benefits

The findings from this study will provide (i) an understanding of hydro-climatic variability and upstream water management impacts on hydropower generation, (ii) an insight into the dynamics of past and future LULC in the NRB, (iii) detailed information on the impact of climate change on future rainfall and temperature using 10 ISIMIP3b models over the basin as well as the individual and combined effects of climate and land use changes on hydropower potential, and (iv) knowledge

about the impacts of water management change on hydropower generation at the Bagré dam. The results of this study provide a decision-support tool for policy-makers. For instance, the results obtained from this study can be useful for the SONABEL to adapt the operation of the dam to future climate and land use conditions. Additionally, the NRB Agency and the Volta Basin Authority can get an instrument for estimating scenario impacts on water availability in the White Volta Basin. The results of this study can help to design adaptation strategies regarding the development of irrigated land in the basin.

1.9. Outline of the thesis

Eight chapters compose the current thesis. Chapter 1 deals with the general introduction. In this chapter, the context of study, the problem statement and the objectives are presented. Afterwards, the study area is presented in chapter 2 with an emphasis on the description of physical, demographic, and socio-economic environment of the NRB. Chapter 3 describes the methodology used to achieve the results of the study. In this chapter, data, materials, and methods used are detailed step by step following the specific objectives. The phases of set-up, calibration and validation of the SWIM model are also described. Chapters 4 to 7 present the results of the study. While chapter 4 analyses the hydro-climatic trends and effects of upstream water management on hydropower generation, chapter 5 inspects the dynamic of past and future LULC in the NRB. In chapters 6 and 7, the impacts of climate and land use changes, as well as water management change are presented and discussed, respectively. Finally, conclusions and perspectives are provided in chapter 8.

CHAPTER 2: STUDY AREA

This chapter describes the physical and biophysical environment of the study area. First, the area of interest is located and the landscape is presented. Afterwards, its characteristics of vegetation, climate, hydrography, soil and land use are described. Finally, the demography and the socio-economic aspects are described.

2.1. Localization

The NRB is located in the Upper White Volta Basin in Burkina Faso. The basin is laying between longitudes 2° 1’ and 0° 3' West and latitudes 11° 11’ and 14° 1' North (Figure **1**). Its area is about 32,623 km^2 at Niaogho station. The Bagré dam was built in 1992 in the region of the basin. It has a water storage capacity of 1.7 billion m^3, a water surface of 255 km^2, a length of 80 km and a width of 3 to 4 km (Zoungrana, 2007). It is a multi-purpose dam with the main purpose to generate hydropower of 44 million kWh per year to supply 20% of the national power need (Kabore and Bazin, 2014). The installed hydropower plant (HPP) has a capacity of 16 MW (two units which operate simultaneously and produce 8 MW each during peak periods). The dam is also used for fishery and supplying irrigation water for over 30,000 ha, of which around 6,000 ha are used for rice cultivation (Zoungrana, 2007).

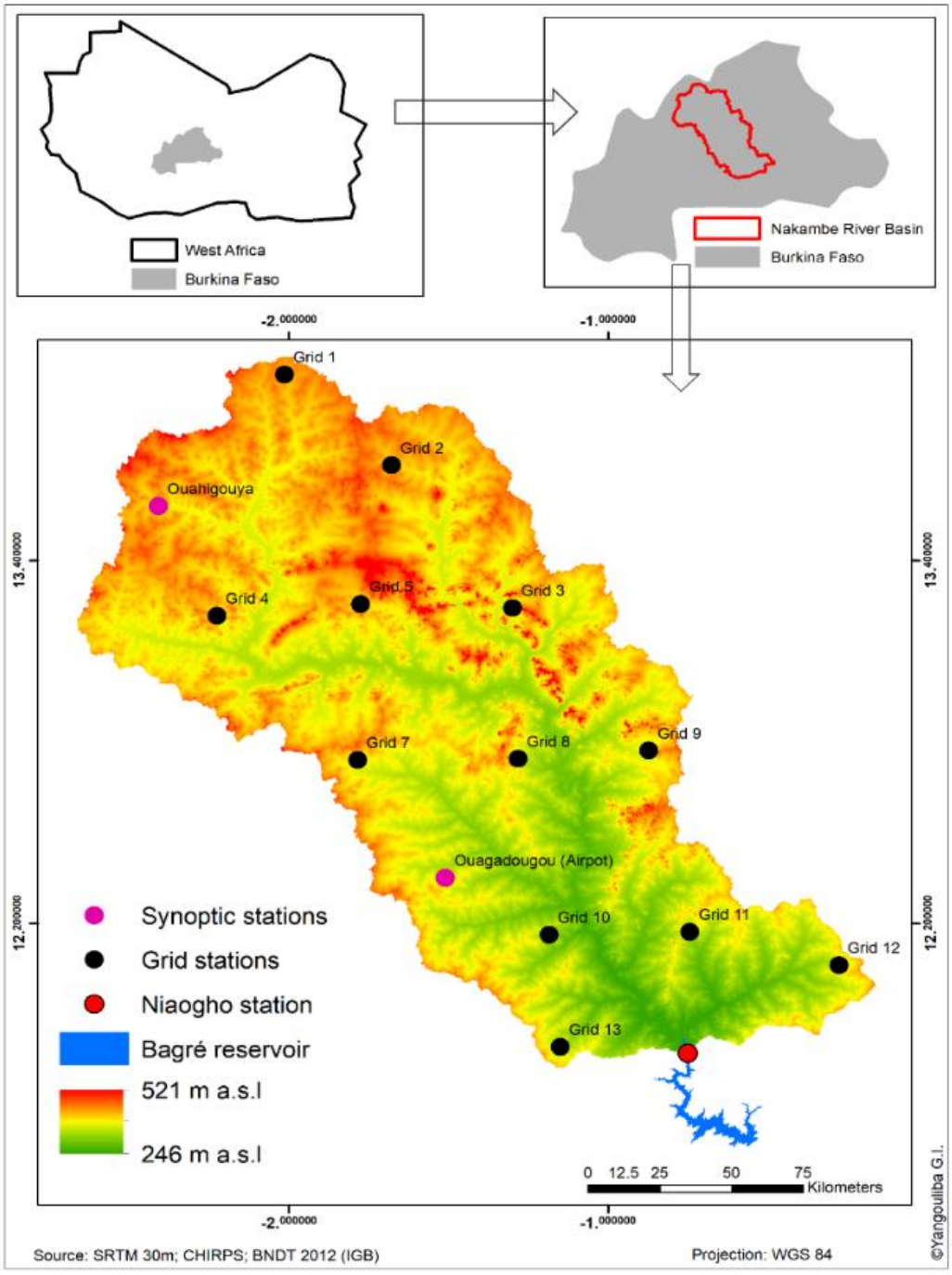

Figure 1. Location of the NRB, Bagré dam, climate and hydrological stations

2.2. Relief

The landscape of the NRB is characterised by a soft landscape, with small rocky outcrops in some areas. The highest and the lowest altitude being 521 and 246 m a.s.l., with a moderate slope ranging

between 0 and 84 degrees. There are also small hills, granite stone chaotic balls and barely marked ridges. The above-mentioned slope formations occupy a vast surface, which is lightly undulated and scattered by occasional deep ravines towards the headwaters of the tributaries (AEN, 2015). At mid-slope, these constitute valleys, whereas at the downstream end, there are larger flat areas. One of the main collectors of water from these incisions is the River Nakambé. The entire flow of the Nakambé and the part of the river that runs downhill from certain small lakes are bordered by alluvial deposits interspersed with depressions and valleys (AEN, 2015).

2.3. Vegetation

The NRB is essentially spread over the South Sahelian and North-Sudanese phytogeographical territories, and a little in the South Sudanese (DGRE, 2010). The vegetation is dominated by savannah and is continuous in the southern part and discontinuous in the northern part (Deme, 2001). In the northern NRB, the vegetation cover is in an advanced state of degradation and occupied by stunted, thorny shrubs and a few occasional tall trees of *Acacia albida, Acacia seyal, Bombax costatum and Adansonia digitata* (Deme, 2001; Diello et al., 2005). The southern part is covered by shrublands and woodlands dominated by tall species of *Parkia biglobosa, Khaya senegalensis et Vitellaria paradoxa*. Along the rivers are encountered riparian formations notably gallery forests composed mainly of *Mitragyna inermis, Kaya senegalenssis, Mimosa pigra* while the terrestrial herbaceous is dominated by grasses, including *Andropogon pseudapricus, Andropogon gayanus* and *Cympopogon shoenanthus* (DGRE, 2010). The degradation of the vegetation cover contributes to the silting up of the water bodies through the increase of soil erosion.

2.4. Climate

Two climatic zones divide the NRB, namely the Sahelian and the North-Sudanese zones. According to DGRE (2010), the Sahelian zone (northern and southern Sahelian) covers the Upper Nakambé sub-basin and is located above the 13°N latitude and has an average annual rainfall of between 300 and 600 mm, a short rainy season length (June-July to September-October), a high variability in the distribution of rainfall, high potential evaporation of 4,800 mm per year and large diurnal and annual thermal amplitudes (AEN, 2015; Deme, 2001; DGRE, 2010). The average daily

maximum temperature is 43°C in April, while the minimum temperature is 14°C in January (Diello et al., 2005).

Besides, the North-Sudanese zone covers the whole sub-basins of the mid and lower Nakambé. It lays between latitudes 11° and 13°N and is characterized by a rainy season length of about 4 to 5 months (May-September), an average annual rainfall ranging between 600 and 900 mm (AEN, 2015; Deme, 2001; DGRE, 2010). In this climatic zone, the mean daily maximum and minimum temperatures are above 30°C and below 15°C, leading to an annual potential evaporation of 2,600 mm (Diello et al., 2005)).

2.5. Hydrography

The Nakambé is the main stream in the study area. It flows from the north (Sahelian zone) at an altitude of 335 m a.s.l. near Ouahigouya (Deme, 2001). It receives on its west branch small tributaries from Tikaré region and outflow from water bodies in Kongoussi and Kaya regions. Afterwards, it feeds the Ziga reservoir and collects on its right branch the Massili, which feeds the Loumbila and Ouagadougou dams and flows through the Gonsé station (AEN, 2015). Between Yilou and Wayen, the slope of the Nakanbé River is moderately low (0.01%) (DGRE, 2010). The river then flows to the Bagre dam after receiving water from tributaries such as Bomboré, Dougoula Mondi and Tcherbo. Furthermore, it flows to Ghana and takes the name of White Volta River. According to Deme (2001), the river network is degraded although it is well densified. Moreover, the flow of the Nakambé river is intermittent and slowed down either by man-made or natural reservoirs which retain a large part of the runoff, or by channels whose slopes are very shallow and do not allow the runoff to drain away (Deme, 2001).

2.6. Soil and land use

2.6.1. Soils

Soil distribution and characteristics have an important impact on the hydrological cycle. An assessment at 1:500,000 scale by the national soil office (BUNASOLS) reported seven types of soil described by the DGRE (2010) as following:

- Lithosols: this type of soil comprises all the rocky and armoured surfaces. Lithosols in the NRB are very shallow (<10 cm), slender, and skeletal. The organic matter content is

extremely low and the water holding capacity is almost nil except in the fractured zones where it allows rainwater to penetrate.

- The poorly evolved alluvial soils contain only the poorly developed soils with hydromorphic alluvial deposits. They are very rich and deep soils (>120 cm) with weak internal drainage created by the presence of alluvial deposits. The surface texture is silty-sandy while the deeper layers are clayey-silty (DGRE, 2010).
- Tropical eutrophic brown soils: this type of soil includes ferruginous tropical eutrophic brown soils, hydromorphic tropical eutrophic brown soils and hydromorphic tropical eutrophic brown soils. These are deep soils (>120 cm). At the subsurface the texture is silty-clay whereas it is clayey in the depth. The tropical eutrophic brown soils have a high mineral potential and a good water holding capacity due to the high proportion of swelling clay of the montmorillonitic type (DGRE, 2010).
- Tropical ferruginous leached soils: this group covers the southern half of the basin. They are divided into three subgroups composed of concretionary leached tropical ferruginous soils, speckled and concretionary leached tropical ferruginous soils and indurated leached tropical ferruginous soils. The two first cited are deep soils (>120cm) with a silty-sandy texture at the surface and silty-clay to clay at depth. Their water holding capacities are moderate and their nitrogen, phosphorus and potassium contents are very low. These soils are highly sensitive to erosion. The last subgroup is characterised by the presence of carapace at varying depths (20 to more than 60 cm) with a very low water holding capacity (DGRE, 2010).
- The hydromorphic soils with low humus and pseudogley are found in the lowlands and alluvial plains. These are deep soils with silty-sandy texture on subsurface and clayey at depth. The drainage on this group of soil is poor although the water holding capacity is good (DGRE, 2010).
- The vertisols: This group of soils is localised in the southern NRB. They have a good chemical fertility (DGRE, 2010).
- The last group is the sodic soils. These soils are not suitable for agriculture (DGRE, 2010).

However, details information on the physical and chemical characteristics of these groups of soils are missing.

2.6.2. Land use

The land use in the basin is mainly cropland (rainfed and irrigated agricultural areas) and bare land/built-up areas (Figure 2-A). The natural vegetation is dominated by savannah which includes shrubland and a small proportion of woodland mainly located in 9 protected areas of around 1,301 Km^2 (Table 2). Most of these protected areas are under pressure of anthropogenic activities and exist simply by virtue of their name. The basin has several water bodies. According to (DGRE, 2010), more than 400 dams comprising big and small reservoirs were built in the basin for domestic, irrigation, livestock and hydropower purposes. The spatial distribution and the storage capacity (in m3) of the reservoirs are shown in Figure 2-B.

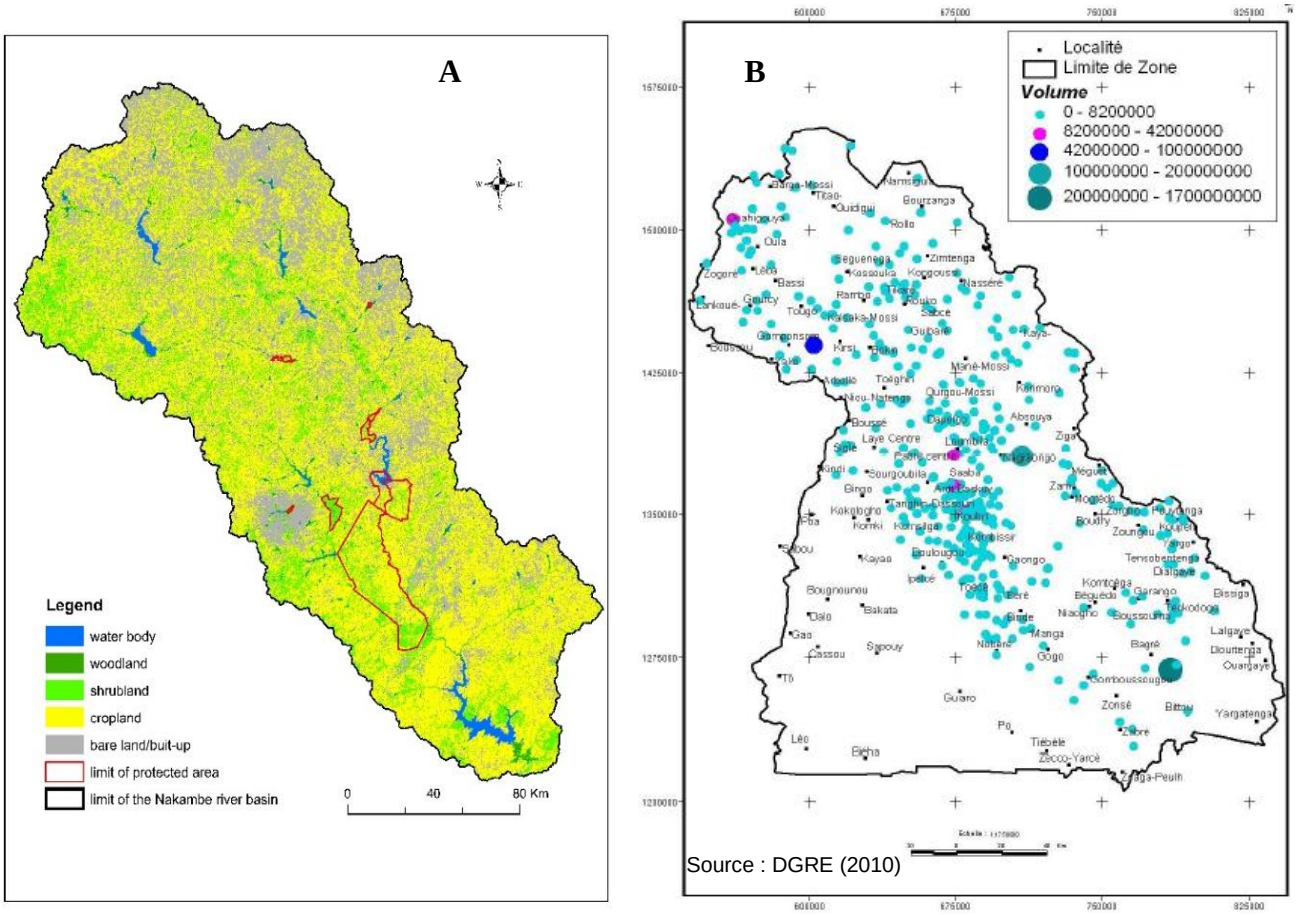

Figure 2. Land use land cover of 2020 (A) and spatial distribution of reservoirs (B) in the NRB

Table 2. Protected areas within the NRB

Name	Area (km^2)	Municipality covered
Protected area of Bissiga	32.1	Zitenga
Protected area of Gonse	62.8	Saaba
Protected area of Dem	2.75	Kaya
Protected area of Nakambé	1,055.1	Nagreongo, Koubri, Bere, Kombissiri, Gaongo, Binde
Protected area of Ouilengore	24.8	Zabre
Protected area of Wayen	173.3	Zam
Protected area of Ziga	94.1	Nagreongo
Protected area of Nakabe	8.8	Korsimoro
Bangre Weogo Urban Parc	3.5	Ouagadougou
Total	1,301.4	

Source: AEN (2015)

2.7. Demography, environmental, social and economic activities

The population survey carried out by the National Institute of Statistics and Demography (INSD) estimated the total population of the NRB to around 6,200,000 inhabitants in 2006. The gender is dominated by women who represent more than 52% of the population (DGRE, 2010). The annual population increase rate was 3.24% which is greater than the national rate (3.1%). High densities (more 200 inhabitants per km^2) are encountered in the large cities such as Ouagadougou, Ouahigouya, Koupela and Tenkodogo while low densities of population are found in the northern basin in the Titao region (less than 50 inhabitants per km^2). The main ethnic group are Mossi and Fulani. These people are recognized are farmers and breeders, respectively.

The main economic activity is agriculture (85%). Of these farmers, 90% are men who are household's chiefs. Rainfed agriculture is used for cereals and food crops including sorghum, maize and millet. Rice is cultivated either rainfed or irrigated. In addition to the food crops, cash crops (groundnut, cowpeas and voandzou) are grown in small quantities (DGRE, 2010).

2.8. Partial Conclusion

The NRB is characterised by a soft landscape with savannah-dominated vegetation. The average annual rainfall is about 600 mm and is collected by the Nakambé River which flows towards Ghana. As the rainy season is short and unimodal, several dams have been built to collect as much water as possible for domestic water supply, irrigation, livestock and hydropower generation. The

continuous increase in the population whose main occupation is agriculture leads to a perpetual change of LULC in the basin. Although nine protected areas exist in the NRB, they are under human activities pressure and in a state of degradation. These permanent changes coupled with climate change may have some impacts on the hydrological response of the basin and the hydropower generation at the Bagré dam.

CHAPTER 3: DATA, MATERIALS AND METHODS

The NRB is a data scarce area characterized by a low distribution of climate and hydrological stations. Data on withdrawals from dams are often not available, leading sometimes to the use of secondary data. This chapter presents all data used in this study. Furthermore, the technical materials used to collect the data as well as the methods applied to obtain the results are described.

3.1. Data

Datasets used in this study included climate, hydrological, soil, topography and land use land cover data. This section presents each data type and its temporal and spatial scale.

3.1.1. Station and Gridded Climate Data

The climatic data used comprise rainfall, minimum, maximum and mean temperature, solar radiation, and relative humidity (Table 3). They are composed of observational and satellite data, and were collected from two sources. On the one hand, observed data were obtained from the National Meteorological Agency (ANAM) from 1985 to 2015. On the other hand, data for 13 gridded cells (Figure 1) were obtained from the bias adjusted ERA5 reanalysis data (W5E5) at https://data.isimip.org/10.5880/PIK.2019.023 and were used to complement the limited spatial distribution of the observed climate stations. W5E5 is a merged dataset whose version 2.0 combines WFDE5 data over land with ERA5 data over the ocean and covers the entire globe at 0.5° horizontal and daily temporal resolution from 1979 to 2019 (Hersbach et al., 2020; Lange et al., 2021). The quality of the climate data was checked. It comprised the identification of missing data in satellite and climate stations time series and their comparison in the period 1985–2015. No missing data were found in the time series of the two stations. As suggested by Okafor et al. (2017), visual inspection has been also used to detect outliers and to ensure internal consistency.

Besides the aforementioned climate data, the Oceanic Niño Index (ONI) was used for this study. The ONI was taken from Golden Gate Weather Services (GGWS) at https://ggweather.com/enso/oni.htm. It presents the running 3-month mean SST anomaly for the Niño 3.4 region (5 °N–5 °S, 120°–170 °W).

Table 3. Observed and Reanalysis climate data used in the study

Data type	Resolution	Temporal	Spatial	Source
Rainfall (mm)	daily	1985-2015	Ouagadougou & Ouahigouya	ANAM
		1979-2019	NRB	W5E5
Min & Max Temperature (^oC)	daily	1985-2015	Ouagadougou & Ouahigouya	ANAM
		1979-2019	NRB	W5E5
Solar radiation (J/cm^2)	daily	1985-2015	Ouagadougou & Ouahigouya	ANAM
		1979-2019	NRB	W5E5
Relative humidity (mm)	daily	1985-2015	Ouagadougou & Ouahigouya	ANAM
		1979-2019	NRB	W5E5

3.1.2. Hydrological data

Regarding hydrological data, observed monthly inflow, outflow, irrigation withdrawals, turbined flow, evaporation, water level, and hydropower generation at Bagré dam were first collected from SONABEL for 1993 to 2018. In addition, observed daily discharge at Niaogho (1964-1997) and Wayen (1990-2014) stations and daily volume from nine reservoirs (Bagré, Ziga, Loumbila, Dourou, Goinre, Seguenega, Tougou, Bam, Dem) were collected from the National hydrological service (DGRE) for 1999 to 2019. Daily discharge at Niaogho station contains many missing data (>20% for all years in rainy season), making its use difficult.

3.1.3. Landsat images and reference data

The dataset used is composed of Landsat 5 Thematic Mapper-TM images of the years 1990 and 2005, and Landsat 8 Operational Land Imager-OLI images of the year 2020. Landsat images have a spatial resolution of 30 meters and can be used to detect LULCC (Midekisa et al., 2017). For 1990 and 2020, Landsat 5 TM and Landsat 8 OLI surface reflectance image collections respectively from January 01 to December 31 were extracted from Google Earth Engine (GEE) Data Catalogue and used as inputs for the LULC analysis. To avoid having missing data due to the line scan corrector problem of Landsat 7, Landsat 5 TM was preferred for the year 2005. However, to obtain a cloud free image composite for the year 2005, the Landsat 5 TM surface reflectance images from 2003 to 2007 were used. This 2-year temporal window around 2005 was due to the low availability of Landsat 5 TM images covering the whole basin for the single year. Table 4 summarizes the scenes and bands of Landsat 5 TM and Landsat 8 OLI images used.

Table 4. Characteristics of Landsat satellite images used

Landsat images	Scenes	Selected bands	Spatial resolution	Temporal range
Landsat 5 (TM) Surface Reflectance	193052-53/194050-53/195050-53/196050-53	1,2,3,4,5,7	30m	01-01-1990 to 31-12-1990
Landsat 5 (TM) Surface Reflectance	193052-53/194050-53/195050-53/196050-53	1,2,3,4,5,7	30m	01-01-2003 to 31-12-2007
Landsat 8 (OLI) Surface Reflectance	193052-53/194050-53/195050-53/196050-53	2,3,4,5,6,7	30m	01-01-2020 to 31-12-2020

Five LULC classes were identified following an adapted LULC classification scheme of Zoungrana et al. (2015) (Table 5). These are water body, woodland, shrubland, cropland and bare land/built-up. Training samples were collected from three sources. The training samples of the years 1990 and 2005 were collected using historical high-resolution images from Google Earth and land use/land cover databases from the National Geographic Institute of Burkina Faso, whereas a field survey was undertaken to collect samples for the year 2020. Overall, 992, 451, and 239 disproportional stratified random samples comprising the five LULC classes were used to classify the images of 1990, 2005 and 2020, respectively (Table 5).

Table 5. Sample sizes of LULC units for 1990, 2005, and 2020

LULC units	Sample sizes		
	1990	**2005**	**2020**
Water body	50	34	35
Woodland	170	52	30
Shrubland	346	84	32
Cropland	204	99	52
Bare land/built-up	222	182	90
Total	**992**	**451**	**239**

3.1.4. Global Climate Models

The future climate data used in this study were downloaded from the Inter-Sectoral Impact Model Intercomparison Project (ISIMIP3b) repository https://data.isimip.org/. The ISIMIP3b protocol is dedicated to a quantification of climate-related risks at different levels of climate change and socio-

economic conditions. It is a total of ten Global Climate Models under shared socioeconomic pathways (SSP) 126 and 370, composed of daily rainfall, minimum maximum and mean temperature, solar radiation and relative humidity from 1960 to 2100. The SSP370 represents a scenario with both substantial land use change and high NTCF emissions, closing the gap between RCP6.0 and RCP8.5 (O'Neill et al., 2016). In the contrary, the SSP126 scenario represents an update of the RCP2.6, assuming an increase of global forest cover. It is anticipated that it will produce a multi-model mean of significantly less than 2°C warming by 2100, and therefore can support analyses of this policy goal (O'Neill et al., 2016).

ISIMIP3b input is based on output of phase 6 of the CMIP (Eyring et al., 2016). ISIMIP3b data are bias adjusted and statistically downscaled using version 2.0 of W5E5 as observational reference dataset (Lange, 2021). The details of the ISIMIP3b models used are summarized in Table 6.

Table 6. Global climate models and their spatial resolution before and after downscaling

Models	**Modelling institution**	**Resolution before downscaling**	**Resolution after downscaling**
CanESM5	Canadian Centre for Climate Modelling and Analysis	2.0°	0.5°
CNRM-CM6-1	National Centre for Meteorological Research	1.0°	0.5°
CNRM-ESM2-1	Centre National de Recherches Météorologiques	1.0°	0.5°
EC-Earth3	EC-EARTH consortium	0.5°	0.5°
GFDL-ESM4	Geophysical Fluid Dynamics Laboratory	1.0°	0.5°
IPSL-CM6A-LR	Institute Pierre-Simon Laplace	2.0°	0.5°
MIROC6	Model for Interdisciplinary Research on Climate	1.0°	0.5°
MPI-ESM1.2-HR	Max Planck Institute for Meteorology Earth System Model	1.0°	0.5°
MRI-ESM2-0	Meteorological Research Institute	1.0°	0.5°
UKESM1-0-LL	Met Office Hadley Centre	2.0°	0.5°

Source: Lange et al. (2021)

3.1.5. SWIM model inputs data

The required input data for SWIM model comprise of daily climate data (rainfall, minimum, maximum and mean temperature, solar radiation and relative humidity), Digital Elevation Model

(DEM), LULC and soil maps. W5E5 data were used as meteorological inputs as it is a consistent and continuous data set, able to capture the climate patterns of the study area. The DEM was obtained from the Shuttle Radar Topography Mission 90m available at https://bigdata.cgiar.org/srtm-90m-digital-elevation-database/. From the DEM were retrieved the river network, the river routing, the slope, and the delineation of the basin outline. The soil map was obtained from the Harmonized World Soils Database (HWSD) Version 1.1 of the Food and Agriculture Organization of the United Nations (FAO). The HWSD is a 30 arc-second (1 km) raster database with over 15,000 different soil mapping units that combines existing regional and national updates of soil information worldwide (FAO, 2009). This dataset compared to BUNASOLS soil map gives more information on soils parameters that are required by the SWIM model. It is composed of eleven layers (Dewitte et al., 2013). The spatial distribution of the soils is presented in Figure **3** and their coverage areas are shown in Table **7**. The LULC map was obtained from the Landsat image classification of the year 2005. The accordance of the land use units in SWIM and the description of land use units are presented in Table 8.

Table 7. HWSD in the NRB

Soil type	**Area (km^2)**
Hypoluvic Arenosols (ARwl)	1,166.5
Vertic Cambisols (CMvr)	1,406.4
Lithic Leptosols (LPli)	2,033.1
Gleyic Luvisols (LVgl)	2,775.5
Haplic Lixisols (LXha)	2,248.3
Plinthic Lixisols (LXpl)	68.2
Solodic Planosols (PLsc)	1,865.0
Petric Plinthosols (PTpt)	8,354.1
Pisoplinthic Plinthosols (PTpx)	7,837.3
Eutric Regosols (RGeu)	6,103.4
Haplic Vertisols (VRha)	2,109.2

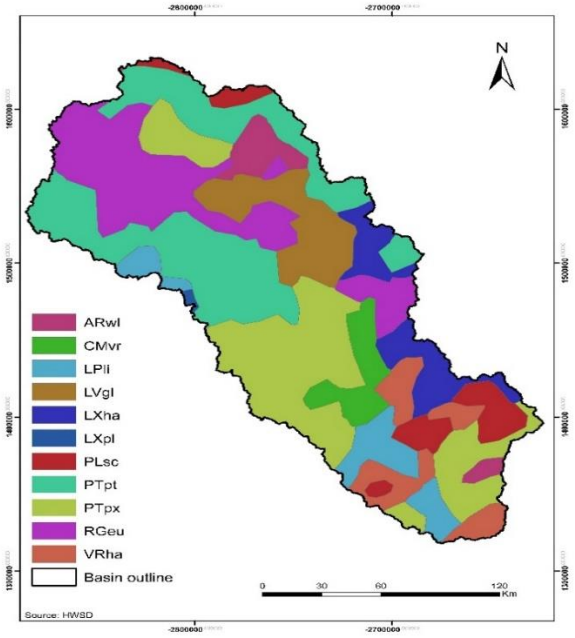

Figure 3. Spatial distribution of soil layers (HWSD) in the NRB

Table 8. Equivalence of LULC units with SWIM land use

LULC units	Description	SWIM LULC units
Water body	Permanent water areas (rivers, dams, lakes)	Water
Woodland	Areas where natural vegetation is dominated by trees whose highs are > 3 m	Forest_closed
Shrubland	Areas where natural vegetation is dominated by trees whose highs are < 3 m	Savanna_dry
Cropland	Cultivated and harvested areas	Cropland_lt_50pc
Bare land/built-up	Bare land, Bare surface, Built up, Tarred Road, Rock	Cities_settlement

NB: Physical characteristics of heat unit and Leaf Area Index (LAI) have been adapted to the climate of the region

In addition to the above-mentioned data, water management and operation of the nine reservoirs was included in SWIM (Table **9**). These are: active and dead storage, reservoir gross capacity, infiltration, volume of water entering the reservoir, volume of rainfall and evaporation over the reservoir surface area, volume of water outflow from the reservoir, volume of water used in the hydropower plant, volume of required minimum outflow from the reservoir, minimum and maximum volumes of the reservoir, minimum and maximum water level, and volume of water withdrawals from the reservoir used for irrigation and fresh water supply. All these data were collected from SONABEL and the literature.

Table 9. Reservoirs and their capacity storage used in SWIM

Reservoirs	Reservoir capacity (Mm^3)	Data source
Bagré	1,700	SONABEL ; de Condappa et al. (2008) ; Ouedraogo (2017)
Ziga	288	Akpaud (2007)
Loumbila	42.2	Adjivon (1991)
Dourou (Kanazoe)	125	Lamizana Diallo (2009)
Seguenega	2.35	Zoungrana (2012); Coulidiati (2016)
Bam	49.1	Nikiema (2017); Pouyaud (1975)
Dem	15.8	Ilboudo (2019)
Tougou	5.5	Diabri (2008)
Goinre	16	Poda (2018)

3.2. Methods

This subsection describes the methods used to compute the results per specific objective.

3.2.1. Hydro-climatic trend and upstream dam management impact on hydropower generation

3.2.1.1. Data quality control and validation

Data quality control comprised the identification of missing data and outliers' detection in hydro-climatic time series to ensure their internal consistency (Okafor et al., 2017). Only solar radiation at Ouahigouya station was excluded because it has missing data of more than 30%. Then, climate data have been aggregated at monthly scale. Observational climate data were used to validate the satellite climate. For this purpose, the W5E5 climate data were compared to the station's climate at the monthly scale using statistical indicators such as Pearson correlation coefficient (R), Normalized Root Mean Square Error (NRMSE), Nash-Sutcliffe Efficiency (NSE), and Percentage bias (PBias) (equations 1, 2, 3, and 4).

$$R = \frac{n(\sum xy) - (\sum x)(\sum y)}{\sqrt{[n\sum x^2 - (\sum x)^2][n\sum y^2 - (\sum y)^2]}} \quad (1)$$

where R is the Pearson Coefficient, n is the number of the pairs of the times series, x is the observations, y is the W5E5 product.

$$NRMSE = \frac{\sum(S_i - O_i)^2}{\sum {O_i}^2} \quad (2)$$

Where O_i are observed values and S_i are simulated values

$$NSE = 1 - \frac{\sum_{i=1}^{n}(O_i - S_i)^2}{\sum_{i=1}^{n}(O_i - \bar{O})^2} \quad (3)$$

where O_i and $\bar{O}$ are the observed discharge and average observed data, respectively, S_i and $\bar{S}$ are the simulated discharge and average simulated data, correspondingly.

$$PBias = \frac{\sum_{i=1}^{n}(Y_i - X_i)}{\sum_{i=1}^{n}(X_i)} * 100 \quad (4)$$

where X_i and Y_i are the observed and the W5E5 climate variables, respectively.

Over the 1985-2015 period, the W5E5 was used to investigate the mean basin rainfall temporal trend, whereas the stations (Ouagadougou and Ouahigouya) were used to investigate the trend at different locations in the NRB.

3.2.1.2. Change year detection

Breakpoint detection in hydro-climatic time series helps to identify regime shifts (Badou et al., 2017). It aims at detecting abrupt changes, called breakpoints, in the distribution of a signal (Bock et al., 2020). Many methods exist for breakpoint detection in climate variability and change studies (Caussinus and Mestre, 2004; Mestre et al., 2013). The Pettitt's test (Pettitt, 1979) considers a sequence of random variables X_1, X_2,..., X_T, which is said to have a change point at τ if X_t for t = 1,..., τ have a common distribution function $F_1(x)$ and X_t for t = τ +1,..., T has a common distribution function $F_2(x)$, with $F_1(x)$ and $F_2(x)$ different, but continuous (Rybski and Neumann, 2011). In this study, the Pettitt's test and the Standard Normal Homogeneity Test (SNHT) were applied to the hydro-climatic variables following equations (5) to (7) and (8) to (10), respectively (Pettitt, 1979; Tuomenvirta and Alexandersson, 1997).

$$U_{t,T} = \sum_{i=1}^{t}\sum_{j=t+1}^{T} sgn(X_i - X_j), 1 \leq t < T \quad (5)$$

where

$$sgn(x) = \begin{cases} 1, if\ x > 0 \\ 0, if\ x = 0 \\ -1, if\ x < 0 \end{cases} \quad (6)$$

The change point τ is computed as follow:

$$K_\tau = U_{\tau,T} = \max\left|U_{t,T}\right|, 1 \le t < T \quad (7)$$

The SNHT was also used to detect non-homogenity in times series (Alexandersson, 1986). This method is capable to identify a break by comparing the average of the first *n* observations with the average of the residual (*n* – *d*) observations with *n* data points (Ahmed et al., 2018).

$$T_d = d_{z_1}^{-2} + (n-d)_{z_2}^{-2} \quad ; \quad d = 1, 2, 3, 4, \ldots\ldots n \quad (8)$$

where

$$\overline{z_1} = \frac{1}{d}\sum_{i=1}^{d} \frac{(Y-\bar{Y})}{sd} \quad (9)$$

$$\overline{z_2} = \frac{1}{n-d}\sum_{i=d+1}^{d} \frac{(Y-\bar{Y})}{sd} \quad (10)$$

where Y is the observed value, $\overline{Y_i}$ is the average and sd is the standard deviation of the time series.

3.2.1.3. Trend analysis

Several statistical methods exist for detecting trends in climate variables. These are mainly composed of Innovative Trend Analysis approach (Sen, 2012), Cumulative Sum (CUSUM), Mann–Kendall (MK) trend test, Bayesian analysis, etc. (Sonali and Kumar, 2013). Commonly used is MK (Sonali and Kumar, 2013). In this study, the trends of hydro-climatic variables and the hydropower generation were analysed using the modified MK trend test, a non-parametric trend test used to identify monotonic trends present in time series data (Mann, 1945; Sen, 1968; Kendall, 1975). This statistical method requires no specific distribution of the data (Kendall, 1975). The method is robust against outliers (Abungba et al., 2020; Sanogo et al., 2015) and can cope with missing values and values below the detection limit (Gavrilov et al., 2016). It measures the correlation of a variable with time and gives information on the direction, magnitude and significance of observed trends (Gulakhmadov et al., 2020; Koudahe et al., 2017). More

information on the modified MK test is available in the literature (Abungba et al., 2020; Gavrilov et al., 2016; Gulakhmadov et al., 2020; Hamed, 2008; Hamed and Rao, 1998; Pingale et al., 2016; Tabari et al., 2011).

First, all time series were checked for autocorrelation. For cases of auto-correlated data, time series were pre-whitened before the trend computation following equations (11) to (16) (Pingale et al., 2016). The variance is underestimated in case of positive auto-correlation in the times series. Therefore, the variance correction factor $\frac{n}{n_s^*}$ is calculated using significant values of *ρk* (Pingale et al., 2016).

$$\frac{n}{n_s^*} = 1 + \frac{2}{n(n-1)(n-2)} \sum_{i=1}^{n-1} (n-i)(n-i-1)(n-i-2)\, \rho_s(i) \qquad (11)$$

where n is the total observations, n_s^* is the "effective" observations to consider for the autocorelation in the time series, $\rho_s(i)$ is the autocorrelation function of the ranks of the observations.

$$\rho_s(i) = \sin^{-1}\left(\frac{\rho(i)}{2}\right) \qquad (12)$$

where $\rho(i)$ is the parent autocorrelation function of rank of the observation.

Therefore, the corrected variance is calculated as follow:

$$V^*(S) = V(S) \,.\, \frac{n}{n_s^*} \qquad (13)$$

where $V(S)$ is the variance of the simple Mann Kend trend test computed as follow (Kendall, 1975):

$$S = \sum_{k=1}^{n-1} sgn\left(x_j - x_k\right) \qquad (14)$$

$$V(S) = \frac{[n(n-1)(2n+5) - \sum_t t(t-1)(2t+5)]}{18} \qquad (15)$$

where $\left(x_j - x_k\right)$ is the signum function and S is the test statistic.

The modified Mann Kendall test statistic Z_{mmk} is computed as follow:

$$Z_{mmk} = \begin{cases} \frac{S-1}{\sqrt{V^*(S)}} & if\ S > 0 \\ 0 & if\ S = 0 \\ \frac{S+1}{\sqrt{V^*(S)}} & if\ S < 0 \end{cases} \quad (16)$$

All statistical analyses were performed with the R software packages *modifiedmk*, *hydroGOF*, *correlation and trend*. The trend analysis was performed for annual and monthly time series of rainfall, mean temperature (minimum and maximum), inflow, outflow, irrigation, turbined flow, evaporation, water level, Ziga volume and hydropower generation. Results with a p-value ≤ 0.05 indicate a significant trend while a p-value > 0.05 indicates an insignificant trend.

3.2.1.4. Correlation between hydro-climatic variables, ENSO and hydropower generation

Variability in hydro-climatic variables and upstream dam management influences downstream river discharge and hydropower generation (Annys et al., 2020; Beilfuss, 2012). To assess the relationship between hydro-climatic variables, upstream dam management and hydropower generation, Spearman correlation tests were performed (equation 17). The Spearman correlation test is a non-parametric test based on the rank and it measures the strength of the monotonic relationship between paired variables (Badou et al., 2017). The annual hydropower generation was correlated to annual rainfall sums, annual inflow, annual outflow, annual irrigation, annual mean water level, annual lake evaporation and annual Ziga volume over the period 1993–2012 and 2001–2012 (corresponding to the availability of hydropower generation and Ziga volume data). A 3 month mean basin rainfall, inflow, mean water level, lake evaporation and hydropower standardized anomaly indices were computed and correlated to the 3 months' ENSO index. Spearman rho results are interpreted as follows: 0–0.20 is negligible, 0.21–0.40 is weak, 0.41–0.60 is moderate, 0.61–0.80 is strong and 0.81–1.00 is considered a very strong correlation (Prion and Haerling, 2014).

$$r_s = 1 - \frac{6\sum d_i^2}{n(n^2-1)} \quad (17)$$

where r_s is the rho coefficient, n is the lenght of the time series, d represents the difference in the ranks between each point (x_i and y_i) of the time series.

3.2.2. Land use land cover classification and future land use prediction

3.2.2.1. Data pre-processing

The pre-processing steps involved scaling, cloud masking and additional bands computation. The scaling consisted of applying the respective scale factors and offsets to the images in order to get the true surface reflectance values. The cloud masking involved the identification of all pixels with the clouds and shadows to exclude them from further analysis. The median filter was then applied to the resulting images for each year to obtain a cloud free composite. In addition to the five raw surface reflectance bands, the Normalized Difference Vegetation Index (NDVI) and the Normalized Difference Built-up Index (NDBI) were computed and used as additional features. The NDVI allows to get a clear differentiation of vegetation from non-vegetation classes (Asenso Barnieh et al., 2020; Feng et al., 2016; Hackman et al., 2017; Yu et al., 2014) while NDBI allows to get a differentiation of built-up and bare land areas from other land uses (Hackman et al., 2020; Prasomsup et al., 2020).

3.2.2.2. Image classification and accuracy assessment

The pre-processed images were classified using the training samples mentioned in the sub-section 3.1.3. For each year, 70% of samples were used to train the classification algorithm while 30% were utilized for the validation. The method of classification was based on Random Forest supervised classification. Random Forest is an ensemble classifier formed by the combination of multiple trees, resistant to noise, overfitting issues, and is able to process massive high-dimensional data while maintaining high accuracy (Gislason et al., 2006; Shetty, 2019). It has been successfully used for LULC assessment in Burkina Faso by different researchers (Dimobe et al., 2017; Zoungrana et al., 2015). Furthermore, it is the best classifier for soil and LULC mapping compared to SVM and SGB in Burkina Faso and Ghana, respectively (Forkuor et al., 2017; Hackman et al., 2017). Thus, Nery et al. (2016) suggested that RF should be prioritised when classifying time series imagery for LULCC detection.

The classification accuracies were assessed through overall accuracy and kappa index following the equations (18) and (19) and described below by Rwanga and Ndambuki (2017).

$$OA = \frac{\sum_1^n x}{\sum_1^n X} \quad (18)$$

where *x* is the number or correct samples and *X* is the total of samples

$$K = \frac{N\sum_{i=1}^{r} x_{ii} - \sum_{i=1}^{r}(x_i + Xx_{+1})}{N^2 - \sum_{i=1}^{r}(x_{ii} + Xx_{+1})} \quad (19)$$

where *r* = number of rows and columns in error matrix, *N* = total number of observations (pixels), *Xii* = observation in row *i* and column *i*, *Xi+* = marginal total of row *i*, and *X+i* = marginal total of column *i*.

Also, the confusion matrix for the LULC maps, 1990-2005, 2005-2020, and 1990-2020, was computed. The confusion matrix allows for detecting the sources of misclassification for a LULC unit (Liu et al., 2020).

3.2.2.3. LULCC analysis and spatial trend of anthropogenic land use

The dynamics between the different LULC classes were examined following the change analysis module of the Land Change Modeler (LCM). Moreover, percent change was computed following equation (20) (Hussien et al., 2022).

$$p = \frac{(A_l - A_e)}{A_e} \text{ x } 100 \quad (20)$$

where p is the percent change, $A_l$is the area of a class in the later LULC map (km^2), and A_e is the area of a class in the earlier LULC map (km^2).

The spatial trend of anthropogenic land use was assessed with the spatial trend tool of the LCM. It consists of mapping the conversion from one or multiple classes of LULC to another following a polynomial function. The study used a third-degree polynomial function to map the spatial trend (Eastman, 2020).

3.2.2.4. Land use change driver variables and transition potentials mapping

Changes in land use result from multiple variables consisting of physical and human factors. Many variables are commonly used in LCM to explain the change in land use. These are composed of the slope, elevation, soil, distance to reservoirs, distance from rivers, distance from roads, distance to urban, etc. (Hussien et al., 2022; Larbi et al., 2019; Gharaibeh et al., 2020; Kim et al., 2020). In this study, four drivers namely, (i) distance to roads, (ii) distance to urban, (iii) distance to rivers, and (iv) evidence likelihood, were considered and used as inputs in the Transition Sub-Model Structure.

The major potential transitions from one LULC class to another were mapped using the MLP neural network algorithm (Larbi et al., 2019). According to Eastman (2020), MLP neural networks are the most robust technique for transition potential mapping, even though the logistic regression method is also viable. Moreover, it allows one to model several or even all transitions at once and is quite capable of modelling non-linear relationships (Eastman, 2020). In this study, nine major transitions greater than 100,000 hectares, derived from the change analysis, were considered to model the potential transitions. These are shrubland to woodland; woodland to shrubland; cropland to shrubland; woodland to cropland; shrubland to cropland; bare land/built-up to cropland; shrubland to bare land/built-up; and cropland to bare land/built-up. After running the transition sub-model using an MLP neural network, the transition potential maps were successfully implemented. The output of the transition sub-model gives the model skill and the most and least influencing driver variables. According to Hussien et al. (2022) and Clark Labs (2020), a model that forces a single independent variable to be constant while keeping one variable constant at a time explains better the power of explanatory drivers than the Cramer's V method. Figure 4 summarizes the methodology used in this study.

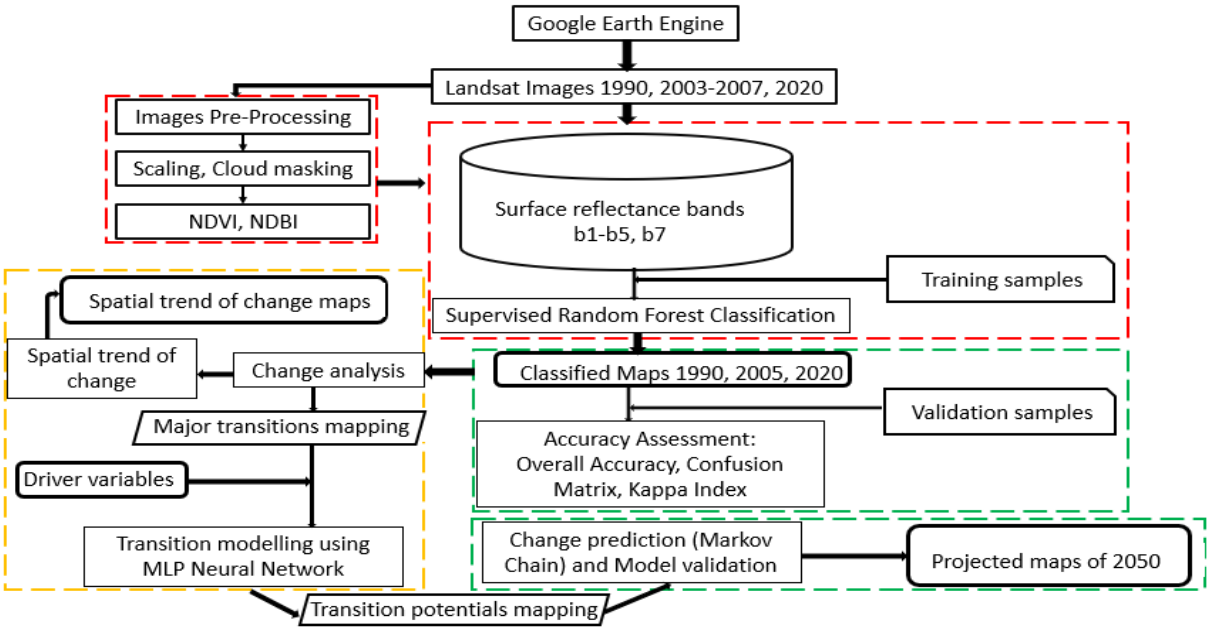

Figure 4. LULC mapping and modelling Flowchart

3.2.2.5. Model validation and LULCC projection

To simulate the LULC of 2020, the first period of 1990-2005 was considered for calibration while the period 2005-2020 was considered for validation. The simulation was done using the Markov Chain Model. This technique is described and used in several studies to project future LULC (Larbi et al., 2019; Mehrabi et al., 2019; Näschen et al., 2019; Shade and Kremer, 2019; Koko et al., 2020). The simulated and classified maps of 2020 were compared by using the VALIDATE module in Idrisi software, which allows the computation of the Kappa index (Pontius, 2000). The Kappa index ranges from -1 to 1 and shows the agreement or disagreement between the actual and simulated maps (Pointus, 2000). K_{no} evaluates the overall accuracy of the model, while $K_{locality}$ indicates the model's ability to identify correct locations (Sibanda and Ahmed, 2021). After the model validation, the future LULC of 2050 was computed based on the same drivers and parameters, and changes detected in LULC between 1990 and 2020. Two futures scenarios were adopted, which were included in the Markov Chain Model editing matrix to model the 2050 LULC. The BAU scenario assumes a probability of decreasing natural vegetation (woodland and shrubland) to the benefit of cropland and bare land/built-up, and a decrease of cropland to the benefit of bare land/built-up. The afforestation scenario assumes a probability of increasing natural vegetation (shrubland + woodland) at the expense of cropland and a decrease in bare land/built-up

to the benefit of cropland, as summarized in Table 10. The choices for these transitions in the scenarios are based on the master plan of the NRB (AEN, 2015).

Table 10. Probability of changes used for BAU and afforestation scenarios

BAU	AFFORESTATION
10% Woodland to cropland	5% Cropland to woodland
10% Woodland to bare land/built-up	5% Bare land/built-up to woodland
15% Shrubland to cropland	15% Cropland to shrubland
10% Shrubland to bare land/built-up	5% Bare land/built-up to shrubland
30% Cropland to bare land/built-up	30% Bare land/built-up to cropland

Source: Adaptation from NRB master plan (AEN, 2015)

3.2.3. Assessment of impact of climate and LULC changes on hydropower generation at the Bagré dam

3.2.3.1. ISIMIP3b data quality control

The quality checking of ISIMIP3b was performed following the same technique for W5E5 datasets validation in section 3.2.1.1. Therefore, monthly values of ISIMIP3b rainfall and mean temperature were compared to monthly W5E5 and observations at Ouagadougou and Ouahigouya stations using statistical indicators of Pearson correlation and PBias (equations (1) and (4)).

3.2.3.2. Hydrological modelling

3.2.3.2.1. SWIM model hydrological components

The hydrological modelling was carried out using the SWIM model. SWIM is a continuous-time spatially semi-distributed process-based hydrological model, made from two previous developed tools SWAT and MATSALU (Krysanova et al., 2000). It integrates the relevant eco-hydrological processes including water flow, nutrient transport and turn-over, vegetation (crop) growth, land use and water management needed to investigate climate and land use change impacts on hydrological systems and vegetation at the regional scale (Figure **5**).

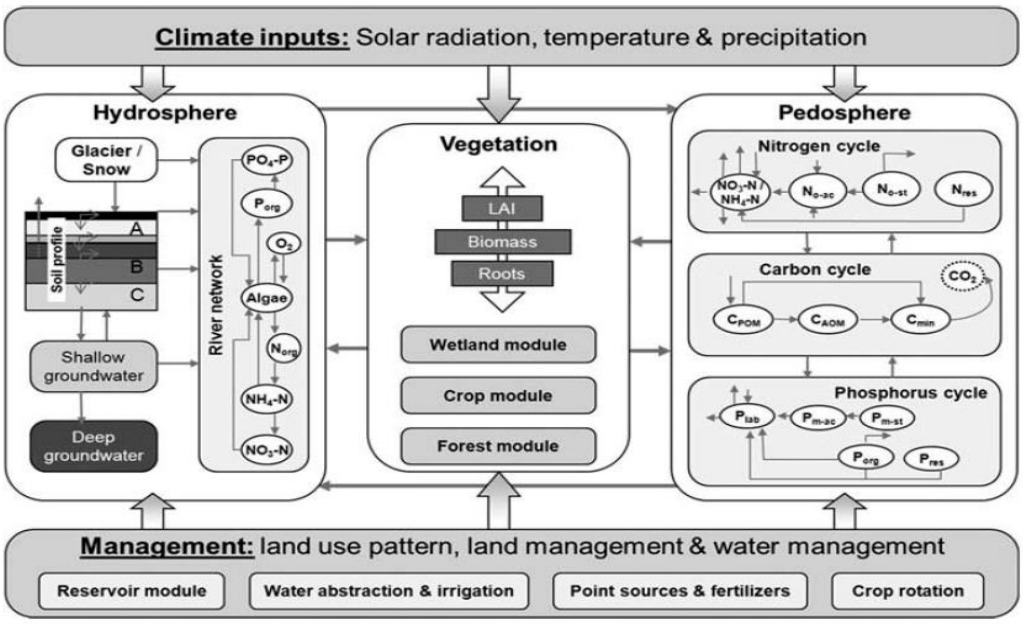

Figure 5. SWIM model structure (Krysanova et al., 2022)

The last version of SWIM used in this work integrates the water allocation and management modules, which allow the computation of reservoirs water level, irrigation supply and electricity production from hydropower plants (Koch et al., 2013). SWIM was developed to investigate impacts of land use and climate changes on hydrology and vegetation (crop yields). The three-level disaggregation scheme 'basin – sub-basins – hydrotopes' used in SWIM can be derived based on a DEM (Krysanova et al., 2022). The simulations are run from hydrotopes to sub-basins and basins levels with uniform land use, soil, slope and climate patterns following the water balance equation (21) (Krysanova et al., 2022).

$$SW(t+1) = SW(t) + PRECIP - Q - ET - PERC - SSF \qquad (21)$$

where *SW(t)* is the soil water content in the day *t*, *PRECIP* is rainfall, *Q* is surface runoff, *ET* is evapotranspiration, *PERC* is percolation, and *SSF* is subsurface flow at daily amounts in mm.

Surface runoff (Q): the runoff volume is estimated based on Soil Conservation Service (SCS) curve number technique following the equation described by Wyseure (1991). This method does not require many inputs and relates runoff to soil type, land use, and management practices. Therefore, the retention coefficient varies spatially and temporally.

$$Q = \frac{(PRECIP - 0.2\,.SMX)^2}{(PRECIP + 0.8\,.SMX)}, \qquad PRECIP > 0.2\,.SMX \qquad (22)$$

or

$$Q = 0, \qquad PRECIP \leq 0.2\,.SMX \qquad (23)$$

where Q is the daily runoff in mm, $PRECIP$ is the daily rainfall in mm, and SMX is the retention coefficient and defined as:

$$SMX = 254\,.\left(\frac{100}{CN} - 1\right) \qquad (24)$$

where *CN* represents the curve number which expresses the quantity of water allowed to percolate into the soil.

Evapotranspiration (ET): The potential evapotranspiration is estimated in SWIM using the Priestley-Taylor method while the actual evapotranspiration is estimated following the method of Ritchie (1972).

The potential evapotranspiration is defined as:

$$ETp = 1.28\,.\left(\frac{RAD}{HV}\right)\,.\left(\frac{\delta}{\delta+\gamma}\right) \qquad (25)$$

where *ETp* is the potential evapotranspiration in mm, *RAD* is the net radiation in MJ/m^2, *HV* is the latent heat of vaporization in MJ/kg, δ is the slope of the saturation vapor pressure curve in kPa/C, and γ is a psychrometer constant in kPa/C.

The actual evapotranspiration is defined as:

$$ETa = EP + ESO \qquad (26)$$

where *ETa* is the actual evapotranspiration, *EP* is the plant water transpiration, and *ESO* is the potential soil evaporation. All units are in mm/d.

"Plant transpiration is simulated as a linear function of potential evapotranspiration and leaf area index. When soil water is limited, plant transpiration is reduced, taking into account the root depth" (Krysanova et al., 2022; p.17). The plant water transpiration is computed as follow:

$$EP = \frac{ETp \,.\, LAI}{3}, \qquad 0 \leq LAI \leq 3 \tag{27}$$

or

$$EP = ETp, \qquad LAI > 3 \tag{28}$$

"Actual soil evaporation is computed in two stages. It is equal to the potential soil evaporation predicted by means of an exponential function of leaf area index until the accumulated soil evaporation exceeds the upper limit of 6 mm. After that stage two begins. The actual soil evaporation is reduced and estimated as a function of the number of days since stage two began" (Krysanova et al., 2022; p.17). The potential soil evaporation is defined as:

$$ESO = ETp \,.\, e^{(-0.4 \,.\, LAI)} \tag{29}$$

where *LAI* is the leaf area index (area of plant leaves relative to the soil surface area) and *ETp* is the potential evapotranspiration in mm.

Percolation (PERC): Downward flow occurs when field capacity of the soil layer is exceeded, and as long as the layer below is not saturated. This component is treated as the recharge to shallow aquifer and is expressed as a function of soil water content following the equation (30).

$$PERC_i = SW_i \,.\, \left[1 - e^{\left(\frac{-\Delta t}{TT_i}\right)}\right] \tag{30}$$

Where *SWi* is the soil layer water content in mm/d, Δt is the time interval (24 h), and *TTi* is the travel time through layer *i* in h.

Lateral subsurface flow (SSF): In SWIM, SSF is computed simultaneously with percolation and is based on the mass continuity equation in the finite difference form with the entire soil profile as the control volume.

$$SSF = 0.024 \,.\left(\frac{2\,.SUP\,.SC\,.\sin(v)}{PORD\,.\,SL}\right) \quad (31)$$

where *SSF* is the lateral subsurface flow in mm/d, *SUP* is the water above field capacity in m/month, *SC* is the saturated conductivity in mm/h, *PORD* is the drainable porosity of the soil in m/month, and *SL* is the hillslope length in m.

Groundwater flow: This component in SWIM is the same as in SWAT, where shallow and deep aquifers are simulated in each sub-catchment at hydrotopes level (Arnold et al., 1993). The groundwater recharge equation is described as follow in equation (32).

$$GWQ = 8\,.\left(\frac{KD\,.GWH}{DS^2}\right) \quad (32)$$

where GWQ is the return flow or groundwater contribution to streamflow, *KD* is the hydraulic conductivity of groundwater in mm/d, *DS* is the drain spacing in m, and *GWH* is the water table height in m.

In semi-arid regions like NRB, some alluvial channels can abstract large quantities of stream flow. A special module that accounts for transmissions losses, takes into account this phenomenon because it can reduce runoff volumes when the flood wave travels downstream (Krysanova et al., 2022). It is based on the use of regression equations which allow the user to estimate transmission losses for similar channels of arbitrary length and width using channel geometry parameters (width and depth) and Manning's "n" (Krysanova et al., 2022). More details on SWIM hydrological components are available in the SWIM manual (Krysanova et al., 2022).

3.2.3.2.2. SWIM model set up

The model step up is mainly done in GRASS GIS. It starts with the watershed delineation using a DEM. With the different gauge stations, 19 sub-catchments and 162 subbasins as well as the accumulation flow have been created. From there, the routing network was checked to ensure that the river flows through the correct subbasins. Thereafter, the substats (subbasin statistics of routing and groundwater), the hydrotopes and the climate files can be created. In SWIM, climate data are spatially interpolated using the Thiessen polygon method. Each hydrotope shares the same LULC and soil units. Adapted LULC of 2005 from Landsat images and Harmonized World Soil Database

from FAO were used to create 1,302 hydrotopes. There is no lateral interaction between the hydrotopes. However, the area-weighted hydrotopes fluxes are added at each sub-basin outlet and routed through the river network to the basin outlet, at daily time step (Koch et al., 2020).

The potential evaporation was calculated directly by SWIM using the Priestley-Taylor method (Ritchie, 1972). This method requires few inputs (temperature and radiation data), and is considered as one of the most precise among the simplified methods with reduced parameters (Aschonitis et al., 2015; Sumner and Jacobs, 2005).

The reservoir and water allocation modules were applied in the model step implemented by Koch et al. (2013) and Liersch et al. (2013), respectively. The reservoir module is a storage-release process based on three management options: (i) minimum discharge downstream considering minimum and maximum reservoir volumes for each month; (ii) daily release based on hydropower generation demand considering the minimum and maximum reservoir volumes and (iii) daily release based on the water level of the reservoir (Koch et al., 2013). In this study, only the first two options were considered for 9 reservoirs operation. The water allocation module enables to transfer water from a source (subbasin, river, reservoir, external of the basin) to a destination (hydrotope, subbasin, river section, outside of the basin) for industrial, domestic and agricultural uses (Liersch et al., 2013). For the purpose of this study, destination was set to “0” as water withdrawals from Bagré dam are used to irrigate developed lands in the downstream of the dam. The different steps of the SWIM model set-up are represented in Figure 6.

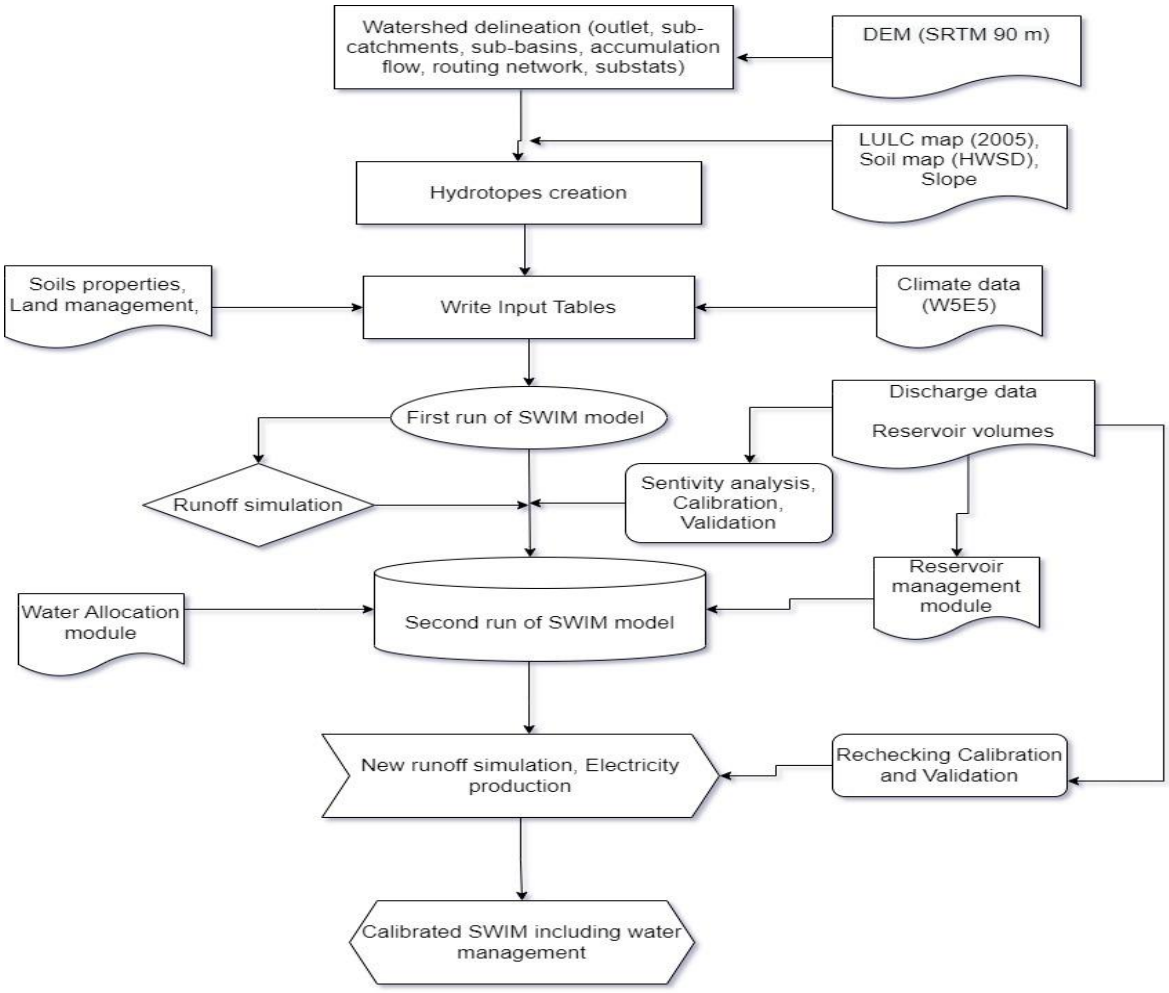

Figure 6. Flowchart of SWIM model set up, calibration, and validation for the NRB

3.2.3.2.3. Model parameters sensitivity, calibration and validation

One of the best ways to achieve a better calibration of a model is based on the assessment of its parameters' sensitivity in the study area. SWIM is composed of 24 parameters including climate, soil, and groundwater. The sensitivity analysis consisted of varying one parameter after one, step by step, in order to detect the most sensitive parameters. Based on previous studies in semi-arid regions such as Koch et al. (2020) and Krysanova et al. (2015), the emphasis was put on 8 parameters (Annex 1a).

The SWIM model was manually calibrated and validated using observed daily/monthly discharge at Wayen and Niaogho stations before the construction of Ziga dam (year 2000). Due to lack or poor discharge data for many stations on the upstream of reservoirs, daily water volumes were also

used for reservoir calibration and validation. For most of the dams, the calibration period is within 1985-2010 while the validation period is within 2009-2018. Table **11** gives more details for the calibration and validation periods. The performance of the model was assessed using three statistical indicators namely NRMSE, NSE, Coefficient of Determination (R^2) and PBias defined in equations (2), (3), (34) to (35), respectively. PBias estimates the percentage trend of simulated data to be higher or lower than the observed data; a PBias of 0 indicates an optimal value while negative and positive values indicate an overestimation and underestimation of observations, respectively (Gupta et al., 1999). NRMSE varies from −1 to +∞, where zero is the optimal case (Getirana and Peters-Lidard, 2013). The R^2 is used to estimate the correlation between the observations and simulations. It is ranged from 0 to 1; 0 indicates no correlation while 1 indicates a perfect correlation. Although R^2 can estimate the linear regression between observations and simulations, it does not take into consideration the variation in maximum and minimum flows. Hence, the suggestion of using it with other statistical indicators like NSE is recommended (Krause et al., 2005). NSE coefficient varies from −∞ to 1; An NSE of 1 indicates a perfect fit between observations and simulations. The use of NSE in semi-arid regions was discussed in many studies (Costelloe et al., 2005; Koch et al., 2020; Love et al., 2011) especially when it comes to daily discharge time series and the use of satellite rainfall products as input. However, Koch et al. (2020) suggested the use of graphical analysis or mean daily discharge over a long-term period. In this study, the lack of long-term discharge data for Niaogho did not allow the use of this method. Nevertheless, the simulated inflow, turbined, hydropower generation, and water level were also compared to observations from SONABEL at monthly and mean monthly scales from 2005 to 2010.

It is important to highlight that reservoir operation (and hydropower generation) in SWIM is based on observed reservoir operation. It is flexible and adapted to wetter/drier conditions. However, if the climate/inflow changes considerably, an adjustment of the reservoir operation may be necessary.

Table 11. Period of calibration and validation of discharge and reservoir volumes

	Stations/Dams	Calibration	Validation	Scale
Discharge	Wayen	1989-1993	1995-1999	daily
	Niaogho	1980-1984	1987-1991	monthly
Volume	Bagré	2004-2008	2009-2013	daily
	Ziga	2005-2011	2013-2018	daily
	Loumbila	2006-2010	2011-2015	daily
	Dourou	2006-2010	2011-2015	daily
	Séguénega	2006-2009	2015-2018	daily
	Bam	2009-2012	2013-2016	daily
	Dem	1985-1986	---	daily
	Tougou	2005-2008	2011-2013	daily
	Goinré	1999-2001	2004-2007	daily

$$R^2 = \left[\frac{\sum_{i=1}^{n}(O_i-\bar{O})(S_i-\bar{S})}{\left[\sum_{i=1}^{n}(O_i-\bar{O})\right]^{1/2}\left[\sum_{i=1}^{n}(S_i-\bar{S})\right]^{1/2}}\right]^2 \quad (34)$$

$$PBias = \frac{\sum_{i=1}^{n}(O_i-S_i)}{\sum_{i=1}^{n}(O_i-\bar{O})} * 100 \quad (35)$$

where O_i and $\bar{O}$ are the observed discharge and average observed discharge data, respectively, S_i and $\bar{S}$ are the simulated discharge and average simulated discharge data, correspondingly.

3.2.3.3. Calculation of hydropower generation

The Bagré dam is operated under option 2 and the electricity generated by the hydropower plant is calculated in SWIM using the following equation 36.

$P_{el} = Q * h * k$ with $Q = MIN(V_{outfl}, Cap_{HPP})$ (36)

where P_{el} is the electricity produced (kW), Q is the flow through the turbine (m^3/s), h is the water head (m), k is the efficiency factor (kN/m^3), Cap_{HPP} is the maximum turbine flow capacity (m^3/s) and V_{outfl} is the actual outflow. Here, the outflow depends on the actual volume and is calculated using the water level–volume relationship data (Annex 1b).

3.2.3.4. Impact of climate and land use changes assessment

As in many other studies (Obahoundje et al., 2021b; Larbi, 2019), three scenarios were determined to assess the possible impacts of climate and land use changes on runoff and hydropower:

(i) climate change (SSP126 and SSP370) impact assessment on hydropower generation by running the SWIM model with 2005 LULC map and ISIMIP3b for the mid (2035-2065) and far (2065-2095) future periods;

(ii) LULCC impact assessment on hydropower generation by running the calibrated SWIM model with W5E5 (1979-2019) and the LULC maps 2050;

(iii) combined climate and LULC changes impact assessment by running the SWIM model with the future ISIMIP3b models and the two scenarios of land use change of 2050.

The changes in inflow and hydropower generated were assessed by estimating the relative and absolute changes of the median inflow and hydropower generation during the mid (2035-2065, "P1") and far (2065-2095, "P2") futures compared to the baseline period (1984-2014, "P0"). Although the Bagré dam started operating in 1993, the baseline starts in 1984. The objective of this choice is to cover the reference period of the Sixth IPCC Assessment Report (1995-2014), and to reduce uncertainty in the interpretation of model simulations because the historical period should cover a minimum of 30 years (Liersch et al., 2020).

The relative change is defined in equation (37) while the absolute change is defined in equation (38).

$$EP_{relchange} = \frac{EP_{ft} - EP_{bl}}{EP_{bl}} \times 100 \quad (37)$$

$$EP_{abschange} = EP_{ft} - EP_{bl} \quad (38)$$

where $EP_{relchange}$ is the relative change of electricity produced in %; $EP_{abschange}$ is the absolute change of electricity produced in MW; EP_{ft} is the quantity of electricity produced in the future period; EP_{bl} is the quantity of electricity produced during the baseline period.

The contribution rate to hydropower change by climate and LULCC was evaluated by using equations (41) and (42). Here, the assumption is that the impact resulted from the interaction between climate and LULC is negligible (Gbohoui et al., 2021; Yonaba et al., 2021).

$EP_{CC_{LULCC}} = EP_{LULCC} + EP_{CC} + EP_{CC\&LULCC}$ with $EP_{CC\&LULCC} = 0$ (39)

therefore, $EP_{CC_{LULCC}} = EP_{LULCC} + EP_{CC}$ (40)

Where $EP_{CC_{LULCC}}$ is the electricity produced under combined effects of climate and land use changes, EP_{LULCC} is the electricity produced under land use change, EP_{CC} is the electricity produced under climate change, $EP_{CC\&LULCC}$ is the electricity produced from the interaction between climate and land use.

$$LULCCpart = \frac{EP_{CC_{LULCC}} - EP_{CC}}{EP_{CC_{LULCC}}} \times 100 \quad (41)$$

$$CCpart = \frac{EP_{CC}}{EP_{CC_{LULCC}}} \times 100 \quad (42)$$

Where $LULCCpart$ and $CCpart$ are the percentage of contribution of LULCC and climate change, respectively; $EP_{CC_{LULCC}}$ is the quantity of electricity produced under combined impact of climate and land use changes in MW; EP_{CC} is the quantity of electricity produced under sole impact of climate change in MW.

3.2.4. Assessment of impact of water management changes on hydropower generation at the Bagré dam

3.2.4.1. Estimation of withdrawal changes for the Ziga and Bagré dams

Population projections and estimates of water needs confirm that Burkina Faso could face water scarcity in the future (GFDRR, 2020). Therefore, an increment in water demand and food production is expected. The future withdrawal at Bagré dam was determined using linear regression equation while the future water withdrawal from Ziga was retrieved from a study by (Newborne, 2016). For the Bagré dam, the withdrawals from 2000 to 2018 increased from 0.65 m^3/s to 8.5 m^3/s. following a linear trend. The full development of the irrigated area downstream Bagré is about 57,800 ha (Bagré Pôle, 2011) and was extrapolated with the withdrawals. By assumption, the baseline water withdrawals correspond to the year 2010 while the future withdrawals correspond to the year 2045 (Table **12**).

Table 12. Mean withdrawals from Bagré and Ziga under baseline and future water management

Reservoirs	Baseline water withdrawals (m^3/s)	Future water withdrawals (m^3/s)
Bagré	6.9	17.2
Ziga	0.196	2.3

It is important to mention that the different scenarios identified in this study are all based on the master plans of the NRB and the “Bagré Pôle”.

3.2.4.2. Assessment of water management change impact on hydropower

To assess the water management change, the methodology described in section 3.2.3.4 was used with new operations for the Ziga and Bagré dams. Then, the impact of water management change is assessed by calculating the difference between the electricity produced under future water management and electricity produced under baseline water management.

3.3. Partial Conclusion

Datasets used are composed of hydrological-climatic data. W5E5 was used as historical observed climate data while ISIMIP3b was used to drive the future climate. Hydrological data comprised historical discharge, water levels, volumes and reservoir parameters. In addition, soil, DEM, and ground truth data of LULC were collected and used in many materials. The GEE and LCM were used for LULC mapping and prediction while the SWIM model was used to simulate inflow and hydropower generation at the Bagré dam. All graphs were drawn using R studio and Microsoft Excel.

CHAPTER 4: HYDRO-CLIMATIC VARIABILITY AND UPSTREAM WATER MANAGEMENT IMPACTS ON HYDROPOWER GENERATION AT THE BAGRÉ DAM

This chapter presents the impact of hydro-climatic variability and upstream reservoir management on the hydropower generation at the Bagré dam. The first section inspects the suitability of the reanalysis W5E5 climate data for the NRB. The second and third sections investigate the homogeneity and trend analysis in annual and monthly hydro-climatic variables. Furthermore, the correlation between hydro-climatic variables and hydropower generation is examined in section four. The last section discusses the results of the chapter.

4.1. W5E5 datasets performance

At the monthly scale over the period 1985–2015, the statistics showed a good correlation between the W5E5 products and the observed climate patterns at the two stations (Table **13**). W5E5 slightly overestimates rainfall and relative humidity at Ouagadougou station while at Ouahigouya station, these are slightly underestimated. The maximum and minimum temperatures are underestimated during all the months of the year except for Ouahigouya station that overestimates the maximum temperature from May to September (Figure **7**). Figure **7** further shows that W5E5 underestimates solar radiation during the rainy season whereas during the dry season, it is overestimated. Nevertheless, the lowest bias is observed in the solar radiation and maximum temperature at Ouagadougou station (0.2 and -0.2), while the highest bias is detected for rainfall at Ouahigouya station (-8.4). However, none of the biases is important, considering -20 to +20% as an acceptable performance range for a satellite product (Cohen et al., 2012; Diem et al., 2014). The W5E5 dataset was then used as climate inputs for the rest of the work.

Table 13. Comparison statistics of monthly observed climate variables and monthly W5E5 products at Ouagadougou (south of the basin) and Ouahigouya (north of the basin) stations

Climate variables	**Ouagadougou**				**Ouahigouya**			
	R	PBias	NSE	NRMSE	R	PBias	NSE	NRMSE
Rainfall (mm)	0.97	3.8	0.94	19.6	0.98	-8.4	0.97	13.9
Minimum Temperature (^{o}C)	0.98	-1	0.95	0.23	0.98	-3.2	0.97	0.16
Maximum Temperature (^{o}C)	0.98	-0.2	0.96	0.18	0.98	0.8	0.97	0.2
Relative humidity (mm)	0.99	0.6	0.98	9	0.98	-2.3	0.98	11
Solar radiation (J/cm^2)	0.72	0.2	0.7	31	-	-	-	-

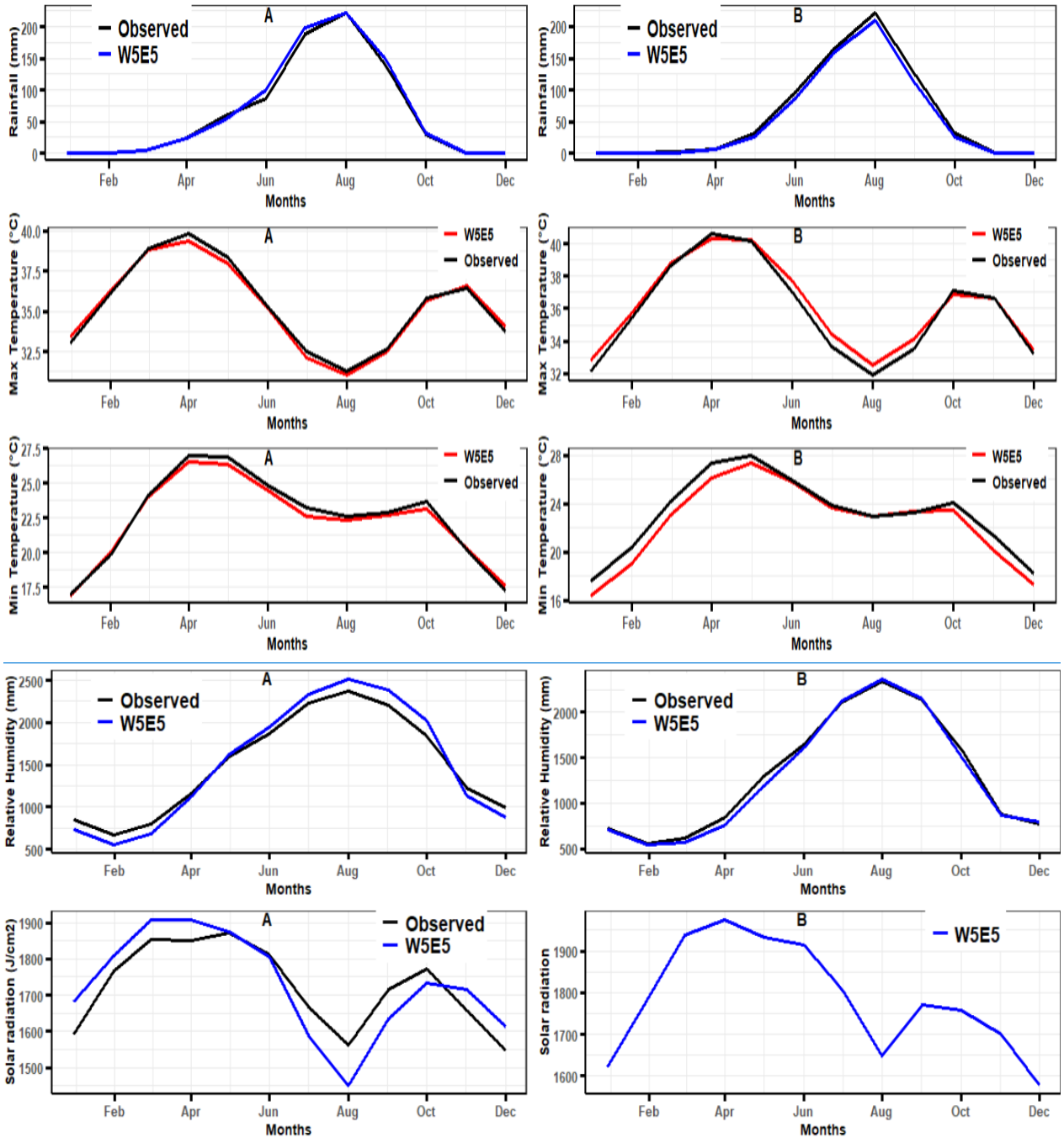

Figure 7. Mean monthly observed and W5E5 of rainfall, min and max temperature, relative humidity, and solar radiation at Ouagadougou (A) and Ouahigouya (B) from 1985-2015.

4.2. Homogeneity and trend analysis of annual hydro-climatic variables and hydropower generation

The results of the homogeneity test show break years for many variables. The break years are calculated for all climatic variables using the Pettitt test or SNHT. For hydrological variables, only outflow, water level, and lake evaporation do not have a breakpoint whether from the Pettit test or the SNHT (Table **14**).

The results of the Modified Mann-Kendall trend test are presented in Table **14**. All variables showed an increasing trend over their respective considered periods. Rainfall, temperature, inflow, turbined flow, irrigation and hydropower generation show a significant increasing trend at the 95% confidence level, while the increasing trends of lake evaporation, outflow and water level were not significant. The annual slopes of rainfall were 5.27 mm over the basin, 6.17 mm at Ouagadougou station, 8.77 mm at Ouahigouya station, 68.08 hm^3 for inflow, 17.99 hm^3 for turbined flow, 12.54 hm^3 for irrigation and 2,168 MWh for hydropower generation. The results also show that minimum and maximum temperature increased significantly by 0.04°C per year at Ouagadougou station, while Ouahigouya station recorded significant annual increasing slope of 0.02°C. Figure **8** and Figure 9 show the trends of annual hydro-climatic variables.

Table 14. Modified Mann Kendall, Pettitt's test and SNHT statistics of annual hydro-climatic variables and hydropower in the NRB

Variables	Modified Mann Kendall trend test			Pettitt's test		SNHT	
	trend	p-value	Sen's slope	change	year	change	year
Mean Basin Rainfall (mm)	+	**0.02** [c]	5.27	Yes	2007	No	---
Ouagadougou Rainfall (mm)	+	**0.01** [c]	6.17	Yes	2007	Yes	2008
Ouagadougou Tmin (°C)	+	**0.000** [a]	0.04	Yes	1997	Yes	1996
Ouagadougou Tmax (°C)	+	**0.000** [a]	0.03	Yes	2001	Yes	1995
Ouahigouya Rainfall (mm)	+	**0.006** [b]	8.77	Yes	2006	Yes	2006
Ouahigouya Tmin (°C)	+	**0.008** [b]	0.02	Yes	2003	Yes	2003
Ouahigouya Tmax (°C)	+	**0.03** [c]	0.02	No	---	Yes	1995
Lake evaporation (hm^3)	+	0.9	0.2	No	---	No	---
Inflow (hm^3)	+	**0.01** [c]	68.08	Yes	2006	No	---
Outflow (hm^3)	+	0.11	0.00	No	---	No	---
Water level (m)	+	0.53	0.01	No	---	No	---
Turbined flow (hm^3)	+	**0.03** [c]	17.99	Yes	2002	Yes	2002
Irrigation (hm^3)	+	**0.000** [a]	12.54	Yes	2006	Yes	2007
Hydropower generation (MWh)	+	**0.002** [b]	2168.26	Yes	2002	Yes	2002

Significance codes of confidence level: 100% 'a'; 99% 'b'; 95% 'c'

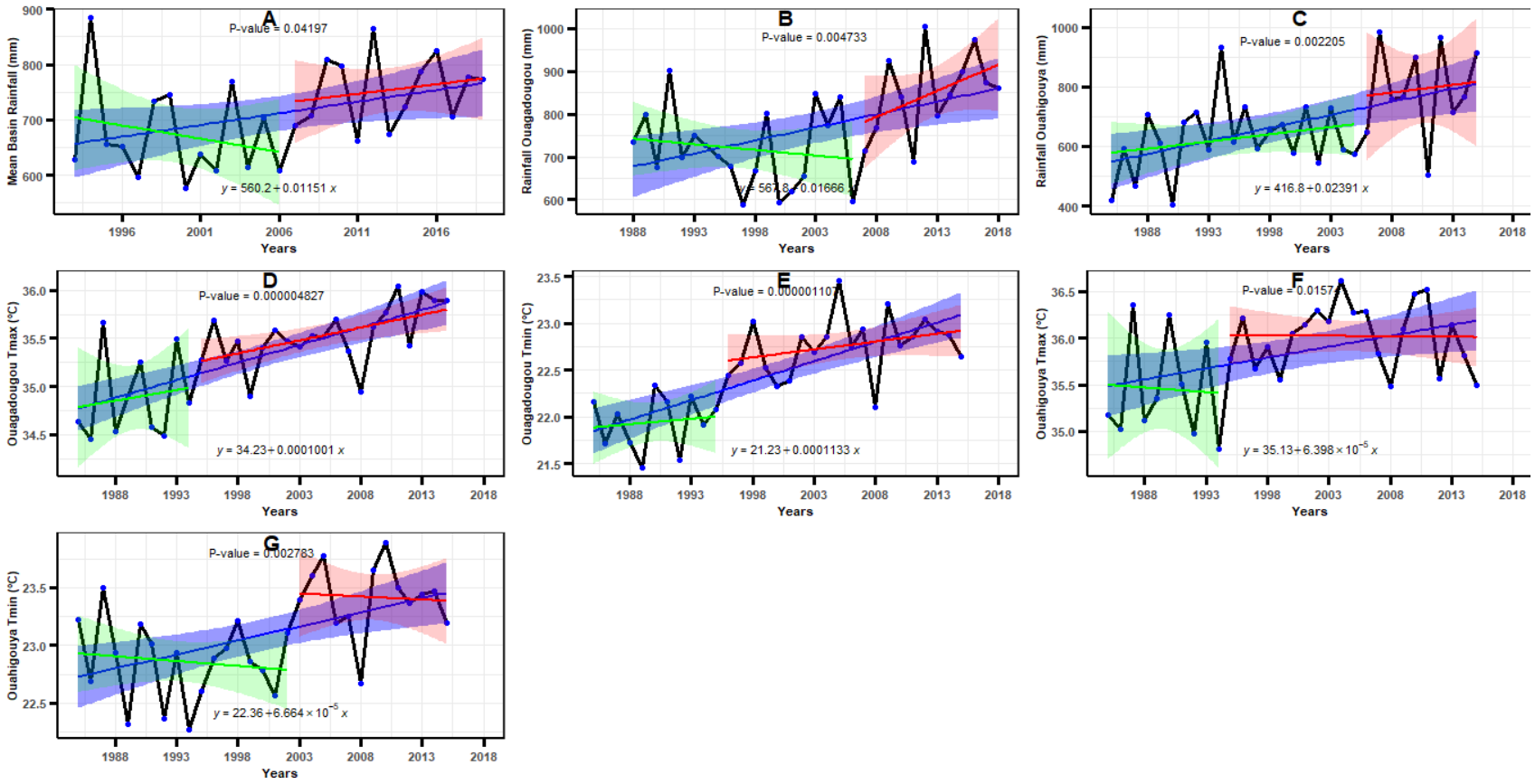

Figure 8. Annual trend of climatic variables: Mean basin rainfall (A); Rainfall at Ouagadougou station (B); Rainfall at Ouahigouya station (C); Maximum temperature at Ouagadougou station (D); Minimum temperature at Ouagadougou station (E); Maximum temperature at Ouahigouya station (F); Minimum temperature at Ouahigouya station (G). Blue line: trend over the whole time series; green line: trend before the break year; red line: trend after the break year. The blue, green and red shadows represent their respective confidence intervals (5-95%).

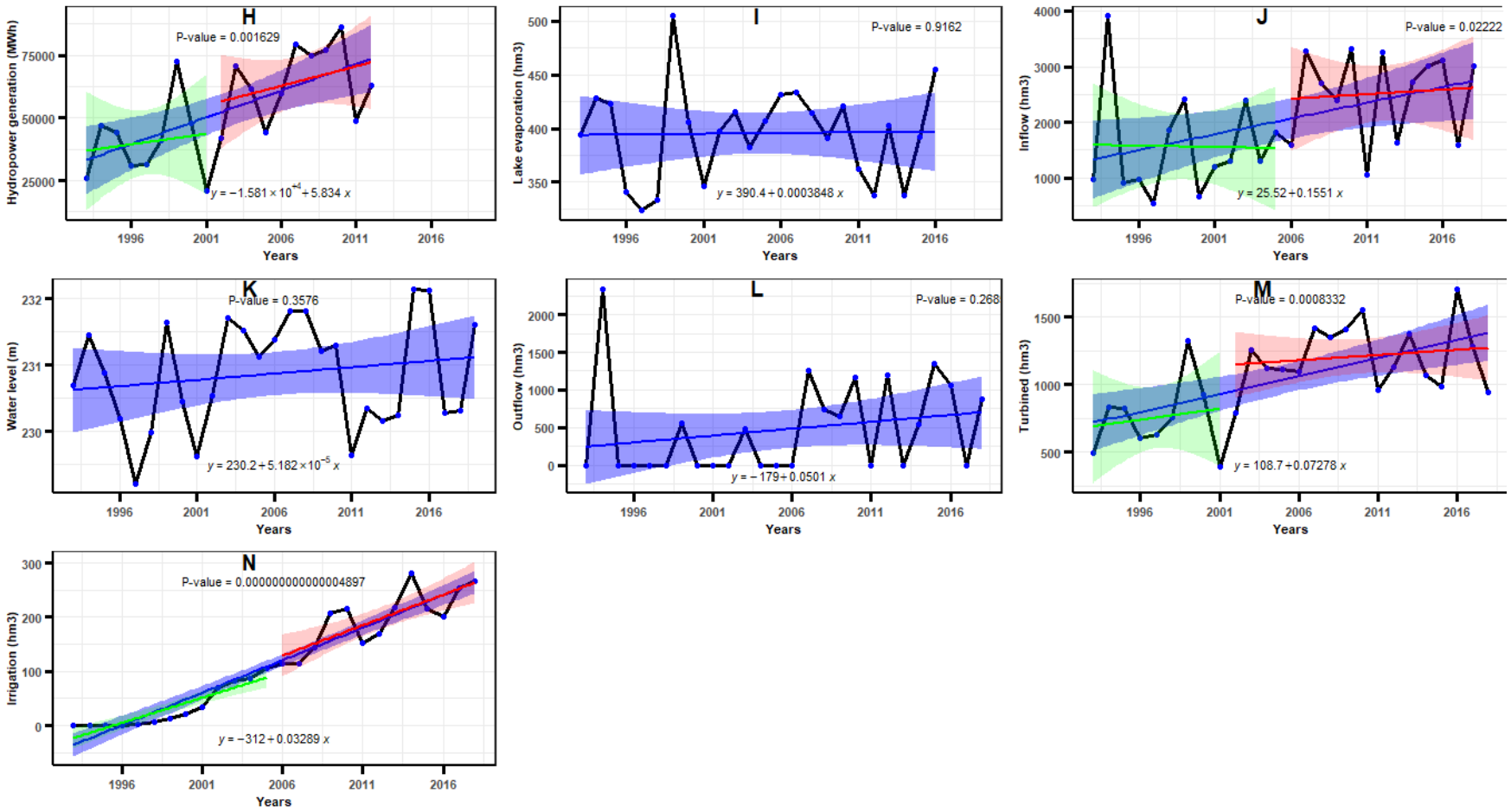

Figure 9. Annual trend of hydrological variables: Hydropower generation (H); Lake evaporation (I); Inflow (J); Water level (K); Outflow (L); Turbined flow (M); Irrigation (N). Blue line: trend over the whole time series; green line: trend before the break year; red line: trend after the break year. The blue, green and red shadows represent their respective confidence intervals (5-95%).

4.3. Trend analysis of monthly hydro-climatic variables and hydropower generation

The Modified Mann-Kendall trend test was performed for the monthly times series of all variables. Table **15** and Table **16** summarize the trend direction, the significance and the slope of each month over the variables and considered periods. Mean basin rainfall increased from May to October over the period 1985-2015. Only in the month of July rainfall increases significantly at 99% (Table **15**). At the station level, rainfall in Ouagadougou increased significantly in July and September (rainy season) while in Ouahigouya a significant increase in February (dry season) is observed. This significant increase of rainfall in the dry season has a negligible annual slope (Table **15**) and is therefore not relevant in terms of water balance. Minimum temperature increased in all months at the two stations whereas maximum temperature increased differently. In Ouagadougou, maximum temperature increased for all months while in Ouahigouya, it decreased from August to October, but not significantly.

For lake evaporation, significantly increasing trends were found for September and December, while for March, August and October non-significant increasing trends were found. Decreasing lake evaporation trends were found for January, February, from April to July and in November, but these were not significant. Meanwhile for inflow, the months of February to November show increasing trends between 1993 and 2018. However, significant trends are only noticed in May, July, August and September. During the same period, decreasing trends of mean lake water levels were found from March to July and increasing trends from August to February. Significant negative trends are observed in May and June, while significant positive trends were perceived in September and October (Table **16**). Outflow increased from August to October, with a significant increasing trend of water spill in September. The volume of irrigation water supply increased significantly for all months. The turbined flow and the hydropower generation increased for all months except in May and June, where it decreased. Turbined flow increased significantly in January, March and July to December while for hydropower generation, the months that showed significant increasing trends are February, March, and August to December.

Table 15. Modified Mann Kendall statistics of monthly climatic variables in the NRB

Climatic variables	Statistics	Jan	Feb	Mar	Apr	May	Jun	Jul	Aug	Sep	Oct	Nov	Dec
Mean Basin Rainfall (mm)	Trend	+	+	-	-	+	+	+	+	+	+	-	+
	p-value	0.06	0.6	0.59	0.56	0.94	0.69	**0.01** [c]	0.10	0.09	0.35	0.27	0.88
	Sen's slope	0.001	0.001	-0.02	-0.08	0.02	0.17	1.90	1.23	0.97	0.21	-0.003	0.0009
Ouagadougou Rainfall (mm)	Trend	+	+	+	-	+	+	+	+	+	-	-	-
	p-value	0.24	0.07	0.37	0.34	0.27	0.38	0.05 [c]	0.34	**0.04** [c]	0.25	0.39	0.68
	Sen's slope	00	00	00	-0.37	0.56	0.53	1.76	1.07	2.23	-0.48	00	-0.4
Ouagadougou Tmin (ºC)	Trend	+	+	+	+	+	+	+	+	+	+	+	+
	p-value	0.5	0.06	0.1	0.07	**0.02** [c]	**0.000** [a]	**0.004** [b]	**0.001** [b]	**0.007** [b]	**0.000** [a]	0.11	0.3
	Sen's slope	0.02	0.06	0.03	0.03	0.03	0.06	0.03	0.04	0.02	0.06	0.04	0.03
Ouagadougou Tmax (ºC)	Trend	+	+	+	+	+	+	+	+	+	+	+	+
	p-value	0.29	**0.04** [c]	**0.008** [b]	0.11	0.9	**0.005** [b]	**0.02** [c]	**0.05** [c]	0.11	0.08	0.01	0.07
	Sen's slope	0.03	0.05	0.05	0.02	0.001	0.04	0.04	0.02	0.02	0.02	0.04	0.05
Ouahigouya Rainfall (mm)	Trend	+	+	+	+	-	+	+	+	+	+	-	+
	p-value	0.9	**0.05** [c]	0.9	0.7	0.5	0.1	0.4	0.29	0.09	0.28	0.29	0
	Sen's slope	00	00	00	00	-0.3	2.03	1.05	2.4	1.97	0.76	00	0
Ouahigouya Tmin (ºC)	Trend	+	+	+	+	+	+	+	+	+	+	+	+
	p-value	0.7	0.3	0.3	**0.04** [c]	**0.01** [c]	0.08	**0.007** [b]	**0.01** [c]	0.3	**0.01** [c]	0.09	0.24
	Sen's slope	0.01	0.03	0.02	0.03	0.04	0.02	0.03	0.02	0.009	0.03	0.03	0.03
Ouahigouya Tmax (ºC)	Trend	+	+	+	+	+	+	+	-	-	-	+	+
	p-value	0.26	0.17	**0.004** [b]	**0.03** [c]	0.29	0.13	0.8	0.62	0.49	0.78	**0.03** [c]	0.2
	Sen's slope	0.03	0.04	0.06	0.03	0.01	0.03	0.001	-0.01	-0.02	-0.007	0.03	0.04

Significance codes of confidence level: 100% 'a'; 99% 'b'; 95% 'c'

Table 16. Modified Mann Kendall statistics of monthly hydrological variables in the NRB

Hydrological variables	Statistics	Jan	Feb	Mar	Apr	May	Jun	Jul	Aug	Sep	Oct	Nov	Dec
Inflow (hm^3)	Trend	***	+	+	+	+	+	+	+	+	+	+	***
	p-value	0	0.1	0.7	0.19	**0.003** [b]	0.27	**0.03** [c]	**0.02** [c]	**0.01** [c]	0.2	0.09	0
	Sen's slope	0	0	0	0.09	2.15	1.2	11.99	29.4	26.58	2.36	0	0
Outflow (hm^3)	Trend	***	***	***	***	***	***	***	+	+	+	***	***
	p-value	0	0	0	0	0	0	0	0.13	**0.04** [c]	0.84	0	0
	Sen's slope	0	0	0	0	0	0	0	0	0	0	0	0
Water level (m)	Trend	+	+	-	-	-	-	-	+	+	+	+	+
	p-value	0.49	0.6	0.6	0.07	**0.03** [c]	**0.006** [b]	0.29	0.13	**0.017** [c]	**0.008** [b]	0.07	0.2
	Sen's slope	0.02	0.01	-0.01	-0.06	-0.086	-0.071	-0.02	0.07	0.09	0.05	0.05	0.05
Lake evaporation (hm^3)	Trend	-	-	+	-	-	-	-	+	+	+	-	+
	p-value	0.82	0.28	0.70	0.53	0.22	0.08	0.63	0.07	**0.007** [b]	0.53	0.47	**0.02** [c]
	Sen's slope	-0.06	-0.31	0.11	-0.24	-0.30	-0.30	-0.04	0.37	0.30	0.17	-0.21	0.80
Irrigation (hm^3)	Trend	+	+	+	+	+	+	+	+	+	+	+	+
	p-value	**0.000** [a]	**0.000** [a]	**0.000** [a]	**0.000** [a]	**0.000** [a]	**0.000** [a]	**0.002** [b]	**0.000** [a]	**0.000** [a]	**0.000** [a]	**0.009** [b]	**0.005** [b]
	Sen's slope	0.53	1.05	1.57	1.57	1.94	0.67	0.21	0.52	0.74	0.58	0.32	0.32
Turbined flow (hm^3)	Trend	+	+	+	+	-	-	+	+	+	+	+	+
	p-value	**0.02** [c]	0.07	**0.02** [c]	0.27	0.41	0.27	**0.02** [c]	**0.000** [a]	**0.000** [a]	**0.005** [b]	**0.001** [b]	**0.001** [b]
	Sen's slope	1.88	1.82	2.40	1.27	-1.15	-0.97	2.31	4.75	4.91	3.78	3.65	3.23
Hydropower generation (MWh)	Trend	+	+	+	+	-	-	+	+	+	+	+	+
	p-value	0.07	**0.05** [c]	**0.04** [c]	0.58	0.77	0.82	0.20	**0.02** [c]	**0.001** [b]	**0.001** [b]	**0.001** [b]	**0.01** [c]
	Sen's slope	158.54	166.66	201.34	52.9	-30.36	-16.82	81.75	272.09	427.21	421.42	341.31	270.74

Significance codes of confidence level: 100% 'a'; 99% 'b'; 95% 'c'; '***' No trend

4.4. Relationship between hydro-climatic variables, ENSO and hydropower generation

The results of the Spearman correlation test showed that all correlation coefficients between annual hydropower generation and hydro-climatic variables vary from 0.49 to 0.98 (Table **17**). The hydropower generated at the Bagré dam over the period 1993-2012 is very strongly correlated to turbined flow, strongly correlated to irrigation, water level, outflow and inflow, while correlation with mean basin rainfall and lake evaporation is moderate. The results show that with annual increasing inflow and water level, annual hydropower generation increases. This can be observed in the monthly trends where the simultaneous increase of inflow and water level leads to a significant increase of hydropower generation from August to December (Table **16**).

Table 17. Spearman correlation coefficient between annual hydropower generation and hydro-climatic variables.

Hydro-climatic variables	MBR	Infl	Evap	WL	Outf	Irr	Turb
HP	0.49	0.68	0.55	0.73	0.5	0.71	0.98

MBR = Mean Basin Rainfall (mm); Infl = Inflow (hm^3); Evap = Lake Evaporation (hm^3); WL = Water Level (m); Outf = Outflow (hm^3); Irr = Irrigation (hm^3); Turb = Turbined flow (hm^3); HP = Hydropower generation (MWh).

The monthly hydropower generation anomaly is less correlated to ENSO index (-0.23) (Figure **10**), but the correlation is significant. The correlation coefficient between ENSO index and mean basin rainfall and inflow anomalies are negligible (0.02, -0.05). This indicates the need to investigate on the ENSO indices and classification methods in the prediction of rainfall, inflow and hydropower generation in the study area.

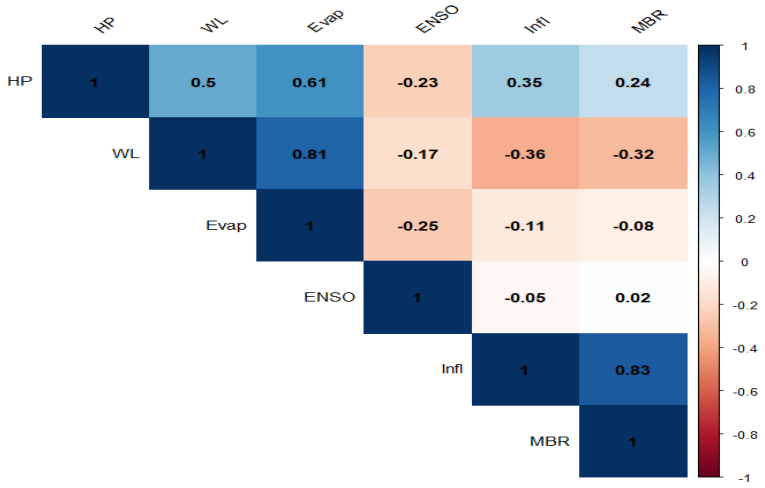

Figure 10. Correlation coefficients between the hydro-climatic variables, ENSO and hydropower generation anomalies. MBR = Mean Basin Rainfall (mm); Infl = Inflow (hm^3);

Outf = Outflow (hm^3); Evap = Lake Evaporation (hm^3); WL = Water Level (m); HP = Hydropower generation (MWh)

For a detailed investigation of the relationship between monthly hydropower anomaly and ENSO index, Figure 11 shows that during El Niño phases in 1997 and 2002, there was a decrease in hydropower generation. In opposite, during La Niña phases in 1999, 2000, 2008-2009 and 2011, there was an increase of hydropower generation. During El Niño events of 1995, 2007 and 2010, the hydropower generation was abundant while it fell short during La Niña years of 1996 and 2006. This necessitates a thorough examination of reservoir management.

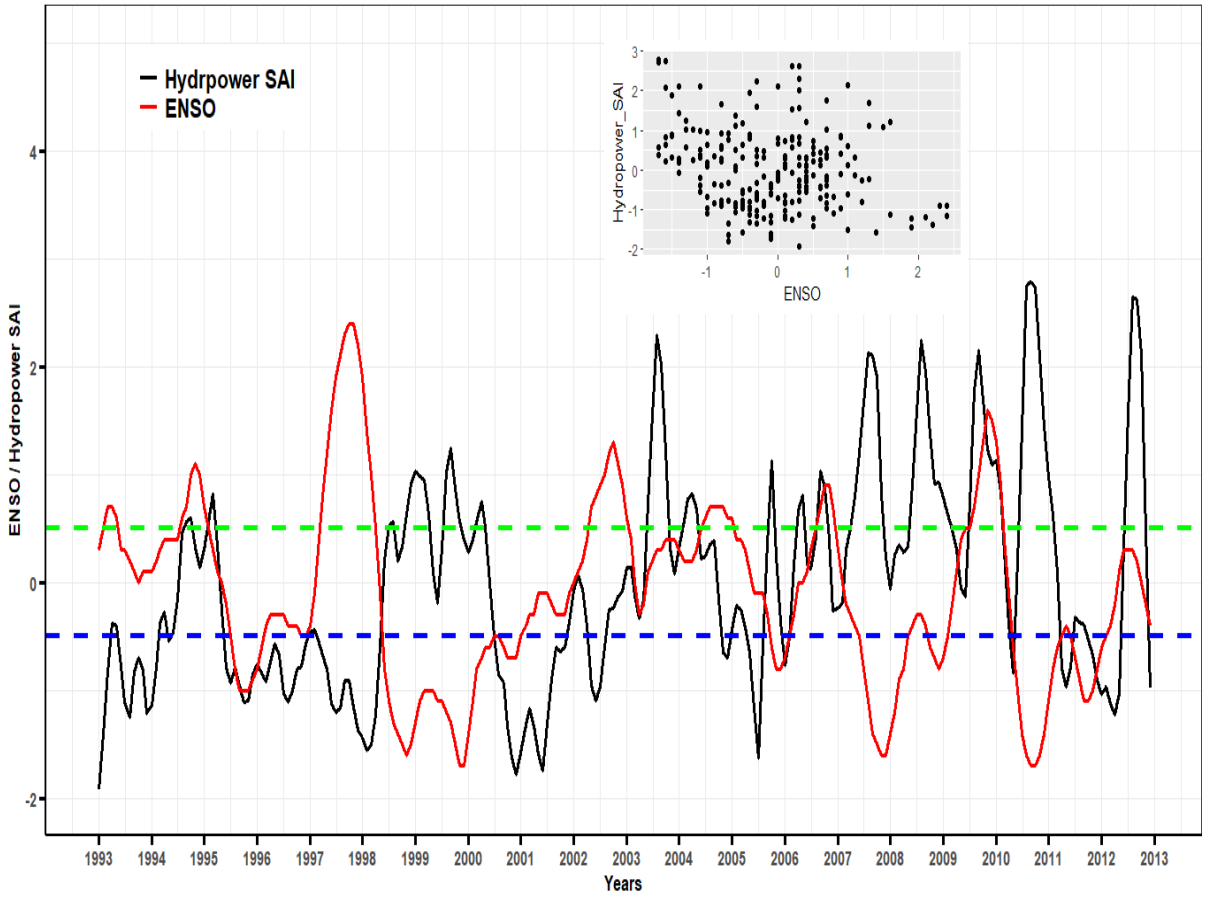

Figure 11. Comparison of ENSO index and hydropower generation anomaly. El Niño phases are greater than 0.5 (above the green dash line); La Niña phases are less than -0.5 (below the blue dash line).

4.5. Discussion

The results in this study show the ability of W5E5 to reproduce the climate variables in the NRB. Besides, there was an annual increasing trend for all climatic variables analysed from

1985-2015. The slope of the mean basin rainfall increased by 158 mm in 30 years (1985-2015). This increase is higher in the northern part (263 mm in Ouahigouya) than the southern part (185 mm in Ouagadougou). As found by Lebel and Ali (2009) and Sanogo et al. (2015), after the dry 1970s some parts of West Africa have experienced a return to wetter conditions in the 1990s and 2000s. Several studies are in agreement with the findings carried out with the Modified Mann-Kendall trend test. Sylla et al. (2016) found an increasing rainfall trend in Burkina Faso over 1983-2010. A similar study of Ibrahim (2012) also showed that annual rainfall in Burkina Faso has increased by about 15% over 1991-2009 compared to 1971-1990. In the Black Volta, the results of the Mann-Kendall trend test showed that annual rainfall increased significantly over 1980-2010 (Aziz and Obuobie, 2017).

Although annual rainfall and inflow show a significant positive trend, increase in annual mean lake water level was found to be not significant. This is a consequence of operator decision-making and dam design specifications (Jia et al., 2017). Indeed, outflow and turbined flow increased between 1993 and 2018. The increase in outflow resulted in flooding recurrence of some villages downstream in Burkina Faso and Ghana (UNEP-GEF Volta Project, 2013). Likewise, from 1996 onwards the increasing withdrawals for irrigated areas developed downstream are directly taken from the Bagré reservoir, and are not exploitable for hydropower generation. This is supported by Yanogo (2012), who indicated that irrigated areas have been developed in the upstream and downstream areas of the Bagré dam since 1997.

The overall positive annual trends found for hydro-climatic variables seem to be profitable to hydropower generation at the Bagré dam. The electricity output doubled from 1993 to 2012 (Figure 9). In addition, the mean electricity output generated by the dam is about 53 GWh per year compared to the planned 44 GWh per year (Kaboré and Bazin, 2014). The feasibility study of the dam construction was done in the 1970s when rainfall in the basin was low (Mahé et al., 2005). The results of the study are in disagreement with those of Machina and Sharma (2017) who found a decrease of hydropower generation at the Kainji dam (Nigeria) although inflow increased between 2009 and 2011. This decrease could be explained by the increase of withdrawals for irrigation.

At the monthly scale, the study highlighted a decreasing trend of hydropower generation and turbined flow in May and June. This is mainly due to the prioritization of agricultural activities. Indeed, irrigation withdrawals increased significantly in May and June, with May being the month recording the highest slope (1.94 hm^3 per year). In fact, during these months the

evapotranspiration is high due to a combined increase of minimum and maximum temperatures (Table **15**), as also observed in the neighbouring Black Volta Basin (Abungba et al., 2020; Neumann et al., 2007) and over West Africa (Kabo-Bah et al., 2016; Koubodana et al., 2020; Oguntunde and Abiodun, 2013; Touré et al., 2017). This led to higher crop water demand and need for additional irrigation withdrawals, decreasing water levels although an increase of inflow is observed in May and June. These months also correspond to the cessation of the dry season and the onset of the rainy season in the Sahel region (Sanogo et al., 2015), where many water bodies are almost dried out. The strong correlation coefficients between irrigation (0.73), water level (0.72), and inflow (0.68) with hydropower generation confirm the above-mentioned explanation. Several studies also confirmed that the variability of rainfall, inflow and water level influenced hydropower generation (Boadi and Owusu, 2017; Kabo-Bah et al., 2016; Kaunda et al., 2012; Perera and Rathnayake, 2019). Interestingly, hydropower generation is less correlated with mean basin rainfall (0.49) which should be the main driver for inflows. Several small dams were built in the upstream basin (Karambiri et al., 2011; Mahe et al., 2005) and might have impacted the inflow. This indicates the need for further studies on the role of LULCC in runoff generation in the NRB, as Mahe et al. (2002) also found an increase of runoff in the upper NRB at Wayen station in the 1990s, despite a decrease of rainfall.

Furthermore, hydropower generation anomaly is less correlated to ENSO index but is statistically significant (p-value < 0.05). This finding is also supported by Jia et al. (2017) who stated that hydropower generation correlates significantly with Multivariate ENSO Index for 27% of reservoirs in the world. Moreover, Boadi and Owusu (2017) using 5-month running mean of spatially averaged sea surface temperature anomalies over the tropical Pacific (4°S–4°N, 150°W–90°W) found that ENSO is significantly correlated to hydropower generation at the Akosombo plant in the lowermost part of the Volta basin from 1991-2010. They further emphasized that ENSO index is a good predictor for hydropower generation at the Akosombo plant. Though, despite the significance the correlation between hydropower generation anomaly and ENSO index found in the NRB is weak (-0.23) and is inversely proportional to the correlation between hydropower generation and rainfall anomalies (0.24). The low correlation could be due to the datasets used and the method of hydro-climatic variables anomalies calculation. In fact, the magnitude of hydro-climatic anomalies could change significantly depending on the dataset used, the method of anomalies estimation and the phase of ENSO (Salas Parra, 2020). It could also be due to the short records of hydropower generation (1993-

2012) as it limits the prospects for finding robust ENSO-driven anomalies in hydropower generation (Jia et al., 2017).

4.6. Partial conclusion

The impact of hydro-climatic trends and upstream dam management on hydropower generation in the NRB was investigated in this chapter. On the annual scale, all hydro-climatic variables increased significantly, except for water level, lake evaporation and outflow. This increase, combined with the construction of the Ziga dam and its management change, impacted positively the annual inflow and hydropower generation at the Bagré dam. However, the monthly trend analysis showed that hydropower generation decreases each May and June due to the significant increase in water withdrawals for irrigation. The results ultimately show that annual hydro-climatic variables can moderately be used to predict hydropower generation. However, as the climate and land-use change simultaneously occur in the basin, there is a need to assess the dynamics of LULC in the basin.

CHAPTER 5: PAST AND FUTURE LAND USE LAND COVER DYNAMICS IN THE NAKAMBÉ RIVER BASIN

This chapter presents the findings of the past and future LULC dynamics in the NRB. First of all, the accuracy of the LULC classification is presented. Moreover, past LULC maps and their change statistics, and the conversion of anthropogenic land uses are inspected. Furthermore, the results of future LULC are presented. Lastly, the different results are discussed.

5.1. Accuracy of Land Use and Land Cover Classification

The results of the classification have an overall accuracy varying from 81% to 93% and the Kappa coefficients are 91%, 82% and 76% for 1990, 2005 and 2020, respectively. Table 18, Table 19
Table 20 show the statistics of the confusion matrix for LULC of 1990, 2005 and 2020, respectively.

Table 18. Confusion matrix of the LULC classification in 1990

LULC 1990	Water body	Woodland	Shrubland	Cropland	Bare land/built-up
Water body	**100.0**	0.0	0.0	0.0	0.0
Woodland	0.0	**85.4**	14.6	0.0	0.0
Shrubland	0.0	5.2	**94.8**	0.0	0.0
Cropland	0.0	0.0	3.9	**94.1**	2.0
Bare land/built-up	0.0	0.0	0.0	2.0	**98.0**

Table 19. Confusion matrix of the LULC classification in 2005

LULC 2005	Water body	Woodland	Shrubland	Cropland	Bare land/built-up
Water body	**100.0**	0.0	0.0	0.0	0.0
Woodland	0.0	**66.7**	33.3	0.0	0.0
Shrubland	0.0	14.3	**85.7**	0.0	0.0
Cropland	0.0	0.0	7.7	**76.9**	15.4
Bare land/built-up	0.0	0.0	0.0	2.7	**97.3**

Table 20. Confusion matrix of the LULC classification in 2020

LULC 2020	Water body	Woodland	Shrubland	Cropland	Bare land/built-up
Water body	**100.0**	0.0	0.0	0.0	0.0
Woodland	0.0	**62.5**	37.5	0.0	0.0
Shrubland	0.0	0.0	**66.7**	33.3	0.0
Cropland	0.0	0.0	0.0	**87.5**	12.5
Bare land/built-up	0.0	0.0	0.0	20.0	**80.0**

In Tables 18-20, the bold values represent the percentage of fitted pixels for each row while the non-bold represent the percentage of confusion with the other LULC classes represented in the corresponding column

5.2. Land Use and Land Cover maps in 1990, 2005, and 2020

The results of the LULC maps of 1990, 2005 and 2020 are shown in Figure 12 and Table 21. In 1990, the NRB was mainly covered by shrubland (44%) and cropland (36%). These were followed by bare land/built-up, woodland and water bodies with coverages of 16%, 3% and 0.5% respectively. By contrast, in the year 2005 the order was reversed. Cropland and shrubland covered 49% and 29%, respectively. As in 1990, woodland and water bodies were the less represented LULC. In 2020, the basin's land cover was dominated by cropland (54%), followed by bare land/built-up (29%) and shrubland (14%). From 1990 to 2020, the natural vegetation has given place to anthropogenic land uses (cropland and bare land/built-up) (Figure 12).

Table 21. Proportion of LULC units in 1990, 2005 and 2020

LULC units	1990		2005		2020	
	km^2	%	km^2	%	km^2	%
Water body	131	0.40	202	0.62	436	1.34
Woodland	946	2.90	646	1.98	522	1.60
Shrubland	14,491	44.4	9,500	29.1	4,652	14.3
Cropland	11,739	36.0	15,950	48.9	17,691	54.2
Bare land/Built-up	5,316	16.3	6,326	19.4	9,322	28.6
Total	32,623	100.0	32,623	100.0	32,623	100.0

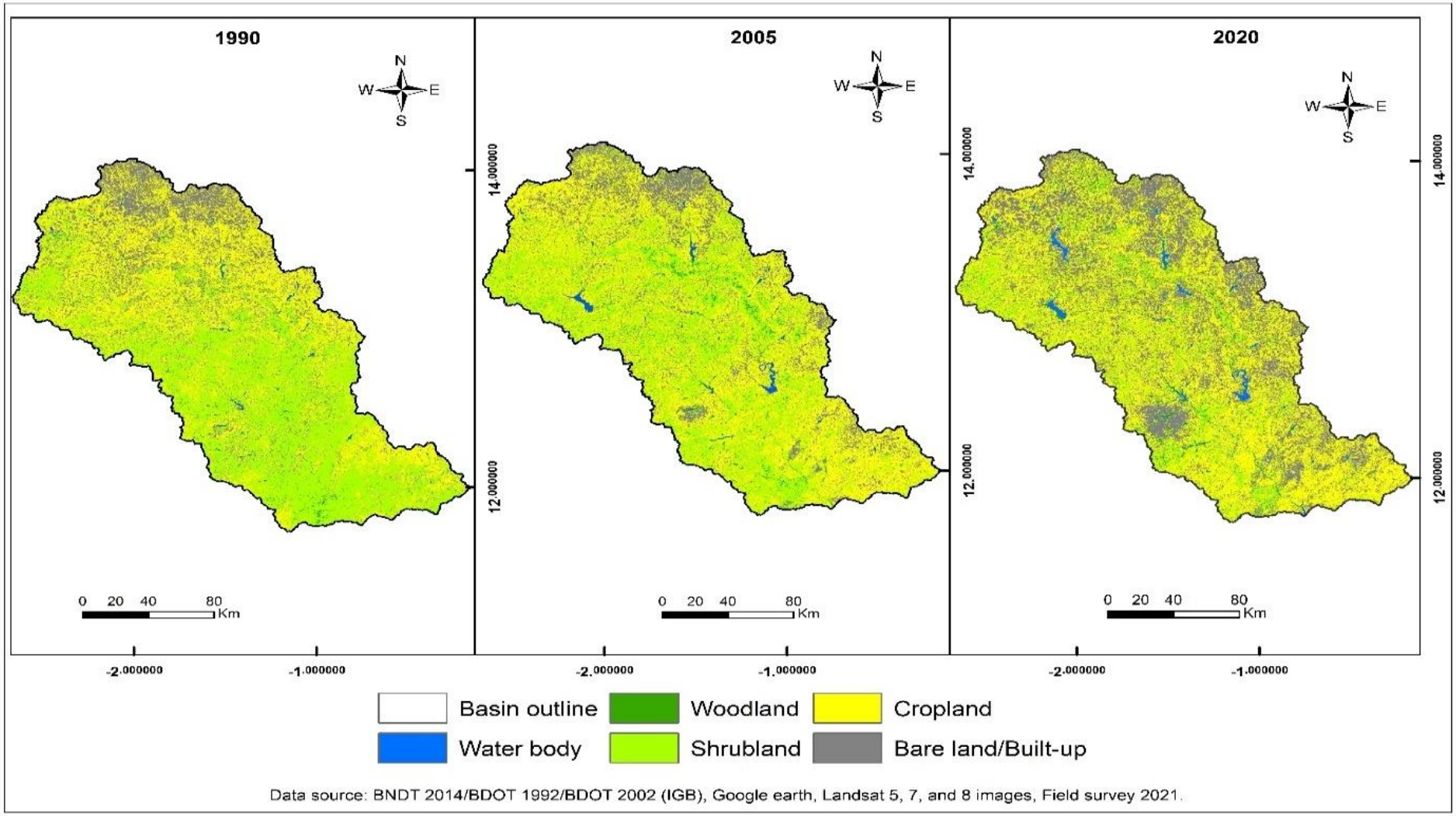

Figure 12. LULC maps of 1990, 2005, and 2020

5.3. Changes in Land Use and Land Cover between 1990-2005, 2005-2020, and 1990-2020

During 1990-2020, losses and gains were observed in LULC units. For the first fifteen years (1990-2005), the LULC classes that decreased were woodland (-32%) and shrubland (-34%), while water bodies, cropland, and bare land/built-up increased by 54%, 36%, and 19%, respectively (Figure 13). From 2005–2020, the same dynamics were noticed, with different percentages of change. Woodland and shrubland decreased by 19% and 51%, respectively, while an increase of 116%, 11%, and 47% was observed for water bodies, cropland, and bare land/built-up, correspondingly. The high increase in water bodies' area is due to the construction of the Ziga and Dourou dams (275 million m^3). Overall, during the last 31 years, the NRB experienced an increase in water bodies (233%), cropland (51%), and bare land/built-up (75%). These increases were at the expense of woodland and shrubland, which decreased by -45% and -68%, respectively, from 1990-2020 (Figure 13).

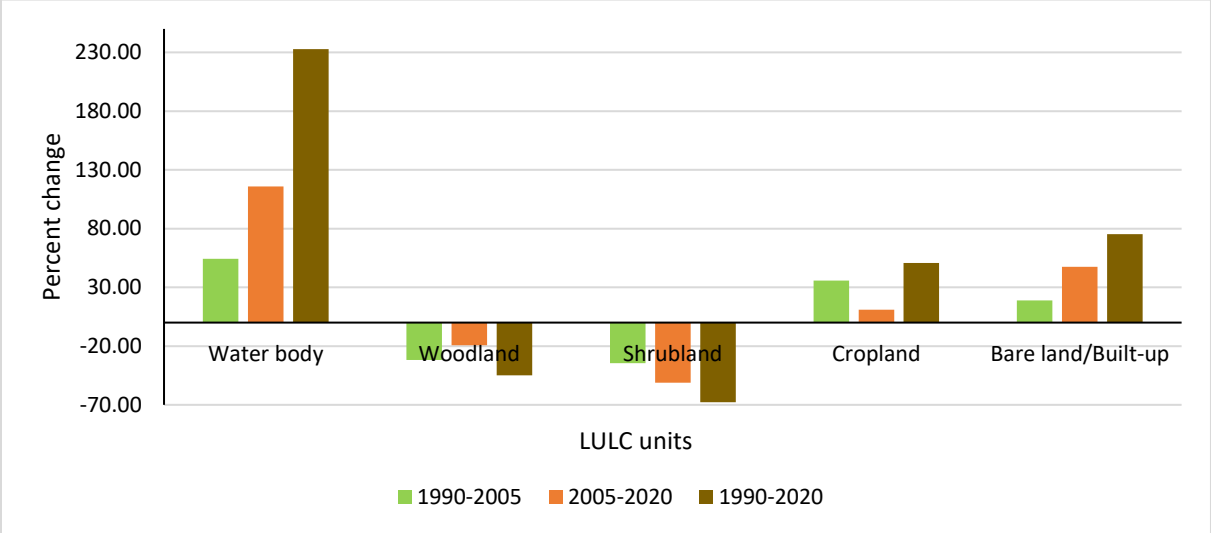

Figure 13. Percent of changes of LULC units between 1990-2005, 2005-2020, and 1990-2020

5.4. Contributors to cropland and bare land/built-up increase

The contributors to the increase in cropland and bare land/built-up are shown in Figure 14. During the period 1990-2005, the increase in cropland could mostly be attributed to the decrease in shrubland of 3,200 km^2 while the increase in bare land/built-up could be attributed to the decrease in cropland of 900 km^2. However, from 2005 to 2020 almost 4,000 km^2 of shrubland were transformed to cropland, even though more than 3,000 km^2 of the existing cropland in 2005 had been transformed into bare land/built-up in 2020. This is illustrated in Figure 14 as the gains in bare land/built-up between 2005 and 2020 are typically from cropland and

shrubland, respectively. Overall, from 1990-2020, the increase in cropland could be attributed to the major loss of 6,000 km^2 of shrubland, representing 19% of the total area. Meanwhile, the increase in bare land/built-up from 2005-2020 could be attributed to the losses in cropland (2,000 km^2) and shrubland (1,800 km^2) areas.

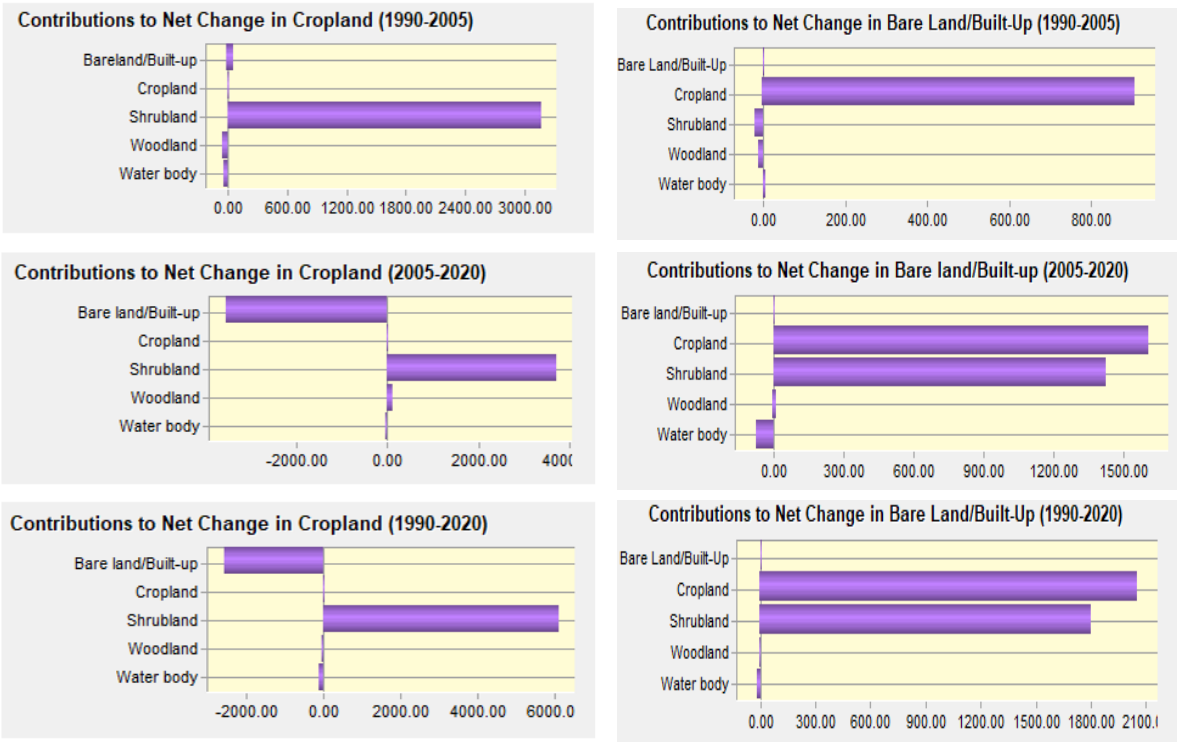

Figure 14. Contribution to net changes in cropland and bare land/built-up (in km^2) for 1990-2005, 2005-2020 and 1990-2020.

5.5. Spatial trend of anthropogenic land uses

The spatial trend of other land use conversions to cropland and bare land/built-up from 1990 to 2005 and 2005 to 2020 are shown in Figure 15 and Figure **16**. It can be observed that the transformation of other LULC classes to cropland and bare land/built-up is South-Eastward from 1990-2005 while during the period 2005-2020, the conversion trend is North-Westward. Also, there is a strong correlation between cropland and bare land/built-up classes. During the first fifteen years, the intensity of change was higher for cropland (0.4) than for bare land/built-up (0.15), whereas from 2005 to 2020, the amplitude of change for cropland (0.24) and bare land/built-up (0.26) was quiet the same (Figure 15 and Figure **16**).

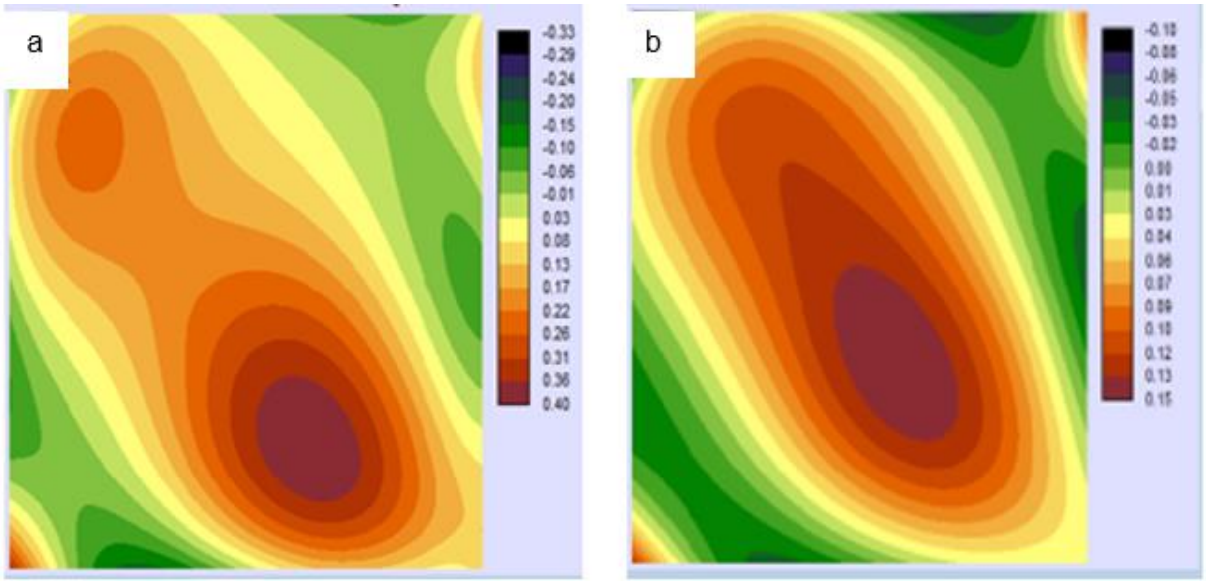

Figure 15. Spatial trend of conversion from all LULC classes to cropland (a) and bare land-built-up (b) during the period 1990-2005. Negative values represent a reverse spatial development for the analysed trend, whereas increasing positive values characterize an increasing intensity for the analysed trend.

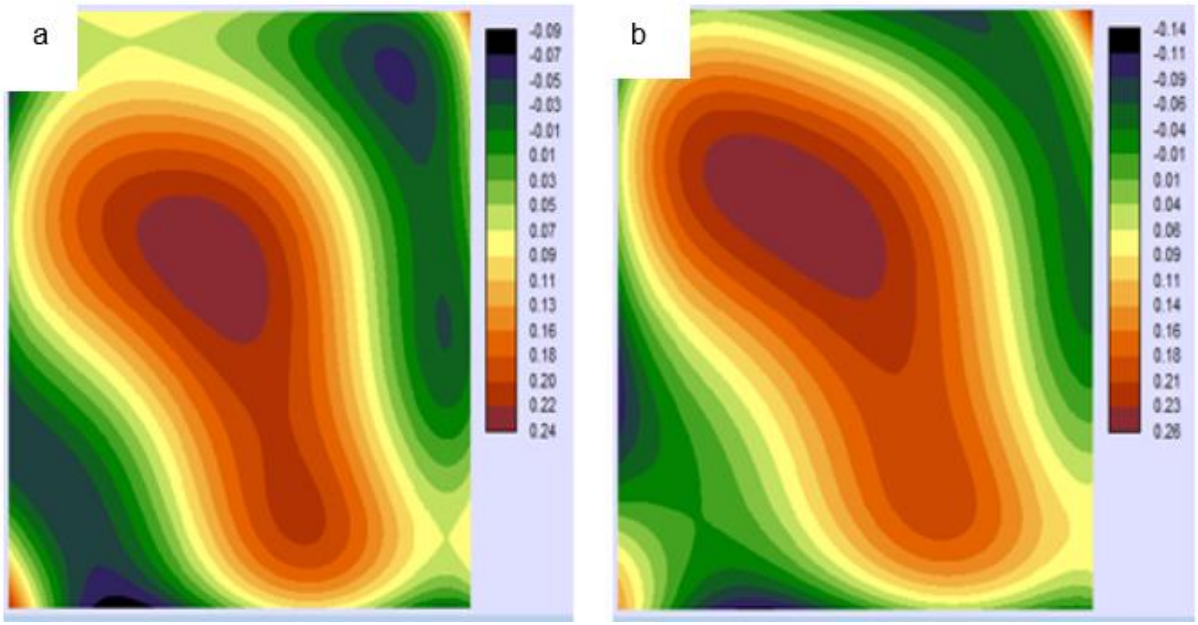

Figure 16. Spatial trend of conversion from all LULC classes to cropland (a) and bare land-built-up (b) during the period 2005-2020. Negative values represent a reverse spatial development for the analysed trend, whereas increasing positive values characterize an increasing intensity for the analysed trend.

5.6. Land use change driver variables and potential transition mapping

Four driver variables (Figure 17) were used to run the potential transition from one class to another. The model succeeded in creating the potential transition maps with an acceptable accuracy rate of 76% (Eastman, 2020). The results also highlight the relationship between the

driver variables and land use change during the period 1990-2005. Indeed, the evidence likelihood was found to be the most influential variable (0.5) driving the land use change, while the distance to rivers was found as least influential variable (0.23).

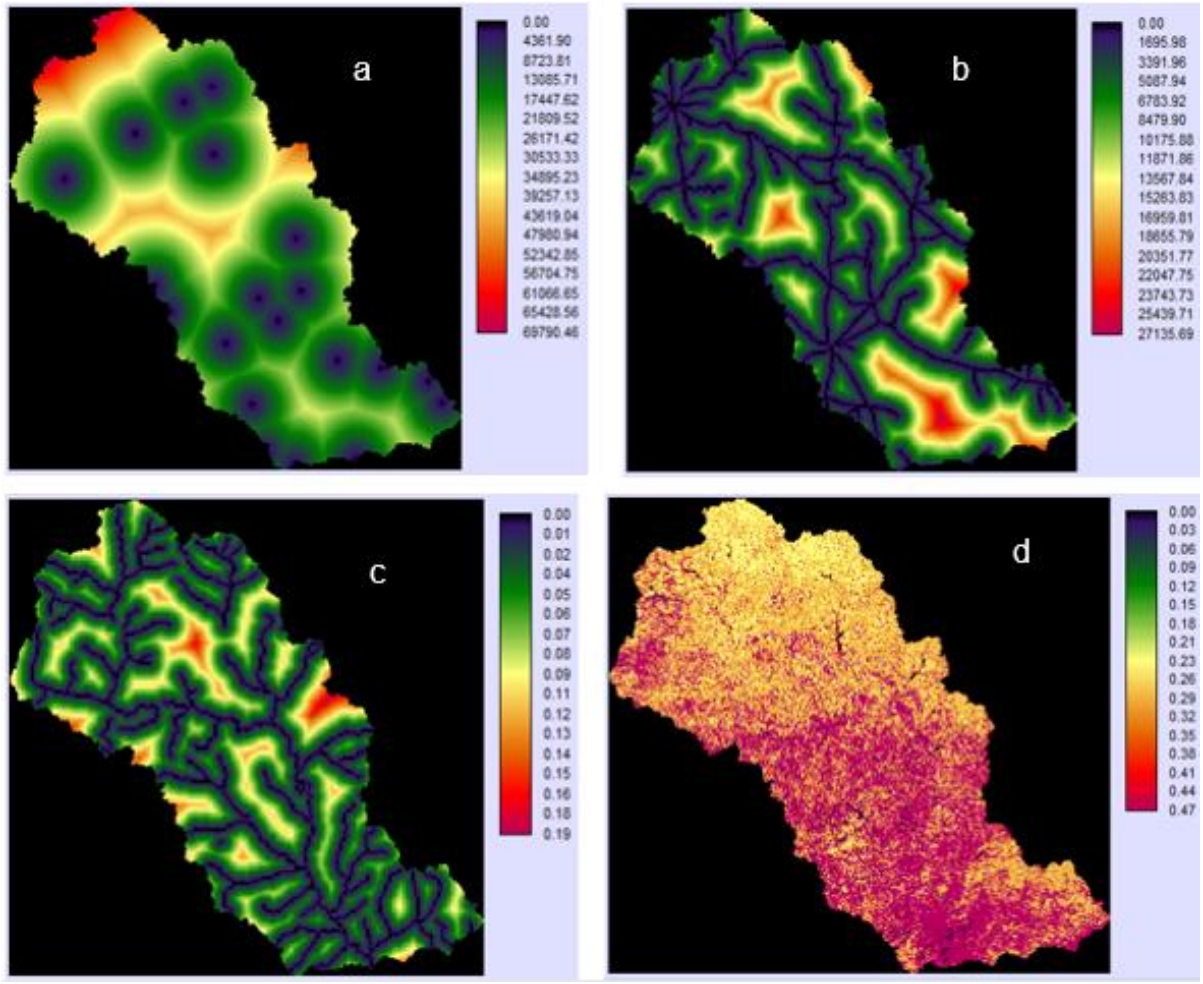

Figure 17. Explanatory variables used for the transition potential mapping (a) Distance to urban, (b) Distance to roads, (c) Distance to rivers, (d) Evidence Likelihood.

5.7. LULC model validation

The results of the comparison between the actual and simulated LULC maps of 2020 showed a K_{no} of 0.86 and a $K_{locality}$ of 0.85, indicating the model's ability to project the LULC of 2020 although there are some slight differences between the two maps (Figure 18). The model tends to overestimate bare land/built-up, shrubland, and woodland areas while it underestimates water bodies and cropland areas (Table **22**). For instance, the difference between the simulated and the classified bare land/built-up is 2,276 km^2, indicating an error of 24.4%. As for cropland, the area of the simulated map (14,936 km^2) is less than the classified map (15,950 km^2), showing an error of 5.7% (Table **22**). The great difference between the simulated and classified water

bodies' class are be due to the fact that the simulation was done with LULC maps (1990 and 2005) before Tougou and Seguenega dams' construction.

Table 22. Proportion of classified and simulated LULC units in 2020 and their associated errors

LULC units	Classified 2020		Simulated 2020		Error (difference between simulated 2020 and classified 2020)	
	km^2	%	km^2	%	km^2	%
Water body	436	1.34	235	0.72	-201	46.1
Woodland	522	1.60	660	2.33	138	26.4
Shrubland	4,652	14.3	5,091	15.6	439	9.44
Cropland	15,950	48.9	15,039	45.8	-911	5.71
Bare land/Built-up	9,322	28.6	11,598	35.5	2276	24.4
Total	32,623	100.0	32,623	100.0		

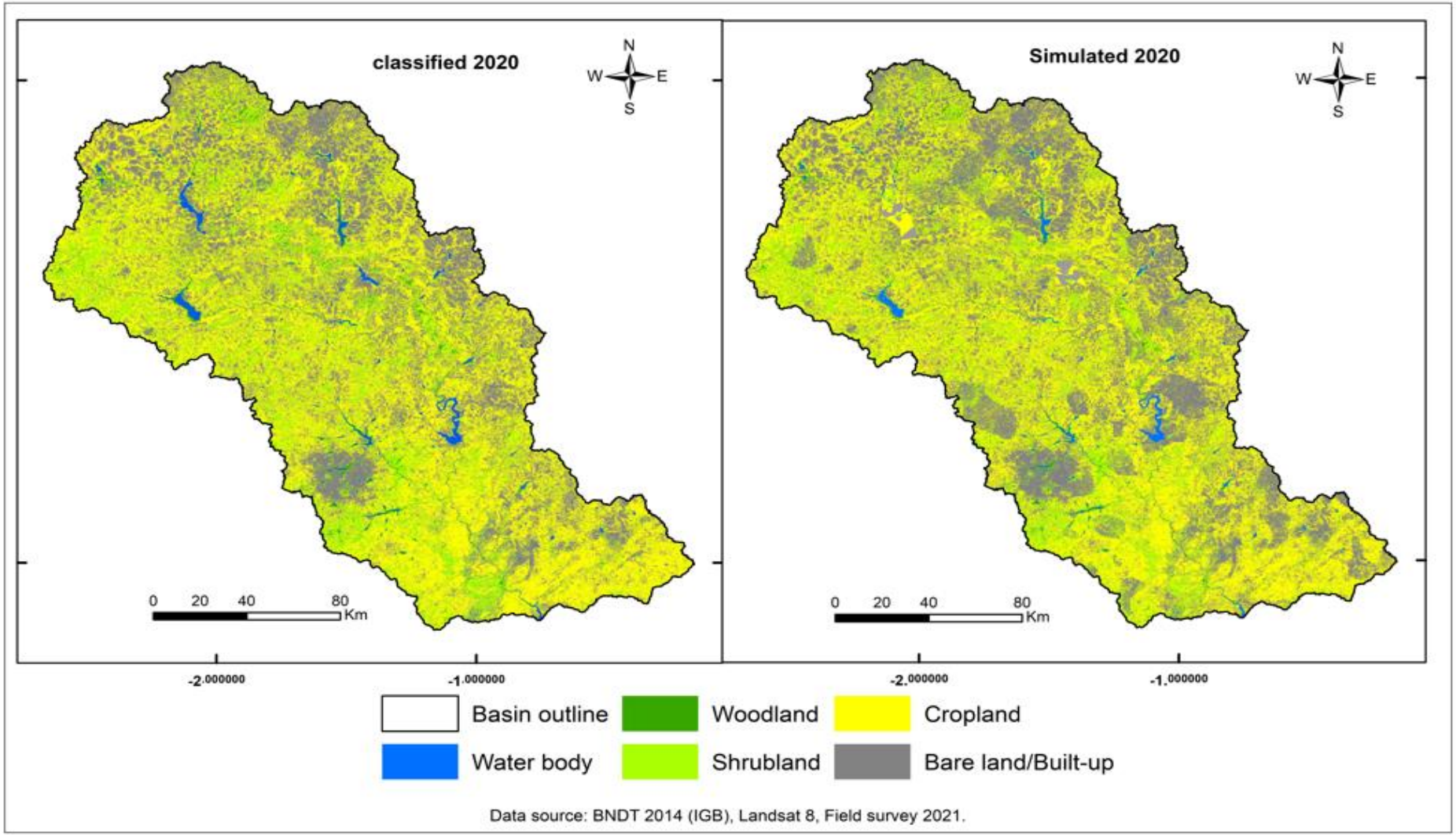

Figure 18. Actual classified (left) and simulated (right) LULC for 2020

5.8. Future LULC dynamics

The results of the LULC projection are shown in Table 23 and Figure 19. Under the BAU scenario, the basin area would be dominated in 2050 by bare land/built-up whose coverage would increase to 57.1% (Table 23), followed by cropland, shrubland, water body, and woodland with coverages of 32.9%, 7.58%, 1.35%, and 1.06%, respectively. The percentage of changes from 2020 to 2050 showed that bare land/built-up area would double while the area covered by cropland would decrease by -32% under the BAU. Natural vegetation like woodland and shrubland would decrease by -33.9% and -46.9%, respectively in 2050. On the contrary, under the afforestation scenario the basin would be mainly covered by cropland (57.7%) in 2050. Yet, woodland and shrubland would increase by 22.2% and 51.6%, respectively relative to 2020. Meanwhile the area covered by cropland would increase by 18.1% whereas bare land/built-up and water body would decrease by -39.0% and -6.16%, respectively (Table 23).

Table 23. Proportion of LULC units in 2050 under the BAU and afforestation scenarios and their percentage of changes

LULC units	Afforestation 2050		BAU 2050		Classified 2020-Afforestation 2050	Classified 2020-BAU 2050
	km^2	%	km^2	%	% Change	% Change
Water body	409	1.25	441	1.35	-6.16	1.15
Woodland	638	1.96	345	1.06	22.2	-33.9
Shrubland	7,051	21.6	2,472	7.58	51.6	-46.9
Cropland	18,842	57.7	10,749	32.9	18.1	-32.6
Bare land/Built-up	5,683	17.4	18,617	57.1	-39.0	99.7
Total	32,623	100.0	32,623	100.0		

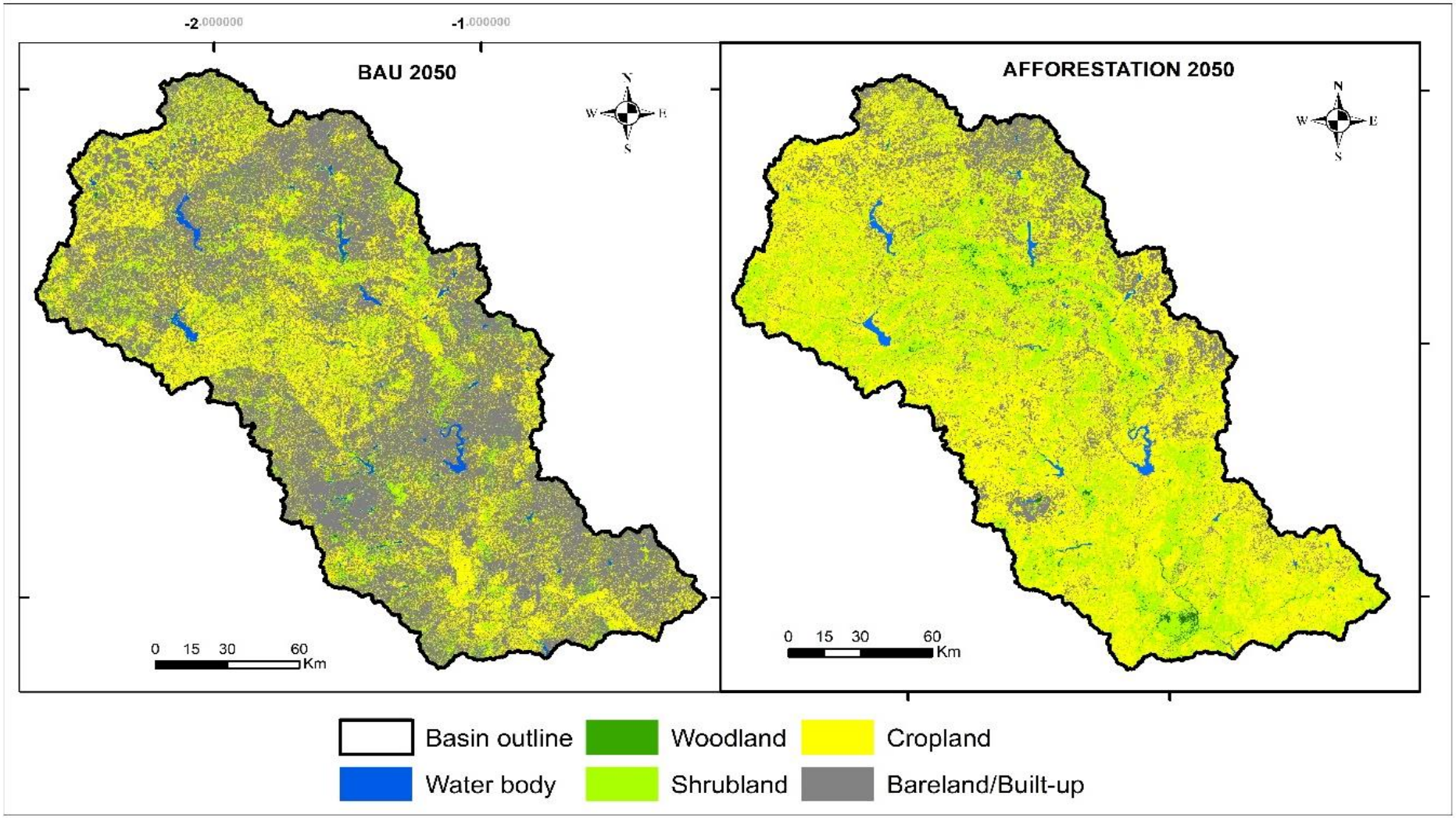

Figure 19. Projected future LULC maps for 2050 under the BAU and Afforestation scenarios

5.9. Discussion

The study investigated the LULC dynamic in the NRB through satellites images processing. The supervised RF classification of Landsat images on GEE gives satisfactory accuracy with Kappa > 0.75 (Fitzgerald and Lees, 1994). For the different years, the accuracy of the classification seemed to be related to the number of samples used as RF performs better when the number of samples is high (Ramezan et al., 2021). However, the low performance could also be attributed to the errors in the choice of samples. The confusion matrices show more misclassifications in samples for the year 2020 compared to 2005 and 1990, respectively. For instance, it was observed that most of confusion are between cropland and natural vegetation. This could be due to the fact that in many croplands, some selective trees are not cut because of the ecosystems services they provide. The finding is congruent with the results of Forkuor (2014) and Larbi et al. (2019) who noted a confusion between cropland and grassland classification due to the presence of grasses and trees in harvested croplands in Vea, a sub-basin of the White Volta Basin where the NRB is located.

The LCM successfully modelled the potential transitions from 1990 to 2005 with an accuracy rate of 76%. Even though Eastman (2020) suggested a threshold of 80% as acceptable performance, he also highlighted that only modelling with an accuracy lower than 75% is not effective. Yet, Rodríguez Eraso et al. (2013) agreed on a 50% threshold when using the MLP neural network to run the sub model transitions of LULCC in the Colombian Andes. Moreover, the evidence likelihood was found as most influential driver variable that explained the LULCC from the 1990-2020 in the NRB. This was also reported in the Abbay and Nashe watersheds in Ethiopia by Hussien et al. (2022) and Leta et al. (2021), respectively. Furthermore, the model showed some errors between the classified and the simulated LULC of 2020. Some LULC units were overestimated while some were underestimated. As stated by Larbi et al. (2019), these errors could be attributed to the model structure because it cannot extrapolate stationary changes from the calibration (1990-2005) to the validation period (2005-2020). These authors also emphasized the difficulty in modelling the non-linearity relationship between humans and nature.

In terms of historical LULC dynamics in the NRB, the study highlighted a continuous decrease in woodland and shrubland, and a continuous increase in water bodies, cropland, and bare land/built-up from 1990 to 2020. During the last 31 years, about 50% of woodland and shrubland was converted to anthropogenic land use. This rapid conversion could be explained

by the rapid population growth. Indeed, the population of the country increased from 10,312,609 to 20,487,979 inhabitants from 1996 to 2019 (INSD, 2020). This population growth could result in further deforestation for farming activities. For example, a study by (Ministère de l'Environnement et du Developpement Durable, 2015) showed that deforestation for agriculture purposes is one of the driving factors of natural vegetation degradation in Burkina Faso. Moreover, the world forest assessment report highlighted that about 1% of forest is lost each year in the country (FAO, 2010). In fact, farming in the region is still based on a familial and extensive agriculture type where farms are always expanded to increase yield with little soil amendment (Larbi et al., 2019). Such farming techniques including slash and burn farming, aggravated by the use of non-adaptive tools and chemical fertilizers are not suitable for soil conservation (Nyamekye et al., 2018). As a result, many farms lose their fertility and become degraded. This could explain why most of the bare land/built-up net gains are from cropland conversion (Figure 12). A study by Braimoh and Vlek (2004) showed that 3% of cropland was abandoned from 1984-1992 in the Volta River Basin due to a decline in soil fertility. This finding is also evidenced by the result of the spatial trend of change. In Figure 15 and Figure **16** for instance, where cropland replaced woodland and shrubland, there is an increase of bare land/built up area. This systematic process of transitions has been observed in other places in West Africa and South America (Barnieh et al., 2020). In addition, many cities in Burkina Faso are experiencing increase in their areas this last decade due to a somewhat urban planning (Sodore, 2022). The results of the historical LULC dynamics are congruent with those of Larbi et al. (2019), Okafor et al. (2019), Yonaba et al. (2021), and Zoungrana et al. (2015) who found an expansion of cropland, bare land and settlement areas, and a decrease in natural vegetation in the Vea, Dano, Tougou, and Southern Burkina, which are all part of the Volta River Basin where the NRB is located.

The future LULC map of 2050 in NRB was projected under the BAU and afforestation scenarios. Under the BAU scenario, a strong increase in bare land/built-up and a decrease in natural vegetation and cropland from 2020 to 2050 is projected. The decrease in cropland is the result of the different transitions allowed in the Markov Chain model to compute the LULC of 2050. The results are not in agreement with many studies, which projected an increase in cropland in the future (Gupta and Sharma, 2020; Larbi et al., 2019; Leta et al., 2021). However, the findings are congruent with the results of Hussien et al. (2022) who projected a decrease in cropland (-5,623.2 km^2) and an increase in settlement (1,073.4 km^2) from 2021 to 2056 in the Abbay River Basin of Ethiopia. In the same country, a study by Sibanda and Ahmed (2021)

projected an increase of 40% and a decrease of -18% for cropland in 2035 and 2045, respectively in the Shashe River Basin. The results of future LULC could have many impacts on water resources in the NRB. As reported by (Mechal et al., 2022), the expansion of bare land could highly increase the discharge and decrease infiltration due to the higher runoff coefficient. It could also increase floods occurrence due to peak discharges (Yira et al., 2016). This situation could jeopardize the life and goods of the thousands of people who live downstream of the dams. For instance, water releases from the Bagré dam caused many deaths and economic losses in Burkina Faso and Ghana in 2009 (UNEP-GEF Volta Project, 2013). The peak flows could also favour dams' siltation due to an increase in sediment transport. The high coverage of the basin by bare land/built-up could ultimately decrease low flows and affect the water yield (Balist et al., 2022).

Under the afforestation scenario, the NRB would be mostly covered by cropland (57.7%) in 2050. However, as set-up in the Markov Chain model, the area of woodland and shrubland would increase. Yet, the bare land/built-up would decrease by -39%. The statistics of LULC units in 2050 under the afforestation scenario are close to those of LULC 2005 (Table 21 and Table 23). Several studies have projected a decrease in cropland to the benefit of forest in the future under the afforestation scenario (Han et al., 2015; Larbi et al., 2019). However, in this study, the increase in cropland could be attributed to bare land/built-up decrease. Indeed, the modelling assumption is set in such a way that the area covered by bare land/built-up in 2020 is mainly due to the degradation of cropland area from 2005. However, with some techniques of soil conservation such as *zaï, stone bunds, and half-moons*, some of the degraded lands could be successfully converted for agriculture purpose (Nyamekye et al., 2018). Such a policy for the designed afforestation scenario could lower the peak flows and increase the groundwater recharge through a better percolation (Tanksali and Soraganvi, 2021).

5.10. Partial conclusion

This chapter investigated the dynamics of past and future LULC in the NRB. The method used was the RF classification in GEE, which produced acceptable maps for 1990, 2005 and 2020. The future LULC was assessed using the MLP neural network and the Markov Chain model of the LCM. The model was successfully validated using the LULC of 2020 as reference year. The dynamics of LULC from 1990 to 2020 showed a continuous decrease in woodland and shrubland areas, a continuous increase of cropland, bare land/built-up, and water bodies. The trend of LULC units showed strong effects of human activities on land cover change in the

basin. On the one hand, the future LULC map in 2050 based on the BAU scenario showed that human pressure would exacerbate the decrease of the natural vegetation, with a probable decrease in cropland. On the other hand, under the afforestation scenario, the natural vegetation could increase while bare land/built-up could decrease. The Bagré dam, a RAMSAR site located downstream of the NRB, relies on the LULC dynamics of the upstream basin. Therefore, a better understanding of the impacts of LULCC on the hydrological system of the dam could be of great interest.

CHAPTER 6: IMPACTS OF CLIMATE AND LAND USE CHANGES ON HYDROPOWER GENERATION

This chapter presents the results of the future climate projections and the investigation of the impacts of climate and land use changes on hydropower generation at the Bagré dam. The first section assesses on the one hand the performance of the ISIMIP3b data to reproduce the historical climate patterns and analyses rainfall and temperature projections in the NRB. On the other hand, the results of the parameter sensitivity analysis and the SWIM model calibration and validation are presented. The second section inspects the impact of climate change on hydropower generation under SSP126 and SSP370. The third section examines the possible impact of LULCC (BAU and afforestation scenario) on hydropower generation. The fourth section investigates the changes in hydropower generation due to the combine effects of climate and land use changes. The last section discusses the different results.

6.1. Global climate models projections and hydrological modelling parameterization

6.1.1. Performance of ISIMIP3b

ISIMIP3b GCMs are already downscaled and bias corrected. However, the consistency of these bias adjusted data on the NRB was checked. Therefore, rainfall and temperature from ISIMIP3b at selected subbasins were compared to W5E5 and observations at Ouagadougou and Ouahigouya stations. The monthly rainfall from 1985-2015 shows acceptable correlation coefficients for all the models at Ouagadougou (0.72 - 0.84) and Ouahigouya (0.70 – 0.82) stations (Table **24**). UKESM1-0-LL depicts the highest correlation, while the lowest correlations are found for CNRM-ESM2-1 and CNRM-CM6-1. Moreover, the percentage of bias ranges between -3.5 and 4.3 (Ouagadougou), and -11.7 and -4.3 (Ouahigouya). The lowest bias is observed for CNRM-ESM2-1 whereas the highest bias is observed for CanESM5 for Ouagadougou. For Ouahigouya, the highest and lowest biases are observed from CNRM-CM6-1 and MRI-ESM2-0, respectively. Furthermore, the annual cycle at Ouagadougou shows that most of the models underestimate rainfall in May, June and September. However, most of the models overestimate rainfall in July and August (Annex 1c). The ISIMIP3b monthly temperatures also show acceptable correlation with W5E5 and observations over 1985-2015 (Table **24**). The mean temperature is underestimated from October to May (dry season). During the rainy season, all ISIMIP3bmodels are capable to represent the mean W5E5 temperature (Annex 1c). Therefore, it was reasonably concluded that overall, the ISIMIP3b GCMs are able to represent the monthly climate patterns in the NRB.

Table 24. Comparison statistics of monthly ISIMIP3b rainfall and mean temperature and monthly observations and W5E5 products at Ouagadougou and Ouahigouya stations

ISIMIP3b models	Rainfall				Mean Temperature				Rainfall				Mean Temperature			
	R								PBias							
	Ouagadougou		Ouahigouya		Ouagadougou		Ouahigouya		Ouagadougou		Ouahigouya		Ouagadougou		Ouahigouya	
	Obs	W5E5	Obs	W5E5	Obs	W5E5	Obs	W5E5	Obs	W5E5	Obs	W5E5	Obs	W5E5	Obs	W5E5
CanESM5	0.80	0.80	0.78	0.79	0.89	0.88	0.90	0.92	4.3	0.4	-6.2	2.4	-3.9	-2.9	-2.3	-1.1
CNRM-CM6-1	0.76	0.76	0.70	0.72	0.87	0.86	0.88	0.90	-3.5	-7.1	-11.7	-3.6	-3.6	-2.6	-2	-0.9
CNRM-ESM2-1	0.72	0.74	0.73	0.74	0.89	0.88	0.89	0.92	-1	-4.6	-6.2	2.3	-3.6	-2.6	-2	-0.8
EC-EARTH3	0.82	0.84	0.76	0.76	0.90	0.89	0.91	0.93	-3.3	-6.9	-9.3	-1.1	-3.6	-2.6	-1.9	-0.8
GFDL-ESM4	0.82	0.84	0.78	0.77	0.88	0.87	0.89	0.91	-1.4	-5.1	-9.5	-1.2	-3.8	-2.7	-2.1	-0.9
IPSL-CM6A-LR	0.79	0.80	0.77	0.79	0.88	0.87	0.89	0.91	-1.1	-4.7	-8.4	0	-3.7	-2.7	-2	-0.9
MIROC6	0.80	0.81	0.80	0.81	0.88	0.86	0.89	0.92	3	-0.8	-7.1	1.4	-4.3	-3.3	-2.6	-1.5
MPI-ESM1-2H	0.78	0.78	0.77	0.81	0.89	0.88	0.90	0.92	-1.7	-5.3	-9.5	-1.3	-3.9	-2.9	-2.2	-1
MRI-ESM2-0	0.81	0.84	0.78	0.80	0.88	0.86	0.88	0.90	2.2	-1.5	-4.3	4.5	-3.9	-2.9	-2.2	-1.1
UKESM1-0-LL	0.84	0.85	0.82	0.83	0.90	0.89	0.91	0.93	3.3	-0.5	-6.2	2.3	-3.7	-2.7	-2.1	-1
ISIMIP3b Ensemble median	0.91	0.92	0.90	0.91	0.93	0.91	0.94	0.96	0	-3.7	-8	0.4	-3.8	-2.8	-2.1	-1

6.1.2. Climate projections in the NRB

6.1.2.1. Annual rainfall and mean temperature changes

The results of the climate projections are summed up in Table **25**. The median annual rainfall increases in the future (P1 and P2), relatively to the reference period (P0). An increase of median rainfall by 10.7-21.1% and 8.11-23.9% during the mid and far future, respectively, is projected. Likewise, mean temperature median increases by 1.36-1.82 °C and 1.58-3.66 °C during the periods 2035-2065 and 2065-2095, correspondingly. All models are unanimous on the change direction of the mean temperature in the basin under SSP126 and SSP370 (Figure **20**).

However, models show different directions regarding future annual rainfall change. From 2035-2065, all models project an increase in annual rainfall apart from MIROC6, CNRM-ESM2-1, and CNRM-CM6-1 under SSP126 (Figure **20**-A). Only GFDL-ESM4 and MIROC6 give a declining rainfall in both future periods under SSP370. In addition to MIROC6 and CNRM-CM6-1 which already projected a decrease in rainfall in the mid future under SSP126, MPI-ESM1-2-HR gives annual rainfall decline in the far future under the same scenario (Figure **20**-B).

Table 25. Median annual rainfall and temperature and percentage of changes over 1984-2014, 2035-2065, and 2065-2095

Climate variables	1984-2014 (P0)	2035-2065 (P1)	% Change (P1-P0)	2065-2095 (P2)	% Change (P2-P0)
Median					
Rainfall [mm]	635.7	703.6 (769.7)	10.7 (21.1)	687.24 (787.86)	8.11 (23.9)
Tmean [°C]	28.3	29.7 (30.1)	1.36 (1.82)	29.94 (31.99)	1.58 (3.66)

NB: values in brackets indicate the results under SSP370; P1-P0 and P2-P0 are in absolute value for Tmean

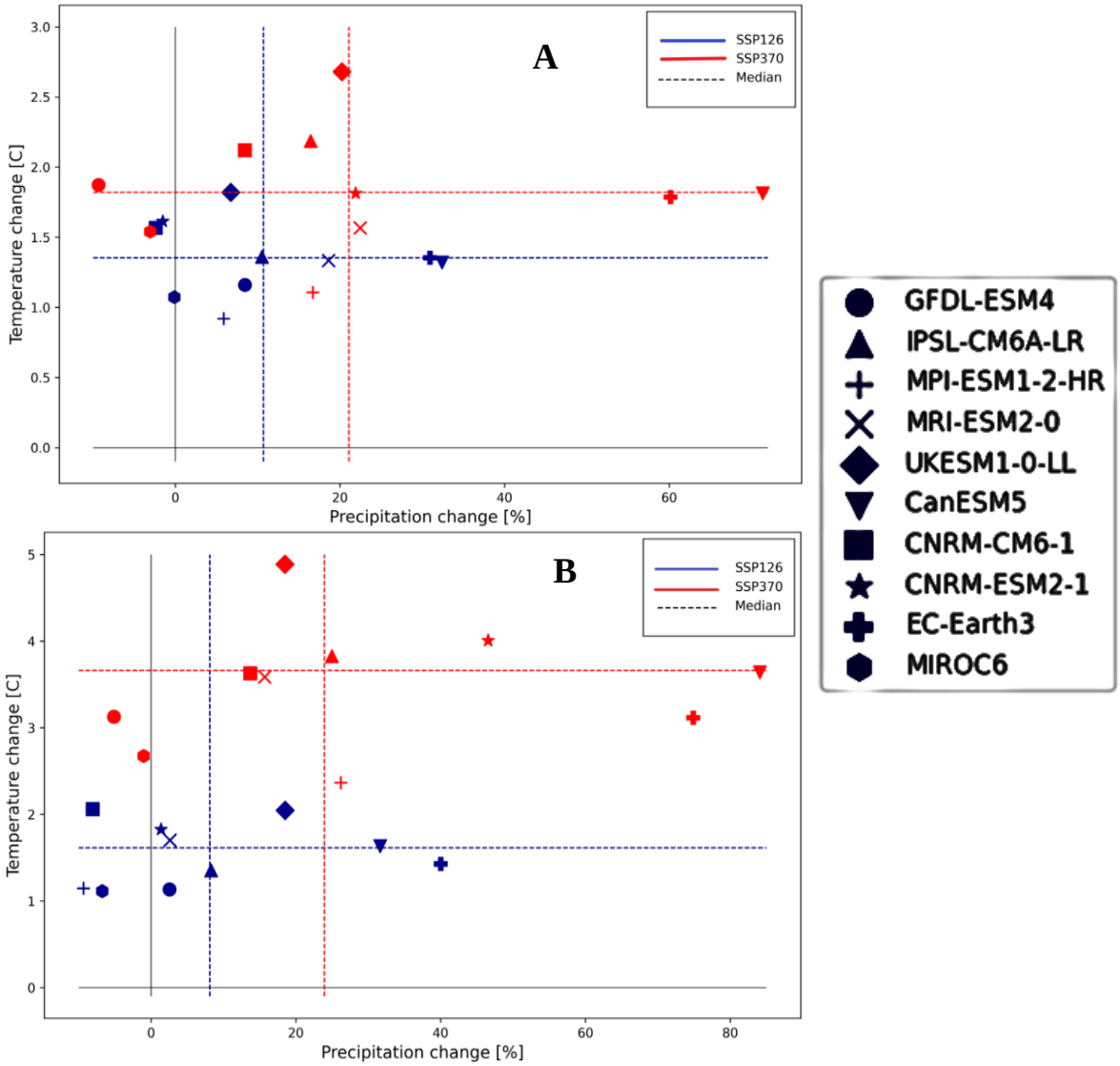

Figure 20. Changes in median annual rainfall and mean temperature from 2035-2065 (A) and 2065-2095 (B), compared to 1984-2014.

6.1.2.2. Monthly rainfall and temperature changes

The future seasonal rainfall and temperature changes are analysed by calculating the absolute change between the future periods and the baseline. Figure **21** and Figure **22** present the monthly rainfall and mean temperature absolute changes under SSP126 and SSP370.

Under SSP126, from 2035 to 2065, more than half of the models project an increment of rainfall for all months except May. The ensemble median show that the net increase would be during the rainy season from June to October. During the period 2065-2095, more than 60% of the models project a decrease in rainfall from March to April. However, the rainy season would

experience an increase in rainfall (May-September) according to projections from 50-70% of ISIMIP3b models. Moreover, the ensemble median gives a slight increase of rainfall during the period of May to September. The mean temperature experiences an increase for all months in the future. Apart from the month of September (2035-2065), where only one model projects a decrease of mean temperature, all models are unanimous on the increase of mean temperature for all months in the mid and the far future. The ensemble median shows that the increase would be greater in the far future compared to the mid future.

Under SSP370, the mean temperature follows the same trend as under SSP126, even though the rate of increase would be higher. For rainfall, more than half of the models project an increase in rainfall for all months during the period 2035-2065. However, from 2065 to 2095, it is expected less rainfall in April compared to the period 1984-2014. Nevertheless, the ensemble medians show an increase of rainfall during the rainy season from May/June to October.

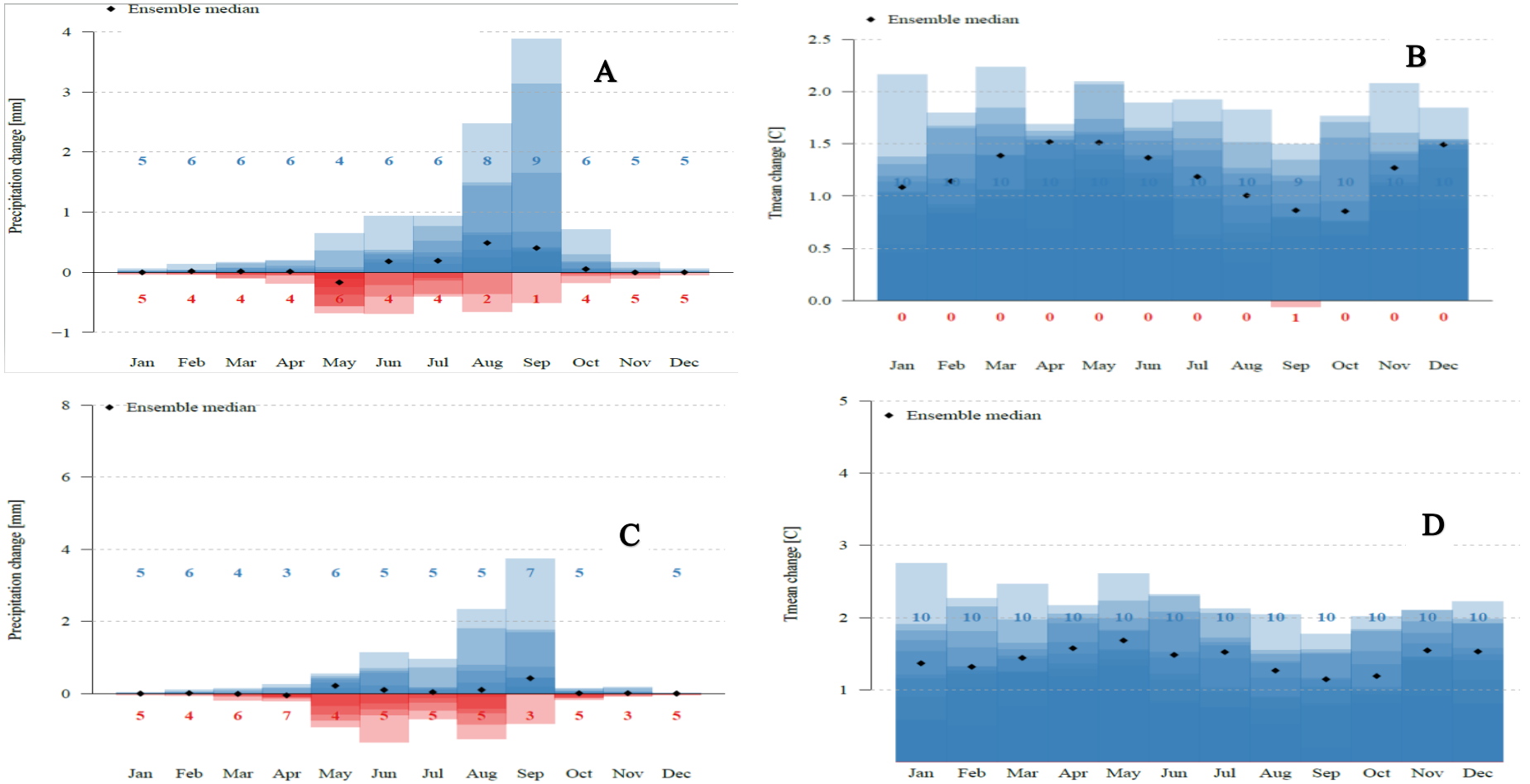

Figure 21. Monthly absolute changes in rainfall and mean temperature during the periods 2035-2065 (A, B) and 2065-2095 (C, D) relative to 1984-2014 under SSP126. The red colour indicates the number of models and amplitude of decrease while the blue colour indicates the number of models and amplitude of increase

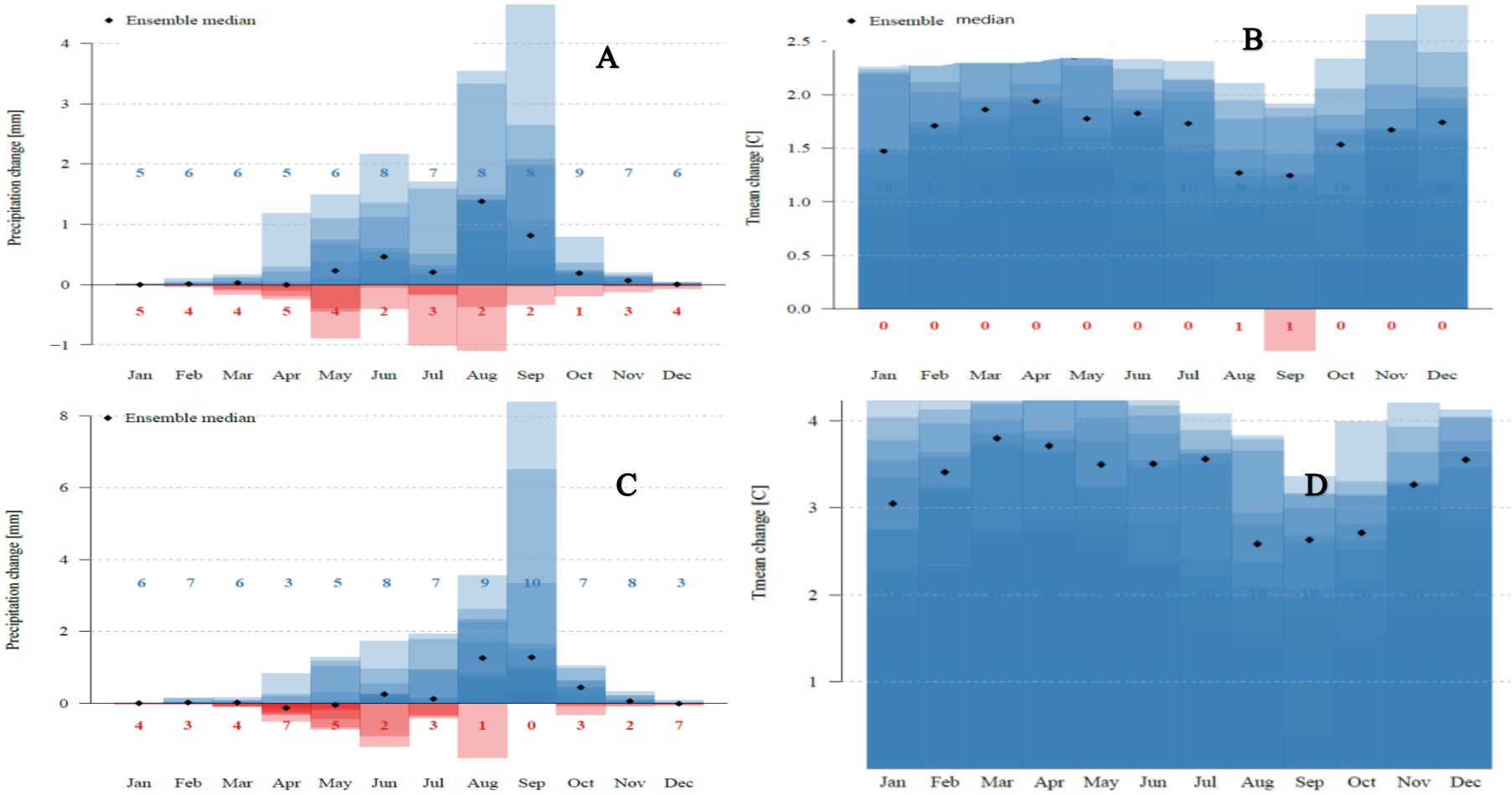

Figure 22. Monthly absolute changes in rainfall and mean temperature during the periods 2035-2065 (A, B) and 2065-2095 (C, D) relative to 1984-2014 under SSP370. The red colour indicates the number of models and amplitude of decrease while the blue colour indicates the number of models and amplitude of increase

6.1.3. Parameters' sensitivity, calibration and validation of SWIM

The sensitivity analysis shows that 8 parameters are sensitive in the study area. According to their importance, they are composed of base flow factor (bff), alpha factor for groundwater (abf), correction factor for curve number (cncor), correction factor for soil hydraulic conductivity (sccor), river routing coefficients (roc2, roc4), groundwater delay (delay), and transmission losses (tlrch). Koch et al. (2020) also found that potential evapotranspiration (ecal), roc, sccor, bff, delay, and abf were the sensitive parameters in SWIM when studying the effects of model calibration on hydrological and water resources management in the semi-arid Pajeú watershed in north-eastern Brazil. The values determined for the 8 parameters are presented in Annex 1a.

The simulated runoff is compared with observed discharges at daily scale for Wayen (Figure 23), and at monthly scale for Niaogho (Figure 24). The performance of the SWIM model for the calibration and validation periods at Wayen and Niaogho stations are shown in Table **26**. The NSE and R^2 coefficients for the calibration periods are 0.67 and 0.7 at Wayen, and 0.81 and 0.83 at Niaogho, respectively. For the validation period, NSE values are 0.74 and 0.6, while R^2 are 0.75 and 0.68 at Wayen and Niaogho stations, respectively. In addition, PBias was -5% during the calibration phase whereas the validation showed a higher PBias (11%), indicating an overestimation (calibration) and underestimation (validation) of runoff by SWIM at Wayen station. At Niaogho station, the PBias is higher (-7.3% and -22%) and indicates an overestimation of flows by SWIM during the calibration and the validation phases. Nevertheless, the statistical indicators are acceptable as they fall in the given satisfactory intervals of NSE > 0.50, R^2 > 0.60, and ±25% of PBias in hydrological studies as given by Moriasi et al. (2007). For all stations and dams, the computation of NRMSE ranges between 0.33 (validation at Tougou) and 0.7 (calibration at Dem).

Table 26. Performance of the calibration and validation of daily (Wayen) and monthly (Niaogho) discharges, and daily reservoir volumes

Stations/Dams		Calibration				Validation			
		Period	NSE	R^2	PBias	Period	NSE	R^2	PBias
Discharge	Wayen	1989-1993	0.67	0.7	-5	1995-1999	0.74	0.75	11
	Niaogho	1980-1984	0.81	0.83	-7.3	1987-1991	0.6	0.68	-22
Volume	Bagré	2004-2008	0.73	0.89	-12	2009-2013	0.76	0.85	2.2
	Ziga	2005-2011	0.78	0.85	-6.6	2013-2018	0.73	0.78	-5.8
	Loumbila	2006-2010	0.84	0.90	-8.2	2011-2015	0.82	0.85	2.6
	Dourou	2006-2010	0.74	0.74	0.5	2011-2015	0.72	0.72	0.5
	Séguénega	2006-2008	0.78	0.78	-3.5	2016-2018	0.75	0.79	13.6
	Bam	2009-2012	0.84	0.85	-2.8	2013-2016	0.76	0.76	1.2
	Dem	1985-1986	0.75	0.86	-12.6	---	---	---	---
	Tougou	2005-2008	0.69	0.79	15.1	2011-2013	0.87	0.89	-2.9
	Goinré	1999-2000	0.58	0.68	8.8	2004-2007	0.74	0.76	17

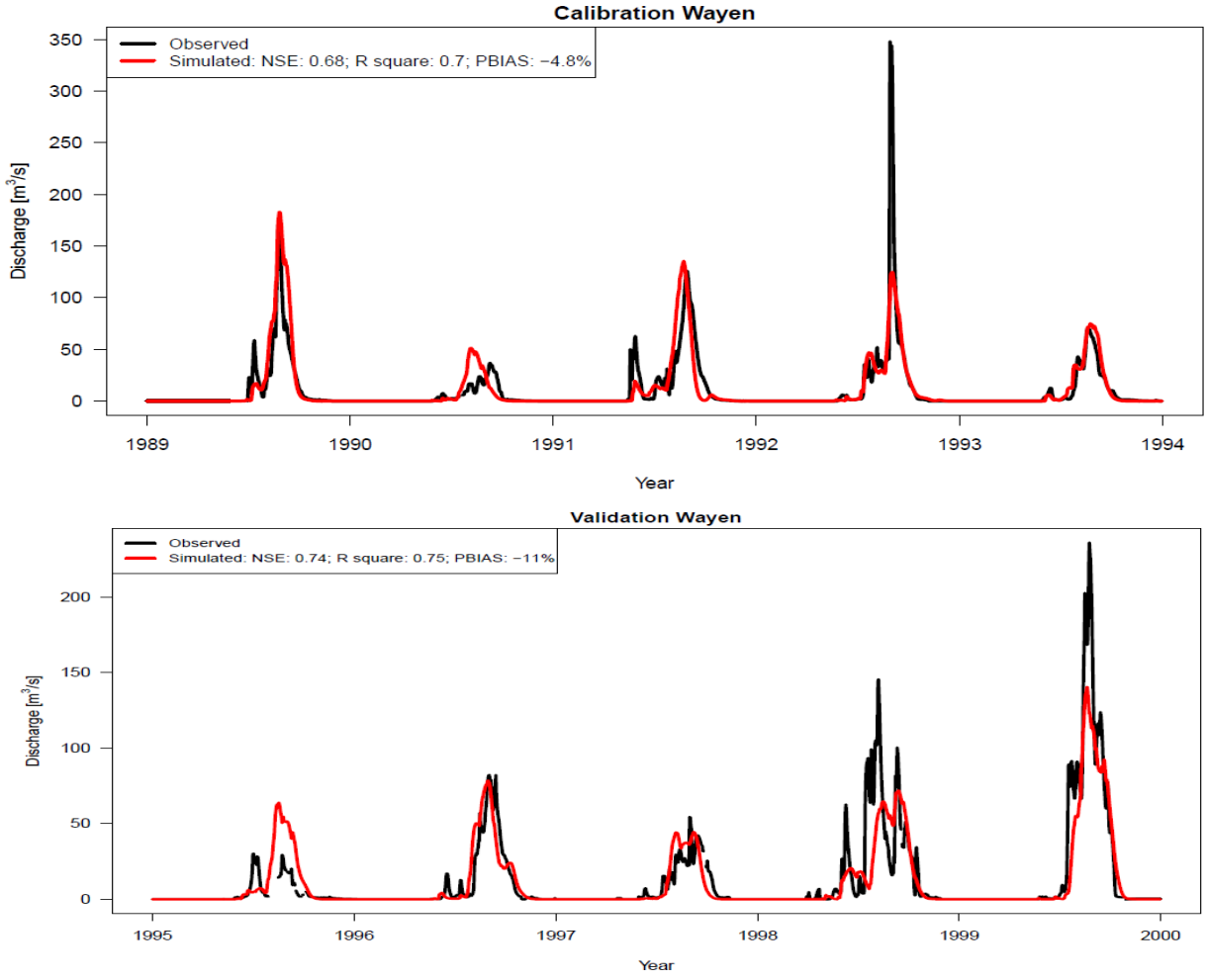

Figure 23. Calibration and validation of discharge at Wayen station

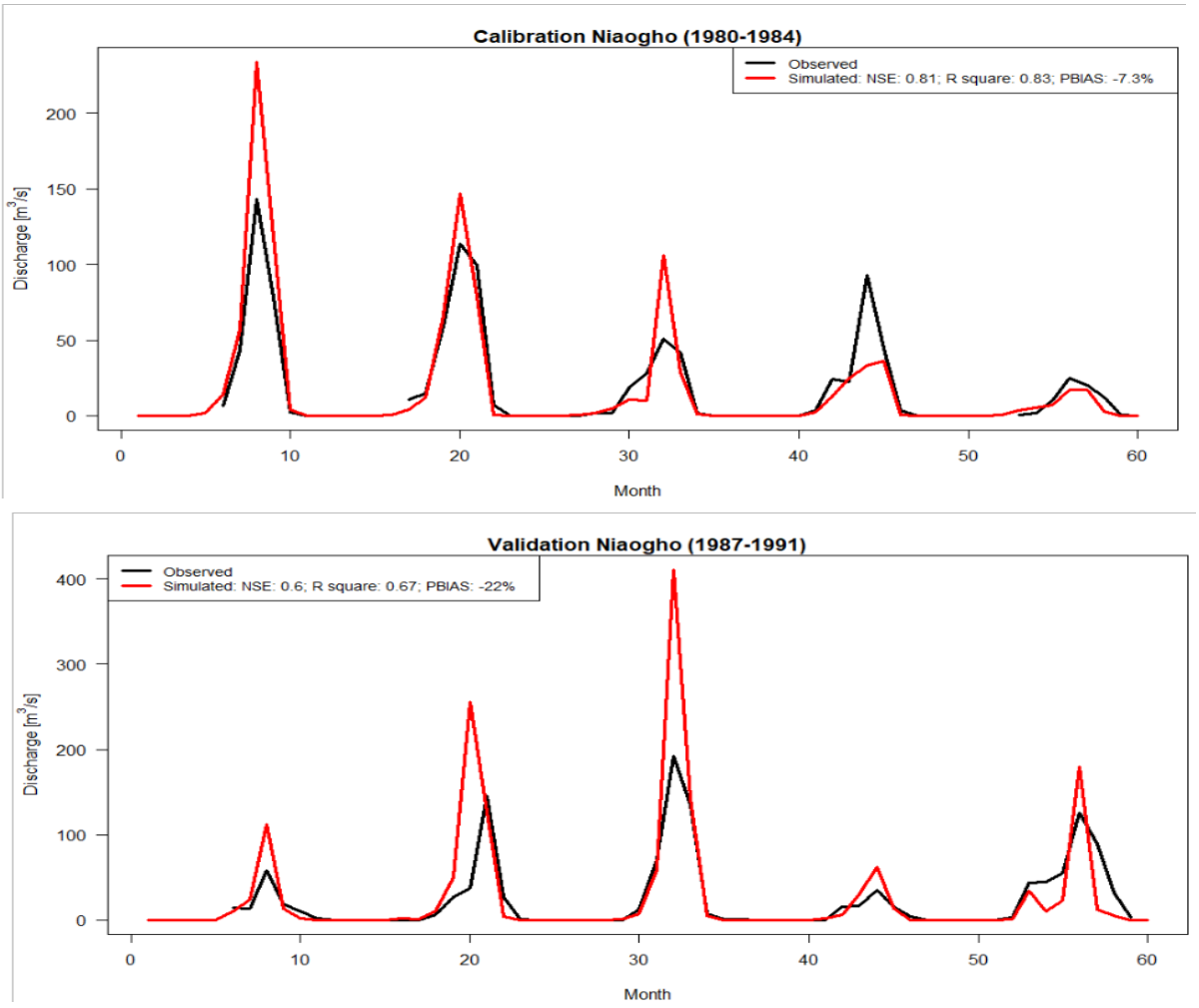

Figure 24. Calibration and validation of discharge at Niaogho station

Figure 24 shows a low goodness fit between the observations and simulations at Niaogho station. This can be explained by the poor quality of discharge data, and the use of reanalysis data. However, the simulation of reservoirs' volume, water level, turbined volume and hydropower generation show a relative goodness of fit (Table **26** and Annex 1d & 1e).

6.2. Impacts of climate change on inflow and hydropower generation

6.2.1. Changes in inflow and hydropower generation under climate change impact

The changes in inflow and hydropower generation medians at Bagré dam are presented in Table **27**. Under SSP126, the period 2035-2065 would be wet in the NRB. This increase in annual rainfall median by 10.7% will favour an increase in daily median inflow and hydropower by 21.1% and 15.6%, respectively. However, the increase in rainfall by 8% during the period 2065-2095 will induce a decline in daily median inflow by -8%, but an increase in daily hydropower generation median by 1.7% (Table **27**). The decrease in inflow could be explained by the

increase of actual and potential evapotranspiration. The hydropower increase could be explained by the additional rainfall over the dam (260 mm per year). Here, the decrease in outflow is mainly due to the decrease of spills. Overall, inflow and hydropower generation could increase during the period 2035-2065 whereas the period 2065-2095 would experience a return to baseline hydropower generation.

Under SSP370, climate conditions are much wetter than under SSP126. Indeed, the increase of annual median rainfall by 21% and 24% during the periods 2035-2065 and 2065-2095, respectively, induces high increases in inflow by 54.5% and 75.1%, respectively, relative to the baseline. Therefore, hydropower generation is expected to increase by 24.4% and 35.8% during 2035-2065 and 2065-2095, respectively relative to 1984-2014 (Table **27**).

Table 27. Multi-models hydro-climatic median changes during 1984-2014, 2035-2065, and 2065-2095 under SSP126 and SSP370

Hydro-climatic variables	1984-2014 (P0)	2035-2065 (P1)	% Change (P1-P0)	2065-2095 (P2)	% Change (P2-P0)
ETa [mm/a]	2037	2,122 (2,077.5)	4.1 (2)	2,128 (2,130)	4.5 (4.6)
ETp [mm/a]	2523.5	2,563 (2,520.5)	1.6 (-0.1)	2,591 (2,556)	2.7 (1.3)
Inflow [m^3/s]	65.1	78.9 (100.7)	21.1 (54.5)	59.9 (114.1)	-8 (75.1)
Outflow [m^3/s]	55.6	68.1 (90)	22.3 (61.7)	50.1 (103.6)	-10 (86.2)
Energy [MW]	6.7	7.7 (8.3)	15.6 (24.4)	6.8 (9.1)	1.7 (35.8)

NB: values in brackets indicate the results under SSP370

6.2.2. Changes in seasonal inflow and hydropower generation under climate change impact

The results of the changes in seasonal inflow and hydropower generation are presented in Figure 25 and Figure **26**. Under SSP126, most of the models project a positive change in inflow, except for March, May, and July from 2035 to 2065, relative to the baseline. Some changes would not be important considering the ensemble median. Substantial positive changes can be observed from July to October, whereas a significant negative change would be noticed in June. The highest ensemble median inflow change occurs in August and September, with an increase of about +100 m^3/s (Figure 25-A). For hydropower generation, the majority of the models project a positive change for all months, except July (Figure 25-B). The ensemble median is positive for all months, although September and October record the highest absolute change of about

+1.5 MW, relative to the baseline. For the period 2065-2095, a positive change is observed for all months, except March, June, August, and December. Considering the ensemble median, positive changes are noticed in September and October, with September recording the highest change of about +60 m^3/s (Figure 25-C). During the same period, a negative change of about -30 m^3/s is expected in August. Meanwhile, the majority of the models project a decrease of hydropower generation in August and an increase from September to April. The models seem uncertain on the trend in hydropower generation from May to July. However, looking at the ensemble median, a positive change is observed from September to May while a negative change is observed for July and August. The highest positive change is observed in September (+0.5 MW), whereas the highest negative change is observed in August (-0.5 MW).

Under SSP370, the majority of the models project a positive change in inflow for all the months in the future (Figure 26-A&C). Based on the ensemble median, the changes can be observed from June to October. During the period 2035-2065, the highest change (+210 m^3/s) is observed in August, while September shows the highest change (+260 m^3/s) during the period 2065-2095. The consequence on the hydropower generation is positive, because 80% and 70% of the models project a positive change in hydropower generation during the periods 2035-2065 and 2065-2095, respectively, relative to the period 1984-2014. The ensemble median shows that a supplementary hydropower of 1 to 3.MW can be generated during the period 2035-2065 while for the period 2065-2095, the gain reaches 1 to 3.8 MW (Figure 26-B&D).

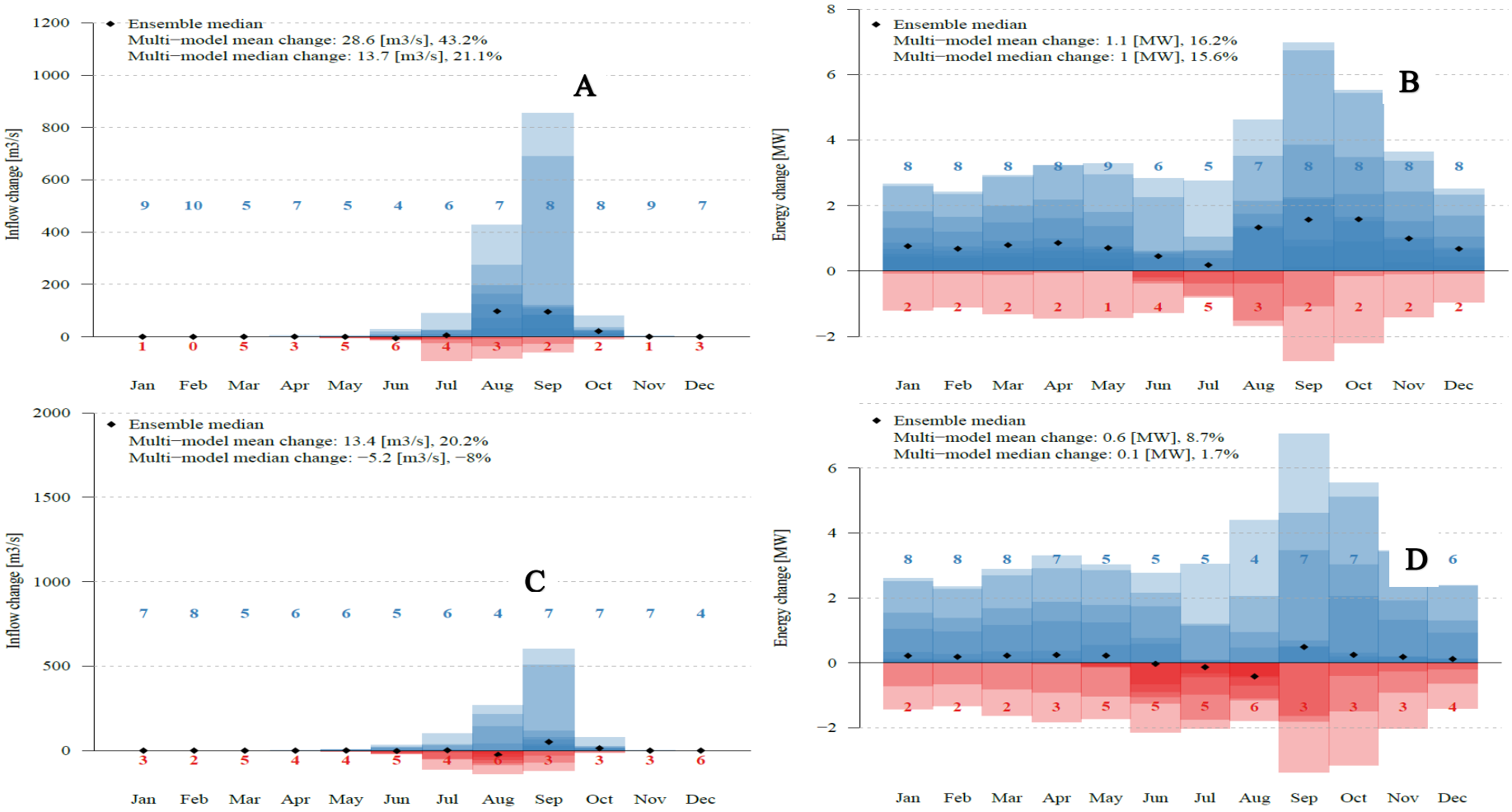

Figure 25. Monthly absolute changes in inflow and hydropower generation during the periods 2035-2065 (A, B) and 2065-2095 (C, D) relative to 1984-2014 under SSP126. The red colour indicates the number of models and amplitude of decrease while the blue colour indicates the number of models and amplitude of increase

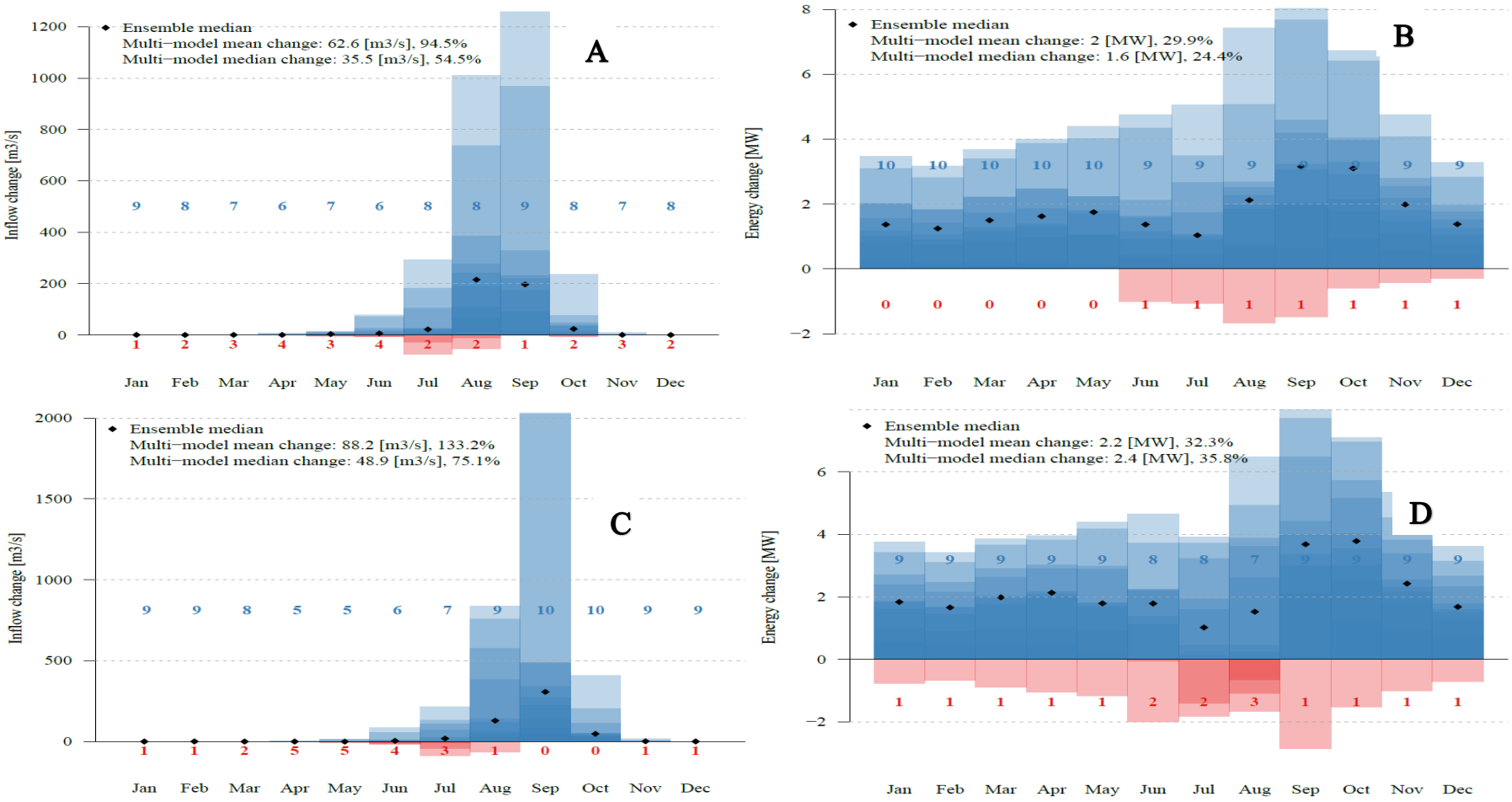

Figure 26. Monthly absolute changes in inflow and hydropower generation during the periods 2035-2065 (A, B) and 2065-2095 (C, D) relative to 1984-2014 under SSP370. The red colour indicates the number of models and amplitude of decrease while the blue colour indicates the number of models and amplitude of increase

6.3. Impact of land use change on inflow and hydropower generation

Assuming no change in climate patterns, the results of the changes in inflow and hydropower generation under various land use are presented in Table **28**. The LULC 2005 is considered as baseline. Overall, inflow increases from 54.4 m^3/s (LULC 2005) to 74.3 m^3/s (LULC 2020). However, the trend would follow two directions using the future LULC 2050. Under the afforestation scenario (LULC 2050 AFF), inflow increases slightly to 56.3 m^3/s whereas under the business-as-usual scenario (LULC 2050 BAU), it increases strongly to 101.1 m^3/s (Table **28**). This increase occurs mainly from May to October (Figure 27-A). In terms of energy conversion, hydropower generation increases from 6.66 MW (LULC 2005) to 8.57 MW (LULC 2020). Likewise, hydropower generation increases by 2.85% under LULC 2050 AFF. However, under the LULC 2050 BAU, it increases by 48.2% (Table **28**). All months are expected to experience an increase in hydropower generation with any kind of LULC (Figure 27-B).

Table 28. Changes in median inflow and hydropower generation for different land use land cover scenarios

LULC	LULC 2005	LULC 2020	LULC 2050 AFF	LULC 2050 BAU
	bl	bl	bl	bl
Inflow [m^3/s]	54.4	74.3	56.3	101.1
Energy [MW]	6.66	8.57	6.85	9.87

bl = baseline water management

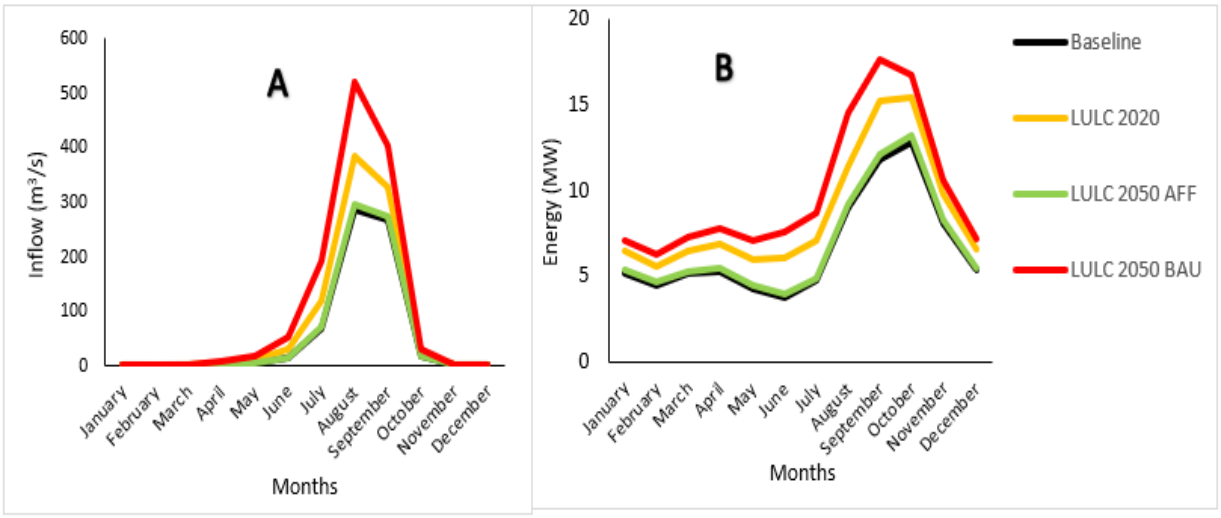

Figure 27. Monthly inflow (A) and hydropower generation (B) under different land use land cover scenarios

6.4. Impact of combined climate and land use changes on inflow and hydropower generation

6.4.1. Changes in inflow and hydropower generation under combined impact of climate and land use changes

This subsection examines the changes in daily inflow and hydropower generation under combined effects of climate and land use changes under afforestation and BAU scenarios.

6.4.1.1. Afforestation LULC

The future hydro-climatic conditions under climate and afforestation land use changes are presented in Table **29**. The results are close to the impacts of climate change (Table **27**). Indeed, inflow and hydropower generation evolve similarly from 2035-2065 and 2065-2095. Under SSP126, the inflow into the Bagré dam increases by 20.9% during the period 2035-2095 and decreases by -7.8% for 2065-2095, relative to the baseline. Nevertheless, the change in hydropower generation is positive in the future even though the increase for 2035-2065 (14.9%) is higher than for 2065-2095 (1.9%). Under SSP370, an increase in inflow by 53.8% and 74% is expected for 2035-2065 and 2065-2095, respectively. Therefore, hydropower generation would increase by 23.2% and 34.4% for 2035-2065 and 2065-2095, correspondingly. The results ultimately show that the changes in inflow would be attributed at 97-98% to climate change and 2-3% to land use change in the future under the afforestation scenario. In terms of hydropower generation, the contribution of land use change is estimated between 1 and 3% (Table **30**).

Table 29. Multi-models median hydro-climatic variables changes during 1984-2014, 2035-2065, and 2065-2095 under SSP126 and SSP370, and afforestation LULC 2050

Hydro-climatic variables	1984-2014 (P0)	2035-2065 (P1)	% Change (P1-P0)	2065-2095 (P2)	% Change (P2-P0)
ETa [mm/a]	2,039	2,123 (2,079)	4.1 (2)	2,130 (2,131)	4.5 (4.5)
ETp [mm/a]	2,521	2,559.5 (2,518)	1.5 (-0.1)	2,589 (2,553.5)	2.7 (1.3)
Inflow [m^3/s]	67.1	81.1 (103.2)	20.9 (53.8)	61.8 (116.7)	-7.8 (74)
Outflow [m^3/s]	57.5	70.2 (92.4)	22.2 (60.8)	51.8 (106.2)	-9.8 (84.8)
Energy [MW]	6.8	7.9 (8.4)	14.9 (23.2)	7 (9.2)	1.9 (34.4)

NB: values in brackets indicate the results under SSP370

Table 30. Contribution of climate and afforestation LULCC to inflow and hydropower changes

	Climate change (%)		**Afforestation LULC 2050 (%)**	
	SSP126	SSP370	SSP126	SSP370
2035-2065				
Inflow	97	98	3	2
Hydropower	97	99	3	1
2065-2095				
Inflow	97	98	3	2
Hydropower	97	99	3	1

6.4.1.2. Business-as-usual LULC

For the BAU scenario, the combined impacts of climate and land use changes are presented in Table **31**. The results show an increase by 16.9% and 5.9% in inflow and hydropower generation, respectively, under SSP126 during 2035-2065 relative to the baseline. However, from 2065-2095 a decrease by -3.1% in inflow is expected, while an increase by 3.8% in hydropower generation is observed. Under SSP370, the wetter conditions increase the inflow by 40.6% and 58.1% during the mid and the far futures, respectively. Therefore, hydropower generation will also increase by 8.1% and 12.4% from 2035-2065 and 2065-2095, respectively, relative to the baseline. Under the BAU scenario, the land use change will contribute at 37-46%, while climate change will contribute at 54-63% to inflow changes. Furthermore, the changes in hydropower generation are attributed at 68-83% to climate change and 17-32% to land use change (Table **32**).

Table 31. Multi-models hydro-climatic median changes during 1984-2014, 2035-2065, and 2065-2095 under SSP126 and SSP370, and Business as usual LULC 2050

Hydro-climatic variables	1984-2014 (P0)	2035-2065 (P1)	% Change (P1-P0)	2065-2095 (P2)	% Change (P2-P0)
ETa [mm/a]	2,067	2,144 (2,104)	3.7 (1.8)	2,163 (2,149)	4.6 (4)
ETp [mm/a]	2,468	2,518.5 (2,484)	2.1 (0.7)	2,547 (2,514)	3.2 (1.9)
Inflow [m^3/s]	114	133.3 (160.3)	16.9 (40.6)	110.5 (180.2)	-3.1 (58.1)
Outflow [m^3/s]	102.3	121.2 (148.6)	18.4 (45.2)	98.2 (168.8)	-4 (64.9)
Energy [MW]	9.7	10.2 (10.4)	5.9 (8.1)	10 (10.9)	3.8 (12.4)

NB: values in brackets indicate the results under SSP370

Table 32. Contribution of climate and BAU LULCC to inflow and hydropower changes

	Climate change (%)		**BAU LULC 2050 (%)**	
	SSP126	SSP370	SSP126	SSP370
	2035-2065			
Inflow	59	63	41	37
Hydropower	75	80	25	20
	2065-2095			
Inflow	54	63	46	37
Hydropower	68	83	32	17

6.4.2. Changes in seasonal inflow and hydropower generation under combined effects of climate and land use changes

6.4.2.1. Afforestation scenario

The results of combined effects of climate and afforestation land use show that most of the models project an increase in inflow for all the months, except March, May and June for 2035-2065 under SSP126 (Figure 28-A). The ensemble median shows that the increase occurs from July to October, while the decrease occurs in June. The highest positive change (+105 m^3/s) is observed in August. During the same period, the majority of the models project a positive change in hydropower generation for all months, except July. However, the ensemble median shows that all months will experience a positive change for 2035-2065, relative to 1984-2014. The change will vary from +0.2 to +1.5 MW, with September recording the highest absolute increase (Figure 28-B). Furthermore, the majority of the models project that August and December will experience a negative change in inflow from 2065-2095, compared to the baseline. The ensemble inflow median increases by about +70 m^3/s in September, while in August it decreases by -35 m^3/s. As a consequence, the majority of the models project a negative change in hydropower generation in August. However, the ensemble hydropower median shows that the negative change also affects July (Figure 28-D). The highest positive change (+0.5 MW) is observed in September, whereas the highest negative change (-0.4 MW) is observed in August.

Under SSP370, all months experience a positive change in inflow and hydropower generation during the period 2035-2065, according to the projection by most of the models (Figure 29-A&B). Indeed, all models are unanimous on the increase of hydropower generation from January to May. However, the positive change in the ensemble inflow median is observed during the rainy season (June to October), while for ensemble hydropower generation median

all months will experience a positive change. The highest change in inflow (+210 m3/s) is recorded in August, whereas the highest change in hydropower (+3 MW) is observed in September. Moreover, the majority of the models project an increase in inflow for all months during the period 2065-2095, relative to the period 1984-2014. For instance, all models are unanimous about the positive change in inflow in September and October (Figure 29-C). Yet, considering the ensemble median, positive inflow changes are only noticed from July to October, with the month of September recording the highest change (+280 m^3/s). Besides, most of models also project an increase in hydropower generation for all months (Figure 29-D). The ensemble median shows that the absolute change occurs all months and can reach +3.85 MW in October.

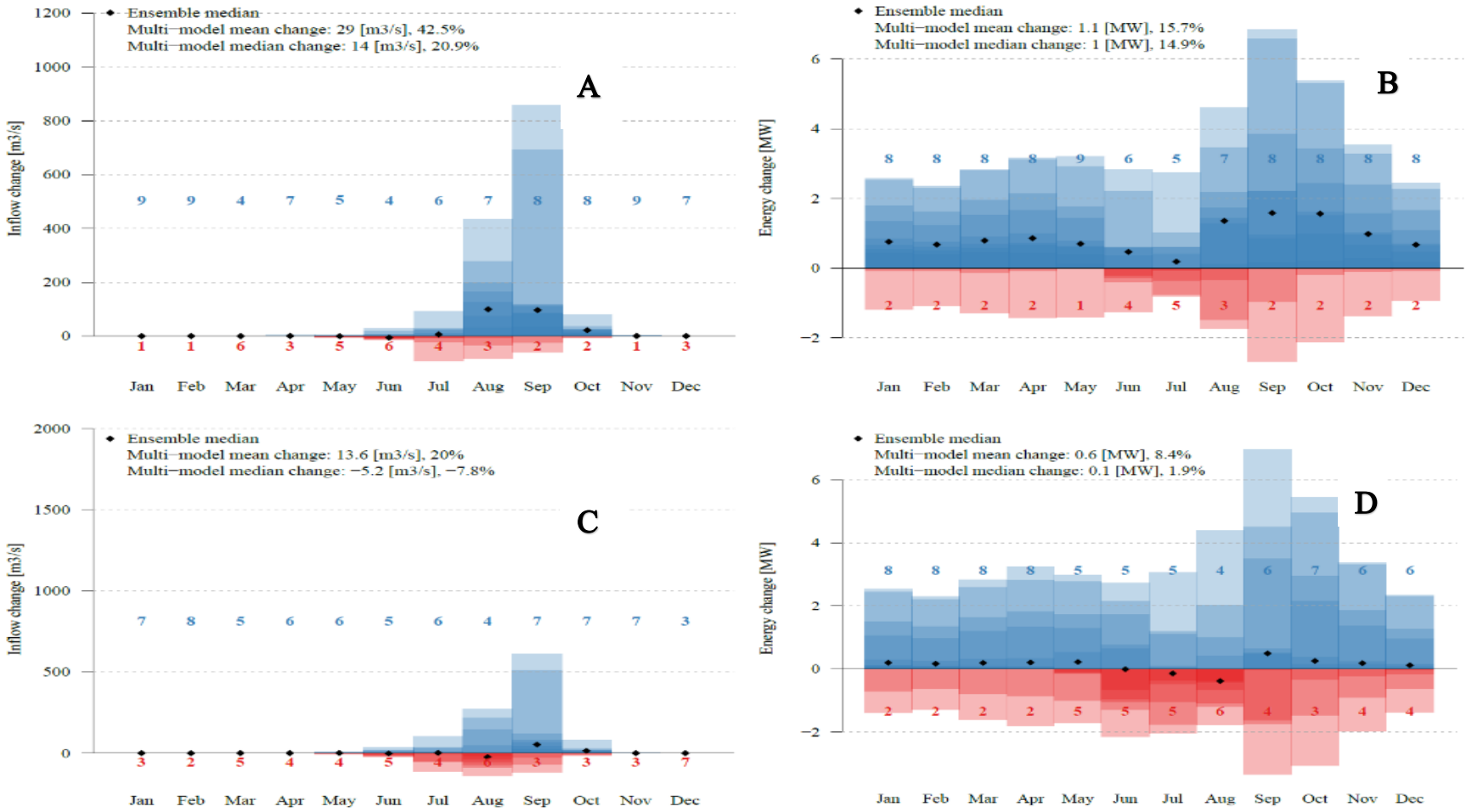

Figure 28. Monthly absolute changes in inflow and hydropower generation during the periods 2035-2065 (A, B) and 2065-2095 (C, D) relative to 1984-2014 under SSP126 and LULC 2050 AFF. The red colour indicates the number of models and amplitude of decrease while the blue colour indicates the number of models and amplitude of increase

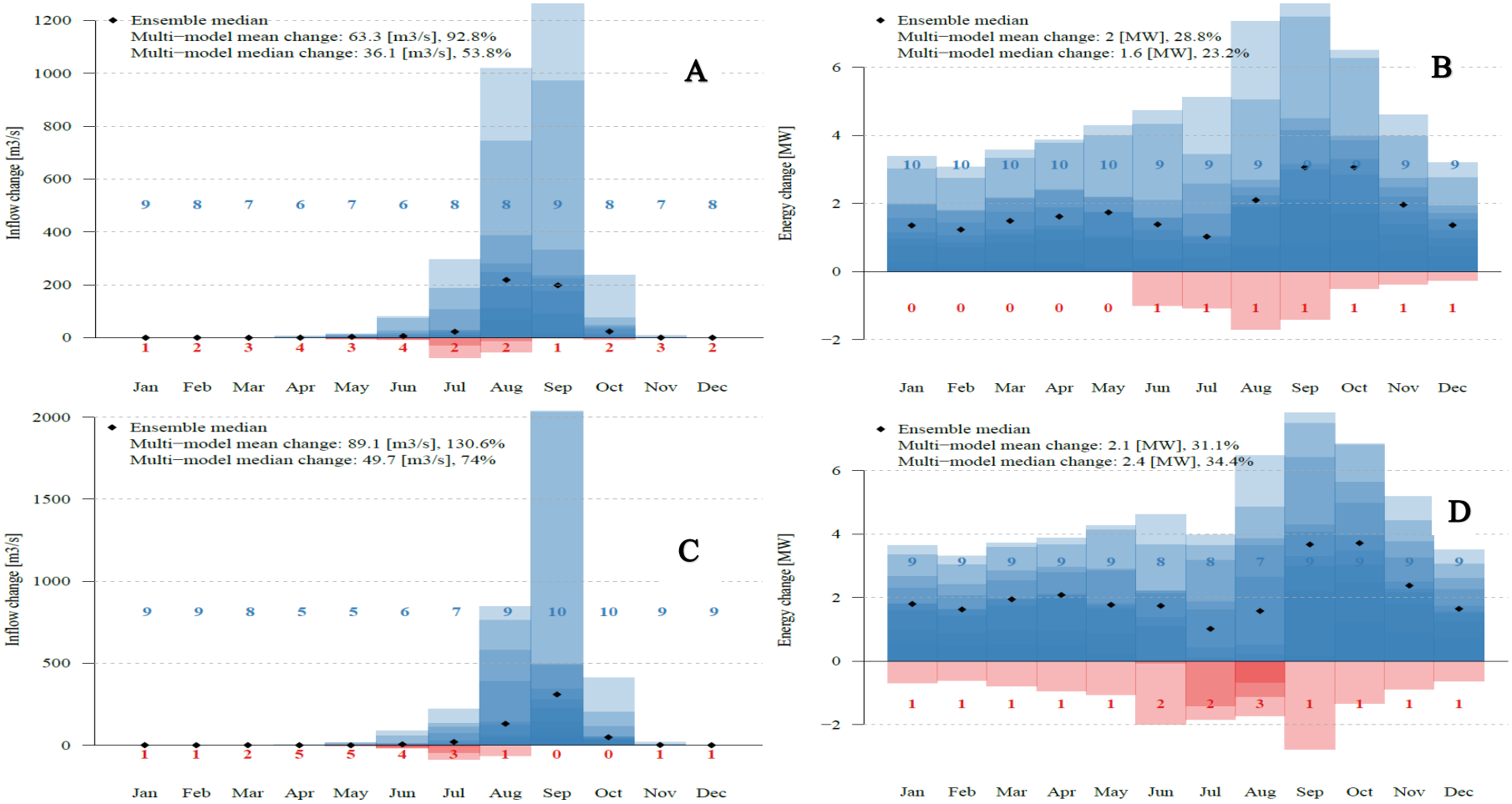

Figure 29. Monthly absolute changes in inflow and hydropower generation during the periods 2035-2065 (A, B) and 2065-2095 (C, D) relative to 1984-2014 under SSP370 and LULC 2050 AFF. The red colour indicates the number of models and amplitude of decrease while the blue colour indicates the number of models and amplitude of increase

6.4.2.2. Business-as-usual scenario

The future inflow and hydropower generation under BAU land use and climate change scenarios are presented in Figures 30 and 31.

Under SSP126, most of the models project an increase of inflow, except in March, May and June, during the period 2035-2065, relative to the baseline. However, net positive changes of the ensemble median are found in July and August. A negative change is found for the month of June and could due to the late onset. This induces an effect on the hydropower generation. Except in June, the majority of the models project an increase in hydropower generation for all months. In addition, the ensemble hydropower generation median shows that only June will experience a negative change in hydropower generation (-0.2 MW). Based on the ensemble median, the maximum inflow change (+150 m^3/s) is observed in August, while the most important change in hydropower generation is observed in September (+1.7 MW) (Figure 30-A&B). From 2065-2095, the ensemble inflow median shows that the positive changes are observed in July, September, and October. Conversely, negative changes are observed in June and August. Meanwhile, the ensemble hydropower generation median illustrates that June to August will experience negative changes, while positive changes are noticed from September to May (Figure 30-D). The greatest inflow and hydropower changes are observed in September (+90 m^3/s and 0.7 MW).

Under SSP370, the majority of the models project an increase in inflow and hydropower generation in both, mid and far future. For inflow, the ensemble median shows that the net positive changes will occur from May to October during the period 2035-2065 and from June to October during the period 2065-2095 (Figure 31-A&C). August will record the highest change (+300 m^3/s) from 2035-2065, whereas from 2065-2095 the maximum change is observed in September (+325 m^3/s). For hydropower generation, all months will experience a positive change in the future relative to the reference period (Figure 31-B&D). The maximum changes are observed in September for both, mid (+1.9 MW) and far (+2.2 MW) future.

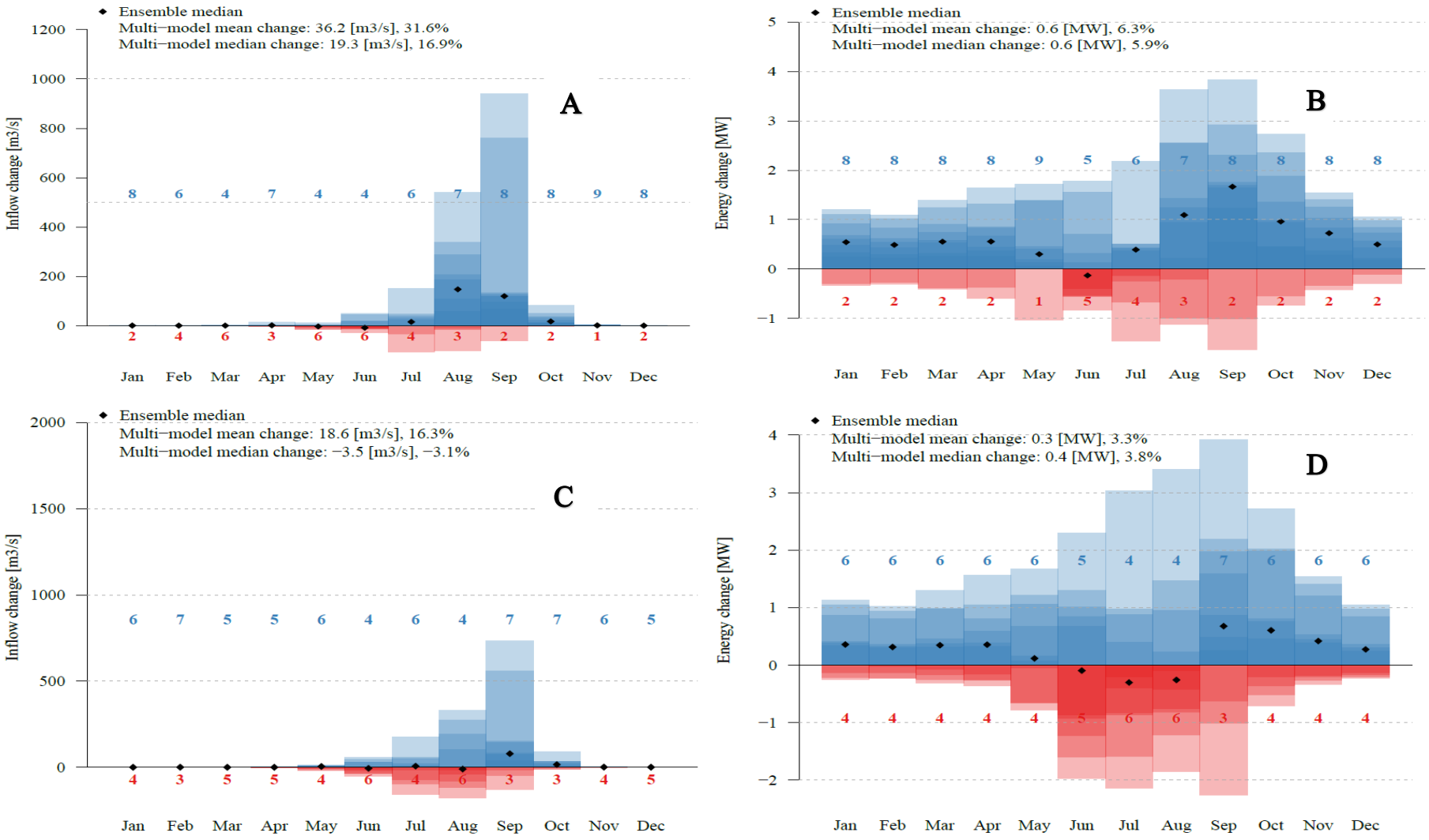

Figure 30. Monthly absolute changes in inflow and hydropower generation during the periods 2035-2065 (A, B) and 2065-2095 (C, D) relative to 1984-2014 under SSP126 and LULC 2050 BAU

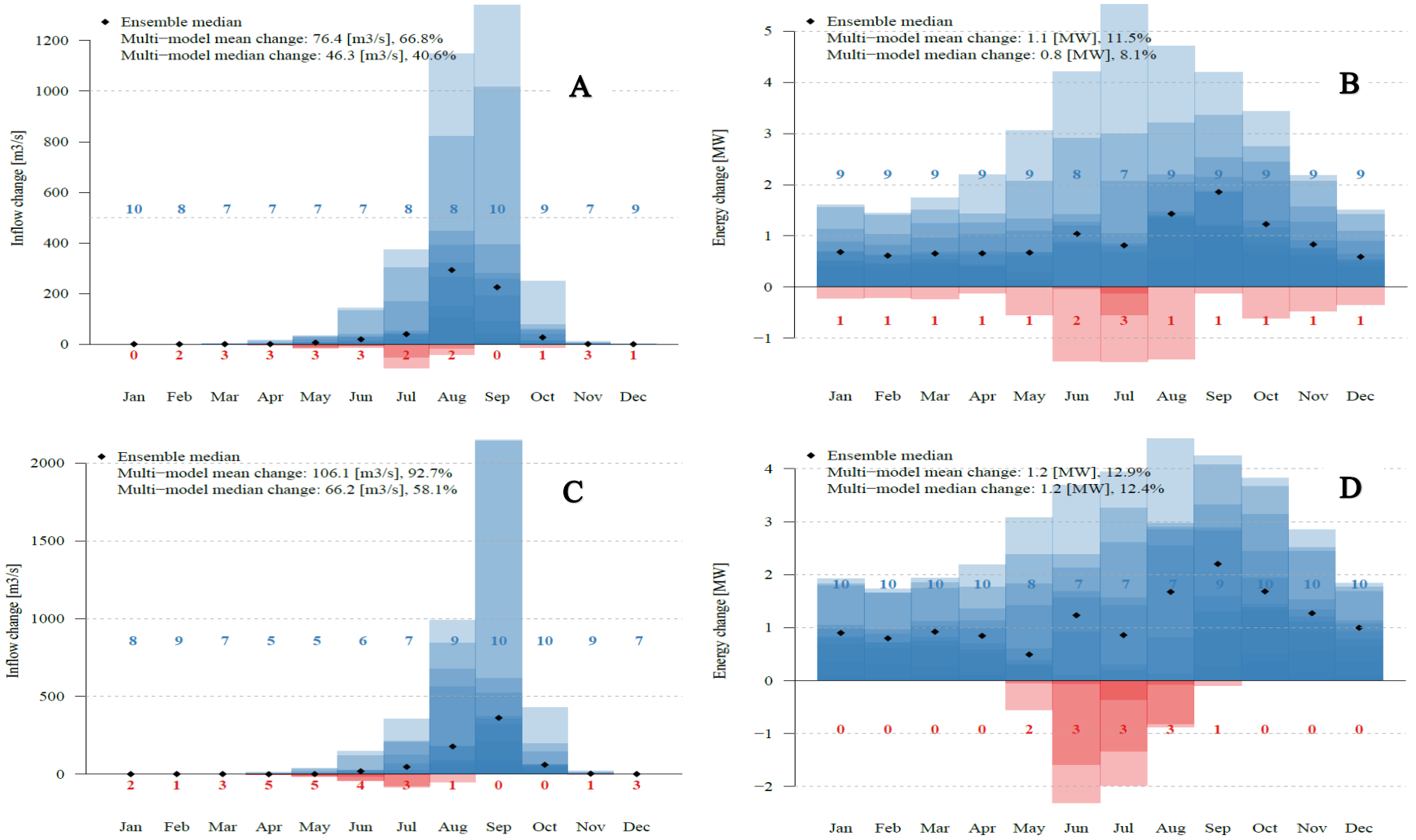

Figure 31. Monthly absolute changes in inflow and hydropower generation during the periods 2035-2065 (A, B) and 2065-2095 (C, D) relative to 1984-2014 under SSP370 and LULC 2050 BAU. The red colour indicates the number of models and amplitude of decrease while the blue colour indicates the number of models and amplitude of increase

6.5. Discussion

Overall, climate projections using ISIMIP3b show an increase of rainfall and temperature in the NRB by 2100. The increase rate would be greater under SSP370 compared SSP126. The results are not congruent with those of Kwawuvi et al. (2022) who found that rainfall would decrease by 2050 in the Oti River Basin, located to the east of the NRB within the Volta River Basin. In contrary, Biasutti (2019), using GCMs from CMIP5, concluded that an increase in rainfall is expected in the Central Sahel by 2100. An increase in annual rainfall is also expected by 2050 in the Vea catchment, part of the White Volta River basin where also the NRB is located (Larbi, 2019). In the NRB, Karambiri et al. (2011) found that rainfall could increase using the RCM RACMO. The monthly changes show a decline in ensemble rainfall median during April and May. This could be due to the delay of the onset in the future as also found by Kwawuvi et al. (2022b) and Kumi and Abiodun (2018). Furthermore, the change in mean temperature is in correspondence with many other studies in the region (Diedhiou et al., 2018; Lawin et al., 2019; Sylla et al., 2018).

Looking at the single climate change impact only, inflow and hydropower generation increases in the mid future under SSP126 and SSP370. However, in the far future, inflow decreases, while a slight increase in hydropower generation occurs under SSP126. This increase could be explained by the additional rainfall over the reservoir. Indeed, about 260 mm per year higher rainfall over the reservoir is projected. Due to higher temperatures and potential evaporation, an increase in rainfall over the upstream basin does not necessarily mean an increase in inflow and hydropower generation. Some months experience a decrease in inflow and hydropower generation. For instance, median inflow decreases in July, while median hydropower generation decreases in July and August. These decreases could be the consequence of the monthly rainfall decrease in April and May in the far future. As found by Yira et al. (2021) and Awotwi et al. (2021), a change of annual discharge can overshadow the changes in monthly discharge, vice-versa. The results are incongruent with those of Obahoundje, et al. (2021b), who projected a decrease in hydropower generation due to climate change at the Nangbeto dam in the Mono River Basin during the periods 2020-2050 and 2060-2090 relative to 1988-2010. Likewise, a study by Yira et al. (2021) found that climate change could reduce hydropower generation by -9.1% and -8.4% during the periods 2020-2049 and 2070-2099 compared to 1983-2005, respectively, in the Bamboi River Basin. Moreover, a study by Turner et al. (2017) projected a -15.3% reduction in hydropower generation for Burkina Faso in the 2050s relative to 1965-2000. However, the results are congruent with a study by Oyerinde et al. (2016) who projected

an increase in hydropower generation by 100 MW and 50 MW under RCP8.5 and RCP4.5, respectively for the Kainji dam in Nigeria from 2010-2100. Most of the increase in hydropower would be due to the increment of inflow. The difference in the direction and magnitude of the change could be justified by the choice of GCMs/RCMs (Liersch et al., 2018; Yira et al., 2021), but also the selected baseline period. As shown by Liersch et al. (2020), a baseline period length less than 30 years (ex: IPCC [1986-2005]) can lead to a distortion on the magnitude of change. Furthermore, they emphasized that the changes between the future simulations and a baseline covering only severe droughts periods would be different compared to a baseline covering wet years. Besides, the monthly hydropower generation at the Bagré dam was reported to decrease each May and June from 1993-2012. This decline could be reduced in May, but would increase in June during the period 2065-2095 under SSP126.

The future LULCC could favour an increase in inflow and hydropower generation. Indeed, the impact of LULC on inflow and hydropower generation changes would be low under an afforestation scenario compared to a BAU scenario. In terms of contribution, land use change impact is almost negligible (3%) under afforestation LULC, whereas under BAU LULC, it could contribute up to 46% and 32% of inflow and hydropower changes in the mid and far futures, correspondingly. Obahoundje et al. (2021a) also found that LULCC (increase of cropland and built-up) has a positive impact on inflow and hydropower generation at the Nangbeto dam. The same finding was found for the Amazon's River discharge; yet, it was not converted to energy due to the inability of the turbines (de Oliveira Serrão et al., 2020). Leta et al. (2022) found that the annual streamflow would not increase significantly (1.6%) under LULCC in 2050 in the Nashe watershed in Ethiopia.

The combined effects of climate and land use changes on inflow and hydropower generation are positive and negative depending on the scenario. The multi-model median shows a positive change in inflow during the mid-future under SSP126 using both future LULC. On the monthly scale, no decreasing inflow and hydropower generation could be observed for all months in the future under SSP370. However, under SSP126, the negative hydropower generation impacts from June to August during the period 2065-2095 due to climate change could be more severe with a BAU land use, while the period of 2035-2065, that did not experience a decrease for most months, would see a decline of hydropower generation in June. Overall, the impact of climate change would dominate the one of LULCC on future inflow and hydropower generation in the NRB. The result is in disagreement with those of Obahoundje et al. (2021b), who found a dominance of LULCC impacts compared to climate change. Many studies attributed the

increasing discharge in the Sahel from the 1970s to LULCC since a decline in rainfall was projected (Karambiri et al., 2011; Mahe et al., 2005). However, because of high variability in West African climate, some uncertainties still exist and could impact the results obtained.

6.6. Partial conclusion

The contribution of climate change and LULCC on future inflow and hydropower generation was assessed. ISIMIP3b GCMs are able to represent the annual cycle of the climate patterns in the NRB. Climate projections show that annual rainfall and mean temperature would increase in the future under both SSP126 and SSP370 scenarios. These changes would increase the inflow and hydropower generation in the future, even though the model median projects a reduction of inflow in far future under SSP126. Likewise, the future LULC under both scenario (afforestation and BAU) would also increase the inflow and hydropower generation. Yet, the increment would be higher under the BAU scenario compared to the afforestation scenario. The combined effects of climate and land use changes would increase even more the ensemble median inflow and hydropower generation. However, these annual increases overshadow some monthly decreases in inflow and hydropower generation. The population of Ouagadougou within the basin is expected to increase. Therefore, drinking water withdrawals from the Ziga dam may also increase. In addition, withdrawals from the Bagré dam are also expected to increase, as the result of the remaining land developments for irrigation purpose. Then, what could be the impact of water management changes for inflow and hydropower generation at the Bagré dam?

CHAPTER 7: IMPACT OF FUTURE WATER ALLOCATION ON HYDROPOWER GENERATION

This chapter presents the findings of future water management impacts on hydropower generation. It is subdivided into four sections. The first section inspects the impact of the future water management on inflow and hydropower generation in the context of climate change. The second section assesses the impact of future water management on inflow and hydropower generation in a context of sole LULCC. The third section investigates the impact of future water management on inflow and hydropower generation under the combined impact of climate and land use changes. At last, the pertinence of the results was discussed.

7.1. Impact of future water management on inflow and hydropower generation in the context of climate change

7.1.1. Changes in inflow and hydropower generation under future water management and climate change

The results of the impacts of water management on median inflow and hydropower generation under future water management and climate change are presented in Table **33**. In this chapter, the reference period is computed with the baseline water management while the future period is computed with the future water management. During the period 2035-2065, it is expected an increase by 18.7% and 52.1% in inflow whereas hydropower generation will decrease by -6.2% and increase by 2.2% under SSP126 and SSP370, respectively. However, during the period 2065-2095, both inflow and hydropower generation will decrease by -10.3% and -20%, respectively, under SSP126. Meanwhile, during the same period an increase by 72.7% and 11.5% is expected for inflow and hydropower generation under SSP370 (Table **33**).

Table 33. Multi-models hydro-climatic median changes during 1984-2014, 2035-2065, and 2065-2095 under future water management and climate changes

Hydro-climatic variables	1984-2014 (P0)	2035-2065 (P1)	% Change (P1-P0)	2065-2095 (P2)	% Change (P2-P0)
ETa [mm/a]	2,037	2,106 (2,064)	3.4 (1.3)	2,114 (2,117)	3.8 (3.9)
ETp [mm/a]	2,523.5	2,591 (2,547)	2.7 (1.0)	2,618 (2,581)	3.8 (2.3)
Inflow [m^3/s]	65.1	77.3 (99.1)	18.7 (52.1)	58.5 (112.5)	-10.3 (72.7)
Outflow [m^3/s]	55.6	59 (80.8)	6 (45.2)	42.1 (93.9)	-24.3 (68.7)
Energy [MW]	6.7	6.3 (6.8)	-6.2 (2.2)	5.3 (7.4)	-20 (11.5)

NB: values in brackets indicate the results under SSP370

7.1.2. Changes in seasonal inflow and hydropower generation under water management and climate changes

The changes in seasonal inflow and hydropower generation due to climate change and future water management are presented in Figure 32 and Figure **33**.

Under SSP126, on the one hand, the majority of the models project a negative change in March, May and June during the period 2035-2065, relative to 1984-2014 (Figure 32-A). Additionally, the ensemble median inflow shows that July to September would experience an increase whereas only June would experience a slight decrease (< -5 m^3/s). The maximum positive inflow change would be observed in September (+90 m^3/s). This increase in inflow during the rainy season would have an impact on hydropower generation, as most of the models project a positive change from August to November. However, all models are unanimous on the negative hydropower generation change experienced in the months of May and June (Figure 32-B). Furthermore, considering the ensemble median, the hydropower generated from December to July would decrease while an increase is expected from August to November. The additional gain could reach 1.1 MW in September whereas May could lose up to -2.5 MW. On the other hand, many months during the period 2065-2095 would experience more positive changes according to most of the ISIMIP3b models. The ensemble inflow median of September and October would change positively (50 and 20 m^3/s, respectively), while August would change negatively (-25 m^3/s), compared to the baseline period. Curiously, the majority of the models project a decrease in hydropower generation for the far future. This is also noticed for the ensemble hydropower generation median, which would experience a negative change from January to December. The lowest change (-0.1 MW) would be observed in September whereas May would depict the maximum change (-2.5 MW). For both future periods, changes in water management at the Bagré would severely impact the hydropower generation as the multi model positive change of inflow does not imply a multi model positive change of hydropower generation (Figure 32).

Under SSP370, most of the models project an increase in inflow for all months, except April and May during the period 2065-2095. Interestingly, the ensemble median inflow would not decrease for all months. On contrary, the months of June to October would experience positive changes in ensemble inflow median. While August records the highest increase of 200 m^3/s for the mid future, a maximum change of 275 m^3/s is observed in September for the far future, both relative to the baseline period (Figure 33-A&C). However, more than half of the models project

a decrease in hydropower generation from April to June in the future. The ensemble hydropower generation median could increase from August to February, while a decrease is observed from March to June, and from April to July during the mid and far futures, respectively. During the period 2035-2065, September would record the maximum positive change (+2.85 MW), while May would record the maximum negative change (-2 MW). However, these extreme changes could reach 3.1 MW in October and -2.1 MW in May during the period 2065-2095.

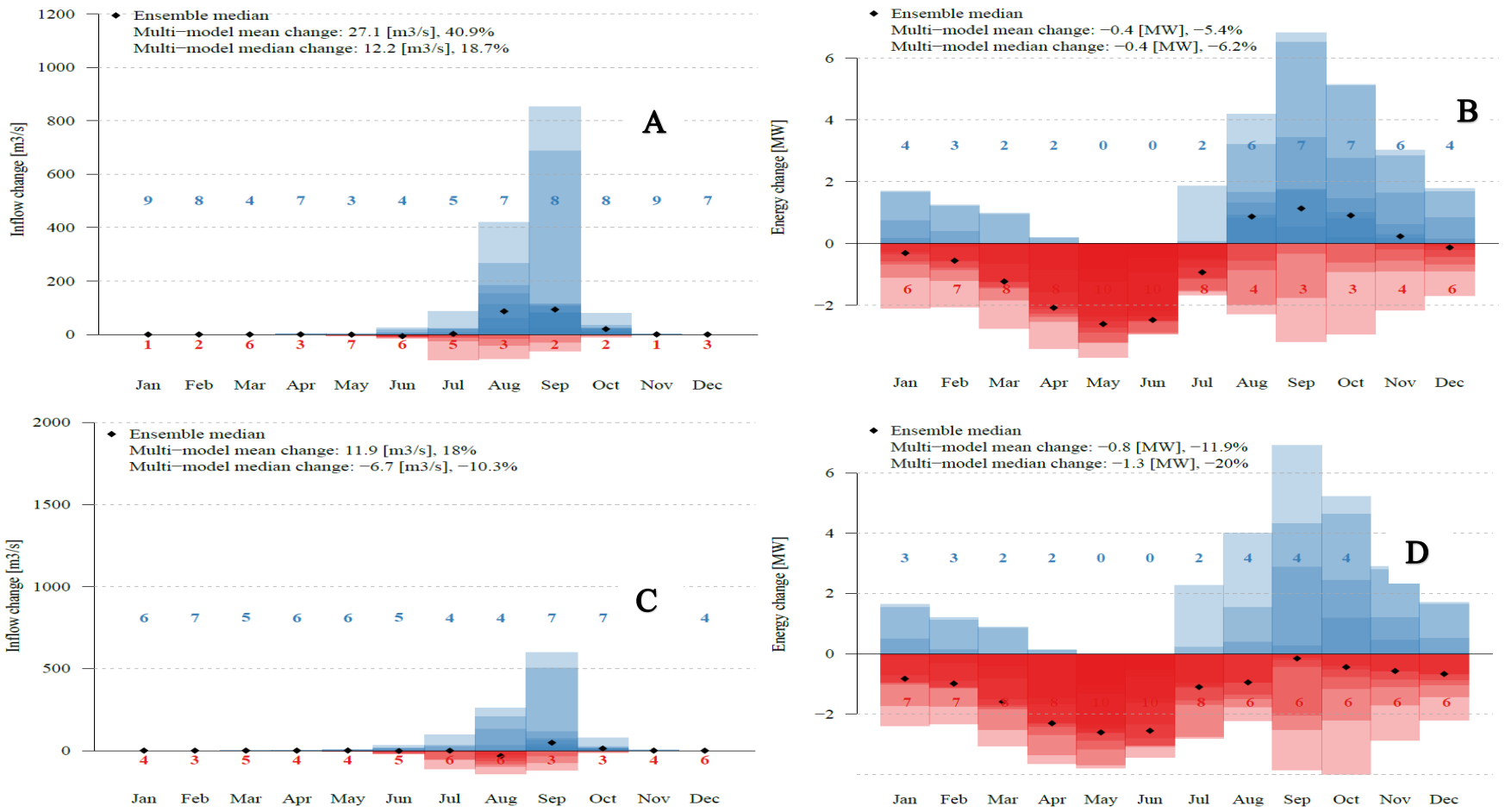

Figure 32. Monthly absolute changes in inflow and hydropower generation due to water management and climate changes (SSP126) during the periods 2035-2065 (A, B) and 2065-2095 (C, D) relative to 1984-2014. The red colour indicates the number of models and amplitude of decrease while the blue colour indicates the number of models and amplitude of increase

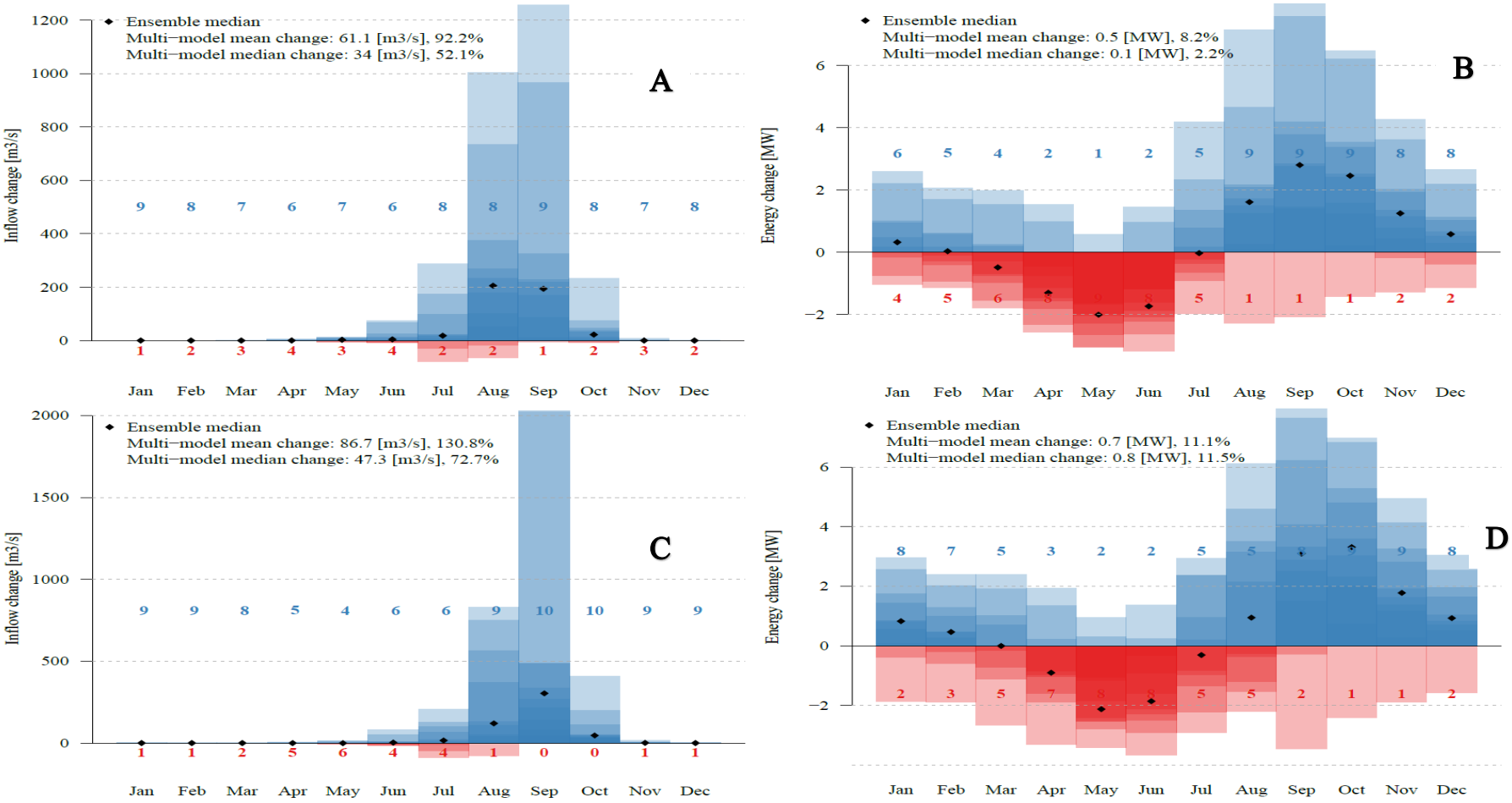

Figure 33. Monthly absolute changes in inflow and hydropower generation due to water management and climate changes (SSP370) during the periods 2035-2065 (A, B) and 2065-2095 (C, D) relative to 1984-2014. The red colour indicates the number of models and amplitude of decrease while the blue colour indicates the number of models and amplitude of increase

7.2. Changes in inflow and hydropower generation under water management and LULC changes

The impact of water management changes on inflow and hydropower generation for different LULC scenarios was assessed at seasonal scale. Under LULC 2005 and baseline water management, inflow is about 54.4 m^3/s. However, under LULC 2020 and future water management, an increase to 72.7 m^3/s is observed. Furthermore, a decrease of inflow to 54.8 m^3/s is expected under the future water management and the afforestation LULC 2050, whereas under LULC 2050 BAU scenario, it will increase to 99.5 m^3/s (Table **34**). This increase in inflow occurs during the rainy season (Figure 34-A).

In terms of energy conversion, the hydropower generation under baseline water management is 6.66 MW. Under LULC 2020 and future water management, it would decrease to 6.93 MW. Also, under LULC 2050 AFF, the future management could decrease the hydropower generation to 5.67 MW (Table **34**). However, hydropower generation could increase to 8.34 MW under LULC 2050 BAU and future water management (Table **34**). Despite the increasing hydropower generation using LULC 2020 and 2050 BAU, some months would experience a severe decrease of hydropower generation. Under LULC 2020, the period of February to June has a lower hydropower generation than the baseline LULC (Figure 34-B). Under LULC 2050 AFF, all months could experience a decline in hydropower generation even though the decrease would be more pronounced from January to July (Figure 34-B). Furthermore, only April and May could experience a decline in hydropower generation under LULC 2050 BAU. In addition, a slight decline in hydropower generation could be observed during the rainy season under LULC 2050 AFF.

Table 34. Changes in median inflow and hydropower generation for different land use land cover and water management scenarios

LULC	LULC 2005	LULC 2020	LULC 2050 AFF	LULC 2050 BAU
	bl-wm	ft-wm	ft-wm	ft-wm
Inflow [m^3/s]	54.42	72.73	54.78	99.51
Energy [MW]	6.66	6.93	5.37	8.34

bl: baseline; ft: future; wm: water management

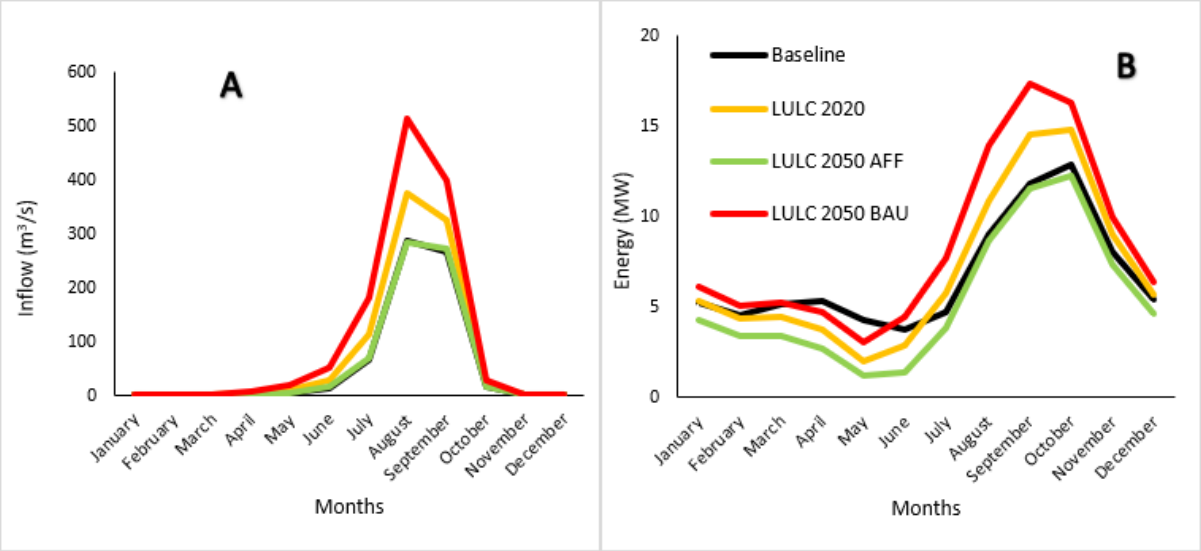

Figure 34. Monthly inflow (A) and hydropower generation (B) due to water management change under various LULC

7.3.Changes in inflow and hydropower generation under the combined impacts of future water management, LULC and climate changes

7.3.1. Changes in inflow and hydropower generation under the combined impacts of future water management, climate and land use changes

The impacts of future water management on inflow and hydropower generation under the combined effects of climate and land use changes are analysed using the afforestation and BAU scenarios. Here, the baseline (P0) corresponds to the results of climate and afforestation/BAU land use changes with historical water management while P1 and P2 are with future water management.

7.3.1.1.Afforestation scenario

The results of the changes in median inflow and hydropower generation due to changes in water management under a combined impact of climate and afforestation land use changes are presented in Table **35**. During the period 2035-2065, an increase in inflow by 18.6% and 49.3% is expected under SSP126 and SSP370, respectively. In terms of hydropower generation, a decrease by -6.7% and a slight increase by 0.1% are expected under SSP126 and SSP370, correspondingly. In the far future, inflow and hydropower generation could decrease by -10% and -19.7%, respectively under SSP126, whereas under SSP370, they could increase by 69.3% and 9.1%, correspondingly.

Table 35. Multi-models hydro-climatic median changes during 1984-2014, 2035-2065, and 2065-2095 under future water management, climate and afforestation land use changes

Hydro-climatic variables	1984-2014 (P0)	2035-2065 (P1)	% Change (P1-P0)	2065-2095 (P2)	% Change (P2-P0)
ETa [mm/a]	2,039	2,108 (2,065.5)	3.4 (1.2)	2,116 (2,118)	3.8 (3.7)
ETp [mm/a]	2,521	2,588 (2,545)	2.6 (1)	2,616 (2,579)	3.8 (2.3)
Inflow [m^3/s]	67.1	79.6 (101.6)	18.6 (49.3)	60.3 (115.2)	-10 (69.3)
Outflow [m^3/s]	57.5	61 (83.1)	6.1 (42.9)	43.7 (96.4)	-23.9 (65.9)
Energy [MW]	6.8	6.4 (6.9)	-6.7 (0.1)	5.5 (7.6)	-19.7 (9.1)

NB: values in brackets indicate the results under SSP370

7.3.1.2.BAU scenario

The changes in annual hydro-climatic variables due to future water management under combined effects of climate and BAU land use changes are presented in Table **36**. The results show an increase in inflow by 15.5% and 39.2% under SSP126 and SPP370, respectively during the period 2035-2065, relative to the baseline. However, this increase would not be profitable to hydropower generation as a decrease by -9.3% and -5.8% occurs under SSP126 and SSP370, correspondingly. Furthermore, the period 2065-2095 would also experience a decrease by -11.5% (SSP126) and -1.3% (SSP370) in hydropower generation, although a low decrease by -4.5% and a high increase by 56.6% in inflow is observed correspondingly.

Table 36. Multi-models hydro-climatic median changes during 1984-2014, 2035-2065, and 2065-2095 under future water management, climate and BAU land use changes

Hydro-climatic variables	1984-2014 (P0)	2035-2065 (P1)	% (P1-P0)	2065-2095 (P2)	% (P2-P0)
ETa [mm/a]	2,067	2,130 (2,090.5)	3 (1.1)	2,149 (2,137)	3.9 (3.4)
ETp [mm/a]	2,468	2,544 (2,509)	3.1 (1.7)	2,573 (2,540)	4.3 (2.9)
Inflow [m^3/s]	114	131.7 (158.7)	15.5 (39.2)	108.9 (178.6)	-4.5 (56.6)
Outflow [m^3/s]	102.3	110.5 (137.9)	8 (34.7)	87.7 (157.8)	-14.3 (54.2)
Energy [MW]	9.7	8.8 (9.1)	-9.3 (-5.8)	8.5 (9.5)	-11.5 (-1.3)

NB: values in brackets indicate the results under SSP370

7.3.2. Changes in seasonal inflow and hydropower generation due to future water management under combined effects of climate and land use changes

The seasonal changes in monthly inflow and hydropower generation due to future water management are analysed under the combined effects of climate and land use (afforestation and BAU) changes.

7.3.2.1. Afforestation scenario

The findings on seasonal inflow and hydropower generation changes due to future water management are presented in Figures 35 and 36.

Under SSP126, the ensemble inflow median increases from August to October (2035-2065) and from September to October (2065-2095). No decrease in ensemble inflow median is observed during the period 2035-2065 (Figure 35-A). September could record the maximum positive changes of 100 m^3/s (2035-2065) and 50 m^3/s (2065-2095). Only August experiences a negative change in ensemble inflow median of -25 m^3/s during the period 2065-2095 (Figure 35-C). These seasonal inflow changes would threaten the seasonal hydropower generation. Indeed, most of the models project a decrease in hydropower generation during the dry season and an increase during the rainy season (Figure 35-B). The ensemble hydropower generation median decreases from December to July from 2035-2065, with a decline of -2.6 MW in May. Meanwhile, September would record the maximum positive change of about 1.1 MW. From 2065-2095, the majority of the models project a decrease in hydropower generation for all months. The ensemble hydropower generation median decreases from January to December, with May recording a decline of -2.7 MW (Figure 35-D).

Under SSP370, the wet conditions would favour an increase in inflow especially during the rainy season in both futures. From 2035-2095, the ensemble inflow median could gain up to 210 m^3/s more in August, compared to the baseline period (Figure 36-A). Furthermore, this inflow gain could reach 275 m^3/s during the period 2065-2095 (Figure 36-C). Overall, no month experiences a decline in ensemble inflow median in the future. In terms of energy conversion, an increase in ensemble hydropower generation median is expected from August to January/February, while a decrease from February/March to July is probable during the periods 2035-2065 and 2065-2095, correspondingly (Figure 36-B & D). The increase could reach + 2.7 MW (September) and +3.1 MW (October) in the mid and far future, respectively. Meanwhile, the decline in hydropower generation would be about -2.2 MW in May in both futures.

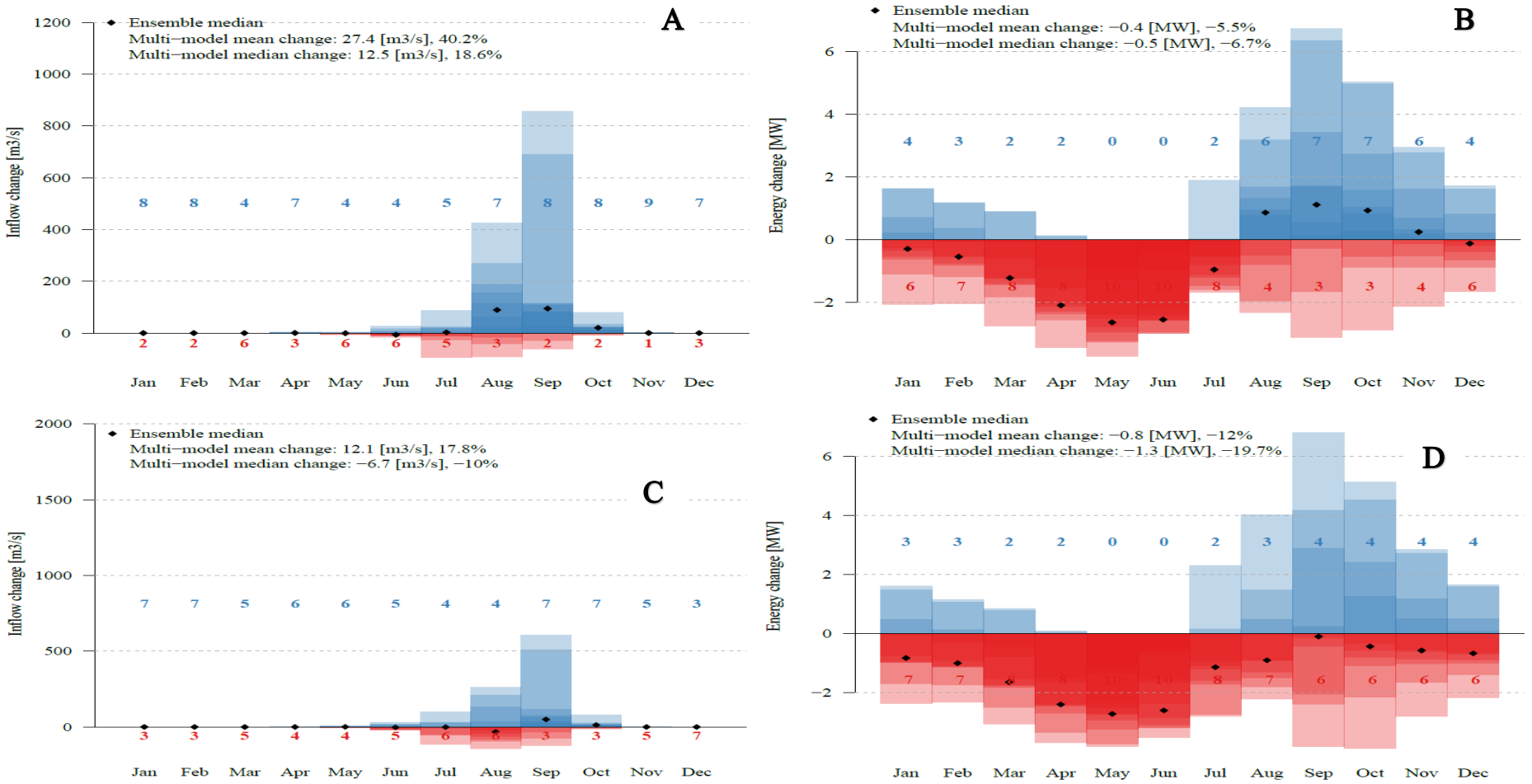

Figure 35. Monthly absolute changes in inflow and hydropower generation due to water management under climate (SSP126) and afforestation land use changes during the periods 2035-2065 (A, B) and 2065-2095 (C, D) relative to 1984-2014. The red colour indicates the number of models and amplitude of decrease while the blue colour indicates the number of models and amplitude of increase

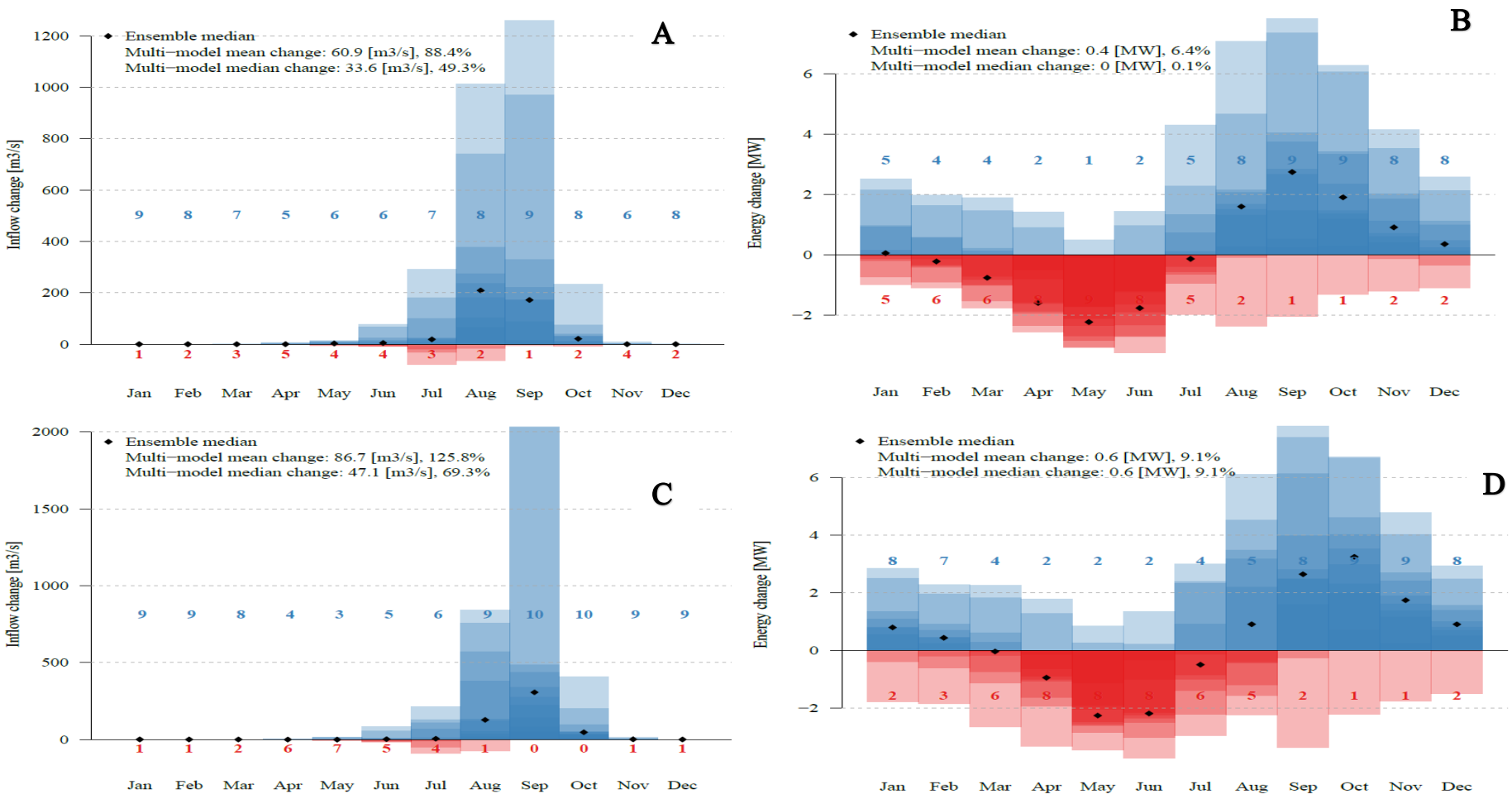

Figure 36. Monthly absolute changes in inflow and hydropower generation due to water management under climate (SSP370) and afforestation land use changes during the periods 2035-2065 (A, B) and 2065-2095 (C, D) relative to 1984-2014. The red colour indicates the number of models and amplitude of decrease while the blue colour indicates the number of models and amplitude of increase

7.3.2.2. BAU scenario

The monthly changes in inflow and hydropower generation due to future water management under climate and BAU land use changes during the mid and far futures are presented in Figure 37 and Figure 38.

Although an inflow increase is observed in general, the ensemble inflow median experiences a decline of -15 m^3/s and -25 m^3/s in June (2035-2065) and August (2065-2095), respectively (Figure 37-A & C). The months that would experience a gain in ensemble inflow median are July to October (2035-2065) and September-October (2065-2095). As a result, the ensemble hydropower generation median could decrease for eight months (December-July) during 2035-2065, while the far future could experience a decline for 10 months (November-August). In both futures, May could record the highest decline of about -3.8 to -3.9 MW (Figure 37-C & D).

Under SSP370, most of the models project an increase in future inflow. No month experiences a decline in inflow based on the ensemble median (Figure 38-A & C). The months of June to October could rather experience an increase in inflow. The maximum increase during the period 2035-2065 is in August (+300 m^3/s), whereas September records the highest increase (+325 m^3/s) during the period 2065-2095. The conversion into hydropower could be less profitable. Indeed, the mid future experiences a decline of hydropower generation from December to June, while this decrease could concern the months of February to July in the far future. Like under SSP126, May would record the maximum hydropower generation decline of -3 MW (2035-2065) and -3.5 MW (2065-2095).

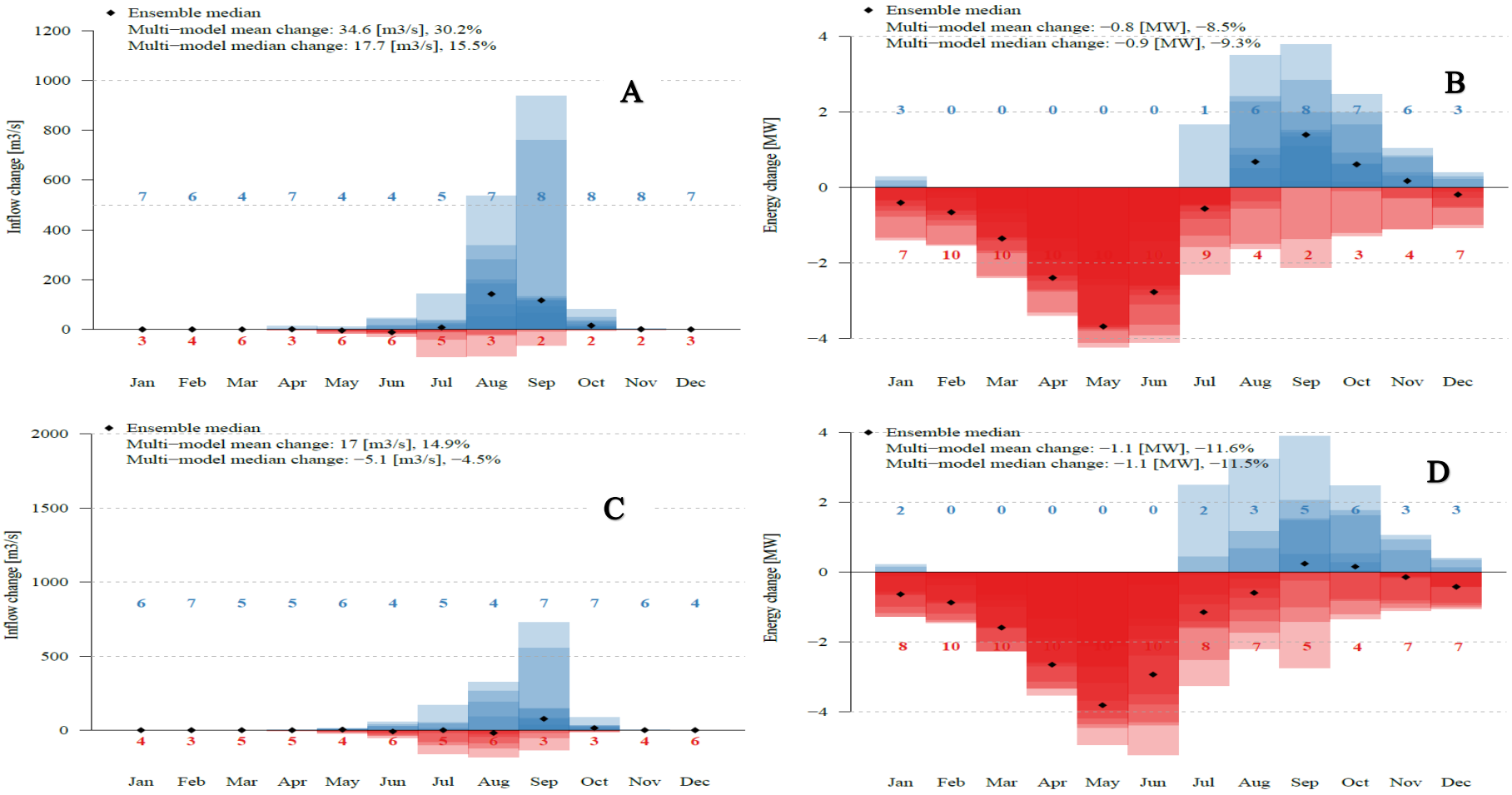

Figure 37. Monthly absolute changes in inflow and hydropower generation due to water management under climate (SSP126) and BAU land use changes during the periods 2035-2065 (A, B) and 2065-2095 (C, D) relative to 1984-2014. The red colour indicates the number of models and amplitude of decrease while the blue colour indicates the number of models and amplitude of increase

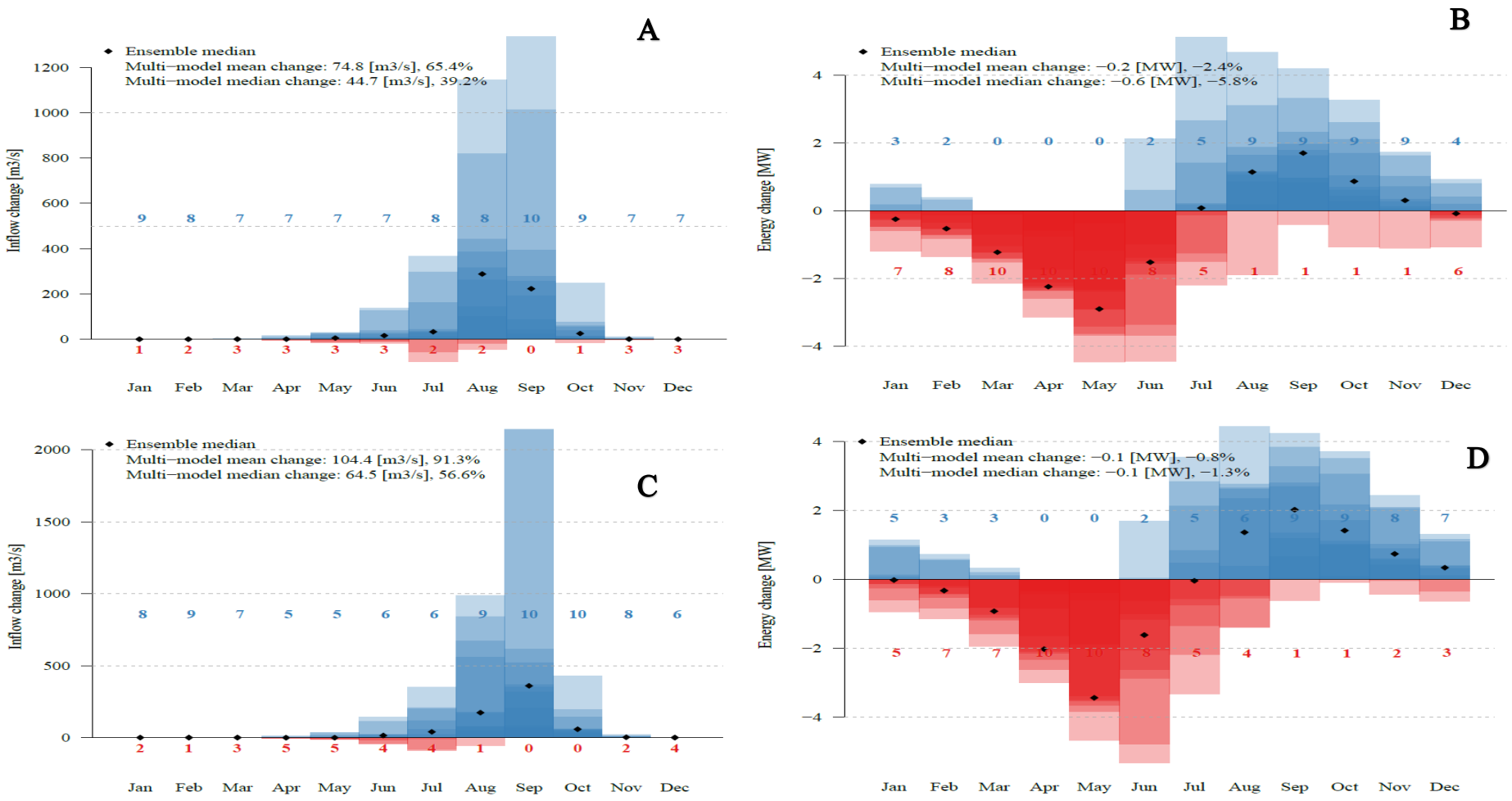

Figure 38. Monthly absolute changes in inflow and hydropower generation due to water management under climate (SSP370) and BAU land use changes during the periods 2035-2065 (A, B) and 2065-2095 (C, D) relative to 1984-2014. The red colour indicates the number of models and amplitude of decrease while the blue colour indicates the number of models and amplitude of increase

7.4.Discussion

The change of Ziga dam management to supply water to Ouagadougou would cause a decrease in inflow median at the Bagré dam. However, compared to the impacts of climate and/or land use changes, this decrease would not be severe and is between -1.4 and -2 m^3/s. As a result, the monthly inflow median could slightly be impacted, but is not visible on Figures 35-38. This means that the increase in withdrawals from 0.196 m^3/s to 2.3 m^3/s at Ziga dam would not affect much the inflow at Bagré dam in the future. The findings are congruent with those of Liersch et al. (2023), who found the future change in Bagré, Pwalugu, and Bui dams management will decrease by -28.4 m^3/s the discharge into the Volta.

The hydropower generation at the Bagré dam would decrease and increase depending on the climate scenario, the land use scenario and the future period. In both futures, the increase of water withdrawals from Bagré for irrigation would lead to a decrease in hydropower generation under SSP126 and both future LULC scenarios. Yet, the decrease rate for the far future would be higher than the decline in the mid-future. This could be explained by the changes in rainfall for the two periods. Indeed, the period 2035-2065 is expected to be much wetter than the period 2065-2095. However, under SSP370, an increase in hydropower generation median is expected except under BAU LULC. In fact, although inflow median is expected to increase under SSP370 and BAU LULC, it would be followed with huge peak flows because of lack of vegetation. Nevertheless, peak flows would fill quickly the dam. In turn, to not expose the dam to risks, water has to be released. This water release could cause more flood events in the downstream villages. Then, maximum hydropower would be generated during the rainy season while during the dry season, the hydropower generation would decline (Figure 38-B & D).

The aforementioned results would impact the socio-economic conditions of the population. In terms of irrigation, it is expected an increase of rice and vegetable crop yields. These additional yields could help the country to be less dependent in rice imports. Moreover, the availability of more developed lands and water for irrigation would reduce the unemployment rate in the region. However, the decline in hydropower generation could lead to more power shortages especially during the dry season. This situation could make the country more dependent on energy imports from neighbouring countries. As a solution to supply the deficit of hydropower generation during the dry season, the country could vary the sources of clean energy by using solar and wind power. The wind power potential in Burkina Faso is estimated to 4,411 MW

using small wind turbines of 50 kW (Landry et al., 2016). In terms of solar energy, the potential is much higher. A study by IRENA (2021) showed that Burkina Faso has a development potential of 95,900 MW and 1,960 MW of photovoltaic solar and wind power, respectively.

7.5.Partial conclusion

Upstream water management change would reduce the inflow of the Bagré dam. However, this decrease is not significant. On the contrary, changes in Bagré dam withdrawals would have a great impact on its hydropower generation. While hydropower generation could increase for some months during the rainy season, it would highly decline during all months of the dry season and also some months of the rainy season.

CHAPTER 8: GENERAL CONCLUSION AND PERSPECTIVES

This chapter is divided into two. On the one hand, it summarizes the main conclusions of the study. On the other hand, the perspectives and future works are discussed.

8.1.Conclusions

The thesis investigated the impact of climate, land use, and water management changes on hydropower potentials of Bagré dam in Burkina Faso based on four assumptions.

The first hypothesis stipulated that "hydropower generation at the Bagré dam is in positive correlation with the trend of rainfall, inflow, water level, and upstream water management". The use of reanalysis climate data (W5E5) and statistical tests (Pettitt test, SNHT, modified Mann-Kendall trend test) showed a presence of break years in the significant increasing trends of rainfall, temperature, inflow, and hydropower generation. These breaks years (2006-2007) show the existing relationship between rainfall and inflow in the basin. However, the break year of hydropower generation was detected in 2002 which corresponds to the Ziga dam construction (2000) in the upstream basin. Furthermore, the change of the Ziga dam management in 2004-2005 could also explain the significant increasing trend of inflow from 2006. The Spearman coefficient confirmed that Ziga dam has an influence on hydropower generation at the Bagré dam as their correlation is moderate (0.5). Therefore, the first hypothesis is confirmed.

"The dynamics of LULC in the NRB is marked by the expansion of anthropogenic land uses" was the second hypothesis of this thesis. Using Landsat satellite images in a GEE platform, with the help of ground truth data, the RF method was able to classify accurately the different states of LULC in the NRB in 1990, 2005, and 2020. The findings showed a continuous decrease of natural vegetation (woodland and shrubland) and an incessant increase of anthropogenic land uses (cropland and bare land/built-up) over the last 31 years. The basin that was mostly covered by shrubland in 1990, was now dominated firstly by cropland in 2005, then bare land/built-up in 2020. The MLP neural network within LCM was able to simulate the future LULCC in the basin. Whatever the scenario, the basin will still be dominated by anthropogenic land uses in 2050. However, cropland area would dominate under the afforestation scenario with little recovering of natural vegetation, while bare land/built-up area would dominate under BAU scenario. These results are congruent with many studies in the region and confirm the aforementioned hypothesis.

The study also inspected the impact of climate and land use changes on hydropower generation at the Bagré dam in mid and far futures. The SWIM model was able to reproduce the hydrological process and the Bagré dam management with acceptable NSE and PBias. The study also showed that downscaled and bias corrected ISIMIP3b models at monthly scale can be used for climate impact studies in the basin. Indeed, it was found that climate change would increase the median hydropower generation in the future under SSP126 and SSP370 scenarios. Likewise, the future LULCC (BAU and afforestation) in 2050 could be favourable for hydropower generation. The results of the combined impacts of climate and land use changes also showed more possibility in hydropower generation. At monthly scale, ensemble hydropower generation median decreases in July and August in the far future under combined impacts of climate change (SSP126) and afforestation LULC 2050. However, under combined impacts of climate change (SSP126) and BAU LULC 2050, the decline could occur in June in the mid future, and in June, July, and August in the far future, relative to baseline. The results ultimately attributed the strongest changes in inflow and hydropower generation to climate change compared to LULC change. Therefore, the third hypothesis whose statement was "future climate and LULC changes will affect positively the hydropower generation at the Bagré dam" is partially confirmed.

The last part of the study examined the impact of water management changes on the hydropower potentials of the Bagré dam. The hypothesis was that "water management changes will negatively impact the seasonal hydropower generation at the Bagré dam". Using the same calibration of SWIM model with new water withdrawals at Ziga (2.3 m^3/s) and Bagré (17.2 m^3/s) for drinking water and irrigation supplies, it was found that the change of water withdrawals at Ziga dam would reduce slightly the median inflow by -1.4 to -2 m^3/s depending on the considered future period, the climate change scenario, and the LULC scenario. In addition to the change of water withdrawals for irrigation from the Bagré dam, the study found that the hydropower generation median could decline severely for 4 (March-June) to 10 (November-August) months depending on the future period, the climate change scenario, and the LULC scenario. Nevertheless, the most important decrease in monthly hydropower median could occur under combined impacts of climate and BAU land use changes. Consequently, the fourth hypothesis is also confirmed.

This work showed the capability of using the SWIM model to assess the impacts of climate, land use and water management changes on the hydropower in a data scarce catchment like the NRB. However, the study contains some limits that must be considered when dealing with the findings. The soil datasets used in this study are at global scale and have an impact in the results. In addition, even though ISIMIP3b GCMs showed an acceptable performance with W5E5 and observations, their reliability could be questioned because the W5E5 products that were used for the bias correction do not really match very well with observations, and could have an effect on the amplitude of the signal in inflow and hydropower generation changes. Moreover, the DEM of 90 m used seems very coarse and the LULC classification was based on Landsat images of 30 m of spatial resolution, which are not very fine especially in West Africa where small farm lands of less than 900 m^2 exist. Moreover, dam sedimentation and siltation are not considered in this study.

8.2.Recommendations

From the results obtained, many recommendations and suggestions can be made:

- Since upstream water management plays an important role in the hydropower generation at the Bagré dam, SONABEL and ONEA (National Water and Sanitation Company) who are in charge of the operation of Bagré and Ziga dams, respectively, should work closely in order to maximize dams' management for hydropower generation, irrigation and water supply.
- Future LULC dynamic will also play a major role in the hydropower generation at the Bagré dam. Therefore, it is important to undertake regular monitoring and evaluation actions to ensure that policies and measures for better land management are successful and relevant.
- As Bagré is a multipurpose dam, it is difficult to prioritize energy production when the country is not food self-sufficient. Therefore, a way to solve this issue would be to use a mix energy system that combines the use of solar power and hydropower. For instance, during the rainy season, hydropower will be produced while during the dry season when sunshine duration is high, solar power will be produced.

8.3. Perspectives

The perspectives of this study are many. Future studies should look at the use of other rainfall data source such as the Climate Hazards Group InfraRed Precipitation with Station (CHIRPS) (0.05°x0.05°) which was found as the best satellite product in Burkina Faso by some researchers (Dembélé and Zwart, 2016). Future works should also be oriented on the use of fine scale resolution RCMs (WASCAL 12 Km RCMs) to assess the hydropower generation of the Bagré dam. As the spill from the Bagré dam is known to have caused many floods in the downstream, a study on the improvement of Bagré dam operation to reduce floods in the downstream is ongoing. This new operation will bring out new results of the hydropower potentials and the water availability for irrigation from the Bagré reservoir. Further studies could also focus on the addition of more small reservoirs and dam siltation in order to investigate the water-food-energy nexus in the basin. Finally, future works should try to assess the uncertainties related to the model structure, the climate change scenarios, and the outputs of the modelling.

REFERENCES

Abungba, J. A., Khare, D., Pingale, S. M., Adjei, K. A., Gyamfi, C., & Odai, S. N. (2020). Assessment of Hydro-climatic Trends and Variability over the Black Volta Basin in Ghana. Earth Systems and Environment, 4(4), 739–755. https://doi.org/10.1007/s41748-020-00171-9

Adeyeri, O. E. (2019). Modelling The Hydrological Response of Komadougu-Yobe Area of the Lake Chad Basin to Climate Change. Ph.D Thesis, University of Abomey-Calavi, Benin.

Adjivon A. S. (1991). Etude hydrologique du bassin versant du Massili a Loumbila: La crue exceptionnelle de Septembre 1986. Master Thesis, Université de Ouagadougou, Burkina Faso.

AEN. (2015). Schema Directeur D'amenagement et de Gestion des Eaux de L'espace de Competance de L'agence de L'eau du Nakanbe: Tome I. Etat Des Lieux. Rapport definitif,

Aich, V., Liersch, S., Vetter, T., Huang, S., Tecklenburg, J., Hoffmann, P., Koch, H., Fournet, S., Krysanova, V., Müller, E. N., & Hattermann, F. F. (2014). Comparing impacts of climate change on streamflow in four large African river basins. Hydrology and Earth System Sciences, 18(4), 1305–1321. https://doi.org/10.5194/hess-18-1305-2014

Ajibola, F. O., Zhou, B., Tchalim Gnitou, G., & Onyejuruwa, A. (2020). Evaluation of the Performance of CMIP6 HighResMIP on West African Precipitation. Atmosphere, 11(10), 1053. https://doi.org/10.3390/atmos11101053

Akinyemi, F. O. (2021). Vegetation Trends, Drought Severity and Land Use-Land Cover Change during the Growing Season in Semi-Arid Contexts. Remote Sensing, 13(5), 836. https://doi.org/10.3390/rs13050836

Akpaud W. A. C. (2007). Analyse des enjeux liés à la gestion de la ressource en eau du barrage de Ziga et perspectives d'un approvisionnement en eau potable adéquat de la ville de Ouagadougou jusqu'en 2025. Master Thesis, Institut International de l'Eau et de l'Environnement, Ouagadougou, Burkina Faso.

Akpoti, K., Antwi, E., & Kabo-bah, A. (2016). Impacts of Rainfall Variability, Land Use and

Land Cover Change on Stream Flow of the Black Volta Basin, West Africa. Hydrology, 3(3), 26. https://doi.org/10.3390/hydrology3030026

Alexandersson, H. (1986). A homogeneity test applied to precipitation data. Journal of Climatology, 6(6), 661–675. https://doi.org/10.1002/joc.3370060607

Ali, S. A., Aadhar, S., Shah, H. L., & Mishra, V. (2018). Projected Increase in Hydropower Production in India under Climate Change. Scientific Reports, 8(1), 12450. https://doi.org/10.1038/s41598-018-30489-4

Amisigo, B. A., McCluskey, A., & Swanson, R. (2014). Modeling impact of climate change on water resources and agriculture demand in the Volta Basin and other basin systems in Ghana. In WIDER Working Paper (Vol. 7, Issue 6). https://doi.org/10.35188/UNU-WIDER/2014/754-7

Amoussou, E., Camberlin, P., & Mahé, G. (2012). Impact de la variabilité climatique et du barrage Nangbéto sur l'hydrologie du système Mono-Couffo (Afrique de l'Ouest). Hydrological Sciences Journal, 57(4), 805–817. https://doi.org/10.1080/02626667.2011.643799

Andersen, J., Refsgaard, J. C., & Jensen, K. H. (2001). Distributed hydrological modelling of the Senegal River Basin — model construction and validation. Journal of Hydrology, 247(3–4), 200–214. https://doi.org/10.1016/S0022-1694(01)00384-5

Annys, S., Ghebreyohannes, T., & Nyssen, J. (2020). Impact of hydropower dam operation and management on downstream hydrogeomorphology in semi-arid environments (Tekeze, Northern Ethiopia). Water (Switzerland), 12(8). https://doi.org/10.3390/w12082237

Arnold, J. G., Allen, P. M., & Bernhardt, G. (1993). A comprehensive surface-groundwater flow model. Journal of hydrology, 142, 47–69

Aschonitis, V., Demertzi, K., Papamichail, D., Colombani, N., & Mastrocicco, M. (2015). Revisiting the Priestley-Taylor method for the assessment of reference crop evapotranspiration in Italy. Italian Journal of Agrometeorology, 20(2), 5–18.

Asenso Barnieh, B., Jia, L., Menenti, M., Zhou, J., & Zeng, Y. (2020). Mapping Land Use Land

Cover Transitions at Different Spatiotemporal Scales in West Africa. Sustainability, 12(20), 8565. https://doi.org/10.3390/su12208565

Awotwi, A, Kumi, M., Jansson, P., Yeboah, F., & Nti, I. (2015). Predicting Hydrological Response to Climate Change in the White Volta Catchment, West Africa. Journal of Earth Science & Climatic Change, 06(01), 1–7. https://doi.org/10.4172/2157-7617.1000249

Awotwi, Alfred, Annor, T., Anornu, G. K., Quaye-Ballard, J. A., Agyekum, J., Ampadu, B., Nti, I. K., Gyampo, M. A., & Boakye, E. (2021). Climate change impact on streamflow in a tropical basin of Ghana, West Africa. Journal of Hydrology: Regional Studies, 34(February), 100805. https://doi.org/10.1016/j.ejrh.2021.100805

Aziz, F., & Obuobie, E. (2017). Trend analysis in observed and projected precipitation and mean temperature over the Black Volta Basin, West Africa. 1400| International Journal of Current Engineering and Technology, 7(4), 2. http://inpressco.com/category/ijcet

Baatuuwie BN (2015) Multi-dimensional approach for evaluating land degradation in the savanna belt of the white volta basin. PhD dissertation, KNUST, Ghana.

Badou, D. F., Kapangaziwiri, E., Diekkrüger, B., Hounkpè, J., & Afouda, A. (2017). Evaluation of recent hydro-climatic changes in four tributaries of the Niger River Basin (West Africa). Hydrological Sciences Journal, 62(5), 715–728. https://doi.org/10.1080/02626667.2016.1250898

Bahati, H. K., Ogenrwoth, A., & Sempewo, J. I. (2021). Quantifying the potential impacts of land-use and climate change on hydropower reliability of muzizi hydropower plant, Uganda. Journal of Water and Climate Change, 12(6), 2526–2554. https://doi.org/10.2166/wcc.2021.273

Balist, J., Malekmohammadi, B., Jafari, H. R., Nohegar, A., & Geneletti, D. (2022). Detecting land use and climate impacts on water yield ecosystem service in arid and semi-arid areas. A study in Sirvan River Basin-Iran. Applied Water Science, 12(1), 1–14. https://doi.org/10.1007/s13201-021-01545-8

Beilfuss, R. (2012). A Risky Climate for Southern African Hydro. September. https://doi.org/10.13140/RG.2.2.30193.48486

Berga, L. (2016). The Role of Hydropower in Climate Change Mitigation and Adaptation: A Review. Engineering, 2(3), 313–318. https://doi.org/10.1016/J.ENG.2016.03.004

Berkun, M. (2010). Hydroelectric potential and environmental effects of multidam hydropower projects in Turkey. Energy for Sustainable Development, 14(4), 320–329. https://doi.org/10.1016/j.esd.2010.09.003

Bessah, E., Raji, A. O., Taiwo, O. J., Agodzo, S. K., Ololade, O. O., & Strapasson, A. (2020). Hydrological responses to climate and land use changes: The paradox of regional and local climate effect in the Pra River Basin of Ghana. Journal of Hydrology: Regional Studies, 27(23), 100654. https://doi.org/10.1016/j.ejrh.2019.100654

Biasutti, M. (2019). Rainfall trends in the African Sahel: Characteristics, processes, and causes. Wiley Interdisciplinary Reviews: Climate Change, 10(4), 1–22. https://doi.org/10.1002/wcc.591

Bidon, S. (1995). Etude de l''impact du barrage de Bagré (Burkina Faso) sur le secteur maraîcher : enquêtes sur trois villages de la zone amont. Mémoire de DESS, Université de Ouagadougou, Burkina Faso

Boadi, S. A., & Owusu, K. (2017). Impact of climate change and variability on hydropower in Ghana. African Geographical Review, 6812, 1–15. https://doi.org/10.1080/19376812.2017.1284598

Bock, O., Collilieux, X., Guillamon, F., Lebarbier, E., & Pascal, C. (2020). A breakpoint detection in the mean model with heterogeneous variance on fixed time intervals. Statistics and Computing, 30(1), 195–207. https://doi.org/10.1007/s11222-019-09853-5

Bozkaya, A. G., Balcik, F. B., Goksel, C., & Esbah, H. (2015). Forecasting land-cover growth using remotely sensed data: a case study of the Igneada protection area in Turkey. Environmental Monitoring and Assessment, 187(3), 59. https://doi.org/10.1007/s10661-015-4322-z

Braimoh, A. K., & Vlek, P. L. G. (2004a). Land-Cover Change Analyses in the Volta Basin of Ghana. Earth Interactions, 8(21), 1–17. https://doi.org/10.1175/1087-3562(2004)8<1:lcaitv>2.0.co;2

Braimoh, A. K., & Vlek, P. L. G. (2004b). Land-Cover Change Analyses in the Volta Basin of Ghana. Earth Interactions, 8(21), 1–17. https://doi.org/10.1175/1087-3562(2004)8<1:LCAITV>2.0.CO;2

Bullock, E. L., Healey, S. P., Yang, Z., Oduor, P., Gorelick, N., Omondi, S., Ouko, E., & Cohen, W. B. (2021). Three Decades of Land Cover Change in East Africa. Land, 10(2), 150. https://doi.org/10.3390/land10020150

Caussinus, H., & Mestre, O. (2004). Detection and correction of artificial shifts in climate series. Journal of the Royal Statistical Society: Series C (Applied Statistics), 53(3), 405–425. https://doi.org/10.1111/j.1467-9876.2004.05155.x

Cherlet, M., Hutchinson, C., Reynolds, J., Hill, .J, Sommer. S. & Von Maltitz, G. (2018) World Atlas of Desertification. Publications Office of the European Union, Luxembourg. https://doi.org/ 10. 2760/ 9205

CILSS. (2016). Les Paysages de l'Afrique de l'Ouest : Une Fenêtre sur un Monde en Pleine Évolution. U.S. Geological Survey EROS, 47914 252nd St, Garretson, SD 57030, United States of America

Clark Labs (2020). TerrSet 2020 geospatial monitoring and modeling system. Clark Labs, Clark University, Worcester, United States of America

Cline, W. R. (2008). Réchauffement climatique et agriculture. Les effets de la sécheresse dans le sud-ouest du Zimbabwé. Finances and Development, 23–27.

Cohen Liechti, T., Matos, J. P., Boillat, J. L., & Schleiss, A. J. (2012). Comparison and evaluation of satellite derived precipitation products for hydrological modeling of the Zambezi River Basin. Hydrology and Earth System Sciences, 16(2), 489–500. https://doi.org/10.5194/hess-16-489-2012

Collier, U. (2004). Hydropower and The Environment: Towards Better Decision-Making. Proceedings of Symposium on Hydropower and Sustainable Development, 27–29. http://ibcperu.org/doc/isis/12015.pdf

Corà, E., Fry, J. J., Bachhiesl, M., & Schleiss, A. (2020). Hydropower Technologies: the state-of-the-art. 826010, 1–87.

Costelloe, J. F., Grayson, R. B., & McMahon, T. A. (2005). Modelling stream flow for use in ecological studies in a large, arid zone river, central Australia. Hydrological Processes, 19(6), 1165–1183. https://doi.org/10.1002/hyp.5558

Coulidiati T. F. A. (2016). Verification d'etudes d'execution de perimetre irrigue de 36 ha de type semi-californien a l'amont du barrage de Seguenega. Matsre Thesis, Institut International d'Ingénierie de l'Eau et de l'Environnement, Ouagadougou, Burkina Faso.

Darbandsari, P., & Coulibaly, P. (2020). Inter-comparison of lumped hydrological models in data-scarce watersheds using different precipitation forcing data sets: Case study of Northern Ontario, Canada. Journal of Hydrology: Regional Studies, 31(April), 100730. https://doi.org/10.1016/j.ejrh.2020.100730

de Condappa, D., Chaponnière, A., & Lemoalle, J. (2008). Decision-support tool for water allocation in the Volta basin. Volta Basin Focal Project Report No 10. IRD, Montpellier, France, and CPWF, Colombo, Sri Lanka.

de Oliveira Serrão, E. A., Silva, M. T., Ferreira, T. R., de Paulo Rodrigues da Silva, V., de Salviano de Sousa, F., de Lima, A. M. M., de Ataide, L. C. P., & Wanzeler, R. T. S. (2020). Land use change scenarios and their effects on hydropower energy in the Amazon. Science of the Total Environment, 744, 140981. https://doi.org/10.1016/j.scitotenv.2020.140981

de Souza Dias, V., Pereira da Luz, M., Medero, G., & Tarley Ferreira Nascimento, D. (2018). An Overview of Hydropower Reservoirs in Brazil: Current Situation, Future Perspectives and Impacts of Climate Change. Water, 10(5), 592. https://doi.org/10.3390/w10050592

Dembélé, M., Vrac, M., Ceperley, N., Zwart, S. J., Larsen, J., Dadson, S. J., Mariéthoz, G., & Schaefli, B. (2022). Contrasting changes in hydrological processes of the Volta River basin under global warming. Hydrology and Earth System Sciences, 26(5), 1481–1506. https://doi.org/10.5194/hess-26-1481-2022

Deme, K. (2001). Evaluation comparee de l'occupation des sols et des ecoulements sur le bassin du Nakambe. Ecole Inter Etats d'Ingenieurs de l'Equipement Rural, Ouagadougou, Burkina Faso.

Desconnets, J., Diallo, A., Traore, O., Chene, J.-M., & Morin, G. (1998). Exemple d '

application du modèle CEQUEAU-ONU : Évaluation de l ’ impact des aménagements sur les écoulements de la rivière Nakambé , Burkina Faso. Water Resources Variability in Africa during the XXth Century.

Descroix, L., Guichard, F., Grippa, M., Lambert, L. A., Panthou, G., Mahé, G., Gal, L., Dardel, C., Quantin, G., Kergoat, L., Bouaïta, Y., Hiernaux, P., Vischel, T., Pellarin, T., Faty, B., Wilcox, C., Abdou, M. M., Mamadou, I., Vandervaere, J. P., … Paturel, J. E. (2018). Evolution of surface hydrology in the Sahelo-Sudanian Strip: An updated review. Water (Switzerland), 10(6). https://doi.org/10.3390/w10060748

Dewitte, O., Jones, A., Spaargaren, O., Breuning-Madsen, H., Brossard, M., Dampha, A., Deckers, J., Gallali, T., Hallett, S., Jones, R., Kilasara, M., Le Roux, P., Michéli, E., Montanarella, L., Thiombiano, L., Van Ranst, E., Yemefack, M., & Zougmore, R. (2013). Harmonisation of the soil map of africa at the continental scale. Geoderma, 211–212, 138–153. https://doi.org/10.1016/j.geoderma.2013.07.007

Dey, N. N., Al Rakib, A., Kafy, A. Al, & Raikwar, V. (2021). Geospatial modelling of changes in land use/land cover dynamics using Multi-layer perception Markov chain model in Rajshahi City, Bangladesh. Environmental Challenges, 4(May), 100148. https://doi.org/10.1016/j.envc.2021.100148

DGRE. (2010). Etat des lieux de la gestion des ressources en eau du bassin du Nakanbé: Rapport final. https://eaunakanbe.bf/wp-content/uploads/2019/06/Rapport-etat-des-lieux-des-RE-du-Nakanbé-de-2010-Final.pdf

Diabri P. (2008). Qualité de l’eau et niveau de comblement du barrage de Tougou (Burkina Faso). Master Thesis, Institut International de l'Eau et de l'Environnement, Ouagadougou, Burkina Faso.

Diasso, U., & Abiodun, B. J. (2017). Drought modes in West Africa and how well CORDEX RCMs simulate them. Theoretical and Applied Climatology, 128(1–2), 223–240. https://doi.org/10.1007/s00704-015-1705-6

Diedhiou, A., Bichet, A., Wartenburger, R., Seneviratne, S. I., Rowell, D. P., Sylla, M. B., Diallo, I., Todzo, S., Touré, N. E., Camara, M., Ngatchah, B. N., Kane, N. A., Tall, L., & Affholder, F. (2018). Changes in climate extremes over West and Central Africa at 1.5 °c

and 2 °c global warming. Environmental Research Letters, 13(6). https://doi.org/10.1088/1748-9326/aac3e5

Diello, P., Mahe, G., Paturel, J.-E., Dezetter, A., Delclaux, F., Servat, E., & Ouattara, F. (2005). Relations indices de Végétation–Pluie au Burkina Faso: Cas du Bassin Versant du Nakambé/Relationship between Rainfall and Vegetation Indexes in Burkina Faso: A Case Study of the Nakambé Basin. Hydrological Sciences Journal, 50(2). https://doi.org/10.1623/hysj.50.2.207.61797

Diem, J. E., Hartter, J., Ryan, S. J., & Palace, M. W. (2014). Validation of satellite rainfall products for Western Uganda. Journal of Hydrometeorology, 15(5), 2030–2038. https://doi.org/10.1175/JHM-D-13-0193.1

Dimobe, K., Goetze, D., Ouédraogo, A., Forkuor, G., Wala, K., Porembski, S., & Thiombiano, A. (2017). Spatio-Temporal Dynamics in Land Use and Habitat Fragmentation within a Protected Area Dedicated to Tourism in a Sudanian Savanna of West Africa. Journal of Landscape Ecology(Czech Republic), 10(1), 75–95. https://doi.org/10.1515/jlecol-2017-0011

DSB (2011). Trends and Implications of Climate Change for National and International Security. DOD Office of Security, Washington, D.C. 20301-3140, United States of America

Dutta, P., & Sarma, A. K. (2021). Hydrological modeling as a tool for water resources management of the data-scarce brahmaputra basin. Journal of Water and Climate Change, 12(1), 152–165. https://doi.org/10.2166/wcc.2020.186

Eastman, J. R. (2020). TerrSet geospatial monitoring and modeling system, Tutorial Version 2020v.19.0. Clark University, Worcester, United States of America

Eyring, V., Bony, S., Meehl, G. A., Senior, C. A., Stevens, B., Stouffer, R. J., & Taylor, K. E. (2016). Overview of the Coupled Model Intercomparison Project Phase 6 (CMIP6) experimental design and organization. Geoscientific Model Development, 9(5), 1937–1958. https://doi.org/10.5194/GMD-9-1937-2016

FAO. (2009). Harmonized World Soil Database????? (Version 1.1). http://www.fao.org/soils-portal/data-hub/soil-maps-and-databases/harmonized-world-soil-database-

v12/en/%0Ahttp://www.fao.org/soils-portal/soil-survey/soil-maps-and-databases/harmonized-world-soil-database-v12/en/

FAO. (2010). Evaluation des ressources forestières mondiales 2010: Rapport principal. In Etude FAO : Forêt. Rome, Italy

Faye, C., Diop, E. H. S., & Mbaye, I. (2015). Impacts des changements de climat et des aménagements sur les ressources en eau du fleuve sénégal: Caractérisation et évolution des régimes hydrologiques de sous-bassins versants naturels et aménagés. Belgeo, 4, 0–25. https://doi.org/10.4000/belgeo.17626

Feng, D., Zhao, Y., Yu, L., Li, C., Wang, J., Clinton, N., Bai, Y., Belward, A., Zhu, Z., & Gong, P. (2016). Circa 2014 African land-cover maps compatible with FROM-GLC and GLC2000 classification schemes based on multi-seasonal Landsat data. International Journal of Remote Sensing, 37(19), 4648–4664. https://doi.org/10.1080/01431161.2016.1218090

Findell, K. L., Berg, A., Gentine, P., Krasting, J. P., Lintner, B. R., Malyshev, S., Santanello, J. A., & Shevliakova, E. (2017). The impact of anthropogenic land use and land cover change on regional climate extremes. Nature Communications, 8(1), 989. https://doi.org/10.1038/s41467-017-01038-w

Fitzgerald, R. W., & Lees, B. G. (1994). Assessing the classification accuracy of multisource remote sensing data. Remote Sensing of Environment, 47(3), 362–368. https://doi.org/10.1016/0034-4257(94)90103-1

Floreano, I. X., & de Moraes, L. A. F. (2021). Land use/land cover (LULC) analysis (2009–2019) with Google Earth Engine and 2030 prediction using Markov-CA in the Rondônia State, Brazil. Environmental Monitoring and Assessment, 193(4), 1–17. https://doi.org/10.1007/s10661-021-09016-y

Forkuor, G. (2014). Agricultural Land Use Mapping in West Africa Using Multi-sensor Satellite Imagery. PhD dissertation, Würzburg University, Germany

Forkuor, G., Hounkpatin, O. K. L., Welp, G., & Thiel, M. (2017). High Resolution Mapping of Soil Properties Using Remote Sensing Variables in South-Western Burkina Faso: A Comparison of Machine Learning and Multiple Linear Regression Models. PLOS ONE,

12(1), e0170478. https://doi.org/10.1371/journal.pone.0170478

Gavrilov, M. B., Tošić, I., Marković, S. B., Unkašević, M., & Petrović, P. (2016). Analysis of annual and seasonal temperature trends using the Mann-Kendall test in Vojvodina, Serbia. Idojaras, 120(2), 183–198. https://doi.org/10.2298/TSCI150207062G

Gbohoui, Y. P., Paturel, J. E., Fowe Tazen, Mounirou, L. A., Yonaba, R., Karambiri, H., & Yacouba, H. (2021). Impacts of climate and environmental changes on water resources: A multi-scale study based on Nakanbé nested watersheds in West African Sahel. Journal of Hydrology: Regional Studies, 35(April), 100828. https://doi.org/10.1016/j.ejrh.2021.100828

Gebrechorkos, S. H., Pan, M., Lin, P., Anghileri, D., Forsythe, N., Pritchard, D. M. W., Fowler, H. J., Obuobie, E., Darko, D., & Sheffield, J. (2022). Variability and changes in hydrological drought in the Volta Basin, West Africa. Journal of Hydrology: Regional Studies, 42(March), 101143. https://doi.org/10.1016/j.ejrh.2022.101143

Getirana, A. C. V., & Peters-Lidard, C. (2013). Estimating water discharge from large radar altimetry datasets. Hydrology and Earth System Sciences, 17(3), 923–933. https://doi.org/10.5194/hess-17-923-2013

GFDRR. (2020). Think Hazard ! Identify natural hazards in your project area and understand how to reduce their impact : Burkina Faso. https://thinkhazard.org/en/report/42-burkina-faso/DG

Gharaibeh, A., Shaamala, A., Obeidat, R., & Al-Kofahi, S. (2020). Improving land-use change modeling by integrating ANN with Cellular Automata-Markov Chain model. Heliyon. https:// doi. org/ 10.1016/j. heliy on. 2020. e05092

Giertz, S., Diekkrüger, B., Jaeger, A., & Schopp, M. (2006). An interdisciplinary scenario analysis to assess the water availability and water consumption in the Upper Ouémé catchment in Benin. Advances in Geosciences, 9, 3–13. https://doi.org/10.5194/adgeo-9-3-2006

Girma, R., Fürst, C., & Moges, A. (2022). Land use land cover change modeling by integrating artificial neural network with cellular Automata-Markov chain model in Gidabo river

basin, main Ethiopian rift. Environmental Challenges, 6(December 2021), 100419. https://doi.org/10.1016/j.envc.2021.100419

Gislason, P. O., Benediktsson, J. A., & Sveinsson, J. R. (2006). Random forests for land cover classification. Pattern Recognition Letters, 27(4), 294–300. https://doi.org/10.1016/j.patrec.2005.08.011

Goodarzi, M. R., Vagheei, H., & Mohtar, R. H. (2020). The impact of climate change on water and energy security. Water Science and Technology: Water Supply, 20(7), 2530–2546. https://doi.org/10.2166/ws.2020.150

Goula, B. T. A., Kouadio, Z. A., Kouakou, K. E., N'go, Y. A., N'doume, C., & Savane, I. (2009). Simulation du Comportement Hydrologique du Bassin Versant de L'Agneby, en Cote D'ivoire. Rev. Ivoir. Sci. Technol, 13(ISSN 1813-3290), 91–113.

Gulakhmadov, A., Chen, X., Gulahmadov, N., Liu, T., Davlyatov, R., Sharofiddinov, S., & Gulakhmadov, M. (2020). Long-Term Hydro–Climatic Trends in the Mountainous Kofarnihon River Basin in Central Asia. Water, 12(8), 2140. https://doi.org/10.3390/w12082140

Gupta, R., & Sharma, L. K. (2020). Efficacy of Spatial Land Change Modeler as a forecasting indicator for anthropogenic change dynamics over five decades: A case study of Shoolpaneshwar Wildlife Sanctuary, Gujarat, India. Ecological Indicators, 112(23), 106171. https://doi.org/10.1016/j.ecolind.2020.106171

Gupta, For, A., With, O., By, A., Vijai, H., Sorooshian, S., & Yapo, P. O. (1999). Status of Automatic Calibration for Hydrologic Models : Comparison with Multilevel Expert Calibration. Journal of Hydrologic Engineering, April, 135–143.

Hackman, Kwame O., Li, X., Asenso-Gyambibi, D., Asamoah, E. A., & Nelson, I. D. (2020). Analysis of geo-spatiotemporal data using machine learning algorithms and reliability enhancement for urbanization decision support. International Journal of Digital Earth, 13(12), 1717–1732. https://doi.org/10.1080/17538947.2020.1805036

Hackman, K. O., Gong, P., & Wang, J. (2017). New land-cover maps of Ghana for 2015 using landsat 8 and three popular classifiers for biodiversity assessment. International Journal of

Remote Sensing, 38(14), 4008–4021. https://doi.org/10.1080/01431161.2017.1312619

Hamed, K. H. (2008). Trend detection in hydrologic data: The Mann-Kendall trend test under the scaling hypothesis. Journal of Hydrology, 349(3–4), 350–363. https://doi.org/10.1016/j.jhydrol.2007.11.009

Hamed, K. H., & Rao, A. R. (1998). A modified Mann-Kendall trend test for autocorrelated data. Journal of Hydrology, 204, 182-196. https://doi.org/10.1200/JCO.2018.36.15_suppl.522

Han, H., Yang, C., & Song, J. (2015). Scenario simulation and the prediction of land use and land cover change in Beijing, China. Sustainability (Switzerland), 7(4), 4260–4279. https://doi.org/10.3390/su7044260

Hassen, G., Bantider, A., Legesse, A., Maimbo, M., & Likissa, D. (2021). Land Use and Land Cover Change for Resilient Environment and Sustainable Development in the Ethiopian Rift Valley Region. Ochrona Srodowiska i Zasobow Naturalnych, 32(2), 24–41. https://doi.org/10.2478/oszn-2021-0007

Hersbach, H., Bell, B., Berrisford, P., Hirahara, S., Horányi, A., Muñoz-Sabater, J., Nicolas, J., Peubey, C., Radu, R., Schepers, D., Simmons, A., Soci, C., Abdalla, S., Abellan, X., Balsamo, G., Bechtold, P., Biavati, G., Bidlot, J., Bonavita, M., … Thépaut, J. N. (2020). The ERA5 global reanalysis. Quarterly Journal of the Royal Meteorological Society, 146(730), 1999–2049. https://doi.org/10.1002/qj.3803

Hounkpè, J., Diekkrüger, B., Afouda, A. A., & Sintondji, L. O. C. (2019). Land use change increases flood hazard: a multi-modelling approach to assess change in flood characteristics driven by socio-economic land use change scenarios. Natural Hazards, 98(3), 1021–1050. https://doi.org/10.1007/s11069-018-3557-8

Hussien, K., Kebede, A., Mekuriaw, A., Asfaw Beza, S., & Haile Erena, S. (2022). Modelling spatiotemporal trends of land use land cover dynamics in the Abbay River Basin, Ethiopia. Modeling Earth Systems and Environment, 0123456789. https://doi.org/10.1007/s40808-022-01487-3

Ibrahim, B. (2012). Caractérisation des saisons de pluies au Burkina Faso dans un contexte de changement climatique et évaluation des impacts hydrologiques sur le bassin du Nakambé.

Thèse de doctorat en Hydrologie, Université Pierre et Marie Curie – Paris VI, France. https://tel.archives-ouvertes.fr/tel-00827764

Ibrahim, B., Karambiri, H., Polcher, J., Yacouba, H., & Ribstein, P. (2014). Changes in rainfall regime over Burkina Faso under the climate change conditions simulated by 5 regional climate models. Climate Dynamics, 42(5–6), 1363–1381. https://doi.org/10.1007/s00382-013-1837-2

Idrissou, M., Diekkrüger, B., Tischbein, B., Op de Hipt, F., Näschen, K., Poméon, T., Yira, Y., & Ibrahim, B. (2022). Modeling the Impact of Climate and Land Use/Land Cover Change on Water Availability in an Inland Valley Catchment in Burkina Faso. Hydrology, 9(1), 12. https://doi.org/10.3390/hydrology9010012

IFC. (2010). L ' éclairage solaire pour la base de la pyramide - Panorama d ' un marché émergent. https://www.ifc.org/wps/wcm/connect/c2d295d0-1e8b-4c64-83d4-274e91da386d/SolarLightingBasePyramid_French.pdf?MOD=AJPERES&CVID=je3NyGg

International Hydropower Association. (2018). 2018 hydropower status report: sector trends and insights. https://www.hydropower.org/publications/2018-hydropower-status-report

International Hydropower Association. (2020). Hydropower Status Report 2020. International Hydropower Association, 1–83. https://www.hydropower.org/sites/default/files/publications-docs/2019_hydropower_status_report_0.pdf

International Hydropower Association. (2021). 2021 Hydropower Status Report: Sector trends and insights. In International Hydropower Association, iha: Vol. Report (Issue 2021). https://www.hydropower.org/publications/2021-hydropower-status-report

Ilboudo D. F. (2019). Réhabilitation des retenues d'eau du Burkina Faso : cas du lac Dem. Master Thesis, Institut International de l'Eau et de l'Environnement, Ouagadougou, Burkina Faso.

INSD. (2020). Résultats Préliminaires du RGPH 5. http://www.insd.bf/contenu/documents_rgph5/RAPPORT_PRELIMINAIRE_RGPH_2019.pdf

IPCC. (2021). Climate Change 2021: The Physical Science Basis. Contribution of Working Group I to the Sixth Assessment Report of the Intergovernmental Panel on Climate Change [Masson-Delmotte, V., P. Zhai, A. Pirani, S.L. Connors, C. Péan, S. Berger, N. Caud, Y. Chen, L. Goldfarb, M.I. Gomis, M. Huang, K. Leitzell, E. Lonnoy, J.B.R. Matthews, T.K. Maycock, T. Waterfield, O. Yelekçi, R. Yu, and B. Zhou (eds.)]. Cambridge University Press. In Press.

IRENA. (2021). Utility-scale solar and wind areas: Burkina Faso, International Renewable Energy Agency, Abu Dhabi. Report. www.irena.org/publications

Jia, Y. N., Turner, S. W. D., & Galelli, S. (2017). Influence of El Niño Southern Oscillation on global hydropower production. Environmental Research Letters, 12(3). https://doi.org/10.1088/1748-9326/aa5ef8

Kabo-Bah, A., Diji, C., Nokoe, K., Mulugetta, Y., Obeng-Ofori, D., & Akpoti, K. (2016). Multiyear Rainfall and Temperature Trends in the Volta River Basin and their Potential Impact on Hydropower Generation in Ghana. Climate, 4(49), 1–17. https://doi.org/10.3390/cli4040049

Kabore, E. & Bazin, F. (2014). Evaluation économique ex-post du barrage de Bagré au Burkina Faso: Rapport final. https://pubs.iied.org/sites/default/files/pdfs/migrate/G04006.pdf

Kanazue, B., Barbier, B. & Thiombiano, T. (2004). Hydroélectricité, énergie thermique et carbone au Burkina Faso Simulation économique à long terme. http://keriel.org/ACT/2009_Ouagadougou_2iE/Theme2/kanazou%C3%A9_B.pdf

Karambiri, B. L. C. N. (2017). Variabilite Climatique et Gestion Integree des Ressources en Eau dans le Bassin-Versant du Sourou au Burkina Faso. These de doctorat, Université Joseph Ki-ZErbo, Ouagadougou, Burkina Faso.

Karambiri, H., García Galiano, S. G., Giraldo, J. D., Yacouba, H., Ibrahim, B., Barbier, B., & Polcher, J. (2011). Assessing the impact of climate variability and climate change on runoff in West Africa: The case of Senegal and Nakambe River basins. Atmospheric Science Letters, 12(1), 109–115. https://doi.org/10.1002/asl.317

Kaunda, C. S., Kimambo, C. Z., & Nielsen, T. K. (2012). Potential of Small-Scale Hydropower for Electricity Generation in Sub-Saharan Africa. ISRN Renewable Energy, 2012, 1–15.

https://doi.org/10.5402/2012/132606

Kendall, M. G. (1975). Rank Correlation Methods, 4th edn. Charles Griffin, London, England.

Khalid, S., Azad, S., Naz, A., Ur Rahman, Z., & Iqbal, A. (2017). Climate Change: A Review of the Current Trends and Major Environmental. Science, Technology and Development, 36(3), 160:176. https://doi.org/10.3923/std.2017.160.176

Kim, Y., Newman, G., & Güneralp, B. (2020). A review of driving factors, scenarios, and topics in urban land change models. Land 9:1–22. https:// doi. org/ 10. 3390/ LAND9 080246

Knutti, R., Masson, D., & Gettelman, A. (2013). Climate model genealogy: Generation CMIP5 and how we got there. Geophysical Research Letters, 40(6), 1194–1199. https://doi.org/10.1002/grl.50256

Koch, H., Liersch, S., & Hattermann, F. F. (2013). Integrating water resources management in eco-hydrological modelling. Water Science and Technology, 67(7), 1525–1533. https://doi.org/10.2166/wst.2013.022

Koch, H., Silva, A. L. C., Liersch, S., de Azevedo, J. R. G., & Hattermann, F. F. (2020). Effects of model calibration on hydrological and water resources management simulations under climate change in a semi-arid watershed. Climatic Change, 163(3), 1247–1266. https://doi.org/10.1007/s10584-020-02917-w

Koko, A. F., Yue, W., Abubakar, G. A., Hamed, R., & Alabsi, A. A. N. (2020). Monitoring and predicting spatio-temporal land use/land cover changes in Zaria City, Nigeria, through an integrated cellular automata and markov chain model (CA-Markov). Sustainability (Switzerland), 12(24), 1–21. https://doi.org/10.3390/su122410452

Komi, K., Neal, J., Trigg, M. A., & Diekkrüger, B. (2017). Modelling of flood hazard extent in data sparse areas: a case study of the Oti River basin, West Africa. Journal of Hydrology: Regional Studies, 10, 122–132. https://doi.org/10.1016/j.ejrh.2017.03.001

Kouadio, Z. A., Kouakou, K. E., & Konan-waidhet, A. B. (2015). Modélisation du comportement hydrologique du bassin versant du Boubo en milieu tropical humide de la Côte d'Ivoire par l'application du modèle hydrologique distribué CEQUEAU. Afrique Science: Revue Internationale Des Sciences et Technologie, 11(3), 82–100.

Kouame, Y. M., Obahoundje, S., Diedhiou, A., François, B., Amoussou, E., Anquetin, S., Didi, S., Kouassi, L. K., Hermann, V., Bi, N., Soro, E. G., & Yao, E. K. (2019). Climate, Land Use and Land Cover Changes in the Bandama Basin (Côte D'Ivoire, West Africa) and Incidences on Hydropower Production of the Kossou Dam. Land, 103(8), 1–21. https://doi:10.3390/land8070103

Koubodana, D. H., Diekkrüger, B., Näschen, K., Adounkpe, J., & Atchonouglo, K. (2019). Impact of the Accuracy of Land Cover Data sets on the Accuracy of Land Cover Change Scenarios in the Mono River Basin, Togo, West Africa. International Journal of Advanced Remote Sensing and GIS, 8(1), 3073–3095. https://doi.org/10.23953/cloud.ijarsg.422

Koubodana, H. D., Adounkpe, J., Tall, M., Amoussou, E., & Atchonouglo, Kossi Mumtaz, M. (2020). Trend Analysis of Hydro-climatic Historical Data and Future Scenarios of Climate Extreme Indices over Mono River Basin in West Africa. American Journal of Rural Development, 8(1), 37–52. https://doi.org/10.12691/ajrd-8-1-5

Koudahe, K., Kayode, A. J., Samson, A. O., Adebola, A. A., & Djaman, K. (2017). Trend Analysis in Standardized Precipitation Index and Standardized Anomaly Index in the Context of Climate Change in Southern Togo. Atmospheric and Climate Sciences, 07(04), 401–423. https://doi.org/10.4236/acs.2017.74030

Krause, P., Boyle, D. P., & Bäse, F. (2005). Comparison of different efficiency criteria for hydrological model assessment. Advances in Geosciences, 5, 89–97. https://doi.org/10.5194/adgeo-5-89-2005

Krysanova, V., Wechsung, F., & SWIM development team. (2022). The Soil and Water Integrated Model (SWIM) User Manual. PIK Report ,250; Potsdam, Germany.

Krysanova, Valentina, Hattermann, F., Huang, S., Hesse, C., Vetter, T., Liersch, S., Koch, H., & Kundzewicz, Z. W. (2015). Modelling climate and land-use change impacts with SWIM: lessons learnt from multiple applications. Hydrological Sciences Journal, 60(4), 606–635. https://doi.org/10.1080/02626667.2014.925560

Krysanova, V, Wechsung, F., Arnold, J., Srinivasan, R., & Williams, J. (2000). SWIM (Soil and Water Integrated Model) User Manual. PIK Report , 69, 239.

Kumar, R., Samaniego, L., & Attinger, S. (2013). Implications of distributed hydrologic model parameterization on water fluxes at multiple scales and locations. Water Resources Research, 49(1), 360–379. https://doi.org/10.1029/2012WR012195

Kumi, N., & Abiodun, B. J. (2018). Erratum: Potential impacts of 1.5 °C and 2 °C global warming on rainfall onset, cessation and length of rainy season in West Africa (Environ. Res. Lett. (2018) 13 (055009) DOI: 10.1088/1748-9326/aab89e). Environmental Research Letters, 13(8). https://doi.org/10.1088/1748-9326/aad5c6

Kwakye, S. O., & Bárdossy, A. (2020). Hydrological modelling in data-scarce catchments: Black Volta basin in West Africa. SN Applied Sciences, 2(4), 1–19. https://doi.org/10.1007/s42452-020-2454-4

Kwawuvi, D., Mama, D., Agodzo, S. K., Hartmann, A., Larbi, I., Bessah, E., Abraham, T., Dotse, S. Q., & Limantol, A. M. (2022a). An investigation into the future changes in rainfall onset, cessation and length of rainy season in the Oti River Basin, West Africa. Modeling Earth Systems and Environment, 8(4), 5077–5095. https://doi.org/10.1007/s40808-022-01410-w

Kwawuvi, D., Mama, D., Agodzo, S. K., Hartmann, A., Larbi, I., Bessah, E., Limantol, A. M., Dotse, S. Q., & Yangouliba, G. I. (2022b). Spatiotemporal variability and change in rainfall in the Oti River Basin, West Africa. Journal of Water and Climate Change, 13(3), 1151–1169. https://doi.org/10.2166/wcc.2022.368

Lamizana Diallo B. M. (2009). Impact de la crue fluviale sur les écosystèmes et les conditions de vie des populations riveraines du Nakambé (Burkina Faso). PhD Thesis. Université de Ouagadougou, Burkina Faso.

Landry, M., Ouedraogo, Y., Gagnon, Y., & Ouedraogo, A. (2016). On the wind resource mapping of Burkina Faso. International Journal of Green Energy, 14(2), 150–156. https://doi.org/10.1080/15435075.2016.1253571

Lange, S, Menz, C., Gleixner, S., Cucchi, M., & Weedon, G. (2021). WFDE5 over land merged with ERA5 over the ocean (W5E5 v2. 0). https://publications.pik-potsdam.de/pubman/faces/ViewItemFullPage.jsp?itemId=item_26192_1

Lange, S. (2019). Trend-preserving bias adjustment and statistical downscaling with

ISIMIP3BASD (v1.0). Geoscientific Model Development, 12(7), 3055–3070. https://doi.org/10.5194/gmd-12-3055-2019

Lange, S. (2021). ISIMIP3b bias adjustment fact sheet. Observational dataset Bias adjustment and statistical downscaling method. 2019, 37. https://www.isimip.org/documents/413/ISIMIP3b_bias_adjustment_fact_sheet_Gnsz7CO.pdf

Larbi, I., Forkuor, G., Hountondji, F. C. C., Agyare, W. A., & Mama, D. (2019). Predictive Land Use Change under Business-As-Usual and Afforestation Scenarios in the Vea Catchment, West Africa. International Journal of Advanced Remote Sensing and GIS, 8(1), 3011–3029. https://doi.org/10.23953/cloud.ijarsg.416

Larbi, I. (2019). Assessment of Climate and Land Use Change Impacts on the Water Balance Components in the Vea Catchment, West Africa. PhD dissertation, University of Abomey-Calavi, Benin

Lawin, A. E., Hounguè, N. R., Biaou, C. A., & Badou, D. F. (2019). Statistical analysis of recent and future rainfall and temperature variability in the Mono River watershed (Benin, Togo). Climate, 7(1). https://doi.org/10.3390/cli7010008

Lebel, T., & Ali, A. (2009). Recent trends in the Central and Western Sahel rainfall regime (1990-2007). Journal of Hydrology, 375(1–2), 52–64. https://doi.org/10.1016/j.jhydrol.2008.11.030

Leta, M. K., Demissie, T. A., & Tränckner, J. (2021). Modeling and prediction of land use land cover change dynamics based on land change modeler (Lcm) in nashe watershed, upper blue nile basin, Ethiopia. Sustainability (Switzerland), 13(7). https://doi.org/10.3390/su13073740

Leta, M. K., Demissie, T. A., & Tränckner, J. (2022). Optimal Operation of Nashe Hydropower Reservoir under Land Use Land Cover Change in Blue Nile River Basin. Water (Switzerland), 14(10). https://doi.org/10.3390/w14101606

Liang, X., Lettenmaier, D. P. Wood, E. F., &. Burges, S. J. (1994). A simple hydrologically based model of land surface water and energy fluxes for general circulation models. Journal of Geophysical Research, Vol. 99, 415-428

Lienou, G. (2013). Integrated Future Needs and Climate Change on the River Niger Water Availability. Journal of Water Resource and Protection, 05(09), 887–893. https://doi.org/10.4236/jwarp.2013.59090

Liersch, S., Koch, H., Abungba, J. A., Salack, S., & Hattermann, F. F. (2023). Attributing synergies and trade-offs in water resources planning and management in the Volta River basin under climate change. Environmental Research Letters, 18(1), 014032. https://doi.org/10.1088/1748-9326/acad14

Liersch, S, Drews, M., Pilz, T., Salack, S., Sietz, D., Aich, V., A D Larsen, M., Gädeke, A., Halsnæ s, K., Thiery, W., Huang, S., Lobanova, A., Koch, H., & Hattermann, F. F. (2020). One simulation, different conclusions—the baseline period makes the difference! Environmental Research Letters, 15(10), 104014. https://doi.org/10.1088/1748-9326/aba3d7

Liersch, S., Tecklenburg, J., Rust, H., Dobler, A., Fischer, M., Kruschke, T., Koch, H., & Hattermann, F. F. (2018). Are we using the right fuel to drive hydrological models? A climate impact study in the Upper Blue Nile. Hydrology and Earth System Sciences, 22(4), 2163–2185. https://doi.org/10.5194/hess-22-2163-2018b

Liersch, S., Koch, H., & Hattermann, F. F. (2017). Management scenarios of the Grand Ethiopian Renaissance Dam and their impacts under recent and future climates. Water (Switzerland), 9(10), 1–24. https://doi.org/10.3390/w9100728

Liersch, S., Cools, J., Kone, B., Koch, H., Diallo, M., Reinhardt, J., Fournet, S., Aich, V., & Hattermann, F. F. (2013). Vulnerability of rice production in the Inner Niger Delta to water resources management under climate variability and change. Environmental Science and Policy, 34, 18–33. https://doi.org/10.1016/j.envsci.2012.10.014

Liersch, S., Kone, B., Koch, H., Diallo, M., Aich, V., Reinhardt, J., Fournet, S., & Hattermann, F. F. (2012). Constraints of future freshwater resources in the Upper Niger Basin - Has the human-environmental system of the Inner Niger Delta a chance to survive? IEMSs 2012 - Managing Resources of a Limited Planet: Proceedings of the 6th Biennial Meeting of the International Environmental Modelling and Software Society, 2907–2915.

Lin, B., Chen, X., Yao, H., Chen, Y., Liu, M., Gao, L., & James, A. (2015). Analyses of landuse

change impacts on catchment runoff using different time indicators based on SWAT model. Ecological Indicators, 58, 55–63. https://doi.org/10.1016/j.ecolind.2015.05.031

Liu, B., Lund, J. R., Liu, L., Liao, S., Li, G., & Cheng, C. (2020). Climate change impacts on hydropower in Yunnan, China. Water (Switzerland), 12(1), 1–20. https://doi.org/10.3390/w12010197

Lobanova, A., Koch, H., Liersch, S., Hattermann, F. F., & Krysanova, V. (2016). Impacts of changing climate on the hydrology and hydropower production of the Tagus River basin. Hydrological Processes, 30(26), 5039–5052. https://doi.org/10.1002/hyp.10966

Love, D., Uhlenbrook, S., & van der Zaag, P. (2011). Regionalising a meso-catchment scale conceptual model for river basin management in the semi-arid environment. Physics and Chemistry of the Earth, 36(14–15), 747–760. https://doi.org/10.1016/j.pce.2011.07.005

Loucks, D. P., & Eelco, van B. (2016). Water resource systems planning and analysis-An Introduction to Methods, Models, and Applications. Advances in Water Resources (Vol. 4, Issue 3). https://doi.org/10.1007/978-3-319-44234-1

Machina, B. M., & Sharma, S. (2017). Assessment of Climate Change Impact on Hydropower Generation : A Case Study of Nigeria. International Journal of Engineering Technology Science and Research, 4(8), 753–762.

Mahe, G., Dray, A., Paturel, J. E., Cres, A., Kone, F., Manga, M., Cres, F. N., Djoukam, J., Maiga, A., Ouedraogo, M., Conway, D., & Servat, E. (2002). Climatic and anthropogenic impacts on the flow regime of the Nakambe River in Burkina Faso. IAHS-AISH Publication, 274, 69–76.

Mahe, Gil, Paturel, J. E., Servat, E., Conway, D., & Dezetter, A. (2005). The impact of land use change on soil water holding capacity and river flow modelling in the Nakambe River, Burkina-Faso. Journal of Hydrology, 300(1–4), 33–43. https://doi.org/10.1016/j.jhydrol.2004.04.028

Mann, H. (1945). Nonparametric tests against trend. Econometrica, 13 (3), 245–259.

McCartney, M., Forkuor, G., Sood, A., Amisigo, B., Hattermann, F., & Muthuwatta, L. (2012). The Water Resource Basin Climate in the Volta River Implications of Changing.

https://doi.org/doi:10.5337/2012.219

Mechal, A., Takele, T., Meten, M., Deyassa, G., & Degu, Y. (2022). A modeling approach for evaluating the impacts of Land Use/Land Cover change for Ziway Lake Watershed hydrology in the Ethiopian Rift. Modeling Earth Systems and Environment, 8(4), 4793–4813. https://doi.org/10.1007/s40808-022-01472-w

Meema, T., Tachikawa, Y., Ichikawa, Y., & Yorozu, K. (2021). Uncertainty assessment of water resources and long-term hydropower generation using a large ensemble of future climate projections for the Nam Ngum River in the Mekong Basin. Journal of Hydrology: Regional Studies, 36(January), 100856. https://doi.org/10.1016/j.ejrh.2021.100856

Mehrabi, A., Khabazi, M., Almodaresi, S. A., Nohesara, M., & Derakhshani, R. (2019). Land use changes monitoring over 30 years and prediction of future changes using multi-temporal landsat imagery and the land change modeler tools in rafsanjan city (Iran). Sustainable Development of Mountain Territories, 11(1), 26–35. https://doi.org/10.21177/1998-4502-2019-11-1-26-35

Mestre, O., Domonkos, P., Picard, F., Auer, I., Robin, S., Lebarbier, E., Böhm, R., Aguilar, E., Guijarro, J., Vertachnik, G., Klancar, M., Dubuisson, B., & Stepanek, P. (2013). HOMER: A homogenization software - methods and applications. Idojaras, 117(1).

Midekisa, A., Holl, F., Savory, D. J., Andrade-Pacheco, R., Gething, P. W., Bennett, A., & Sturrock, H. J. W. (2017). Mapping land cover change over continental Africa using Landsat and Google Earth Engine cloud computing. PLOS ONE, 12(9), e0184926. https://doi.org/10.1371/journal.pone.0184926

Ministère de l'Environnement et du Developpement Durable. (2015). Mécanisme Spécial de Dons (DGM) pour les Peuples Autochtones et les Communautés Locales. 122. https://www.iucn.org/sites/dev/files/import/downloads/cges_dgm_burkina_faso_revu_ccp_17mai15.pdf

Moriasi, D. N., Arnold, J. G., Liew, M. W. Van, Bingner, R. L., Harmel, R. D., & Veith, T. L. (2007). Model Evaluation Guidelines For Systematic Quantification Of Accuracy In Watershed Simulations. American Society of Agricultural and Biological Engineers, 50(3), 885–900.

Mousavi, R. S., Ahmadizadeh, M., & Marofi, S. (2018). A Multi-GCM assessment of the climate change impact on the hydrology and hydropower potential of a semi-arid basin (A Case Study of the Dez Dam Basin, Iran). In Water (Switzerland) (Vol. 10, Issue 10). https://doi.org/10.3390/w10101458

Näschen, K., Diekkrüger, B., Evers, M., Höllermann, B., Steinbach, S., & Thonfeld, F. (2019). The Impact of Land Use/Land Cover Change (LULCC) on Water Resources in a Tropical Catchment in Tanzania under Different Climate Change Scenarios. Sustainability (Switzerland), 11(24). https://doi.org/10.3390/su11247083

Nery, T., Sadler, R., Solis-Aulestia, M., White, B., Polyakov, M., & Chalak, M. (2016). Comparing supervised algorithms in Land Use and Land Cover classification of a Landsat time-series. 2016 IEEE International Geoscience and Remote Sensing Symposium (IGARSS), 8(23), 5165–5168. https://doi.org/10.1109/IGARSS.2016.7730346

Neumann, R., Jung, G., Laux, P., & Kunstmann, H. (2007). Climate trends of temperature, precipitation and river discharge in the volta basin of West Africa. International Journal of River Basin Management, 5(1), 17–30. https://doi.org/10.1080/15715124.2007.9635302

Newborne, P. (2016). Water for cities and rural areas in contexts of climate variability: assessing paths to shared prosperity – the example of Burkina Faso. Field Actions Science Reports. The Journal of Field Actions, Special Issue 14.

Nikiema W. B. (2017). Water balance of Lake Bam in Burkina Faso. Master Thesis, Institut International de l'Eau et de l'Environnement, Ouagadougou, Burkina Faso.

Nonki, R. M., Lenouo, A., Tchawoua, C., Lennard, C. J., & Amoussou, E. (2021). Impact of climate change on hydropower potential of the Lagdo dam, Benue River Basin, Northern Cameroon. Proceedings of the International Association of Hydrological Sciences, 384, 337–342. https://doi.org/10.5194/piahs-384-337-2021

Nowak, D. J., & Greenfield, E. J. (2020). The increase of impervious cover and decrease of tree cover within urban areas globally (2012–2017). Urban Forestry and Urban Greening, 49(February). https://doi.org/10.1016/j.ufug.2020.126638

Nut, N., Mihara, M., Jeong, J., Ngo, B., Sigua, G., Prasad, P. V. V., & Reyes, M. R. (2021). Land Use and Land Cover Changes and Its Impact on Soil Erosion in Stung Sangkae

Catchment of Cambodia. Sustainability, 13(16), 9276. https://doi.org/10.3390/su13169276

Nyamekye, C., Thiel, M., Schönbrodt-Stitt, S., Zoungrana, B., & Amekudzi, L. (2018). Soil and Water Conservation in Burkina Faso, West Africa. Sustainability, 10(9), 3182. https://doi.org/10.3390/su10093182

O'Neill, B. C., Tebaldi, C., Van Vuuren, D. P., Eyring, V., Friedlingstein, P., Hurtt, G., Knutti, R., Kriegler, E., Lamarque, J. F., Lowe, J., Meehl, G. A., Moss, R., Riahi, K., & Sanderson, B. M. (2016). The Scenario Model Intercomparison Project (ScenarioMIP) for CMIP6. Geoscientific Model Development, 9(9), 3461–3482. https://doi.org/10.5194/gmd-9-3461-2016

Obahoundje, S., & Diedhiou, A. (2022). Potential impacts of climate, land use and land cover changes on hydropower generation in West Africa: A review. Environmental Research Letters, 17(4). https://doi.org/10.1088/1748-9326/ac5b3b

Obahoundje, S., Diedhiou, A., Dubus, L., Alamou, E. A., Amoussou, E., Akpoti, K., & Antwi Ofosu, E. (2022). Modeling climate change impact on inflow and hydropower generation of Nangbeto dam in West Africa using multi-model CORDEX ensemble and ensemble machine learning. Applied Energy, 325(August). https://doi.org/10.1016/j.apenergy.2022.119795

Obahoundje, S., Amoussou, E., Youan Ta, M., Kouassi, L. K., & Diedhiou, A. (2021a). Multiyear rainfall variability in the Mono river basin and its impacts on Nangbeto hydropower scheme. Proceedings of the International Association of Hydrological Sciences, 384(November), 343–347. https://doi.org/10.5194/piahs-384-343-2021

Obahoundje, S., Youan Ta, M., Diedhiou, A., Amoussou, E., & Kouadio, K. (2021b). Sensitivity of Hydropower Generation to Changes in Climate and Land Use in the Mono Basin (West Africa) using CORDEX Dataset and WEAP Model. Environmental Processes, 8(3), 1073–1097. https://doi.org/10.1007/s40710-021-00516-0

Obahoundje, S., Diedhiou, A., Ofosu, E. A., Anquetin, S., François, B., Adounkpe, J., Amoussou, E., Kouame, Y. M., Kouassi, K. L., Nguessan Bi, V. H., & Ta, M. Y. (2018). Assessment of Spatio-Temporal Changes of Land Use and Land Cover over South-

Western African Basins and Their Relations with Variations of Discharges. Hydrology, 5(4), 56. https://doi.org/10.3390/hydrology5040056

Obahoundje, S., Ofosu, E. A., Akpoti, K., & Kabo-bah, A. T. (2017). Land Use and Land Cover Changes under Climate Uncertainty : Modelling the Impacts on Hydropower Production in Western Africa. https://doi.org/10.3390/hydrology4010002

Ogega, O.M.; Mbugua, J.; Misiani, H.O.; Nyadawa, M.; Scoccimarro, E., & Endris, H.S. (2021). Detection and Attribution of Lake Victoria's Water-Level Fluctuations in a Changing Climate. Preprints, 2021070575 (doi: 10.20944/preprints202107.0575.v1)

Oguntunde, P. G., & Abiodun, B. J. (2013). The impact of climate change on the Niger River Basin hydroclimatology, West Africa. Climate Dynamics, 40(1–2), 81–94. https://doi.org/10.1007/s00382-012-1498-6

Okafor, G. Chinwendu, Jimoh, O. D., & Larbi, K. I. (2017). Detecting Changes in Hydro-Climatic Variables during the Last Four Decades (1975-2014) on Downstream Kaduna River Catchment, Nigeria. Atmospheric and Climate Sciences, 07(02), 161–175. https://doi.org/10.4236/acs.2017.72012

Okafor, G. C., Annor, T., Odai, S. N., & Larbi, I. (2019). Land Use Landcover Change Monitoring and Projection in the Dano Catchment, Southwest Burkina Faso. International Journal of Advanced Remote Sensing and GIS, 9(1), 3185–3204. https://doi.org/10.23953/cloud.ijarsg.445

Okafor, G. C. (2019). Modeling the Hydrological Response of the Dano Catchment, in the Volta Basin to Landuse Landcover Change and Climate Change. PhD dissertation, KNUST, Ghana

Okudzeto, E., Mariki, W. A., Paepe, G. D. & Sedegah, K. (2014). Ghana 2014. Available from: http://www.africaneconomicoutlook.org/fileadmin/uploads/aeo/2014/PDF/CN_Long_EN/Ghana_ENG.pdf.

Owusu, K., Waylen, P., & Qiu, Y. (2008). Changing rainfall inputs in the Volta basin: Implications for water sharing in Ghana. GeoJournal, 71(4), 201–210. https://doi.org/10.1007/s10708-008-9156-6

Ouédraogo A. K. (2017). Diagnostic et proposition de plan d'amélioration des performances d'un périmètre irrigué de Bagré : cas du v9 et du v10 du périmètre irrigué à l'aval du barrage de Bagré. Master Thesis, Institut International de l'Eau et de l'Environnement, Ouagadougou, Burkina Faso.

Oyerinde, G. T., Wisser, D., Hountondji, F. C. C., Odofin, A. J., Lawin, A. E., Afouda, A., & Diekkrüger, B. (2016). Quantifying uncertainties in modeling climate change impacts on hydropower production. Climate, 4(3). https://doi.org/10.3390/cli4030034

Perera, A., & Rathnayake, U. (2019). Impact of climate variability on hydropower generation in an un-gauged catchment: Erathna run-of-the-river hydropower plant, Sri Lanka. Applied Water Science, 9(3). https://doi.org/10.1007/s13201-019-0925-9

Pettitt, A. N. (1979). A non-parametric approach to the change-point problem. Journal of the Royal Statistical Society. Series C (Applied Statistics) 28 (2), 126–135. http://doi.org/10.2307/2346729.

Piman, T., Cochrane, T. A., & Arias, M. E. (2016). Effect of Proposed Large Dams on Water Flows and Hydropower Production in the Sekong, Sesan and Srepok Rivers of the Mekong Basin. River Research and Applications, 32(10), 2095–2108. https://doi.org/10.1002/rra.3045

Pingale, S. M., Khare, D., Jat, M. K., & Adamowski, J. (2016). Trend analysis of climatic variables in an arid and semi-arid region of the Ajmer District, Rajasthan, India. Journal of Water and Land Development, 28(1), 3–18. https://doi.org/10.1515/jwld-2016-0001

Poda T. L. (2018). Contribution à la réalisation des études techniques détaillées de la réhabilitation du barrage de Goinré dans la commune de Ouahigouya (Burkina Faso). Master Thesis, Institut International de l'Eau et de l'Environnement, Ouagadougou, Burkina Faso.

Pontius, G. R. (2000). Quantification error versus location error in comparison of categorical maps. Photogramm Eng Remote Sens 66:1011–1016

Pouyard B. (1975). Etude hydrologique du lac Bam. Centre ORSTOM de Ouagadougou, Burkina Faso

Prasomsup, W., Piyatadsananon, P., Aunphoklang, W., & Boonrang, A. (2020). Extraction Technic for Built-up Area Classification in Landsat 8 Imagery. International Journal of Environmental Science and Development, 11(1), 15–20. https://doi.org/10.18178/ijesd.2020.11.1.1219

Prion, S., & Haerling, K. A. (2014). Making Sense of Methods and Measurement: Spearman-Rho Ranked-Order Correlation Coefficient. Clinical Simulation in Nursing, 10(10), 535–536. https://doi.org/10.1016/j.ecns.2014.07.005

Ramezan, C. A., Warner, T. A., Maxwell, A. E., & Price, B. S. (2021). Effects of Training Set Size on Supervised Machine-Learning Land-Cover Classification of Large-Area High-Resolution Remotely Sensed Data. Remote Sensing, 13(3), 368. https://doi.org/10.3390/rs13030368

Randall, D. A., Wood, R. A., Bony, S., Colman, R., Fichefet, T., & Fyfe, J. (2007). Kumi M, A. A. (2015). Predicting Hydrological Response to Climate Change in the White Volta Catchment, West Africa. Journal of Earth Science & Climatic Change, 06(01), 1–7. https://doi.org/10.4172/2157-7617.1000249

Ringard, J. , Dieppois B. , Rome S. , Djè Kouakou B., K. D., & Katiellou G. L., Lazoumar R. H., Bouzou-Moussa I., Konaré A., Diawara A., Ochou A.D., Assamoi I. P., Camara M., Diongué A. (10), D. L. et D. A. (2014). Évolution des pics de températures en Afrique de l ’ Ouest : étude comparative entre Abidjan et Niamey. July, 7 pages. https://www.academia.edu/30585648/Évolution_Des_Pics_De_Températures_en_Afrique_De_L_Ouest_Étude_Comparative_Entre_Abidjan_et_Niamey

Ritchie, J. T. (1972). “Model for Predicting Evaporation from a Row Crop with Incomplete Cover”. In: 8.5, pp. 1204–1213. issn: 0043-1397.

Rodríguez Eraso, N., Armenteras-Pascual, D., & Alumbreros, J. R. (2013). Land use and land cover change in the Colombian Andes: Dynamics and future scenarios. Journal of Land Use Science, 8(2), 154–174. https://doi.org/10.1080/1747423X.2011.650228

Rummukainen, M. (2010). State-of-the-art with regional. Clim Change, 1(1), 82–96. https://doi.org/10.1002/wcc.008

Rwanga, S. S., & Ndambuki, J. M. (2017). Accuracy Assessment of Land Use/Land Cover

Classification Using Remote Sensing and GIS. International Journal of Geosciences, 08(04), 611–622. https://doi.org/10.4236/ijg.2017.84033

Rybski, D. & Neumann, J. (2011). A Review on the Pettitt Test. In: Extremis (Kropp, J. & Schellnhuber, H. J., eds.). Springer, Berlin, Heidelberg. https://doi.org/10.1007/978-3-642-14863-7_10

Salas Parra, H. D. (2020). Synchronization and Interdependence Between the Cycles of Colombia's Hydroclimatology and El Nino-Southern Oscillation. Ph.D. Thesis, Universidad Nacional de Colombia, Colombia. https://repositorio.unal.edu.co/handle/unal/78420

Sanogo, S., Fink, A. H., Omotosho, J. A., Ba, A., Redl, R., & Ermert, V. (2015). Spatio-temporal characteristics of the recent rainfall recovery in West Africa. International Journal of Climatology, 35(15), 4589–4605. https://doi.org/10.1002/joc.4309

Sarr, A. B., Camara, M., & Diba, I. (2015). Spatial Distribution of Cordex Regional Climate Models Biases over West Africa. International Journal of Geosciences, 06(09), 1018–1031. https://doi.org/10.4236/ijg.2015.69081

Savenije, H. H. G., & Hoekstra, A. Y. (2002). Water Resources management. In: Knowledge for Sustainable Development: An insight into the Encyclopedia of Life Support Systems, Vol. II, UNESCO Publishing, Paris, France / EOLSS Publishers, Oxford, 2002, pp. 155-180.

Sawsan, A. E. A., Ali Hammad, A. A., & Mohamed, T. F. (2019). The Hydropower Plants Dams. IJISET-International Journal of Innovative Science, Engineering & Technology, 6(4), 193–207. www.ijiset.com

Sen, P. (1968). Estimates of the regression coefficient based on Kendall's tau. Journal of the American Statistical Association 63 (324), 1379–1389. https://doi:10.1080/01621459.1968.10480934.

Sen, Z. (2012). An innovative trend analysis methodology. Journal of Hydrologic Engineering 1943–5584. http://dx.doi.org/10.1061.

SE4ALL (2016). Burkina Faso: Rapid Assessment Gap Analysis. https://www.se4all-

africa.org/fileadmin/uploads/se4all/Documents/Country_RAGAs/Burkina_Faso_RAGA_FR_Released__1_.pdf.

Shade, C., & Kremer, P. (2019). Article predicting land use changes in philadelphia following green infrastructure policies. Land, 8(2). https://doi.org/10.3390/land8020028

Shetty, S. (2019). Analysis of Machine Learning Classifiers for LULC Classification on Google Earth Engine Analysis of Machine Learning Classifiers for LULC Classification on Google Earth Engine. Master Thesis, University of Twente, Enschede, The Netherlands

Shrestha, J. P., Pahlow, M., & Cochrane, T. A. (2020). Development of a SWAT hydropower operation routine and its application to assessing hydrological alterations in the mekong. Water (Switzerland), 12(8). https://doi.org/10.3390/W12082193

Sibanda, S., & Ahmed, F. (2021). Modelling historic and future land use/land cover changes and their impact on wetland area in Shashe sub-catchment, Zimbabwe. Modeling Earth Systems and Environment, 7(1), 57–70. https://doi.org/10.1007/s40808-020-00963-y

Sinha, R. K., Eldho, T. I., & Subimal, G. (2020). Assessing the impacts of land use/land cover and climate change on surface runoff of a humid tropical river basin in Western Ghats, India. International Journal of River Basin Management, 0(0), 1–38. https://doi.org/10.1080/15715124.2020.1809434

Sodore, A. A. (2022). Les Espaces Périurbains de Ouagadougou, entre Politiques de Décentralisation, Interventions des Societes Immobilieres et des Personnes Physiques. GÉOTROPE Revue de Géographie Tropicale et d'Environnement, ISSN: 1817(June).

Sonali, P., & Nagesh Kumar, D. (2013). Review of trend detection methods and their application to detect temperature changes in India. Journal of Hydrology, 476, 212–227. https://doi.org/10.1016/j.jhydrol.2012.10.034

Sridhar, V., Kang, H., & Ali, S. A. (2019). and Their Responses for Hydrology and Water Management in the Mekong River Basin. https://doi.org/10.3390/w11061307

Stanzel, P., Kling, H., & Bauer, H. (2018). Climate change impact on West African rivers under an ensemble of CORDEX climate projections. Climate Services, 11(April), 36–48. https://doi.org/10.1016/j.cliser.2018.05.003

Sumner D.M., Jacobs J.M., (2005). Utility of Penman-Monteith, Priestley-Taylor, reference evapotranspiration, and pan evaporation methods to estimate pasture evapotranspiration. Journal of Hydrology, 308(1-4): 81-104.

Sun, L., Zhou, X., & Gu, A. (2022). Effects of Climate Change on Hydropower Generation in China Based on a WEAP Model. Sustainability (Switzerland), 14(9). https://doi.org/10.3390/su14095467

Sylla, B. M., Diallo, I., & Pal, S. J. (2013). West African Monsoon in State-of-the-Science Regional Climate Models. In Climate Variability - Regional and Thematic Patterns (pp. 3–36). InTech. https://doi.org/10.5772/55140

Sylla, M. B., Giorgi, F., Pal, J. S., Gibba, P., Kebe, I., & Nikiema, M. (2015). Projected changes in the annual cycle of high-intensity precipitation events over West Africa for the late twenty-first century. Journal of Climate, 28(16), 6475–6488. https://doi.org/10.1175/JCLI-D-14-00854.1

Sylla, M. B., Nikiema, P. M., Gibba, P., Kebe, I., & Klutse, N. A. B. (2016). Climate change over West Africa: Recent trends and future projections. In Adaptation to Climate Change and Variability in Rural West Africa (pp. 25–40). Springer International Publishing. https://doi.org/10.1007/978-3-319-31499-0_3

Sylla, M. B., Pal, J. S., Faye, A., Dimobe, K., & Kunstmann, H. (2018). Climate change to severely impact West African basin scale irrigation in 2 °C and 1.5 °C global warming scenarios. In Scientific Reports (Vol. 8, Issue 1). https://doi.org/10.1038/s41598-018-32736-0

Tabari, H., Marofi, S., Aeini, A., Talaee, P. H., & Mohammadi, K. (2011). Trend analysis of reference evapotranspiration in the western half of Iran. Agricultural and Forest Meteorology, 151(2), 128–136. https://doi.org/https://doi.org/10.1016/j.agrformet.2010.09.009

Tamm, O., Luhamaa, A., & Tamm, T. (2016). Modeling future changesinthe north-estonian hydropower production by using SWAT. Hydrology Research, 47(4), 835–846. https://doi.org/10.2166/nh.2015.018

Tanksali, A., & Soraganvi, V. S. (2021). Assessment of impacts of land use/land cover changes

upstream of a dam in a semi-arid watershed using QSWAT. Modeling Earth Systems and Environment, 7(4), 2391–2406. https://doi.org/10.1007/s40808-020-00978-5

Teutschbein, C., & Seibert, J. (2012). Bias correction of regional climate model simulations for hydrological climate-change impact studies: Review and evaluation of different methods. Journal of Hydrology, 456–457, 12–29. https://doi.org/10.1016/j.jhydrol.2012.05.052

Thapar, O. D. (2008). Hydropower Engineering for Diploma Level courses (Department of Technical Education Govt. of Uttarakhand (ed.)).

Thiombiano, A. N. (2011). Variabilite Climatique et Impacts sur les Ressources en Eau au Burkina Faso: Étude de cas du Bassin Hydrographique du Fleuve Nakanbé. Mémoire de Master, Université de Moncton, Canada.

Touré, A. H., Kalifa, T., & Kyei-Baffour, N. (2017). Assessment of changing trends of daily precipitation and temperature extremes in Bamako and Ségou in Mali from 1961- 2014. Weather and Climate Extremes, 18(5), 8–16. https://doi.org/10.1016/j.wace.2017.09.002

Turner, S. W. D., Ng, J. Y., & Galelli, S. (2017). Examining global electricity supply vulnerability to climate change using a high-fidelity hydropower dam model. Science of the Total Environment, 590–591, 663–675. https://doi.org/10.1016/j.scitotenv.2017.03.022

UNEP-GEF Volta Project. (2013). Volta Basin Transboundary Diagnostic Analysis : http://gefvolta.iwlearn.org/project-resources/studies-reports/tda-final/regional-tda/volta-basin-tda-english

UNEP. (2004). Loss and Damage: The Role of Ecosystem Services. In Earth Interactions (Vol. 8, Issue 23). http://collections.unu.edu/view/UNU:5614

United Nations. (2011). World Population Prospects: The 2010 Revision. New York, NY: United Nations, Department of Economic and Social Affairs, Population Division. http://www.un.org/esa/population.

UPDEA. (2009). Etude comparative des tarifs d'électricité pratiqués en Afrique. Report (Issue December).http://www.ecowrex.org/system/files/repository/2009_etude_comparative_tariff_afrique_-_updea.pdf

Vissin, E. W. (2007). Impact de la variabilité climatique et de la dynamique des états de surfacesur les écoulements du bassin béninois du fleuve Niger. In Centre de Recherches en Climatologie (CNRS-UMR 5210): Vol. Thèse de doctorat, Hydrologie. Université de Bourgogne, France. https://tel.archives-ouvertes.fr/tel-00456097

Wei, X., Liu, W., & Zhou, P. (2013). Quantifying the Relative Contributions of Forest Change and Climatic Variability to Hydrology in Large Watersheds: A Critical Review of Research Methods. Water, 5(2), 728–746. https://doi.org/10.3390/w5020728

Winkler, K., Fuchs, R., Rounsevell, M., & Herold, M. (2021). Global land use changes are four times greater than previously estimated. Nature Communications, 12(1), 1–10. https://doi.org/10.1038/s41467-021-22702-2

WMO. (2021). State of the Global Climate 2021. https://library.wmo.int/doc_num.php?explnum_id¼10859

Wyseure, G. C. L. (1991). SWRBB : A basin scale simulation model for soil and water resources management. Agricultural Water Management, 20(1), 82–83. https://doi.org/10.1016/0378-3774(91)90038-K

Yang, C., Wei, T., & Li, Y. (2022). Simulation and Spatio-Temporal Variation Characteristics of LULC in the Context of Urbanization Construction and Ecological Restoration in the Yellow River Basin. Sustainability (Switzerland), 14(2). https://doi.org/10.3390/su14020789

Yanogo, I. P. (2012). Les Strategies d'Adaptation des Populations aux Aleas Climatiques autour du Lac Bagre (Burkina Faso). These de doctorat, Université d'Abomey Calavi, Benin.

Yira, Y., Mutsindikwa, T. C., Bossa, A. Y., Hounkpè, J., & Salack, S. (2021). Assessing climate change impact on the hydropower potential of the Bamboi catchment (Black Volta, West Africa). Proceedings of the International Association of Hydrological Sciences, 384, 349–354. https://doi.org/10.5194/piahs-384-349-2021

Yira, Y., Diekkrüger, B., Steup, G., & Yaovi Bossa, A. (2017). Impact of climate change on hydrological conditions in a tropical West African catchment using an ensemble of climate simulations. Hydrology and Earth System Sciences, 21(4), 2143–2161.

https://doi.org/10.5194/hess-21-2143-2017

Yira, Y., Diekkrüger, B., Steup, G., & Bossa, A. Y. (2016). Modeling land use change impacts on water resources in a tropical West African catchment (Dano, Burkina Faso). In Journal of Hydrology (Vol. 537). Elsevier B.V. https://doi.org/10.1016/j.jhydrol.2016.03.052

Yonaba, R., Koïta, M., Mounirou, L. A., Tazen, F., Queloz, P., Biaou, A. C., Niang, D., Zouré, C., Karambiri, H., & Yacouba, H. (2021a). Spatial and transient modelling of land use/land cover (LULC) dynamics in a Sahelian landscape under semi-arid climate in northern Burkina Faso. Land Use Policy, 103(January). https://doi.org/10.1016/j.landusepol.2021.105305

Yonaba, R., Biaou, A. C., Koïta, M., Tazen, F., Mounirou, L. A., Zouré, C. O., Queloz, P., Karambiri, H., & Yacouba, H. (2021b). A dynamic land use/land cover input helps in picturing the Sahelian paradox: Assessing variability and attribution of changes in surface runoff in a Sahelian watershed. Science of The Total Environment, 757(23), 143792. https://doi.org/10.1016/j.scitotenv.2020.143792

Yu, L., Liang, L., Wang, J., Zhao, Y., Cheng, Q., Hu, L., Liu, S., Yu, L., Wang, X., Zhu, P., Li, X., Xu, Y., Li, C., Fu, W., Li, X., Li, W., Liu, C., Cong, N., Zhang, H., … Gong, P. (2014). Meta-discoveries from a synthesis of satellite-based land-cover mapping research. International Journal of Remote Sensing, 35(13), 4573–4588. https://doi.org/10.1080/01431161.2014.930206

Zoungrana, B., Conrad, C., Amekudzi, L., Thiel, M., Da, E., Forkuor, G., & Löw, F. (2015). Multi-Temporal Landsat Images and Ancillary Data for Land Use/Cover Change (LULCC) Detection in the Southwest of Burkina Faso, West Africa. Remote Sensing, 7(9), 12076–12102. https://doi.org/10.3390/rs70912076

Zoungrana D. K. (2012). Actualisation des etudes techniques pour la rehabilitation du barrage de Seguenega, province du Yatenga. Master Thesis, Institut International de l'Eau et de l'Environnement, Ouagadougou, Burkina Faso.

Zoungrana, T. P. (2007). Problématique de l’accès à l’eau potable sur les rives du lac Bagré, Burkina Faso. Revue de LARBE, 1812–1413, 25–44.

ANNEX

Annex 1a. Sensitive parameters, their fitted values for the NRB, and their ranges in SWIM

Parameter	Description, correction on	Range	Fitted value
ecal	Potential evapotranspiration	0.7 – 1.3	1
roc2, roc4	River routing coefficients for quick and slow components	1-50 (1 = quick routing; 50 = slow routing)	1 - 20 (from north to south)
cncor	Curve number	0.75 – 1.25	0.95 - 0.75 (from north to south)
sccor	Soil hydraulic conductivity	1 – 50 (the higher the value the higher conductivity)	4 - 1.5 (from north to south)
bff	Base flow factor, used to calculate return flow travel time	0.1 – 3	0.15 – 0.6 (from north to south)
abf	Alpha factor for groundwater. This parameter characterizes the ground water recession	0.0005 – 0.95	0.01
delay	Groundwater delay (days). The time it takes for water leaving the bottom of the root zone until it reaches the shallow aquifer where it can become groundwater flow	1 – 200	2
tlrch	Transmission losses, riverbed	0 – 3 (0 = no losses)	1 - 1.1

Annex 1b. Water level-Area-Volume relationship used for the implementation of the nine reservoirs in SWIM

Bam	Water Level (m)	0	295.15	295.65	296.15	296.65	297.15	297.65	298.15	298.65	299.15	299.6	299.8
	Area (Km^2)	0	0.8	1.8	2.8	4.5	6.3	8.5	11.5	16	20	25.5	30
	Volume (Mm^3)	0	0.23	0.88	0.98	3.9	6.5	10.48	15.43	21.58	30.63	41.2	49.1
Bagre	Water Level (m)	0	226	227	228	229	230	231	232	233	234	235	236
	Area (Km^2)	40.5	50.7	61.6	74.1	88.4	106.1	124.3	146	169.9	196.1	228.1	260
	Volume (Mm^3)	0	0	355	445	540	650	775	930	1090	1280	1490	1700
Ziga	Water Level (m)	259	260	261	262	263	264	265	266	266.2	266.5	267	267.5
	Area (Km^2)	0.5	2.6	6.1	12.1	22.1	36.2	55.6	81.8	88	95	110.2	126.5
	Volume (Mm^3)	1.1	6	13.9	27.5	50.2	82.4	126.5	186.1	200.1	218.4	253	288
Loumbila	Water Level (m)	0	0	0	0	0	0	0	0	0	271	272	276
	Area (Km^2)	0	0	0	0	0	0	0	0	0	0.1	1	16.8
	Volume (Mm^3)	0	0	0	0	0	0	0	0	0	0	6	48.2
Dourou (Kanazoe)	Water Level (m)	0	0	0	0	0	0	0	0	0	281	282	295
	Area (Km^2)	0	0	0	0	0	0	0	0	0	0.1	2	55
	Volume (Mm^3)	0	0	0	0	0	0	0	0	0	0	15	125
Goinre	Water Level (m)	0	326.5	327	327.5	328	328.5	329	329.5	330	330.5	331	331.25
	Area (Km^2)	0	0	0.04	0.14	0.35	0.74	1.26	2.03	2.98	4.05	5.18	5.6
	Volume (Mm^3)	0	0	0.12	0.4	1	2.1	3.6	5.8	8.5	11.58	14.8	16
Dem	Water Level (m)	293.5	293.75	294	294.25	294.5	294.75	295	295.25	295.35	295.5	295.75	296.1
	Area (Km^2)	2.59	3.17	3.75	4.28	4.9	5.52	6.11	6.72	6.95	7.32	8.04	10.13
	Volume (Mm^3)	1.29	2.01	2.88	3.88	5.03	6.33	7.78	9.39	10.13	11.14	13.06	15.8
Seguenega	Water Level (m)	294	294.25	294.5	294.75	295	295.25	295.5	295.75	296	296.25	296.5	296.75
	Area (Km^2)	0.209	0.326	0.403	0.489	0.586	0.701	0.807	0.913	1.035	1.157	1.24	1.229
	Volume (Mm^3)	0.163	0.235	0.326	0.437	0.571	0.733	0.922	1.136	1.379	1.657	1.956	2.35
Tougou	Water Level (m)	0	0	0	0	0	0	0	0	0	311	314.2	315
	Area (Km^2)	0	0	0	0	0	0	0	0	0	0.03	4.6	6.99
	Volume (Mm^3)	0	0	0	0	0	0	0	0	0	0.1	4.26	5.5

Annex 1c. Annual cycle of rainfall and mean temperature of bias corrected ISIMIP3b GCMs, W5E5 and Observations over 1985-2015 in Ouagadougou (A, C) and Ouahigouya (B, D)

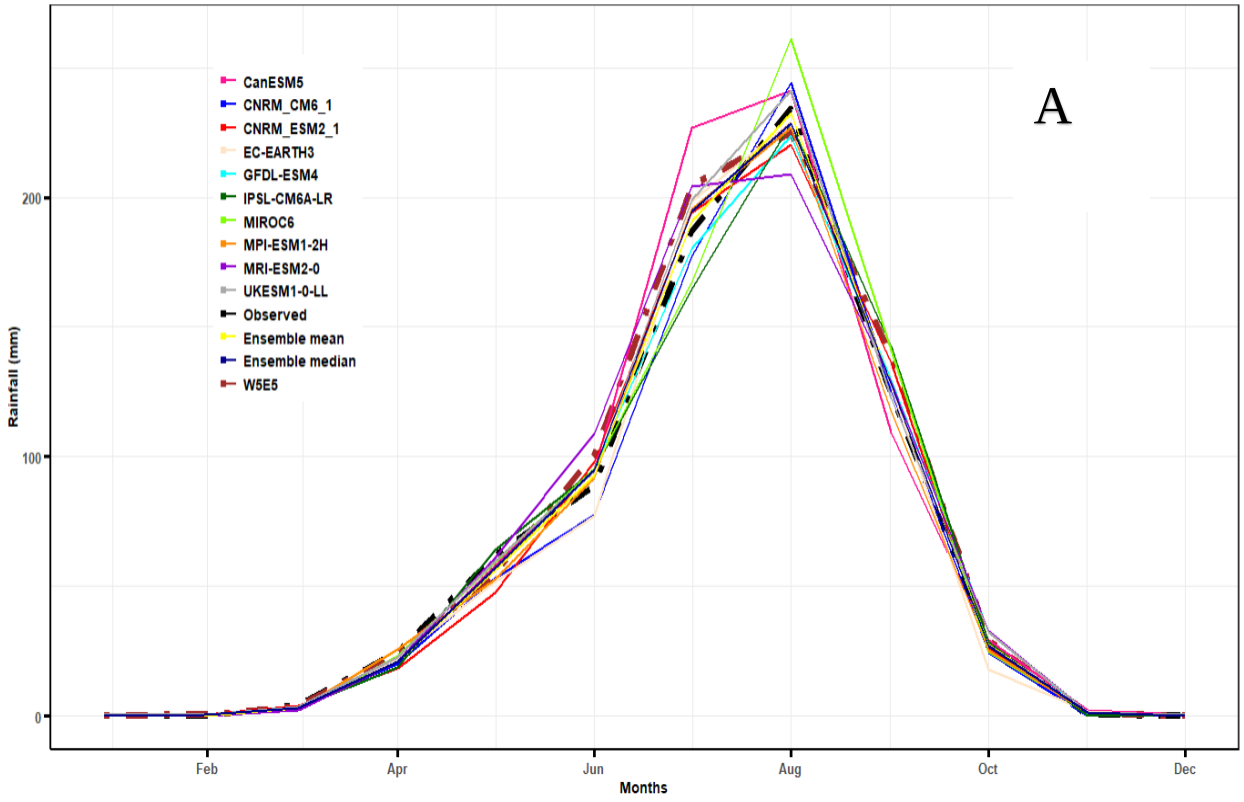

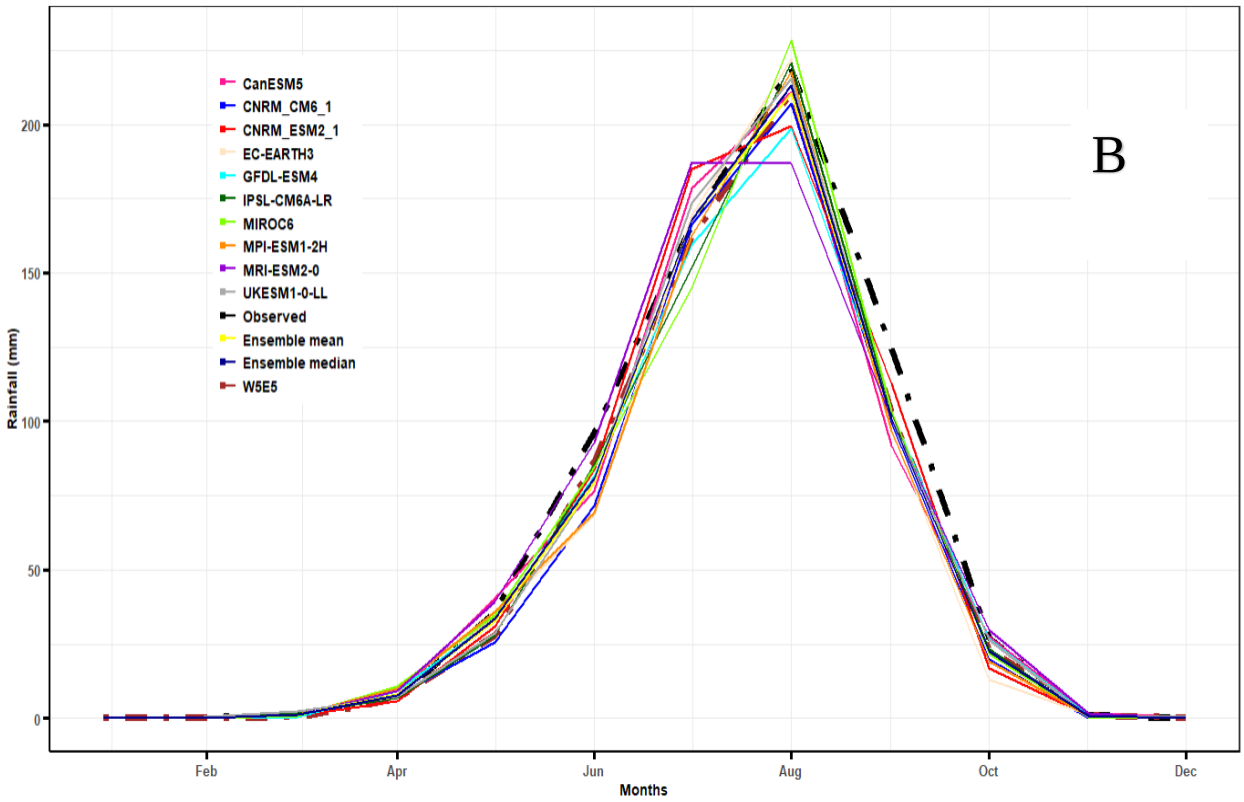

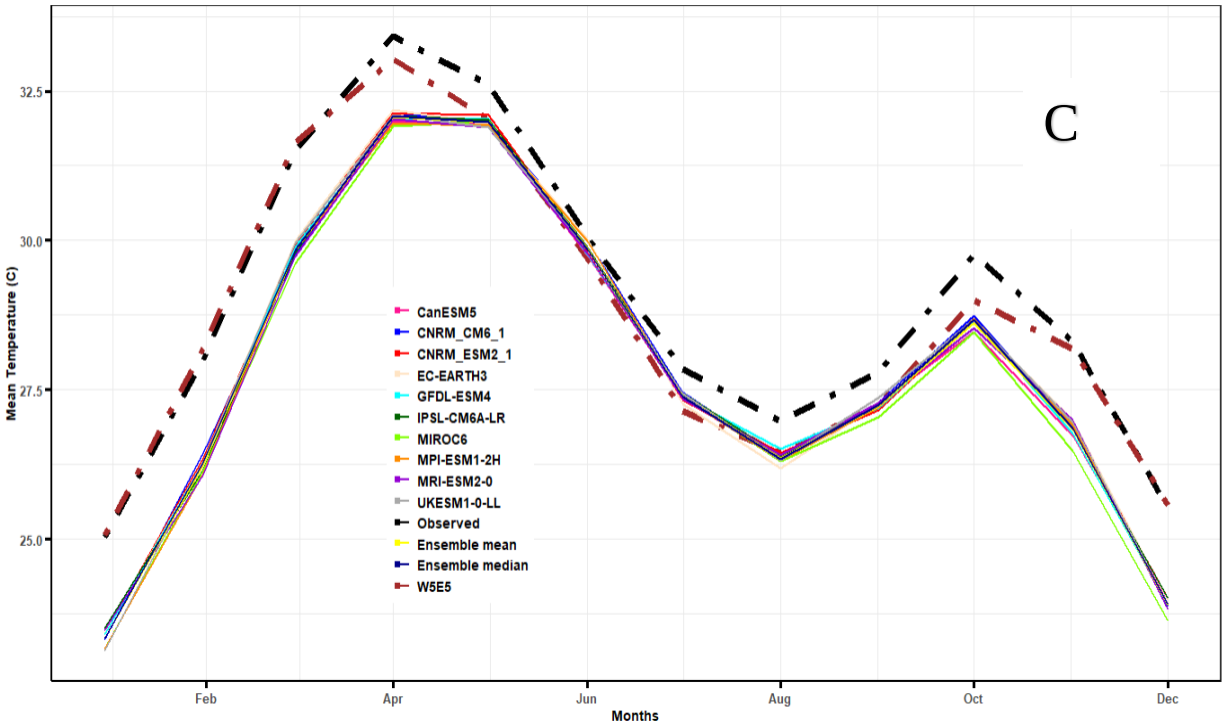
C
Mean Temperature (C)
32.5
30.0
27.5
25.0
Feb
Apr
Jun
Aug
Oct
Dec
Months
CanESM5
CNRM_CM6_1
CNRM_ESM2_1
EC-EARTH3
GFDL-ESM4
IPSL-CM6A-LR
MIROC6
MPI-ESM1-2H
MRI-ESM2-0
UKESM1-0-LL
Observed
Ensemble mean
Ensemble median
W5E5

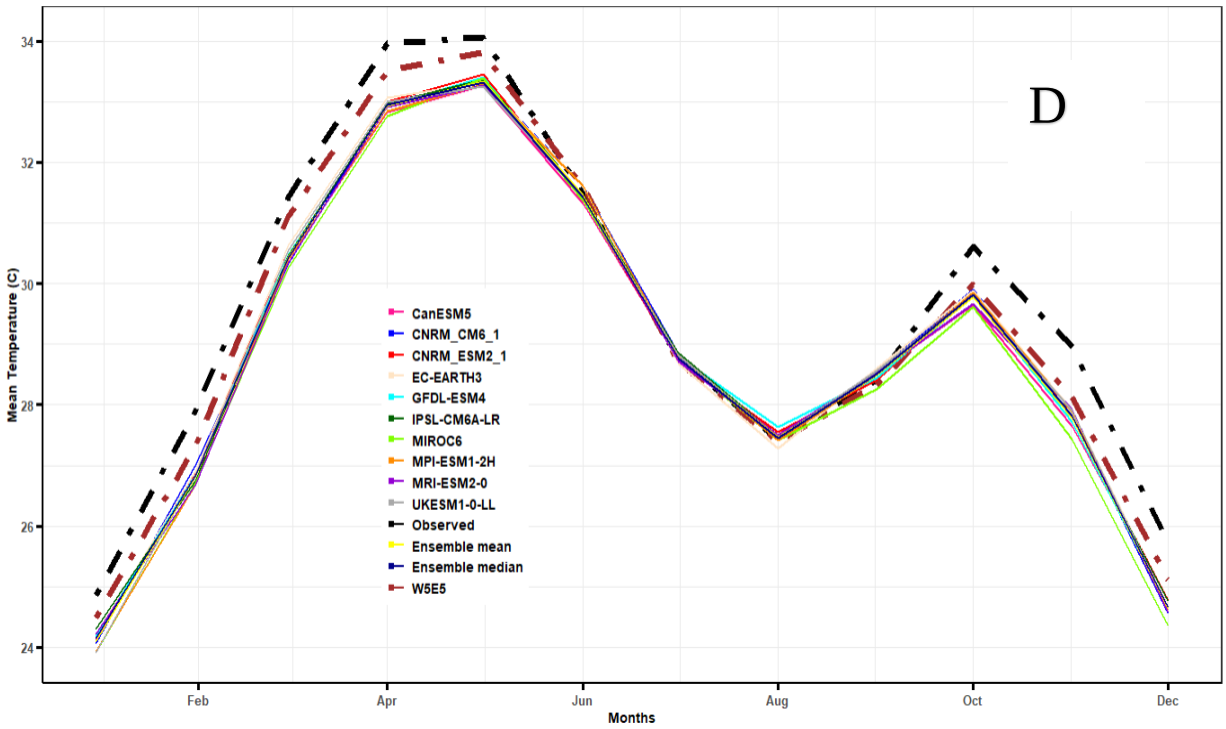
D
Mean Temperature (C)
34
32
30
28
26
24
Feb
Apr
Jun
Aug
Oct
Dec
Months
CanESM5
CNRM_CM6_1
CNRM_ESM2_1
EC-EARTH3
GFDL-ESM4
IPSL-CM6A-LR
MIROC6
MPI-ESM1-2H
MRI-ESM2-0
UKESM1-0-LL
Observed
Ensemble mean
Ensemble median
W5E5

Annex 1d. Calibration and Validation of reservoir volumes

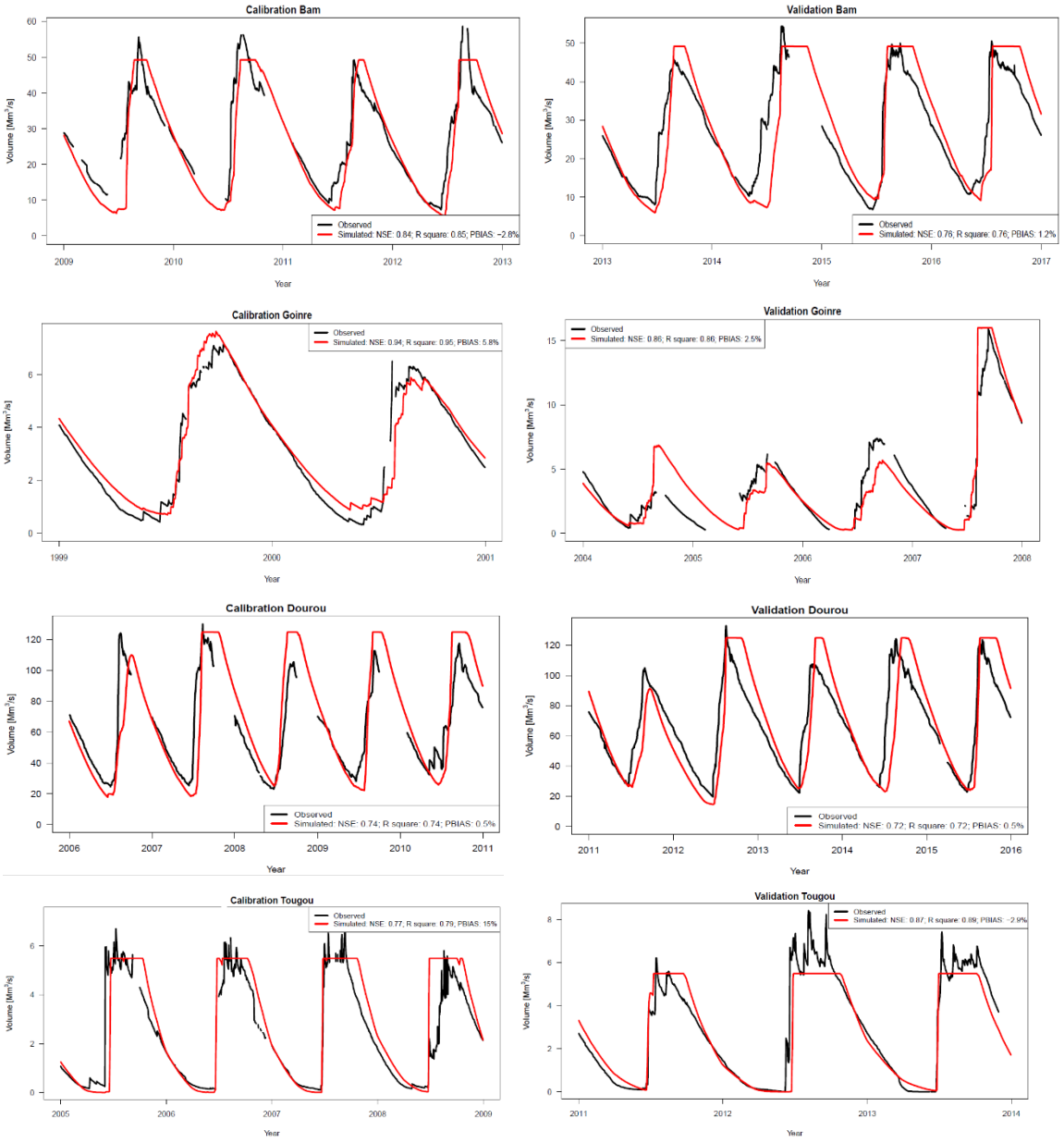

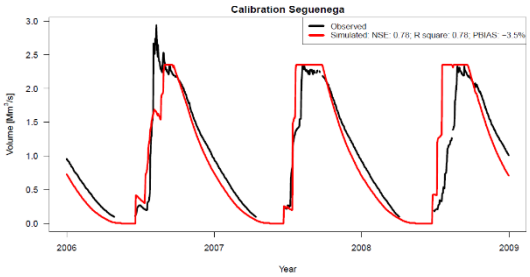
Calibration Seguenega
Observed
Simulated: NSE: 0.78; R square: 0.78; PBIAS: −3.5%
Volume [Mm³/s]
Year

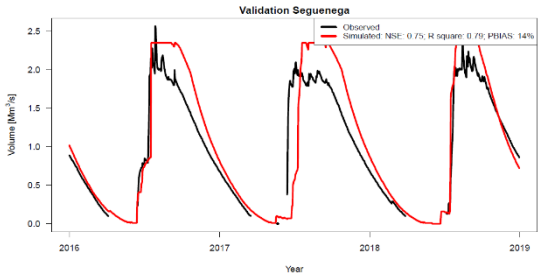
Validation Seguenega
Observed
Simulated: NSE: 0.75; R square: 0.79; PBIAS: 14%
Volume [Mm³/s]
Year

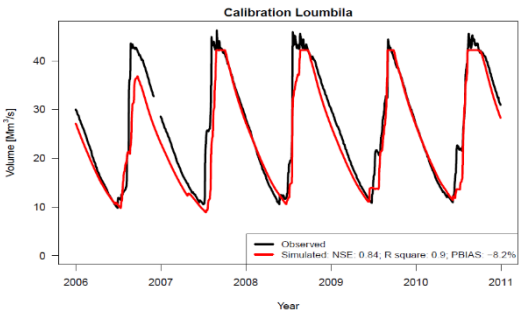
Calibration Loumbila
Observed
Simulated: NSE: 0.84; R square: 0.9; PBIAS: −8.2%
Volume [Mm³/s]
Year

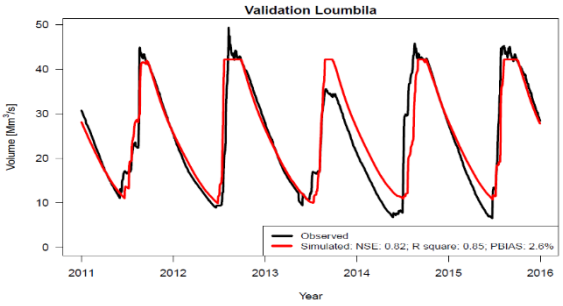
Validation Loumbila
Observed
Simulated: NSE: 0.82; R square: 0.85; PBIAS: 2.6%
Volume [Mm³/s]
Year

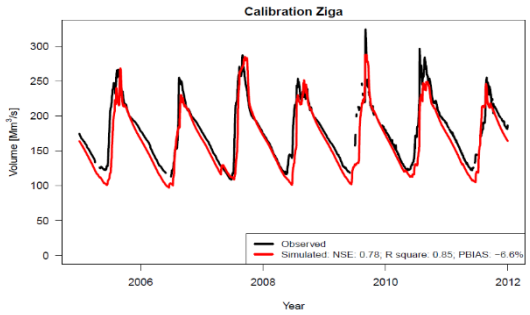
Calibration Ziga
Observed
Simulated: NSE: 0.78; R square: 0.85; PBIAS: −6.6%
Volume [Mm³/s]
Year

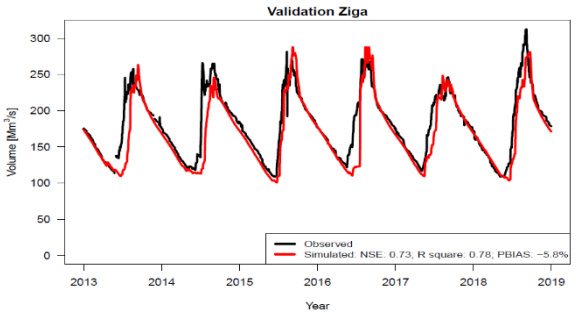
Validation Ziga
Observed
Simulated: NSE: 0.73; R square: 0.78; PBIAS: −5.8%
Volume [Mm³/s]
Year

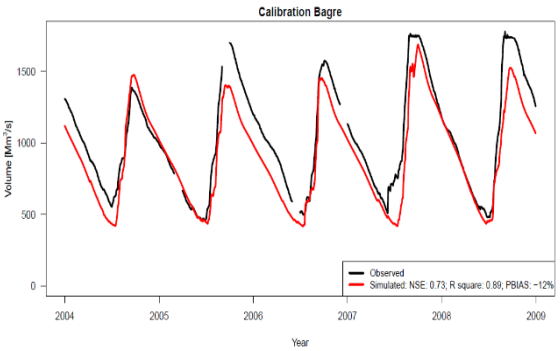
Calibration Bagre
Observed
Simulated: NSE: 0.73; R square: 0.89; PBIAS: −12%
Volume [Mm³/s]
Year

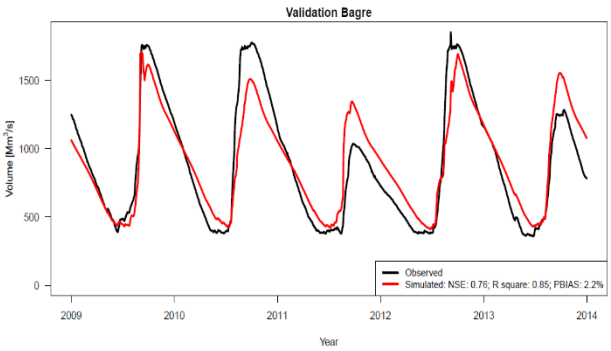
Validation Bagre
Observed
Simulated: NSE: 0.76; R square: 0.85; PBIAS: 2.2%
Volume [Mm³/s]
Year

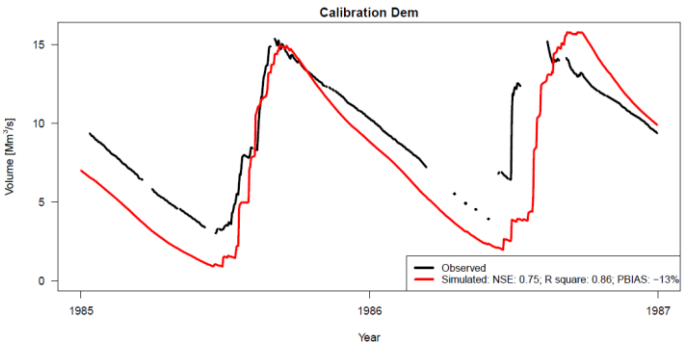
Calibration Dem
Observed
Simulated: NSE: 0.75; R square: 0.86; PBIAS: −13%
Volume [Mm³/s]
Year

Annex 1e. Comparison of simulated and observed monthly water level, inflow, turbined, and hydropower generation from 2005-2010

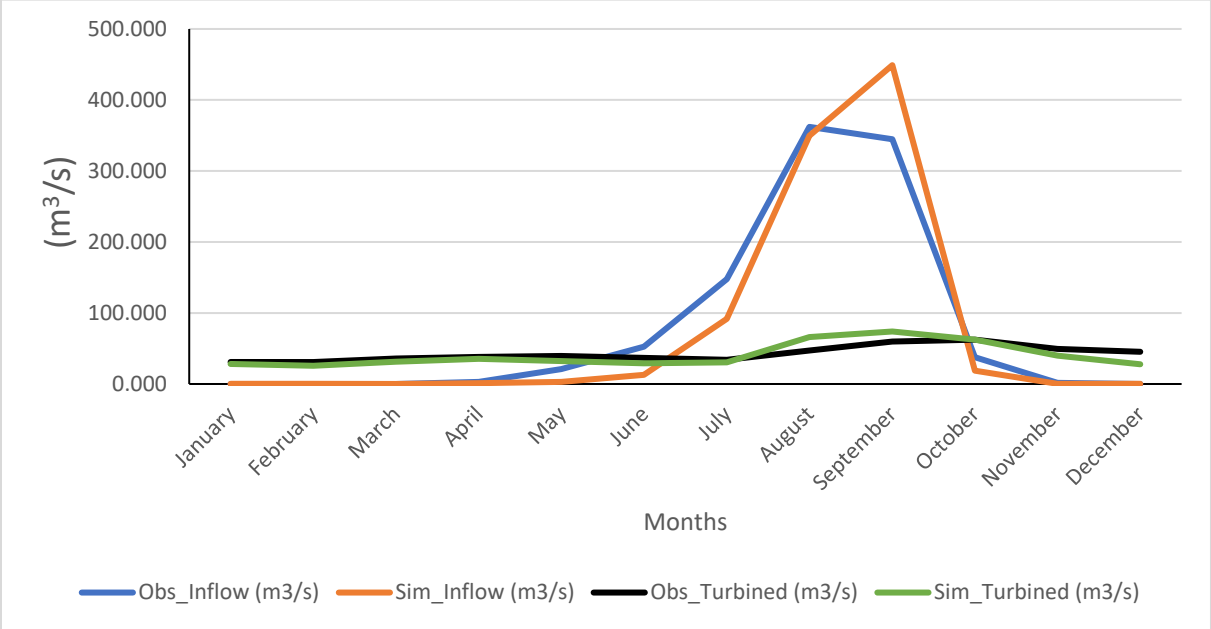

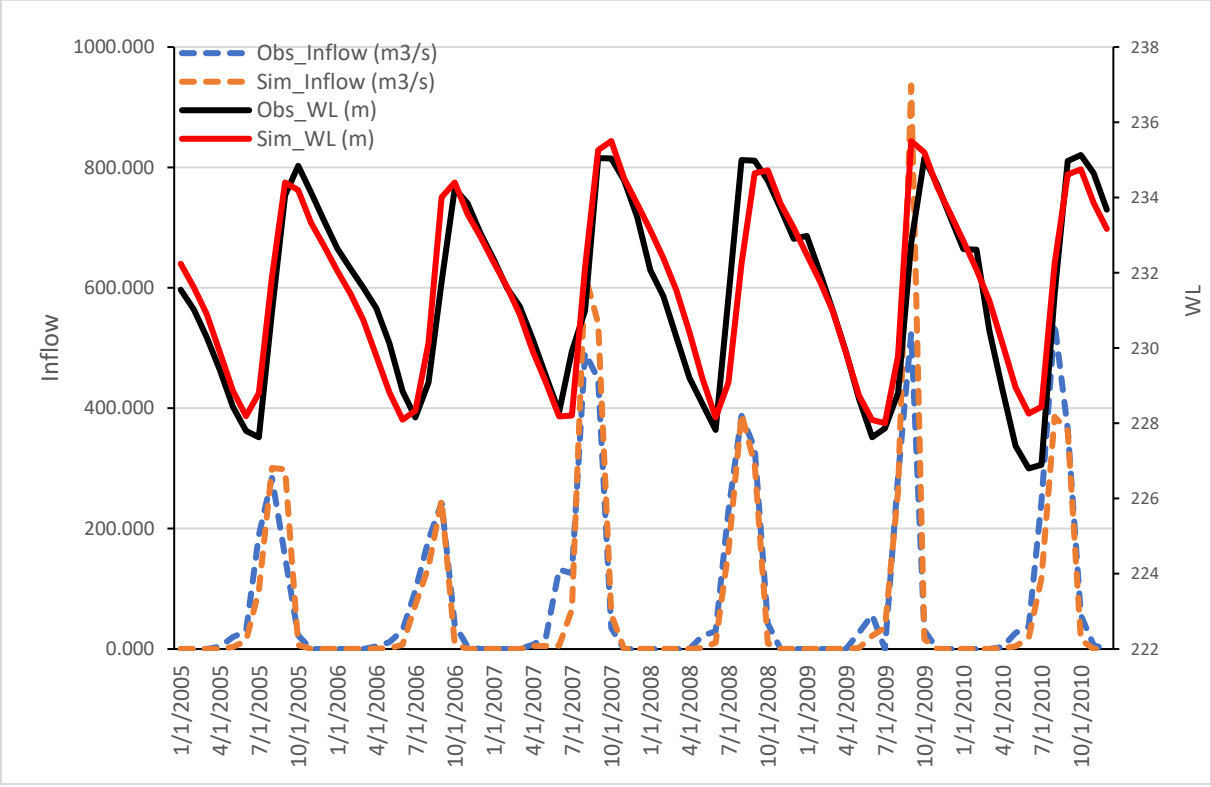

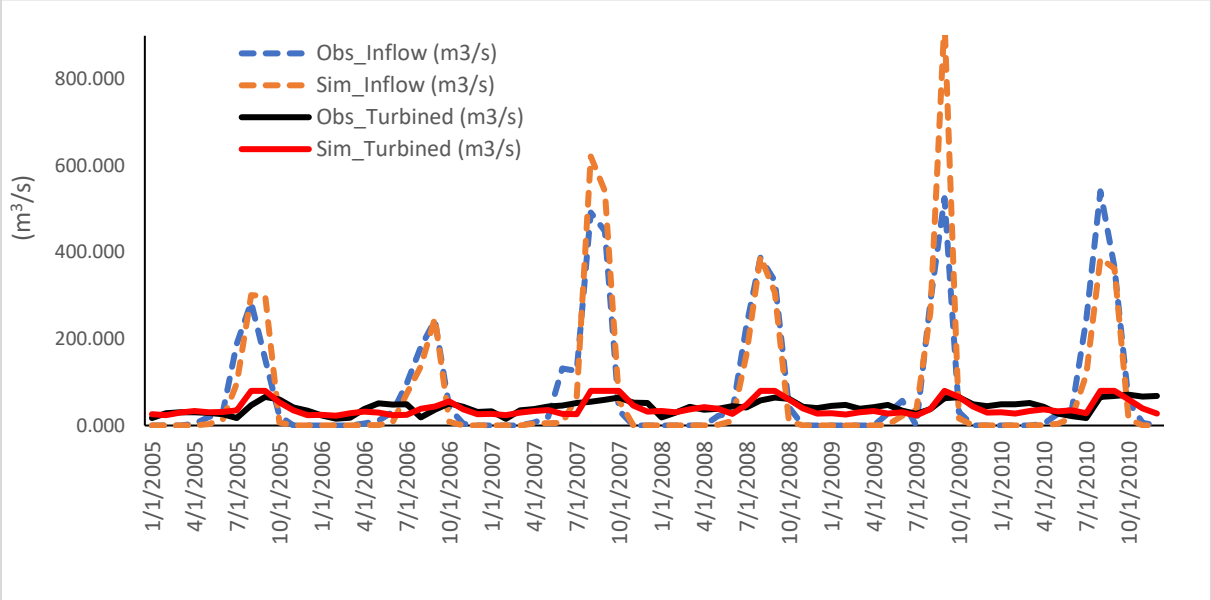
Obs_Inflow (m3/s)
Sim_Inflow (m3/s)
Obs_Turbined (m3/s)
Sim_Turbined (m3/s)
(m3/s)
800.000
600.000
400.000
200.000
0.000
1/1/2005
4/1/2005
7/1/2005
10/1/2005
1/1/2006
4/1/2006
7/1/2006
10/1/2006
1/1/2007
4/1/2007
7/1/2007
10/1/2007
1/1/2008
4/1/2008
7/1/2008
10/1/2008
1/1/2009
4/1/2009
7/1/2009
10/1/2009
1/1/2010
4/1/2010
7/1/2010
10/1/2010

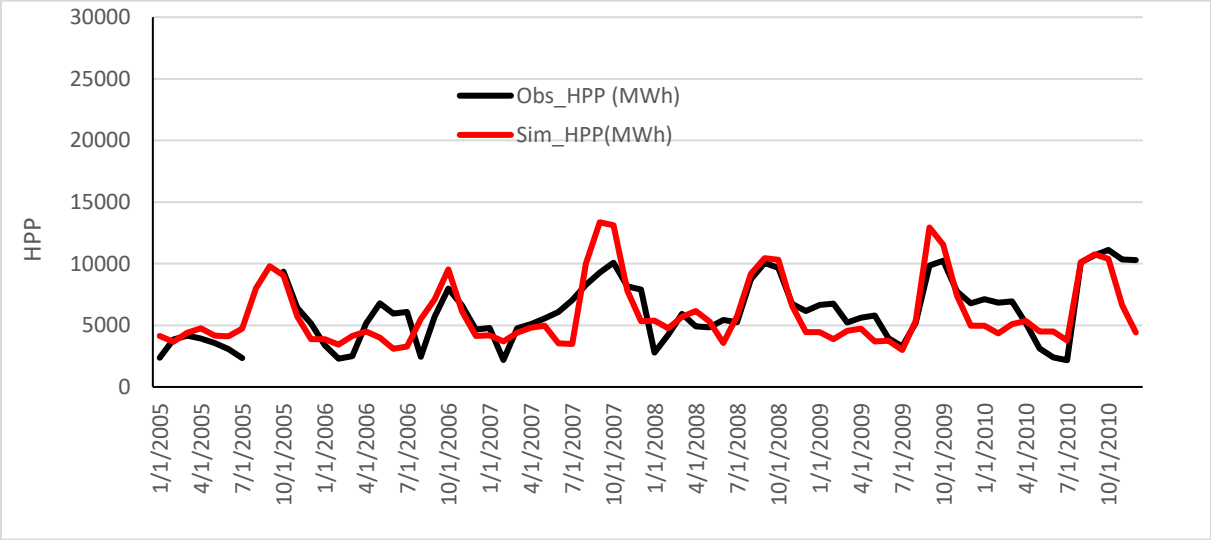
HPP
30000
25000
20000
15000
10000
5000
0
Obs_HPP (MWh)
Sim_HPP(MWh)
1/1/2005
4/1/2005
7/1/2005
10/1/2005
1/1/2006
4/1/2006
7/1/2006
10/1/2006
1/1/2007
4/1/2007
7/1/2007
10/1/2007
1/1/2008
4/1/2008
7/1/2008
10/1/2008
1/1/2009
4/1/2009
7/1/2009
10/1/2009
1/1/2010
4/1/2010
7/1/2010
10/1/2010

Annex 2

Published Papers

1. Yangouliba, G.I., Koch, H., Liersch, S., Sintondji, L.O., Sidibé, M., Larbi, I., Limantol, A.M., Yira, Y., Dipama, J-M., Kwawuvi, D. (2022). Impacts of hydro-climatic trends and upstream water management on hydropower generation at the Bagré dam. *Journal of Water and Climate Change*. https://doi.org/10.2166/wcc.2022.452
2. Yangouliba, G.I., Zoungrana, B.J-B., Hackman, K.O., Koch, H., Liersch, S., Sintondji, L.O., Dipama, J-M., Kwawuvi, D., Ouédraogo, V., Yabré, S., Bonkoungou, B., Sougué, M., Gadiaga, A., Koffi, B. (2022). Modelling past and future land use and land cover dynamics in the Nakambé River Basin, West Africa. *Model. Earth Syst. Environ.* https://doi.org/10.1007/s40808-022-01569-2
3. Yangouliba, G.I., Kwawuvi, D., Almoradie, A. (2020). Suitable Land Assessment for Rice Crop in Burkina Faso Using GIS, Remote Sensing and Multi Criteria Analysis. *Journal of Geographic Information System*, 12, 683-696. https://doi.org/10.4236/jgis.2020.126039
4. Kwawuvi, D., Mama, D., Agodzo, S.K., Hartmann, A., Larbi, I., Bessah, E., Limantol, A.M., Dotse, S-Q., Yangouliba, G.I. (2022) Spatiotemporal variability and change in rainfall in the Oti River Basin, West Africa. *Journal of Water and Climate Change*. https://doi.org/10.2166/wcc.2022.368

Gnibga Issoufou YANGOULIBA was born in 1990 in Guelwongo, in the central-southern region of Burkina Faso. He attended the primary and secondary schools "Ecole Gounghin Sud Protestante" (1995-2001) and Lycée Mixte de Gounghin (2001-2008), respectively. After successfully completing his Baccalaureate in 2008, he joined the University Joseph Ki-Zerbo to study Geography, where he obtained his Bachelor's degree and Master's degree in 2011 and 2017 respectively. He also has a Master of Science in Geomatics obtained at the "Institut Superieur des Etudes Spatiales et Telecommunications" in 2017. After a short career as an independent consultant, he was awarded a WASCAL doctoral fellowship in climate change and water resources in 2019. Issoufou is an expert in geographic information systems (GIS) and remote sensing, natural resource management, climate change, quantitative hydrology, and integrated water resources management.

***Abstract*:** This study focused on the impact of climate, land use, and water management changes on the hydropower potentials of the Bagré dam in Burkina Faso. The specific objectives are (i) the analysis of hydro-climatic variability and upstream reservoir management impact on the hydropower generation at the Bagré dam, (ii) the determination of the past and future land use/land cover (LULC) dynamics in the Nakambé River Basin (NRB), (iii) the assessment of climate and LULC changes impacts on the hydropower potentials at the Bagré dam, and (iv) the assessment of impacts of changed water management on the hydropower potentials at the Bagré dam. Datasets used comprise historical observed and reanalysis climate (W5E5), and hydrological time series for break years detection, trend analysis, and correlation investigation. In addition, Landsat images (1990, 2005, 2020) and ground truth data were used for LULC mapping and projection. Downscaled and Bias corrected data from the Inter-Sectoral Impact Model Intercomparison Project (ISIMIP3b) Global Climate Models, water management, and reservoirs parameters data were integrated into the Soil and Water Integrated Management (SWIM) model to assess the changes in hydropower generation for the mid (2035-2065) and far (2065-2095) future due to climate, land use, and water management changes. The results showed an annual positive trend in hydropower generation and inflow due to the construction of the Ziga dam in 2000 and its management change in 2005, respectively. In terms of LULC dynamics, from 1990 to 2020, woodland and shrubland decrease to the benefit of cropland, bare land/built-up, and water bodies. By 2050, woodland and shrubland may continue to decrease under the Business-as-usual (BAU) scenario. However, under an afforestation scenario, woodland and shrubland would slightly increase even though cropland will be the dominated land use of the basin. The results also showed that hydropower generation would increase in the mid (15-24%) and far (1.7-35%) future under climate change scenarios, relative to the baseline period (1984-2014). Furthermore, the future LULC change could increase the hydropower potential. Yet, the increment would be less under an afforestation scenario compared to a BAU LULC. For the hydropower generation change, climate change is responsible for 60-98% while LULC change is responsible for 2-40%. The future water allocation from Ziga reservoir would reduce the inflow by -2 m3/s in the future. This inflow decrease, in addition to the increasing water withdrawals for irrigation supply at the Bagré dam would cause a strong decrease in hydropower generation, which could be more pronounced under SSP126 and BAU LULC, compared to SSP370 and afforestation scenarios. This work pointed out the challenges for the Bagré dam operation to supply electricity in the future and can be used as a guideline for policy makers to address the future impacts of climate, land use, and water management changes on water resources in the NRB.

Key words: ISIMIP3b, Land Use and Land Cover Change, SWIM Model, Water Management, Hydropower Generation, Nakambé River Basin.

PhD	Gnibga Issoufou YANGOULIBA	IMPACTS OF CLIMATE, LAND USE, AND WATER MANAGEMENT CHANGES ON THE HYDROPOWER POTENTIALS OF THE BAGRE DAM, BURKINA FASO	GRP/CCWR/INE/WASCAL – UAC July, 2023